Molecular Coordination of Skeletal Muscle Capillary Remodelling in Obesity: Implications for Metabolic Homeostasis and Disease

Emmanuel Nwadozi

A Dissertation Submitted to the Faculty of Graduate Studies
in Partial Fulfilment of the Requirements for the Degree of
Doctor of Philosophy

Graduate Program in
Kinesiology and Health Sciences

York University
Toronto, ON.
April 2020

Abstract

Considerable effort has been directed towards the development of preventative and therapeutic strategies against obesity and its clinical sequalae (i.e. type-2 diabetes, cardiovascular disease) that now pose a significant public health and economic burden on healthcare systems worldwide. Over the last ~30 years, the capillary network within skeletal muscle has emerged as a critical determinant of metabolic homeostasis by facilitating the transport of oxygen and nutrients to support the metabolic functions of the underlying myocytes. In fact, it is now widely accepted that the loss (rarefaction) of skeletal muscle capillaries promotes the onset of metabolic dysfunction (i.e. insulin resistance, hyperglycaemia) in obesity. However, other studies have reported unaltered or, in some cases, expansion (angiogenesis) of the skeletal muscle capillary network, thus, the influence of obesity on capillary remodelling within skeletal muscle remains unclear. The purpose of the current dissertation was to define the intrinsic molecular mechanisms that govern these skeletal muscle capillary remodelling responses in obesity. First, I compared two widely used models of obesity: leptin-signalling deficiency, which often results in capillary rarefaction, and a model of diet-induced obesity that has previously been shown to promote angiogenesis in skeletal muscle. Considerable evidence suggests that leptin is a pro-angiogenic factor. Thus, I hypothesized that the capacity for leptin signalling underlies the disparate capillary remodelling outcomes between both models of obesity. Consistent with this hypothesis, I found that capillary rarefaction in leptin receptor mutant (*Lepr*^{db}) mice was a consequence of the underlying leptin resistance more so than obesity. Administration of a 16-week high-fat (HF) diet was associated with increased capillary number within skeletal muscle and promoted the expression of pro-angiogenic factors including leptin and vascular endothelial growth factor-A (VEGF-A). Leptin was shown to promote VEGF-A synthesis by skeletal myocytes. Furthermore, peri-capillary cells known as

pericytes were identified as local sources of leptin within skeletal muscle, indicating a potential paracrine regulation of capillary homeostasis by leptin. To investigate the potential involvement of anti-angiogenic factors in mediating the capillary remodelling response in obesity, I investigated the role of forkhead box O (FoxO) transcription factors that are potent repressors of skeletal muscle angiogenesis and have previously been implicated in the progression of metabolic disorders. In transgenic mice that have an endothelial cell directed depletion of FoxO proteins ($Foxo^{\Delta}$ mice), I demonstrated enhanced angiogenesis after 16-weeks of HF diet, which was associated with the preservation of peripheral insulin sensitivity. Together, these findings demonstrated that angiogenesis is a physiological adaptation to obesity that is governed by the net-influence of pro- and anti-angiogenic molecular factors within skeletal muscle and can mitigate the onset of metabolic dysfunction. Finally, to determine whether the positive influence of obesity on the skeletal muscle capillary network was beneficial in a pathological context, HF-preconditioned mice were subjected to a pre-clinical model of peripheral artery disease, a condition characterized by reduced blood flow (ischemia) to the lower limbs. HF-preconditioning elicited an overall increase in capillary perfusion, which was associated with enhanced microvascular remodelling, blood flow recovery and tissue regeneration following the onset of ischemia, highlighting the potential benefit of vasculo-centric therapies against the clinical progression of obesity. Overall, these findings demonstrate that angiogenesis is a physiological adaptation that preserves metabolic homeostasis and provides mechanistic insight into the coordination of skeletal muscle capillary in obesity.

Acknowledgments

I would like to express my most sincere gratitude and appreciation to everyone who has made this journey possible, including:

Dr. Tara Haas: For taking a chance on me as a clueless 2nd Year Kinesiology student and moulding me into the researcher that I am today. Thank you for teaching me how to think critically about my experiments, for the countless revision hours that has undoubtedly elevated my scientific writing and for giving me the opportunity to present my findings at the most amazing international conferences. You have been a source of great inspiration and I could not have asked for a better supervisor.

Dr. Emilie Roudier: You have been there for me without fail since I joined the lab back in May 2011! Thank you for your mentorship, patience and the excitement you always showed for my research work. je vous en serai éternellement reconnaissant!

Dr. Thomas Gustafsson: For your collaboration, mentorship and teaching me to always look at the 'big picture' with my research. Thank you for taking care of me while I spent time in your lab in Sweden and of course for all the laughs we've had over the years. You are a big part of whom I've become as a researcher and I hope that one day I can pay if forward!

To all my colleagues: Jenn, Cassandra, Eric, Ariella, Dara, Sammy, Suji, Cindy, Martina, Ghoncheh, Matt, Omid and all the undergrads I have had the pleasure of working with over the years. Thank you for your leadership, friendship and support over the years. It's been a great positive and stimulating experience!

To my parents (Clement & Catherine Nwadozi): for instilling in me the attitude of hard work/discipline, the belief that I can achieve anything that I want in life and for allowing me to spread my wings and soar. Your continuous love and support have been the fuel that has kept me going, without which none of this would have been possible.

To my friends and family: For all the laughs, tears, and good times that provided me with a life outside of research, words cannot describe the impact you've had on my life. I love you all.

List of Publications

1. **Nwadozi, E.**, Rudnicki, M., DeCiantis, M., Milkovich, S., Pulbere, A., Roudier, E., Birot, O., Gustafsson, T., Ellis, C.G., and Haas, T.L. (2020a). High fat diet pre-conditioning improves microvascular remodeling during regeneration of ischemic mouse skeletal muscle. Acta Physiol. Oxf. Engl. doi: 10.1111/apha.13449.

2. **Nwadozi, E.**, Rudnicki, M., and Haas, T.L. (2020b). Metabolic Coordination of Pericyte Phenotypes: Therapeutic Implications. Front. Cell Dev. Biol. 8, 77.

3. **Nwadozi, E.**, Ng, A., Strömberg, A., Liu, H.-Y., Olsson, K., Gustafsson, T., and Haas, T.L. (2019). Leptin is a physiological regulator of skeletal muscle angiogenesis and is locally produced by PDGFRα and PDGFRβ expressing perivascular cells. Angiogenesis 22, 103–115.

4. Rudnicki, M., Abdifarkosh, G., **Nwadozi, E.**, Ramos, S.V., Makki, A., Sepa-Kishi, D.M., Ceddia, R.B., Perry, C.G., Roudier, E., and Haas, T.L. (2018a). Endothelial-specific FoxO1 depletion prevents obesity-related disorders by increasing vascular metabolism and growth. ELife 7.

5. Rudnicki, M., Abdifarkosh, G., Rezvan, O., **Nwadozi, E.**, Roudier, E., and Haas, T.L. (2018b). Female Mice Have Higher Angiogenesis in Perigonadal Adipose Tissue Than Males in Response to High-Fat Diet. Front. Physiol. 9, 1452.

6. Mandel, E.R., Uchida, C., **Nwadozi, E.**, Makki, A., and Haas, T.L. (2017). Tissue Inhibitor of Metalloproteinase 1 Influences Vascular Adaptations to Chronic Alterations in Blood Flow. J. Cell. Physiol. 232, 831–841.

7. **Nwadozi, E.**, Roudier, E., Rullman, E., Tharmalingam, S., Liu, H.-Y., Gustafsson, T., and Haas, T.L. (2016). Endothelial FoxO proteins impair insulin sensitivity and restrain muscle angiogenesis in response to a high-fat diet. FASEB J. Off. Publ. Fed. Am. Soc. Exp. Biol. 30, 3039–3052.

8. Haas, T.L., and **Nwadozi, E.** (2015). Regulation of skeletal muscle capillary growth in exercise and disease. Appl. Physiol. Nutr. Metab. Physiol. Appl. Nutr. Metab. 40, 1221–1232.

9. Uchida, C., **Nwadozi, E.**, Hasanee, A., Olenich, S., Olfert, I.M., and Haas, T.L. (2015). Muscle-derived vascular endothelial growth factor regulates microvascular remodelling in response to increased shear stress in mice. Acta Physiol. Oxf. Engl. 214, 349–360.

Table of Contents

Abstract……ii

Acknowledgments……..v

List of Publications v

Table of Contents vii

List of Abbreviations ix

List of Tables xii

List of Figures xiii

Chapter 1: Literature Review 1

1.1 Capillary Networks 1

1.1.1 Basic Morphology, Functions and Cellular Constituents 1

1.1.2 Ultrastructural Classifications & Organotypic Heterogeneity 2

1.2 Skeletal Muscle Capillary Network 4

1.2.1 Structural Organization of the Microvasculature 4

1.2.2 Capillary Architecture & Oxygen Transport 4

1.2.3 Postnatal Capillary Remodelling 7

1.2.4 Regulation of Capillary Remodelling in Skeletal Muscle 10

1.3 Pericyte Functions & Multipotency 17

1.3.1 Pericytes & Capillary Homeostasis 17

1.3.2 Pericyte Plasticity 19

1.3.3 Regulation of Pericyte Stemness and Differentiation Potential 21

1.3.4 Pericytes & Skeletal Muscle Regeneration 22

1.4 Skeletal Muscle Capillaries: Determinants of Metabolic Homeostasis 23

1.4.1 Exchange of Energy Substrates and Regulatory Hormones 24

1.4.2 Microvascular Dynamics in the Postprandial Period 28

1.4.3 Skeletal Muscle Capillarity and Metabolic Homeostasis 30

1.5 Clinical Application: Vascular Remodelling in Peripheral Artery Disease 32

1.6 Scope of Dissertation 35

Chapter 2: Leptin is a Physiological Regulator of Skeletal Muscle Capillary Homeostasis and Angiogenesis: Implications During Post-Natal Myocyte Hypertrophy and Obesity.....37

2.1 Contributions: 37

2.2 Published Data: 37
2.3 Chapter Summary 38
2.4 Results 40
2.5 Discussion 49
Chapter 3: Nutrient-Excess Induces Leptin Production By PDGFRβ+ Perivascular Cells in Skeletal Muscle: Implications for Capillary Remodeling. 55
3.1 Contributions: 55
3.2 Published Data: 55
3.3 Chapter Summary 56
3.4 Results 58
3.5 Discussion 65
Chapter 4: Endothelial FoxO proteins Impair Insulin Sensitivity and Restrain Muscle angiogenesis in response to a high-fat diet. 70
4.1 Contributions: 70
4.2 Published Data: 70
4.3 Chapter Summary 71
4.4 Results 73
4.5 Discussion 88
Chapter 5: High-fat diet pre-conditioning improves microvascular remodeling during regeneration of ischemic mouse skeletal muscle 93
5.1 Contributions: 93
5.2 Published Data: 93
5.3 Chapter Summary 94
5.4 Results 96
5.5 Discussion 106
Chapter 6: Concluding Remarks 110
6.1 Perspectives 110
6.2 Novel Contributions to the Field 113
6.2.1 Angiogenesis is a Physiological Adaptation to Obesity that Contributes to the Preservation of Metabolic Homeostasis 113
6.2.2 Potential Role of Pericytes as Energy-Sensing Cells That Coordinate Myocyte and Microvascular Adaptations Within Skeletal Muscle 114

6.3 Study Limitations 116
6.4 Future Work 117
Chapter 7: Materials & Methods 118
7.1 Human Studies 118
7.2 Animal Studies 118
7.2.1 Transgenic Mouse Models 119
7.2.2 Administration of High-Fat Diet 120
7.2.3 Metabolic Testing 121
7.2.4 *In-vivo* and *Ex-vivo* stimulation of mouse skeletal muscles 121
7.2.5 Mouse Model of Femoral Artery Ligation 122
7.2.6 Isolation of Cell Fragments from Mouse Skeletal Muscle 123
7.3 Histological Assessments 124
7.3.1 Cryopreservation of Skeletal Muscles 124
7.3.2 Staining Protocols 124
7.3.2.1 Capillarity, arterioles and myocyte cross-sectional area 124
7.3.2.2 Intracellular localization of Leptin, Foxo1 and Ki67 125
7.3.2.3 Cellular Infiltration into skeletal muscle 126
7.3.2.4 Skeletal Muscle regeneration 127
7.4 Cell Culture 128
7.5 RNA Analysis 129
7.6 Transcriptome Analyses of HF-Foxo$^{L/L}$ and HF-Foxo$^{\Delta}$ Mouse Muscles 130
7.7 Protein Analyses 131
7.8 Statistical Analysis 132
Appendix A: Nutrient-Overload Induced Leptin Production Within Skeletal Muscle: Potential Role for ZNF423 134
Appendix B: Endothelial-specific Foxo1,3 depletion enhances post-ischemia perfusion recovery in HF-fed mice. 144
Reference List 149

List of Abbreviations

αSMA - alpha-smooth muscle actin
Angpt1 - Angiopoietin-1
Angpt2 - Angiopoietin-2
C:F - Capillary-to-Fibre Ratio
CD - Capillary Density
Cebpa - Ccaat enhancer binding protein alpha
CLI - Critical Limb Ischemia
EC - Endothelial Cell
ECM - Extracellular Matrix
EDL - Extensor Digitorum Longus
eNOS - endothelial nitric oxide synthase
ET-1 - Endothelin-1
FA - Fatty Acid
FATP - Fatty Acid Transport Protein
Foxo - Forkhead box o
Gluts (Glucose transporters)
GTT - Glucose Tolerance Test
HF - High Fat
IGT - Impaired Glucose Tolerance
IPA - Ingenuity Pathway Analysis
ITT - Insulin Tolerance Test
JAK2 - Janus Kinase 2
LEPR - Leptin receptor
MMP - Matrix Metalloproteinase
NC - Normal Chow
NG2 - Neural-Glial Antigen 2
NO - Nitric Oxide
NRP1 - Neuropilin 1
PAD - Peripheral Artery Disease
PDGF-BB - Platelet Derived Growth Factor - BB
PDGFRβ - Platelet Derived Growth Factor Receptor - beta
PDGFRα – Platelet Derived Growth Factor Receptor - alpha
Pparg - Peroxisome Proliferator-Activated Receptor γ
Pparγ – peroxisome proliferator activated receptor gamma
RBC - Red Blood Cell
Runx2 - Runt-Related Transcription Factor 2
SDH - Succinate Dehydrogenase
Sox9 - Sry-Box Transcription Factor 9

Tbx18 - T-box Transcription Factor 18
TET - Transendothelial Transport
TGFβ – Transforming Growth Factor beta
THBS-1 - Thrombospondin-1
TIMP3 - Tissue Inhibitor of Metalloprotenaises - 3
TNFα – Tumor necrosis Factor aplha
TSR - Thrombospondin Type-1 Repeats
VEGF-A - Vascular Endothelial Growth Factor-A
VEGFR2 - Vascular Endothelial Growth Factor Receptor 2
vSMC - Vascular Smooth Muscle Cell
WT - Wildtype
Zfp423 - Zinc Finger Protein 423

List of Tables

Table 4.1: Differentially expressed genes in HF-Foxo$^{\Delta}$ and Foxo$^{L/L}$ mice……..…….84

Table 4.2: GSEA of genes up-regulated in HF-Foxo$^{\Delta}$ and Foxo$^{L/L}$ mice ……..……..85

Table 4.3: Selected functions that are represented within the set of differentially expressed genes…….……..…….86

Table 4.4: Selected upstream regulators of the differentially expressed gene set diet)…….....87

Table 7.1: Taqman primer sets……..…..133

Table 7.2: Antibodies used for western blotting…….…....133

Table A.1: Predicted ZNF423 binding sites on human leptin promoter…...……..141

List of Figures

Figure 1.1: Schematic representation of the different types of capillaries…….....3

Figure 1.2: Architecture of skeletal muscle capillary network.……..5

Figure 1.3: Schematic representation of the angiogenic process……9

Figure 1.4: Scope of the dissertation……36

Figure 2.1: Characterization of 4-week old *Lepr*^{db} cohort……..…….41

Figure 2.2: Skeletal muscle characteristics of *Lepr*^{db} mice at 4 and 13 weeks of age……...…...42

Figure 2.3: Leptin increases *Vegfa* mRNA expression in murine and human skeletal muscle cells.....44

Figure 2.4: Characterization of myocyte-specific leptin-resistant (MLepRb+) mice……..…….45

Figure 2.5: Skeletal muscle capillarization in MLepRb mice..……46

Figure 2.6: Mouse model of diet-induced obesity…...…….47

Figure 2.7: Assessments of insulin sensitivity and glucose tolerance in diet-fed mice……...….48

Figure 2.8: HF-feeding promotes angiogenesis within skeletal muscle……...50

Figure 3.1: Cellular localization of leptin within skeletal muscle……59

Figure 3.2: Leptin is produced in skeletal muscle capillary fragments……60

Figure 3.3: Co-localization of PDGFRα and leptin immunoreactivity……61

Figure 3.4: Co-localization of PDGFRβ and leptin immunoreactivity……62

Figure 3.5: PDGFRβ+ and PDGFRβ+ perivascular cells are leptin producing within skeletal muscle……64

Figure 3.6: Microvascular remodelling in NC- and HF-fed mice……66

Figure 4.1: Diet-induced obesity increases the expression of Foxo1 in the endothelium of WT FVB/n mice……74

Figure 4.2: Endothelial Foxo1 is increased by palmitate and TNFα.……....75

Figure 4.3: Endothelium-directed Foxo deletion protects mice from the development of an obese phenotype……...76

Figure 4.4: Increased vascular-dependent insulin sensitivity in muscle of HF-Foxo$^{\Delta}$ mice (2nd cohort; 8-week diet)…… ..78

Figure 4.5: High-fat diet induces angiogenesis in Foxo$^{\Delta}$ mice……..…...79

Figure 4.6: High fat diet is not associated with skeletal muscle immune cell infiltration……80

Figure 4.7: Differential expression of genes associated with angiogenesis, lipid metabolism, and inflammation in Hf-fed Foxo$^{\Delta}$ vs. Foxo$^{L/L}$ mice……82

Figure 4.8: Indicators of M2 polarization and a potential role of Tgfβ1 as an upstream regulator within muscle of HF-Foxo$^{\Delta}$ mice…….……..83

Figure 5.1: Muscle characteristics after 9 weeks of NC or HF diet…...……...……97

Figure 5.2: Capillary hemodynamics after 8 weeks of NC or HF diet. ……...98

Figure 5.3: Blood flow recovery and muscle characteristics 4 days post-ligation. ……...…..…99

Figure 5.4: Capillary hemodynamics recover better in HF-fed regenerating muscles.....…..100

Figure 5.5: Blood flow recovery in ligated limbs at 14 days post-ligation. …….……..101

Figure 5.6: Greater capillary growth in regenerating muscle from hf-fed mice at 14 days post-ligation…….103

Figure 5.7: Higher arteriole numbers in hf diet-fed regenerating muscles 14 days post-ligation…….104

Figure 5.8: Less adipocyte accumulation and fibrosis in hf-fed muscles 14 days post-ligation…….105

Figure 6.1: Summary of findings……112

App. A, Figure 1: Characterization of unsorted plastic-adherent cell populations from skeletal muscle biopsy……..138

App. A, Figure 2: Nutrient overload induces leptin synthesis in unsorted plastic-adherent cells……..140

App. A, Figure 3: Nutrient overload promotes nuclear translocation of ZNF423 in plastic-adherent cells…..……..141

App. A, Figure 4: Fluorescence activated cell sorting (FACS) of non-adipogenic and adipogenic pericytes……...142

App. B, Figure 1: Endothelial-specific Foxo1/3 depletion enhances post-ischemia perfusion recovery in HF-fed mice…….…….148

Chapter 1: Literature Review

1.1 Capillary Networks

1.1.1 Basic Morphology, Functions and Cellular Constituents

Capillaries are the smallest unit of the vascular tree with an average diameter of 5-10μm and widespread in all body tissues, accounting for an estimated 1000m^2 in total surface area (Pugsley and Tabrizchi, 2000). The primary function of capillaries is to facilitate the exchange of nutrients, oxygen and metabolic waste products (i.e. CO_2) between body tissues and the external environment. However, capillaries also contribute to the regulation of hemodynamics, immunity and thermoregulation. Structurally, capillaries consist of concentric layers of cellular and extracellular components (Bruns and Palade, 1968). The innermost (luminal) layer is comprised of a single layer of endothelial cells (ECs) and is surrounded by a thin (~30nm) outer basement membrane layer rich in collagen IV and laminin. Embedded within the capillary basement membrane are a heterogenous population of mural vascular cells known as pericytes. The pericyte basement membrane is contiguous with that of the endothelial cells. Morphologically, pericytes are characterized by numerous cytoplasmic processes that emanate from a prominent cell body, tracking along several endothelial cells and occasionally spanning adjacent capillaries. Pericyte protrusions (pegs) insert into endothelial cell invaginations (sockets) at occasional interruptions in the basement membrane, providing structural support as well as direct heterotypic cell-cell communications (Armulik et al., 2005). Peg-socket contacts at the pericyte-endothelium interface varies between tissues, but up to 1000 contacts have been described for a single endothelial cell (Armulik et al., 2011).

The primary function of pericytes is to stabilize capillary networks but also includes the regulation of capillary barrier function, blood flow and immunomodulation (Armulik et al., 2011; Bergers

and Song, 2005; Geevarghese and Herman, 2014; Navarro et al., 2016). Additionally, pericytes exhibit broad multipotency and functional plasticity which has led to their classification as multipotent progenitor cells. Pericyte multipotency and regulation of capillary homeostasis will be discussed further in Chapter 1.3.

1.1.2 **Ultrastructural Classifications & Organotypic Heterogeneity**

Capillaries are classified into 3 distinct groups based on their ultrastructural characteristics: continuous, fenestrated, and discontinuous (sinusoidal) (Fig. 1.1). Continuous capillaries are the most ubiquitous in the body and found in tissues such as the heart, lungs, kidney and brain (Augustin and Koh, 2017; Bruns and Palade, 1968). Continuous capillaries are characterized by an uninterrupted layer of endothelial cells held together by junctional proteins that connect adjacent ECs. This type of capillary permits the passage of water, small solutes and lipid-soluble materials to the underlying tissue but not circulating cells or large molecules, which require active transport mechanisms (Augustin and Koh, 2017). Fenestrated capillaries, which are present in tissues such as the kidney glomeruli, are characterized by the presence of anatomically stable cylindrical pores (fenestrae; ~10nm) that perforate individual ECs, allowing for the passage of water and small solutes (Pugsley and Tabrizchi, 2000). Sinusoidal capillaries are present in specialized tissues such as the liver and exhibit 150-250nm wide gaps between adjacent ECs, which allows for the unperturbed passage of large molecules to underlying tissues (Pugsley and Tabrizchi, 2000).

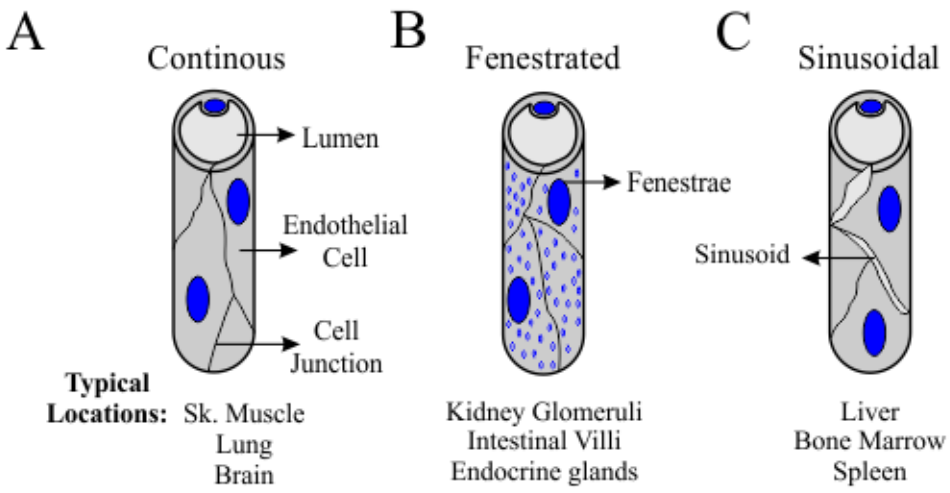

Figure 1.1: **Schematic representation of the different types of capillaries** A) Continuous capillaries are the most common type and are characterized by an uninterrupted layer of endothelial cells held together by proteins at the cell junction. B) Fenestrated Capillaries are characterized by cylindrical pores (fenestrae) that perforate individual endothelial cells and allow for the passage of water and small solutes. C) Sinusoidal Capillaries exhibit wide gaps (sinusoids) between endothelial cells that allow for the passage of large molecules.

Beyond these classifications, capillaries exhibit organotypic heterogeneity that supports the functional specialization of different tissues (Augustin and Koh, 2017). For instance, continuous capillaries in the brain are characterized by specialized tight intercellular junctions that form the blood-brain barrier, which protects the brain from the potential influx of toxic substances. In the glomerulus of the kidney, fenestrated capillaries facilitate the filtration of serum for waste removal and regulation of fluid balance. In the liver, sinusoidal capillaries are necessary to ensure unobstructed transfer of molecules to be detoxified by hepatocytes. The factors that contribute to this organotypic heterogeneity of the capillary network remains to be elucidated (Augustin and Koh, 2017). Nonetheless, structural and functional organization of capillary beds in body tissues is essential to support the optimal functioning of the underlying parenchyma.

1.2 Skeletal Muscle Capillary Network

1.2.1 Structural Organization of the Microvasculature

The skeletal muscle microvasculature consists of arterioles and capillaries. Arterioles are specialized microvessels characterized by a concentric ring of vascular smooth muscle cells (vSMC) that wrap around the luminal endothelial cell layer. Arterioles emanate from feed arteries at the point where the latter penetrates skeletal muscle and regulate the flow of arterial blood into skeletal muscle via the contraction and relaxation of smooth muscle cells to alter luminal diameter (Williams and Segal, 1992). A group of ~8-12 capillaries perfused by a terminal arteriole is termed the microvascular unit and represents the smallest functional unit for blood flow regulation within skeletal muscle (Korthuis, 2011). While arteriolar flow regulation is indispensable for skeletal muscle function, the current dissertation is primarily concerned with the skeletal muscle capillary network which will be the focus of discussion henceforth.

1.2.2 Capillary Architecture & Oxygen Transport

Skeletal muscle is comprised of continuous capillaries that are oriented longitudinally (parallel) along myocytes, with short orthogonal anastomoses that form secondary networks with adjacent capillaries (Fig. 1.2). In cross-sectional imaging of skeletal muscle tissue, capillary endothelial cell thickness ranges from ~3μm in cellular regions occupied by its nucleus but flatten out to 0.2μm in non-nuclear regions (Bruns and Palade, 1968). This morphological feature of endothelial cells together with the close association of capillaries with skeletal myocytes minimizes diffusion distances and establish the capillary as the critical site along the vascular tree for gas exchange.

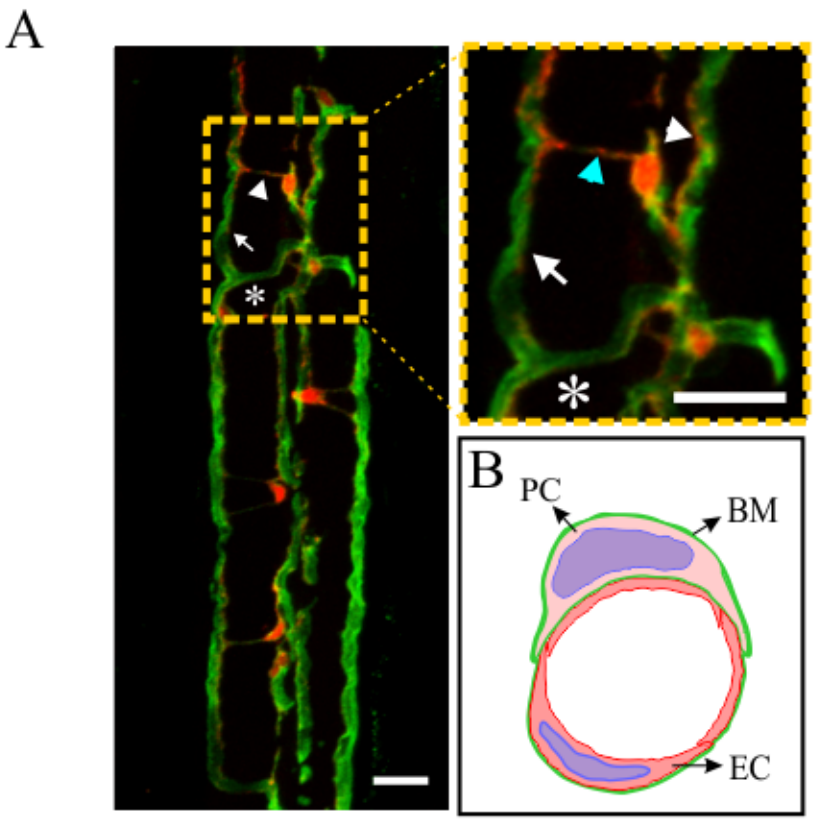

Figure 1.2: **Architecture of Skeletal Muscle Capillary Network.** A) In mice that express DsRed (red fluorescent protein) under the control of the pericyte-specific Ng2 promoter, *extensor digitorum longus* muscle was stained using *Griffonia simplificolia*-fluorescein isothiocyante to detect vascular endothelial cells. Capillaries (arrow) are predominantly oriented parallel with the long axis of muscle fibers (oriented from top to bottom in this image). Orthogonal anastamoses (asterisks) form networks with adjacent capillaries. Pericytes (red cells) are distributed along capillary networks and are characterized by cytoplasmic processes (arrowhead) that track along an individual capillary (white arrowhead) or span several capillaries (blue arrowhead). Scale bar = 20μm. B)Depiction cross-sectional plane of a capillary. PC - Pericyte; BM - Basement membrane; EC - Endothelial cell

The oxygen exchange properties of skeletal muscle capillaries were first modelled by August Krogh in a series of studies that earned him the Nobel Prize in Physiology or Medicine in 1920. In this model, Krogh postulated that capillaries supply a finite cylindrical volume of tissue and

proposed that the metabolic capacity of skeletal muscle is proportional to the extent of capillarization (Krogh, 1919a). Krogh's proposal has since been confirmed by studies that demonstrated a greater number of capillaries surrounding oxidative myofibers compared to neighbouring glycolytic fibres (Krogh, 1919a; Murakami et al., 2010). Thus, capillarization within skeletal muscle is positively correlated with the basal metabolic demands imposed by skeletal myocytes.

Beyond supporting skeletal muscle function in the basal state, the skeletal muscle capillary network must accommodate large increases in blood flow (i.e. up to 100-fold during exercise) to support increases in oxygen demand placed by skeletal myocytes. Two schools of thought currently exist regarding the mechanism by which increasing metabolic demands by skeletal myocytes are accommodated by the capillary network. According to the "capillary recruitment" hypothesis, pre-capillary sphincters at the proximal end of each capillary regulate blood flow such that only a fraction of the total capillaries within skeletal muscle support blood flow at rest and increased blood flow is facilitated by the opening of pre-capillary sphincters to recruit more capillaries (Angleys and Østergaard, 2020; Krogh, 1919b). A second hypothesis, referred to as "longitudinal recruitment" is based on the observation that capillaries exhibit unequal distribution of red blood cells (RBCs) in various segments due to the unique architecture of the skeletal muscle capillary network (i.e. branching pattern and orthogonal anastomoses) (Ellis et al., 1994). According to this hypothesis, blood is re-distributed from capillaries with high flow velocities (main longitudinal capillaries) to capillaries with relatively low-flow velocities (capillary bifurcations and orthogonal anastomoses), resulting in the homogenization of RBC distribution and transit times across the skeletal muscle capillary network (Angleys and Østergaard, 2020). This redistribution of blood flow velocities between capillary segments is thought to enhance

myocyte oxygen extraction by increasing the surface area and time available for blood-myocyte exchange (Angleys and Østergaard, 2020; Poole et al., 2011).

Capillary recruitment has been the subject of extensive research over the last ~100 years and while theoretically plausible, the premise that unperfused capillaries exist in resting skeletal muscle is not consistently supported by experimental models (Angleys and Østergaard, 2020; Poole et al., 2011, 2013). Furthermore, anatomical and functional evidence for the presence of "pre-capillary sphincters" capable of completely occluding flow is weak (Golub and Pittman, 2013). Currently, there is no consensus regarding whether capillary recruitment or longitudinal recruitment best describe the mechanism by which capillaries accommodate large increases in skeletal muscle blood flow. However, there is increasing empirical support for the longitudinal recruitment hypothesis (Poole et al., 2013).

1.2.3 **Postnatal Capillary Remodelling**

Capillary networks within skeletal muscle are not static but demonstrate a remarkable capacity to remodel in response to physiological shifts in the metabolic capacity of skeletal myocytes, as discussed below:

Angiogenesis

Angiogenesis is the growth of new capillaries from pre-existing ones, resulting in an increased surface area available for the exchange of substances between plasma and skeletal myocytes. Post-natal angiogenesis occurs naturally in the female reproductive system (Robinson et al., 2009; Zygmunt et al., 2003), wound healing (Bao et al., 2009), adipose tissue expansion (Rudnicki et al., 2018) and exercise-induced skeletal muscle angiogenesis (Egginton, 2009; Slopack et al., 2014).

Two types of angiogenesis have been described in skeletal muscle: abluminal sprouting and splitting angiogenesis (luminal splitting and intussusception). Abluminal sprouting involves a highly coordinated sequence of events including the activation and proliferation of endothelial cells, spatially restricted proteolytic degradation of the capillary basement membrane by matrix metalloproteinases (MMPs) and migration of endothelial cells into the interstitial space to form a sprout (Carmeliet and Jain, 2011; Geudens and Gerhardt, 2011), as illustrated in Fig. 1.3A. In the ensuing sprout, a single endothelial (tip) cell is selected to lead the sprout towards the angiogenic stimulus while the remaining endothelial (stalk) cells continue to proliferate and elongate the sprout (Carmeliet and Jain, 2011; Geudens and Gerhardt, 2011). Eventually, the sprout forms an anastomosis with a neighbouring capillary and is stabilized by the recruitment of pericytes, forming a patent lumen that allows for blood flow.

Relatively less is known about splitting angiogenesis which occurs when endothelial cells extend luminal protrusions/filopodia (luminal splitting) or form transluminal pillars that fuse opposing endothelial walls (intussusception), generating parallel flow channels that eventually separate to form two capillaries (Makanya et al., 2009; Zhou et al., 1998) (Fig. 1.3B). In contrast to sprouting, splitting angiogenesis involves minimal endothelial cell proliferation and does not require MMP induced degradation of the capillary basement membrane (Styp-Rekowska et al., 2011). Splitting angiogenesis is thought to occur in response to changes in the level of shear stress (frictional force generated by blood flow) experienced by endothelial cells. However, studies have demonstrated evidence of splitting angiogenesis in response to both elevated (Schlatter et al., 1997; Styp-Rekowska et al., 2011) and reduced (Gianni-Barrera et al., 2018) levels of shear. Thus, the precise regulatory mechanisms are not yet elucidated.

Sprouting and splitting angiogenesis should not be considered as dichotomous. Rather, there is evidence to show that both angiogenic processes occur simultaneously under both physiological and pathological contexts and are thus complementary processes during capillary expansion (Djonov et al., 2001; Gianni-Barrera et al., 2011; Hlushchuk et al., 2008; Makanya et al., 2007).

Capillary Rarefaction

Capillary rarefaction or regression refers to the loss of capillaries. During vascular development, regression of vascular networks has been shown to result from the migration of endothelial cells from vessels with low flow/shear stress to vessels from with high flow/shear stress (Franco et al., 2015; Udan et al., 2013), demonstrating the importance of blood flow in maintaining the patency

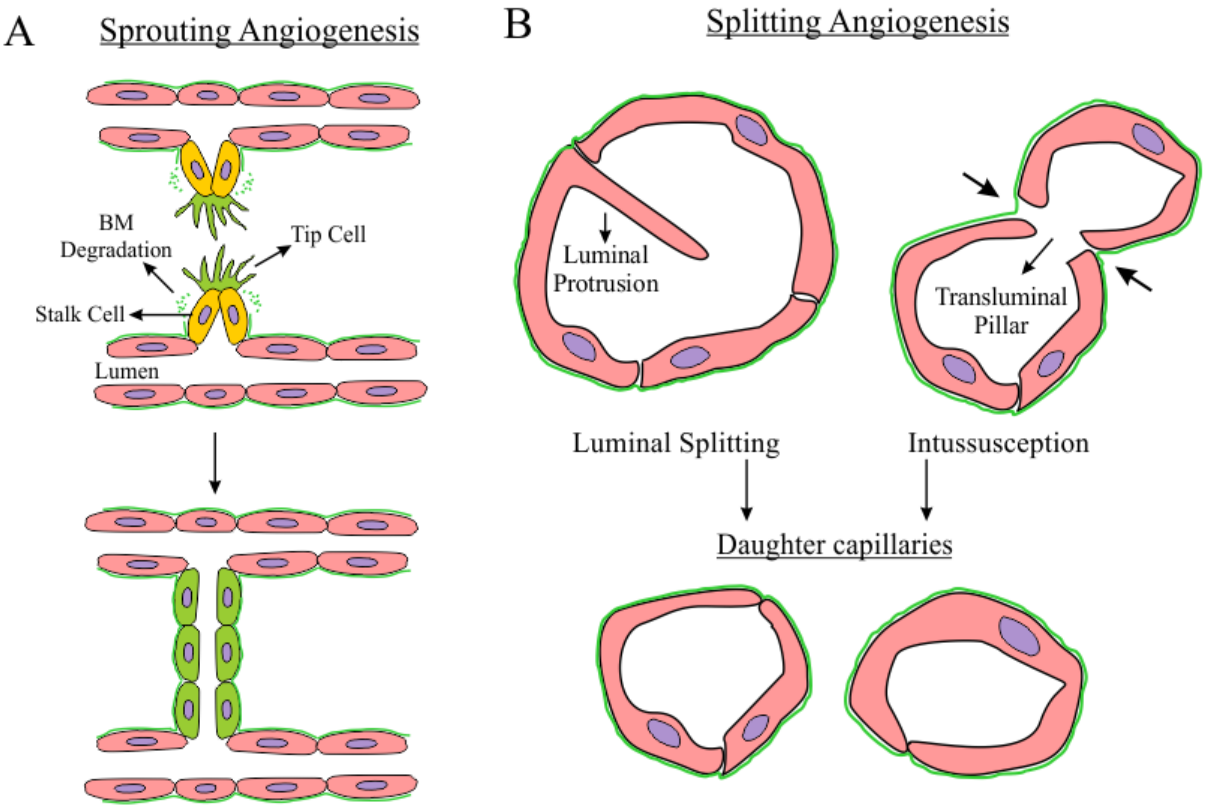

Figure 1.3: **Schematic Representation of the Angiogenic Process.** A) Sprouting angiogenesis involves basement membrane (BM) degradation, proliferation of stalk cells and migration of tip cells to form a new capillary. B) Splitting angiogenesis occurs due to the extension of luminal protrusions (luminal splitting) or formation of transluminal pillars that divide an existing capillary into 2 daughter vessels.

of blood vessels. In skeletal muscle, capillary rarefaction is often observed in experimental models of detraining and hindlimb unloading, whereby capillary supply exceeds the metabolic demands of skeletal myocytes (Olfert, 2016). Moreover, capillary rarefaction has also been reported in conditions such as hypertension (Chen et al., 1981), and type-2 diabetes mellitus (Jonk et al., 2007; Lillioja et al., 1987; Tilton et al., 1981). In these pathological contexts, capillary rarefaction results in a deficit in blood supply, that impairs skeletal muscle function. The molecular mechanisms regulating capillary rarefaction remain largely unknown, but is thought to involve pericyte degeneration, inflammation and the presence of anti-angiogenic factors (discussed below) (Jonk et al., 2007; Tilton et al., 1981).

1.2.4 **Regulation of Capillary Remodelling in Skeletal Muscle**

Capillary remodelling within skeletal muscle is initiated in response to metabolic and/or mechanical changes within the muscle microenvironment. For example, hypoxia, which indicates insufficient capillary supply, is a potent pro-angiogenic stimulus (Krock et al., 2011; Pugh and Ratcliffe, 2003). The resultant capillary expansion would in turn correct for the underlying oxygen deficit. Conversely, oxidative stress, which can result from oxygen surplus, is associated with endothelial cell apoptosis and regression of the capillary network (Korn and Augustin, 2015). In addition, the release of metabolites (i.e. adenosine) during repeated bouts of exercise can also promote angiogenesis (Høier et al., 2010).

Mechanical stress that results from the contraction and lengthening of skeletal myocytes also contribute to the angiogenic process by acting directly on endothelial cells or by promoting the secretion of factors from stromal cell populations that promote the proliferation of endothelial cells (Hellsten et al., 2008; Hoier et al., 2013; Milkiewicz et al., 2007). Furthermore, as previously mentioned, shear stress acts directly on endothelial cells to promote capillary expansion within

skeletal muscle (Gee et al., 2010; Rivilis et al., 2002; Zhou et al., 1998). Previous work in our laboratory has uncovered evidence for an intricate endothelial-myocyte crosstalk involved in the coordination of shear stress induced angiogenesis (Uchida et al., 2015). Specifically, our study indicated that shear stress induced nitric oxide release from endothelial cells, promotes vascular endothelial growth factor-A (a pro-angiogenic factor discussed below) production by skeletal myocytes, which in turn acts on the endothelium to promote angiogenesis (Uchida et al., 2015).

Ultimately, capillary remodelling is governed by the balance of pro- and anti-angiogenic molecular factors that promote the expansion or regression of the skeletal muscle capillary network, respectively (Haas and Nwadozi, 2015; Uchida et al., 2015). In the following sections, I will discuss a few of these angiogenic factors that are well characterized and pertinent to my dissertation.

Vascular Endothelial Growth Factor (VEGF)-A

VEGF-A is a dimeric glycoprotein (~34-42kDa) member of the Platelet Derived Growth Factor superfamily of proteins (Tischer et al., 1989). Of the 5 mammalian VEGF family members, VEGF-A is the most widely studied and well characterized as a potent pro-angiogenic molecule, capable of stimulating all aspects of sprouting angiogenesis (EC proliferation, migration and survival) (Olsson et al., 2006). Several isoforms of VEGF-A (VEGF-A_{121}, VEGF-A_{165}, VEGF-A_{189}, VEGF-A_{206}) are generated as a consequence of alternative splicing of the primary mRNA transcript (Neufeld et al., 1996). These isoforms differ in the presence of a heparan sulfate binding domain (encoded by exon 6) and thus their ability to bind to the extracellular matrix (ECM).

Myocytes constitute the largest source of VEGF-A, accounting for ~90% of all VEGF-A produced within skeletal muscle (Olfert et al., 2009). Heparan sulfate binding isoforms of VEGF-A (VEGF-

$A_{165,189}$) constitute ~70% of skeletal muscle derived VEGF-A and accumulate in the ECM (Gustafsson et al., 2005; Haas and Nwadozi, 2015). ECM-associated VEGF-A can be released by proteolytic enzymes (MMPs) to initiate/amplify angiogenic responses as well as provide chemotactic cues to guide tip cell migration during sprout elongation (Vempati et al., 2014).

Myocyte-derived VEGF-A is indispensable for angiogenesis induced by stimuli such as repeated bouts of endurance exercise (Olfert et al., 2010), elevated shear stress (Uchida et al., 2015) and muscle overload (Gorman et al., 2014). In skeletal muscle, VEGF-A production is enhanced by hypoxia (Hoier and Hellsten, 2014). To exert its pro-angiogenic effects, VEGF-A binds to its cognate receptor VEGF-receptor 2 (VEGFR2) on the surface of endothelial cells, which triggers receptor dimerization and several intracellular signalling cascades that initiate the angiogenic process by promoting the endothelial proliferation, migration and survival (Simons et al., 2016). VEGF-A also binds to VEGF-receptor 1 (VEGFR1) on the surface of endothelial cells. In fact, VEGFA binds to VEGFR1 with greater affinity than VEGFR2 (Terman et al., 1992). However, VEGFR1 signalling is not directly involved in the angiogenic process. Rather, these receptors are thought to act as decoys that control the amount of VEGFA available to bind to and activate VEGFR2 (Simons et al., 2016). A third receptor, neuropilin-1 (NRP1) binds only with heparan sulfate binding isoforms of VEGF-A (Soker et al., 1998). NRP1 does not exert any signalling functions of its own but potentiates VEGF-A binding to VEGFR2 by forming heterodimeric complexes with VEGFR2 (Soker et al., 2002). Furthermore, VEGF-A binding to NRP1 has been shown to be important in the regulation of endothelial cell migration (Herzog et al., 2011).

Leptin

Leptin is a 16kDa peptide hormone produced predominantly by adipocytes and most widely known for its role within the central nervous system to regulate food intake and energy expenditure (Zhou et al., 1997). Five membrane-bound leptin receptors (LEPR) are produced by alternative splicing of a single primary transcript and differ only in the sequence of their cytoplasmic tail (Lee et al., 1996; Tartaglia et al., 1995). The long LEPR isoform (LEPRb) is the primary signalling receptor involved in energy homeostasis. This function is mediated predominantly by activating the protein tyrosine kinase Janus Kinase 2 (JAK2), that subsequently activates the downstream effector protein Signal Transducer and Activator of Transcription 3 (STAT3) (Zhang and Chua, 2017). Besides the JAK2/STAT3 signalling, LEPRb also activates the IRS/PI3k/AKT pathway which coordinates leptin's role in glucose metabolism (Liu et al., 1998; Morton et al., 2005). The short LEPR isoforms lack most of the cytoplasmic sequences in LEPRb and there is very little evidence to suggest that they have any signalling functions. Rather, it has been suggested that short LEPR isoforms are involved in regulating the transport, clearance and bioavailability of leptin (Zhang and Chua, 2017). LEPRs are also expressed at relatively low levels in peripheral tissues and influence metabolic homeostasis (Muoio and Lynis Dohm, 2002). For instance, in skeletal myocytes, leptin enhances the influx of FA and partitions FA disposal towards oxidation and away from storage as triglycerides (Dyck, 2009).

Several pieces of evidence establish leptin as a pro-angiogenic molecule. For example, exogenous administration of leptin has been shown to promote angiogenesis in the context of wound healing (Liapaki et al., 2008) as well as *in-vitro* and *in-vivo* angiogenesis assays (Artwohl et al., 2002; Bouloumié et al., 1998). In culture leptin treatment increases endothelial cell proliferation, migration and survival to a similar extent as VEGF-A (Bouloumié et al., 1998; Garonna et al.,

2011), highlighting the potency of the endothelial leptin response. The mechanisms by which leptin exert its pro-angiogenic effect has yet to be established but may involve the direct release of angiogenic factors such as VEGF-A and MMPs (Cao et al., 2001; Park et al., 2001). Leptin has also been shown to act synergistically with other angiogenic factors including VEGF-A and fibroblast growth factor-2, leading to the suggestion that leptin potentiates the function of other angiogenic factors (Cao et al., 2001). Furthermore, inhibition of VEGFR2 was shown to suppress leptin-induced endothelial cell proliferation and migration (Garonna et al., 2011), demonstrating that the pro-angiogenic functions of leptin requires LEPRb activation of VEGFR2 (Garonna et al., 2011).

Thrombospondin-1

Thrombospondins are a family of secreted matricellular glycoproteins comprised of 5 family members that interact with cell surfaces, cytokines and components of the ECM to regulate tissue specific functions including angiogenesis, synaptogenesis, and connective tissue organization (Adams and Lawler, 2011). Thrombospondin-1 (THBS1) was the first family member discovered (1970s) as a protein associated with thrombin-stimulated platelets (Baenziger et al., 1971; Lawler et al., 1978). Subsequently, in the 1990s, THBS1 was identified as the first endogenous inhibitor of angiogenesis identified (Good et al., 1990). Since then, several research groups have focused on elucidating the mechanisms by which THBS-1 represses angiogenesis and potential clinical application in cancer therapy (Lawler and Lawler, 2012; Maxhimer et al., 2009; Ren et al., 2006; Sargiannidou et al., 2001).

THBS1 is produced by multiple cell types including skeletal myocytes, endothelial cells, and stromal cell populations (i.e. fibroblasts, macrophages). THBS1 function is facilitated by

interactions between specific TSR (Thrombospondin type-1 repeat) domains (TSR1-3) and cell surface receptors such as CD36, CD47 or β1-integrins (Lawler and Lawler, 2012) on endothelial cells. THBS1 exerts its anti-angiogenic function by restricting endothelial cell proliferation and migration as well as the induction of endothelial cell apoptosis (Lawler and Lawler, 2012). In the ECM, THBS1 restricts the bioavailability of VEGF-A by inhibiting the proteolytic degradation of ECM proteins and by direct binding and clearance of VEGF-A via receptor mediated uptake (Greenaway et al., 2007; Gupta et al., 1999; Rodriguez-Manzaneque et al., 2001). Furthermore, CD36 and β1-integrins have been shown to form heterotypic complexes with VEGFR2 that limit endothelial VEGF-A signal transduction in the presence of THBS1 (Zhang et al., 2009). These effects establish THBS1 as a potent anti-angiogenic factor. In line with this, THBS1 null mice exhibit increased capillary number within skeletal muscles and an enhanced exercise capacity (Malek and Olfert, 2009).

Forkhead Box O (Foxo) transcription factors

Foxo proteins belong to the transcription factor family of forkhead proteins that are characterized by a highly conserved DNA binding domain (forkhead box). FoxO proteins are involved in the regulation of numerous cellular processes including development, metabolism, proliferation, apoptosis and stress resistance (van den Berg and Burgering, 2011; Kaestner et al., 2000). In mammals, 4 Foxo family members have been Identified: Foxo1, Foxo3, Foxo4, Foxo6. While Foxo1, Foxo3 and Foxo4 are expressed ubiquitously in all body tissues, their expression varies dynamically between tissues and developmental stage (Oellerich and Potente, 2012). In contrast, Foxo6 expression is confined to the adult brain (Hoekman et al., 2006; Jacobs et al., 2003). FoxO proteins are is regulated by several post-translational modifications including phosphorylation, acetylation, ubiquitination and methylation that regulate its DNA binding, subcellular localization,

and protein stability (van den Berg and Burgering, 2011; Oellerich and Potente, 2012). Notably, the first identified regulator of Foxo activity was insulin signalling through the PI3K/Akt pathway which results in the phosphorylation of Foxo at 3 conserved Ser/Thr residues, nuclear exclusion via binding to the 14-3-3 protein, and consequently, inhibition of Foxo transcriptional activity (van den Berg and Burgering, 2011).

The developmental and physiological roles of FoxO proteins have been elucidated by various studies using loss-of-function transgenic mice. Mice with global deletion of Foxo1 die at E10.5 due to improper formation of the vascular network (Furuyama et al., 2004; Hosaka et al., 2004). This effect was recapitulated when Foxo1 deletion was restricted to endothelial cells, demonstrating the importance of endothelial Foxo1 in vascular development (Dharaneeswaran et al., 2014). In contrast, mice with global deletion of either Foxo3 or Foxo4 are viable and indistinguishable from their control littermates (Hosaka et al., 2004). Foxo1 and Foxo3 are the most abundant family members in adult endothelial cells and inhibit capillary growth by regulating the transcription of angiogenic factors cell cycle regulators, and survival genes (Paik et al., 2007; Potente et al., 2005; Roudier et al., 2013; Shikatani et al., 2012). In contrast, Foxo4 activity appears to be inconsequential for capillary growth (Potente et al., 2005). Transcriptome analysis of Foxo1 or Foxo3 silenced endothelial cells revealed that they regulate an overlapping but functionally non-redundant set of angiogenesis related genes by both FoxO proteins (Potente et al., 2005). In fact, Foxo1 was shown to be a more potent inhibitor of uncontrolled EC proliferation in mice compared to Foxo3, leading to the suggestion that Foxo1 is the primary regulator capillary homeostasis (Paik et al., 2007).

Several studies in our lab have established endothelial FoxO proteins as critical regulators of capillary homeostasis within skeletal muscle. Using mice deficient for endothelial Foxo1, 3, and

4, we demonstrated accelerated skeletal muscle angiogenesis following endurance exercise training and post-ischemic insult, demonstrating that endothelial FoxO proteins are potent repressors of angiogenesis within skeletal muscle (Roudier et al., 2013; Slopack et al., 2014). We found that this effect is likely mediated in part by direct transcriptional regulation of THBS1 by FoxO proteins (Roudier et al., 2013). Furthermore, we showed that overexpression of Foxo1 is associated with reduced levels of VEGF-A (Shikatani et al., 2012).

1.3 Pericyte Functions & Multipotency

1.3.1 Pericytes & Capillary Homeostasis

Pericyte recruitment is essential for the maturation of newly formed capillary networks. During development, pericytes are first attracted to newly formed capillaries via the endothelial-secreted chemoattractant platelet derived growth factor (PDGF)-BB, which binds to PDGF receptor β (PDGFRβ) on pericytes (Benjamin et al., 1998; Lindahl et al., 1997). Interference with PDGFBB-PDGFRβ signalling was shown to disrupt endothelial-pericyte interactions (Lindahl et al., 1997), indicating that perpetual signalling through PDGFRβ is critical to maintain pericyte localization to capillary endothelial cells. Several other pericyte proteins have been implicated in supporting the continued interaction between pericytes and endothelial cells such as Notch receptors and N-cadherin (Gerhardt et al., 2000; Kofler et al., 2015). Juxtacrine signals via these connections as well as secretion of paracrine factors such as angiopoietin-1 (Angpt1) and tissue inhibitor of metalloproteinases 3 (TIMP3) are mechanisms by which pericytes ensure the stability of mature networks and promotes endothelial cell viability and quiescence (Papapetropoulos et al., 2000; Saunders et al., 2006).

Pericytes also play an active role during the process of sprouting angiogenesis. During the initial phase of angiogenesis, elevated levels of angiopoietin-2 (Angpt2), a competitive inhibitor of

Angpt1, disrupts endothelial-pericyte interactions and promotes a pro-migratory pericyte phenotype (Brudno et al., 2013; Maisonpierre et al., 1997; Teichert et al., 2017). During this initial phase of angiogenesis, pericytes also assist in the remodelling the extracellular matrix to enable sprout formation and migration of endothelial cells towards a gradient of chemotactic factors such as VEGF-A (Carmeliet and Jain, 2011). In some instances, pericytes were observed in the leading edge of opposing capillary sprouts leading to the suggestion that pericytes provide guidance cues for the outgrowth of endothelial cells (Nehls et al., 1992; Ribatti et al., 2011; Stapor et al., 2014). Proliferation and migration of pericytes during capillary sprouting ensures pericyte coverage of nascent capillaries. Finally, pericytes re-establish endothelial cell-pericyte contacts and return to a quiescent state (van Dijk et al., 2015; Stapor et al., 2014). Interestingly, it was recently shown that the retention pericytes during the initial stages of angiogenesis favoured splitting over sprouting angiogenesis by limiting endothelial cell proliferation (Gianni-Barrera et al., 2018). Thus, the extent pericyte coverage during angiogenesis may be an important determinant for the type of angiogenesis that occurs.

In mature capillary networks, pericytes are susceptible to metabolic toxicity (i.e. oxidative stress, inflammation, glucotoxicity) that arises due to chronic conditions such as insulin resistance and type-2 diabetes (Hayden et al., 2010). The resultant pericyte degeneration (apoptosis) can be observed histologically as abnormal pericyte morphology during apoptosis (i.e. retracted cytoplasmic processes) or by the presence of empty spaces (“ghost pockets”) within the capillary basement membrane previously occupied by a pericyte. Pericyte degeneration induced by metabolic toxicity has predominantly been studied in the context of non-proliferative diabetic retinopathy, whereby pericyte loss is associated with basement membrane thickening, edema, capillary rarefaction and consequently, vision loss (Ejaz et al., 2008; Hayden et al., 2010; Kusuhara

et al., 2018). In skeletal muscle, ultrastructural assessments demonstrated the presence of pericyte degeneration in humans almost 40 years ago (Tilton et al., 1981). More recently, pericyte degeneration within skeletal muscle was evident in rodent models of type-2 diabetes and has been suggested to precede the onset of capillary rarefaction (Hayden et al., 2010). However, the fate of capillary networks following pericyte degeneration is context dependent, as concurrent elevations in pro-angiogenic molecules (VEGFA, Angpt2) have been associated with angiogenesis (Ramsauer and D'Amore, 2002).

1.3.2 **Pericyte Plasticity**

The presence of "transitional cells" that exhibit intermediate morphological phenotypes between pericytes and vSMCs within the same vessel was demonstrated in early electron microscopic studies (Díaz-Flores et al., 1991) and provided the first evidence that pericytes can adopt structural and functional properties of closely related cell types. Subsequent studies have since shown that pericytes develop a contractile phenotype by modulating levels of contractile proteins such as alpha-smooth muscle actin (αSMA) (Alarcon-Martinez et al., 2019; Ji et al., 2016; Siedlecki et al., 2018). Physiologically, pericyte contractility is thought to underlie the ability of pericytes to regulate blood flow, by modulating the diameter of the capillary lumen. This concept has predominantly been studied in the brain, whereby regional blood flow is thought to be coupled with neuronal activity (Hamilton et al., 2010; Kisler et al., 2017). However, this concept is contentious, as other studies have demonstrated that pericyte contractility is insufficient to substantially alter capillary diameter and regulate blood flow (Fernández-Klett et al., 2010; Hill et al., 2015). Pericytes have also been shown to increase their expression of fibroblast related genes (i.e. PDGFRα, vimentin) and contribute to fibrogenesis (Barron et al., 2016). Given the structural and functional similarities between pericytes, vSMCs and fibroblasts it is challenging to ascertain

whether these described transitions reflect reversible phenotype shift or the terminal conversion of pericytes into vSMCs and/or myofibroblasts.

Pericytes express canonical stem cell markers and demonstrate a capacity to undergo tri-lineage differentiation (osteoblasts, chondrocytes and adipocytes) when cultured (Crisan et al., 2008; Geevarghese and Herman, 2014), analogous to cells belonging to the heterogeneous multipotent stromal population previously referred to as "mesenchymal stem cells" but more commonly described now as "mesenchymal progenitors". In fact, cultured pericytes display broader multipotency compared to mesenchymal progenitors, including differentiation into vascular smooth muscle cells, myofibroblasts as well as parenchymal cells such as skeletal and cardiac myocytes and neuronal cells (Alarcon-Martinez et al., 2019; Barron et al., 2016; Birbrair et al., 2017; Ji et al., 2016; Siedlecki et al., 2018). The broad multipotency reported for pericytes has led some researchers to postulate that pericytes are the predominant source of tissue resident mesenchymal progenitors (Crisan et al., 2008; da Silva Meirelles et al., 2008).

Multipotency is not a universal characteristic of all pericytes. For instance, pericytes expressing T-Box transcription factor 18 (Tbx18) failed to display trans-differentiation capacity in vivo in multiple tissues assessed, including skeletal, cardiac and adipose tissues (Guimarães-Camboa et al., 2017). Notably, not all pericytes express Tbx18, thus it has been proposed that multipotent pericytes are marked by the absence of Tbx18 (Birbrair et al., 2017; Wörsdörfer and Ergün, 2018). In addition, there is evidence that pericyte subsets within and across tissues exhibit distinct transcriptomes and differentiation potentials that may correspond with pre-programmed commitment to specific lineages. This idea is supported by recent single cell profiling of brain and lung derived pericytes (He et al., 2018; Vanlandewijck et al., 2018) that revealed a non-overlapping expression profile of lineage specific regulators including runt-related transcription factor 2

(Runx2; osteogenesis), peroxisome proliferator activated receptor gamma (Pparγ; adipogenesis) and sry-box transcription factor 9 (Sox9; chondrogenesis).

1.3.3 **Regulation of Pericyte Stemness and Differentiation Potential**

Pericyte interactions with their microenvironment provide critical cues that maintain their stemness (potential to differentiate). Laminin, a heterotrimeric glycoprotein, is a major constituent of the capillary basement membrane to which pericytes adhere via integrins. In the brain, disruption of pericyte-laminin interactions reduced PDGFRβ levels, enhanced pericyte dissociation from blood vessels and increased the expression of smooth muscle contractile proteins (αSMA, SM22α) (Durbeej, 2010; Reynolds et al., 2017, 2017), suggesting that pericyte-laminin interactions are important for maintaining pericyte identity. Similarly, signalling via pericyte Notch receptors have been implicated in the regulation of pericyte identity by promoting the expression of PDGFRβ (Weber, 2008) and by facilitating pericyte-laminin interactions (Kofler et al., 2015).

Several cell intrinsic pathways have also been implicated in the regulation of pericyte differentiation including the Wnt and Notch signalling pathways as well as several transcription factors (i.e. Runx2, Pparg, Sox-9) that direct the fate-specification of pericytes during the process of differentiation (Kirton et al., 2007; Pierantozzi et al., 2016; Yang et al., 2019). A recent study revealed a role for epigenetic regulation of pericyte stemness and differentiation potential by demonstrating tissue-specific histone modification patterns within genes that regulate pericyte phenotype, metabolism and fate specificity (Yianni and Sharpe, 2018). Thus, available data support the concept that subsets of pericytes exhibit a degree of pre-programmed commitment to specific lineages. Furthermore, there is some evidence to suggest that pericyte differentiation and

fate-specification depends on the metabolic state of the cells (Nwadozi et al., 2020). However, there is a paucity of studies that have investigated a link between pericyte metabolism and differentiation capacity. Overall, mechanisms that regulate the multi-potency and tissue-specific pre-programming that contribute to pericyte diversity require further elucidation.

1.3.4 **Pericytes & Skeletal Muscle Regeneration**

The multipotent characteristics of pericytes has led to their growing use for cell therapies to promote tissue healing and regeneration. Skeletal muscle has a remarkable intrinsic capacity to regenerate myofibers in response to tissue injury. From a clinical perspective, optimizing muscle regeneration would benefit the loss of skeletal muscle mass and strength in diseases such as muscular dystrophy, cachexia and age associated sarcopenia. The contribution of tissue resident satellite cells to skeletal muscle regeneration has been extensively studied and is well characterized (Tedesco et al., 2010). A growing body of evidence suggests that pericytes contribute to the regeneration process within skeletal muscle. Using transgenic reporter mice to trace the fate of pericytes, Dellavalle et. al demonstrated that pericytes differentiate into myogenic cells and fuse with regenerating myofibers in response to acute injury and muscular dystrophy (Dellavalle et al., 2011). Other studies have identified pericyte subpopulations with distinct differentiation potentials within skeletal muscle. Namely, Type-1 and Type-2 pericytes which are classified based on their expression of cell surface markers PDGFRα (CD140a) and Nestin, respectively (Birbrair et al., 2013a, 2013b, 2014a). Lineage-tracing experiments have demonstrated that only Type-2 pericytes contribute to myogenesis while Type-1 pericytes undergo fibro-adipogenic differentiation during muscle regeneration (Birbrair et al., 2013a, 2013c, 2014a). Additionally, Type-2 pericytes from skeletal muscle have the capacity to differentiate into Schwann cells, thus may contribute to skeletal muscle reinnervation during regeneration (Birbrair et al., 2014a). Interestingly,

angiogenesis, which is important during the process of skeletal muscle regeneration was shown to involve Type-2 but not Type-1 pericytes (Birbrair et al., 2014b). Thus, the available data support the therapeutic potential for Type-2 pericytes in regenerative medicine.

1.4 Skeletal Muscle Capillaries: Determinants of Metabolic Homeostasis

Metabolic homeostasis refers to the systemic intake, expenditure and storage of energy substrates (mainly glucose and fatty acids) to maintain biological set-points (i.e. blood glucose levels) required for optimal tissue functions. Disruption of this balance leads to metabolic dysfunction (i.e. Hyperglycemia, insulin resistance, hypertriglyceridemia) and eventually, diseases including type-2 diabetes. Metabolic homeostasis relies on tightly regulated crosstalk between the brain and peripheral tissues that coordinate the intake and disposal of energy substrates. Skeletal muscle is an important peripheral regulator of metabolic homeostasis, constituting 40% of total body mass and is the primary tissue responsible for the body's energy expenditure.

Metabolic states are generally divided into the 1) postprandial phase, referring to the period immediately following a meal and the 2) postabsorptive or fasting state, which occurs after energy substrates have been absorbed and stored within metabolic tissues. In the fasting state, fatty acids (FA) are the predominant fuel source used by skeletal myocytes whereas in the postprandial state, glucose is primarily used. In fact, skeletal muscle accounts for an estimated 80% of postprandial glucose disposal in human subjects (DeFronzo et al., 1985). Increased post-prandial glucose disposal within skeletal muscle is facilitated by insulin which induces the translocation of glucose trasporter-4 (Glut-4) from the cytosol to the myocyte plasma membrane, where it acts as a gateway for glucose influx. FAs are transported into skeletal myocytes via membrane bound proteins such as FA binding proteins (FABP) (Hotamisligil and Bernlohr, 2015) or FA transport proteins (FATP)

(Kazantzis and Stahl, 2012). Within skeletal muscle, glucose and fatty acids are used for ATP production or storage as glycogen or as triglycerides within lipid droplets, respectively.

The clearance of glucose and FAs within skeletal muscle is critical for metabolic homeostasis. Ultimately, the ability for skeletal muscle to dispose of these energy substrates is not only dependent on the intrinsic metabolic capacity of myocytes but also on the ability of the surrounding microvasculature to deliver energy substrates to the skeletal muscle interstitium. Previously, the capillary network was considered as a passive barrier for the flux of substrates between plasma and the underlying parenchyma. However, capillaries are now recognized to play an active role by acting as a selective barrier for energy substrates and regulatory hormones (i.e. insulin and leptin) to reach skeletal myocytes and regulating blood flow within skeletal muscle. Furthermore, capillary remodeling events that alter the total capillary surface area available for trans-capillary transport of energy substrates and nutrients can influence skeletal muscle function and thus metabolic homeostasis. These aspects of capillary-regulated substrate disposal ultimately underlie the ability of skeletal muscle to maintain metabolic homeostasis.

1.4.1 **Exchange of Energy Substrates and Regulatory Hormones**

The transfer of molecules across the skeletal muscle endothelium can occur by passage between adjacent endothelial cells (paracellular route) or directly through the endothelial cell body (trans-endothelial transport, TET) (Grotte, 1956; Pappenheimer et al., 1951; Rippe et al., 2002). In skeletal muscle, the paracellular route has an average radius of approximately 4.5nm, providing a passageway for small hydrophilic molecules (Bruns and Palade, 1968). TET involved plasmalemmal vesicles that either shuttle molecules across the endothelial barrier (transcytosis) or fuse together to create large transcellular pores (Rippe et al., 2002). Transcytosis is either facilitated by molecule specific receptors on the endothelial cell surface or occurs non-specifically

whereby a quantum of plasma is engulfed into plasmalemmal vesicles (fluid-phase transport) (Rippe et al., 2002). Protein (clathrin or caveolin) coats are used to form the shape of the transcytotic vesicles. In general, receptor mediated TET occurs via clathrin-coated vesicles whereas fluid phase transport is mediated by caveolin coated vesicles (Rippe et al., 2002).

The following sections will discuss the mechanisms by which energy substrates and regulatory hormones cross the endothelial cell barrier. Owing to challenges in directly visualizing TET in-vivo, the studies discussed below have relied on inferences made from experiments performed in monolayer cultures. In other words, the ability of an endothelial cell to 1) ingest, 2) preserve the biological function of, and subsequently 3) release specific molecules are used evidence for TET.

Glucose

Glucose transport is thought to cross the endothelial cell predominantly by passive diffusion via the paracellular route (Michel and Curry, 1999) but can also occur by TET. Using microdialysis probes inserted into the femoral muscle of human subjects, Muller et al. observed that glucose concentration was consistently lower in the interstitium compared the corresponding concentration in arterial blood under both fasting (3.8mM vs. 4.6mM, respectively) and fed (6.2mM and 8.4mM, respectively) states (Müller et al., 1996). This indicates that the endothelial barrier is rate limiting for glucose uptake by skeletal myocytes in skeletal muscle. Studies using endothelial cells isolated from anatomical regions distinct from skeletal muscle have provided further evidence that glucose may cross the capillary wall by TET. In human carotid artery preparations, broad inhibition of glucose transporters (Gluts) with cytochalasin-B resulted in a 35% reduction in endothelial glucose uptake (Gaudreault et al., 2008), suggesting that glucose may also cross the endothelium by Glut-facilitated TET. The constitutively expressed Glut-1 is the predominant Glut isoform expressed on

the surface of endothelial cells and allows for constant influx of glucose at the apical surface and efflux at the basolateral membrane of endothelial cells (Yazdani et al., 2019).

Lipids

Dietary lipids primarily consist of long chain FAs (>12 carbons) and travel the blood stream as triglycerides within lipoproteins or bound to the carrier protein, albumin. Following dissociation of the albumin-FA complex or release from lipoproteins (catalyzed by endothelial lipoprotein lipase), FAs cross the luminal membrane, cytosol and abluminal wall of endothelial cells to reach skeletal muscle. The molecular mechanisms that govern endothelial FA transport remain largely unknown but is thought to be facilitated by endothelial FA transporters (Pi et al., 2018). In skeletal muscle FABP4 and FABP5 are predominantly expressed within capillary endothelium (Iso et al., 2013). In FABP4 and FABP5 knockout mice, fatty acid uptake into skeletal muscle was markedly reduced, leading the authors to conclude that capillary FABP4/5 are required for the lipid transport in skeletal muscle (Iso et al., 2013). However, relatively low levels of FABP4 have been detected in skeletal myocytes (Fischer et al., 2006) and could account, in part, for the impaired FA uptake in FABP4/5 knockout mice. CD36 is another FA transporter that has been demonstrated to facilitate FA TET in-vitro (Harmon and Abumrad, 1993). Recently, endothelial cell specific deletion of CD36 resulted in a significant reduction in the uptake of long chain fatty acids into skeletal muscle (Harmon and Abumrad, 1993). Thus, fatty acid TET is an important determinant for skeletal myocyte FA uptake. However, the capacity of the myocytes to utilize the fatty acids is more consequential for metabolic homeostasis than endothelial barrier function as the accumulation of fatty acids within skeletal myocyte contributes to the pathogenesis of insulin resistance.

Insulin

As previously mentioned, insulin is critical for skeletal myocyte glucose uptake. Several studies have demonstrated that the transfer of insulin from the plasma to skeletal muscle interstitium is rate limiting for skeletal muscle insulin action (Chiu et al., 2008; Freidenberg et al., 1991, 1994; Miles et al., 1995; Yang et al., 1989, 1992, 1994). The precise mechanisms that govern insulin transport across the microvascular walls is still largely unknown. Monomeric insulin has a diameter of approximately 2.69nm (Oliva et al., 2000) and could theoretically cross the endothelial cell barrier passively via the paracellular route. However, early observations demonstrated a consistent insulin concentration gradient of approximately 2:1 between plasma and the skeletal muscle interstitium (Yang et al., 1989), indicating that the endothelium also acts as a selective barrier for insulin transport.

In skeletal muscle, insulin transport was demonstrated to be a saturable process and thus likely involving the insulin receptor on the endothelial cell surface (Majumdar et al., 2012). Indeed, endothelial cell specific depletion of the insulin receptor delayed time (10 vs. 20 minutes) required to achieve comparable levels of insulin activation within skeletal muscle and induced systemic insulin resistance (Konishi et al., 2017). This finding suggests that endothelial insulin receptors are important for insulin TET, but also suggests the presence of other mechanisms with slower kinetics. Recently, mathematical modelling of insulin transport across the skeletal muscle capillary wall was shown to fit the kinetic model of fluid phase transport more so than a receptor mediated process (Williams et al., 2018). Thus, insulin TET in skeletal muscle may involve both receptor mediated transcytosis and fluid phase transport. Further, unlike most cells that bind and internalize insulin (i.e. myocytes, adipocytes), microvascular endothelial cells do not target insulin for

enzymatic or lysosomal degradation (Azizi et al., 2015), further demonstrating the capacity for capillary endothelial cells to facilitate insulin TET.

Leptin

Leptin TET has predominantly been studied in brain endothelial cells and demonstrated saturable kinetics indicating its transport is facilitated by LEPRs on the surface of endothelial cells (Hileman et al., 2002; Maresh et al., 2001). Specifically, the short LEPR isoform, LEPRa, which is abundant in brain microvessels (Bjørbaek et al., 1998), has been shown to mediate the unilateral transport of intact leptin from the apical to basolateral surface in cultured cells (Hileman et al., 2000), demonstrating the involvement of LEPRa leptin TET. In skeletal muscle endothelial cells, the relative expression of the different LEPRs has not been established. However, skeletal muscle leptin uptake from plasma is relatively low (Hill et al., 1998; McMurtry et al., 2004), indicating that circulating leptin does not contribute significantly to the metabolic effects of leptin within skeletal muscle. Moreover, there is now evidence to suggest that leptin is produced within skeletal muscle (Wang et al., 1998), thus paracrine/autocrine leptin signalling may be more important within skeletal myocytes. However, the cellular source and regulation of leptin production within skeletal muscle remain to be defined.

1.4.2 **Microvascular Dynamics in the Postprandial Period**

In addition to its metabolic effects on skeletal myocytes, insulin is a potent vasodilator and promotes its own delivery to skeletal muscle, as well as that of other energy substrates and regulatory hormones via increased blood flow (hyperemia). Insulin induced hyperemia is endothelial cell dependent. Within endothelial cells, insulin activates the PI3K-Akt pathway resulting in the activation of endothelial nitric oxide synthase (eNOS), and subsequent production

of nitric oxide (NO) (Kubota et al., 2011; Zeng et al., 2000). NO is a potent vasodilator that freely diffuses into vSMC's on arterioles and facilitates the relaxation of smooth muscle which results in reduced vascular resistance and consequently, enhanced flow. Insulin also has vasoconstrictor effects in endothelial cells involving the MAP kinase pathway and production of endothelin-1 (ET-1), which induces smooth muscle contraction (Kim et al., 2006). However, under physiological conditions, the net result favors NO production and thus vasodilatation (Potenza et al., 2009).

Insulin induced hyperemia facilitates skeletal muscle metabolic function during periods of nutrient surplus (i.e. in the postprandial period) (Clark et al., 2003; Keske et al., 2017). In male rats, hyperemia was shown to occur early (5 minutes) and preceded skeletal myocyte insulin action and glucose uptake by skeletal myocytes (Vincent et al., 2004). In fact, insulin induced hyperemia accounts for ~40% of skeletal muscle glucose uptake in the postprandial period (Vincent et al., 2003). Furthermore, impaired endothelial insulin signalling in mice significantly reduced glucose uptake into skeletal muscle (Kubota et al., 2011). Thus, insulin induced hyperemia is an important regulator of skeletal muscle metabolic function and impairments in this system can result in metabolic dysfunction.

Endothelial Dysfunction: Early Player in the Pathogenesis of Insulin Resistance and Type-2 Diabetes

Endothelial dysfunction is characterized by a reduced bioavailability of vasodilators such nitric oxide in response to vasoactive stimuli (i.e. insulin) while levels of vasoconstrictors (i.e. ET-1) remain unaffected. In both rodents and humans, a considerable body of evidence suggests that endothelial dysfunction contributes significantly to the onset of insulin resistance (Clerk et al., 2006; Francischetti et al., 2011; Han et al., 2011; de Jongh et al., 2004a, 2004b, 2008; Jonk et al., 2011a, 2011b).

A meta-analysis of thirteen prospective studies demonstrated that the risk of incident hyperglycemia and type 2 diabetes increased (15% and 25%, respectively) per standard deviation increase in endothelial dysfunction (Muris et al., 2012), demonstrating that endothelial dysfunction and metabolic impairments are causally linked. In a mouse model of diet-induced obesity, endothelial dysfunction was evident after only 1 week of a high-fat diet, prior to the onset of weight gain, hyperinsulinemia, hyperglycemia and skeletal myocyte insulin resistance (Kim et al., 2008; Zhao et al., 2015), demonstrating that endothelial dysfunction precedes the development of metabolic dysfunction. Furthermore, endothelial specific ablation of insulin signalling in mice (to induce endothelial dysfunction), resulted in impaired insulin stimulated glucose uptake into skeletal muscle (Kubota et al., 2011). Importantly, in isolated skeletal myocytes from these mice, glucose uptake was normal (Kubota et al., 2011) demonstrating that endothelial dysfunction impairs skeletal muscle metabolic activity independent of skeletal myocyte function. Together, these studies support the idea that endothelial dysfunction is a cause of insulin resistance, by affecting insulin mediated glucose uptake within skeletal muscle (Karaca et al., 2014).

1.4.3 **Skeletal Muscle Capillarity and Metabolic Homeostasis**

Changes in capillarity can influence skeletal muscle metabolic function by altering the total surface area available for the exchange of energy substrates and regulatory hormones. It is well established that repeated bouts of endurance exercise elicit both angiogenesis and enhanced skeletal myocyte insulin sensitivity. To distinguish the myocyte specific adaptations to exercise from the influence of angiogenesis in determining skeletal muscle metabolic function, Prior et al. employed a 2-week detraining period following a 6-month endurance exercise regimen to reverse myocyte specific adaptations (i.e. increased Glut-4 protein levels, mitochondrial enzyme activity) while maintaining increased skeletal muscle capillarity (Prior et al., 2015). They found a significant positive

correlation between capillary density and insulin sensitivity (r=0.70) and that exercise induced improvements in insulin sensitivity were retained even after the detraining period (Prior et al., 2015). In line with this observation, pharmacological induction of elevated shear stress, which resulted in and increase (20%) in skeletal muscle capillarization, enhanced insulin sensitivity independent of any metabolic adaptations in myocytes (Akerstrom et al., 2014). Furthermore, myocyte specific VEGF-A deficient mice, that exhibit a ~60% reduction in skeletal muscle capillary number, also developed skeletal muscle insulin resistance independent of insulin action on skeletal myocytes (Bonner et al., 2013). These studies demonstrate that skeletal muscle capillarity is an independent determinant of metabolic homeostasis.

A growing body of evidence suggests that there is a relationship between skeletal muscle capillarity and metabolic dysfunction. In large cross-sectional population studies, capillary density was lower in obese subjects and inversely related to insulin sensitivity and skeletal muscle glucose uptake (Lillioja and Bogardus, 1988; Solomon et al., 2011). These findings are corroborated by studies that demonstrated reduced capillary number in the skeletal muscles of obese mice or rats (Emanueli et al., 2007; Nascimento et al., 2013; Schiekofer et al., 2005; Solomon et al., 2011). In addition, 3-dimensional assessments of the skeletal muscle capillaries in mice have also demonstrated alterations in capillary architecture with metabolic dysfunction, including reduced capillary diameter, volume and tortuosity (Murakami et al., 2012; Nascimento et al., 2013). The net effect of these alterations is reduced surface area available for the transport of energy substrates and regulatory hormones for skeletal muscle. Thus, it is now generally accepted that obesity induced reduction in skeletal muscle capillarity contributes to the progression of metabolic dysfunction (Frisbee, 2007). However, this conclusion has been challenged by some other studies. For instance, in a 15-year longitudinal study involving subjects with impaired glucose tolerance

(IGT), it was found that subjects who developed diabetes also exhibited an increase in capillary density, compared to control subjects and IGT subjects that did not develop diabetes (Eriksson et al., 1994). Similarly, in mice fed a prolonged high-fat diet to induce obesity, capillary number within skeletal muscle was increased (Silvennoinen et al., 2013; Umek et al., 2019) and no significant alterations in capillary architecture was observed (Umek et al., 2019). These findings are consistent with hypotheses that have been proposed by some researchers, which postulate that enhanced skeletal muscle capillarity serves as an early adaptation to match the increased oxidative capacity (i.e. mitochondrial biogenesis, fatty acid metabolism) of obese muscles and to compensate for other mechanisms of insulin resistance (i.e. endothelial dysfunction) (Chadderdon et al., 2016; Silvennoinen et al., 2013). Thus, while the "obesity-induced capillary rarefaction" hypothesis is widely accepted, there is a growing body of evidence to the contrary. As such, the fate of capillary networks during obesity remains to be established.

1.5 Clinical Application: Vascular Remodelling in Peripheral Artery Disease

The progression of obesity to type-2 diabetes is paralleled by and increased risk for developing cardiovascular complications such as hypertension and atherosclerosis. Peripheral artery disease (PAD) is a debilitating vascular condition that is characterized by reduced blood flow (ischemia) to the lower limb due to an underlying occlusion of a main artery by atherosclerotic plaques. PAD results in the development of structural and functional ischemic myopathies (i.e. myofiber atrophy/death, fibrous/fatty tissue accumulation) that reduce the overall well-being of affected individuals. In its most severe form, PAD can result in severe tissue necrosis requiring limb amputation (Annex, 2013; Katwal and Dokun, 2011), a condition referred to as critical limb ischemia (CLI). These outcomes are further complicated in patients that present with concurrent diabetes, a condition that worsens the prognosis of PAD. According to the Framingham Heart

Study, PAD was more prevalent (up to 8.6-fold) amongst individuals with type-2 diabetes and in patients suffering from both PAD and diabetes concurrently, a greater risk for lower limb amputation and a 3-4 fold higher mortality rate was observed (Jude et al., 2010). Insulin resistance has also been identified as an independent risk factor for the development of PAD, possibly due to underlying microangiopathy including endothelial dysfunction, increased vascular permeability, and generation of a pro-inflammatory environment which promotes of the progression of atherosclerosis (Bonora et al., 2002; Britton et al., 2012; Groen et al., 2014; Jude et al., 2010).

Despite best clinical efforts to restore limb blood flow, PAD continues to pose a significant health challenge and patients experience excessive rates of morbidity and mortality (Bonaca and Creager, 2015; Conte et al., 2019; Fowkes et al., 2017). The limited success to date in establishing effective approaches to treat CLI indicates a limited understanding of mechanisms underlying its pathogenesis and/or a lack of appropriate preclinical models (Cooke and Losordo, 2015; Haghighat et al., 2019; Ziegler et al., 2010). A recognized determinant of PAD prognosis is the degree to which vascular remodelling responses can compensate for the arterial occlusion and resulting ischemia (Annex, 2013; Silvestre et al., 2013). Several innate vascular remodelling responses act to mitigate damage in ischemic tissues, as described below.

Arteriogenesis of Collateral Arteries

The collateral circulation is a network of immature auxiliary vessels that form artery-to-artery connections between two distinct arteries or proximal and distal regions of the same artery. Narrowing of a main artery such as the femoral or iliac arteries (as seen in PAD), progressively forces blood through collateral vessels proximal to the site of occlusion, bypassing the blockage and restoring blood flow to tissues (mostly skeletal muscle) in the distal regions (Faber et al., 2014). Over time, these collateral arteries undergo arteriogenesis; a remodelling process that

involves the outward remodelling of existing arteries, which enables collateral arteries to carry more blood from the proximal to distal regions of the occlusion site.

In rabbits, perfusion through the collateral circulation was observed to occur as early as 30 minutes following the occlusion of the femoral artery and by 3 months post-occlusion, collateral artery diameter had doubled (Longland, 1953). This study demonstrated the capacity of the collateral circulation to compensate for an occlusion in a main artery. However, the remodelling capacity of these vessels is insufficient to fully restore blood flow to pre-occlusion levels and the patency of collateral arteries following arteriogenesis is short-lived (Hoefer et al., 2001; Longland, 1953).

Arteriolarization

Arteriolarization is a remodelling process that involves the transformation of capillaries into arterioles and involves the recruitment of perivascular precursor cells to the capillary wall and differentiation of these cells into contractile smooth muscle cells (Peirce and Skalak, 2003). Arteriolarization has previously described to occur in ischemic skeletal muscles (Bruce and Peirce, 2012; Mac Gabhann and Peirce, 2010) and could compensate for PAD-associated ischemia by diverting more blood to skeletal muscle capillaries.

Angiogenesis

As previously mentioned, capillaries are the site of exchange of key nutrients, hormones and metabolites that ensure the survival and optimal functioning of skeletal myocytes. In PAD, ischemia-induced myopathies (i.e. atrophy, myocyte death, fibrosis) promote reduced skeletal muscle function and while arteriogenesis and arteriolarization partially restores blood flow to the skeletal muscle in PAD, angiogenesis is necessary to maintain adequate distribution of blood flow during periods of ischemia and to support the energy-intensive process of regeneration.

Paradoxically, these microvascular remodelling responses (angiogenesis, arteriolarization) are compromised in ischemic skeletal muscle despite the generation of a hypoxic environment and release of pro-angiogenic factors that should, in theory, promote growth (Annex, 2013; Cherwek et al., 2000; Couffinhal et al., 1998; Lederman et al., 2002; Milkiewicz et al., 2006; Powell et al., 2008). This may be explained by a simultaneous induction of stimuli (i.e. oxidative stress, chronic inflammation) and up-regulation of factors (i.e. Foxo1) that counteract the pro-angiogenic signals (Guillot et al., 2014; Milkiewicz et al., 2011). However, the regulation of microvascular remodelling within ischemic skeletal muscle is not fully understood. Furthermore, the influence of obesity-related metabolic disturbances (i.e. insulin resistance, hyperlipidemia) on the microvascular remodelling capacity within ischemic tissues remains unclear.

1.6 **Scope of Dissertation**

Seminal studies over the last ~30 years have established the skeletal muscle capillary network as a critical determinant of metabolic homeostasis. The primary purpose of this dissertation was to define molecular mechanisms that govern skeletal muscle capillary remodelling in the context of obesity (Fig. 1.4). My first aim was to establish the fate of skeletal muscle capillary networks in obesity. To achieve this aim, I assessed two widely used mouse models of obesity that often report conflicting capillary remodeling outcomes. Specifically, leptin receptor mutant (*Lepr*^{db}) mice, that consistently exhibit capillary rarefaction within skeletal muscle were compared to a physiological model of prolonged administration of a fat-enriched diet, previously shown to promote angiogenesis within skeletal muscle (Silvennoinen et al., 2013). Considering leptin's role as a pro-angiogenic molecule, I asked whether leptin signalling deficiency could induce capillary rarefaction independent of obesity and investigated a potential role for leptin as a physiological regulator of skeletal muscle capillary homeostasis. FoxO proteins are potent anti-angiogenic

factors and have previously been implicated in obesity-related disorders such as insulin resistance (Karki et al., 2015) and atherosclerosis (Tsuchiya et al., 2012). Thus, I hypothesized that depletion of endothelial FoxO proteins would promote capillary growth within skeletal muscle and prevent the development of metabolic dysfunction in high-fat fed mice. Finally, to investigate the contribution of capillary remodeling in determining the prognosis of obesity-related diseases, I assessed the impact of high-fat diet induced alterations to capillary structure and hemodynamics on blood flow recovery and tissue regeneration in a preclinical model of peripheral artery disease (reduced blood flow to the lower limb). Overall, these investigations provide mechanistic insight into the coordination of skeletal muscle capillary remodeling in obesity and identifies potential molecular targets that may be used in the development of vascular-centric therapeutic strategies against clinical sequalae that arise secondary to obesity.

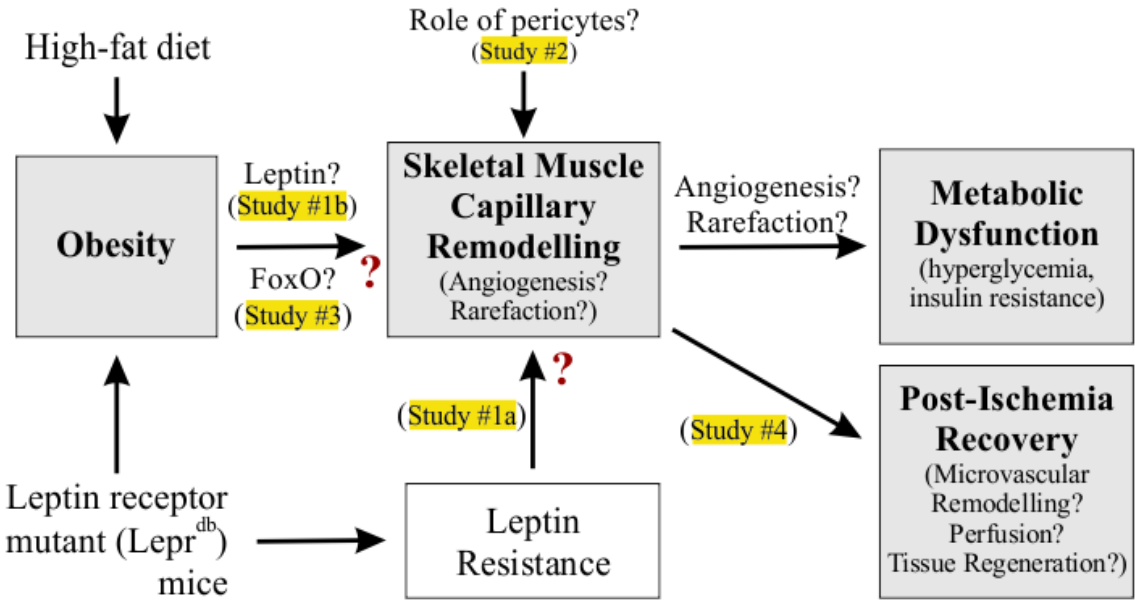

Figure 1.4: Scope of The Dissertation. Two mouse models: high-fat feeding and leptin receptor mutant ($Lepr^{db}$) mice will be used to assess the influence of obesity on capillary remodelling within skeletal muscle In $Lepr^{db}$ mice, the separate influence of leptin resistance will be assessed. The impact of obesity-induced skeletal muscle remodelling on metabolic dysfunction and post-ischemia recovery will also be examined.

Chapter 2:

Leptin is a Physiological Regulator of Skeletal Muscle Capillary Homeostasis and Angiogenesis: Implications During Post-Natal Myocyte Hypertrophy and Obesity.

2.1 Contributions:

I was involved in the development of the conceptual and experimental framework used in the current study. My specific contributions to experiments included the generation and propagation of transgenic mouse models, administration of diets and metabolic testing, as well as biochemical and histological assessments. Additional contributions were made by fellow lab members: Aly Fawzy assisted with assessments in C2C12 cells (Fig. 2.3A) and MLepRb mice (Fig. 2.4B,E,F,G). Hsin-yi Liu assisted with mRNA assessments in *Lepr*^{db} mice (Fig. 2.2E-G). Thomas Gustafsson provided the primary human myoblasts used for experiments (Fig. 2.3B,C,E,F).

2.2 Published Data:

1. **Nwadozi, E.** [1], Roudier, E. [1], Rullman, E. [2,3], Tharmalingam, S. [1], Liu, H.-Y. [1], Gustafsson, T. [2,3], and Haas, T.L[1]. (2016). Endothelial FoxO proteins impair insulin sensitivity and restrain muscle angiogenesis in response to a high-fat diet. FASEB J. 3039–3052.

   Figures: 2.6B, 2.7E, 2.8B, 2.8C, 2.8F

2. **Nwadozi, E.**[1], Ng, A. [1], Strömberg, A. [2,3], Liu, H.-Y. [1], Olsson, K.[2,3], Gustafsson, T.[2,3], and Haas, T.L[1]. (2019). Leptin is a physiological regulator of skeletal muscle angiogenesis and is locally produced by PDGFRα and PDGFRβ expressing perivascular cells. Angiogenesis 22, 103–115.

   Figures: 2.2A-G, 2.3A-G

[1]School of Kinesiology and Health Science, Faculty of Health, York University, Toronto, Canada; [2]Department of Laboratory Medicine, Clinical Physiology, Karolinska Institutet, Stockholm, Sweden; [3]Department of Clinical Physiology, Karolinska University Hospital, Stockholm, Sweden

2.3 **Chapter Summary**

Background/Rationale

Skeletal muscle capillary rarefaction is widely accepted as a consequence of obesity and is thought to contribute to further metabolic dysfunction (i.e. insulin resistance) during the development of diseases such as type-2 diabetes. These assertions are based largely on studies that have used rodent models of leptin- or leptin receptor-deficiency, whereby severe obesity is induced due to hyperphagia caused by abnormal leptin signalling in the hypothalamus. In contrast, metabolic impairments induced by prolonged high-fat feeding does not alter, or even increases, skeletal muscle capillarization (Silvennoinen et al., 2013; Umek et al., 2019). A factor that is often overlooked in studies that used models of deficient leptin signalling, is the increasing body of evidence that has established leptin as a potent pro-angiogenic molecule. Thus, it remains unclear whether skeletal muscle capillary rarefaction occurs secondary to metabolic dysfunction or as a consequence of the underlying leptin signalling deficiency. However, a pro-angiogenic role for leptin has not directly been assessed in skeletal muscle. The divergent capillary remodeling outcomes between leptin resistant and diet-induced (physiological) models of obesity suggest that deficiency in leptin signalling, rather than metabolic dysfunction, contributes directly to the underlying reduction in skeletal muscle capillarity. Thus, I hypothesized that leptin is a physiological regulator of skeletal muscle capillary homeostasis.

Objectives

1) Assess the separate influences of leptin resistance and metabolic dysfunction on skeletal muscle capillarity.

2) Investigate a potential role for leptin as a physiological regulator of the skeletal muscle capillary network.

Experimental Approach

Leptin receptor mutant (*Lepr*^{db}) mice are widely used as a mouse model of obesity and type-2 diabetes. In order to separate the influence of leptin signalling deficiency from metabolic dysfunction, I assessed mice before (by 4 weeks of age) and after (at 13 weeks) development of a sustained period of metabolic dysfunction. Leptin resistance and metabolic dysfunction were further assessed in transgenic myocyte-specific leptin receptor deficient (MLepRb-) mice and mice fed a high-fat diet for 16 weeks, respectively. A potential role for leptin in the regulation of capillary homeostasis was investigated by assessing capillarity and expression of angiogenic factors within skeletal muscle.

For detailed methods, refer to Chapter #7, including methods pertaining to the generation of transgenic mouse models (#7.2.1), Metabolic testing (#7.2.3), assessments of skeletal muscle capillarity (#7.2.3.1), and *in-vivo* and *ex-vivo* stimulation of skeletal muscles (#7.2.4)

2.4 Results

Impaired Angiogenesis and Suppressed VEGF-A Production During Post-Natal Skeletal Muscle Growth of Leptin Resistant (*Lepr^{db}*) Mice

The development of metabolic dysfunction in leptin resistant (*Lepr^{db}*) mice is well characterized, with mice demonstrating a progressive decline in metabolic function beginning at 3-4 weeks of age (www.jax.com). To discriminate the influence of leptin resistance from sustained metabolic dysfunction, two separate age cohorts were assessed: 4 weeks, to coincide with the onset of metabolic dysfunction and 13 weeks, representing a stage of chronic metabolic impairment (Yamauchi et al., 2007). The genotypes of mutant mice in the 4-week old cohort (bred in-house) were confirmed by PCR analysis (Fig. 2.1A). 4-week old mice exhibited higher (13%) body weights (Fig. 2.1B) but no apparent fasting hyperglycaemia (Fig. 2.1C) relative to control age-matched littermates, consistent with being in the early stages of metabolic dysfunction.

Histological assessments of the plantaris muscle (Fig. 2.2A) were performed to evaluate the separate influences of leptin resistance and metabolic dysfunction on skeletal muscle capillarity. At both 4- and 13-weeks, *Lepr^{db}* mice had a lower (18% and 27%, respectively) capillary-to-fibre ratio (C:F) in the plantaris muscle compared to wild-type (WT) (Fig. 2.2B). Control mice exhibited a 30% higher C:F at 13 weeks compared to 4 weeks of age (1.87 ± 0.04 vs. 1.43 ± 0.04, respectively; $P < 0.05$). However, there was no significant increase in *Lepr^{db}* mice over the same time (1.17 ± 0.1 vs. 1.38 ± 0.05; P=0.21) (Fig. 2.2B). Capillary density (CD) also was significantly reduced in *Lepr^{db}* mice at 13 weeks compared to 4 weeks (Fig. 2.2C). Myocyte hypertrophy associated with maturation (i.e. 4 vs. 13 weeks) was blunted in *Lepr^{db}* mice, resulting in smaller myocyte cross-sectional area at 13 weeks relative to control mice (Fig. 2.2D), consistent with a previous report (Tadokoro et al., 2015).

To determine whether the observed differences in muscle capillarization were associated with dysregulated expression of major angiogenic regulators, skeletal muscle levels of THBS1 and VEGF-A were measured. Within both age-cohorts, mRNA levels of *Thbs1* were not altered in *Lepr*^{db} mice compared to WT mice but a genotype-independent decline in *Thbs1* mRNA was observed at 13 weeks (Fig. 2.2E). At 13 weeks, VEGF-A transcripts and protein levels were significantly higher in control but not *Lepr*^{db} mice compared to their respective 4-week cohort (Fig. 2.2F,G). However, mRNA and protein levels of VEGF-A were significantly reduced in *Lepr*^{db} mice at 13-weeks (Fig. 2.2F,G). These data suggest that leptin resistance impairs age-related increased in VEGF-A expression in skeletal muscle, leading to impaired post-natal angiogenesis.

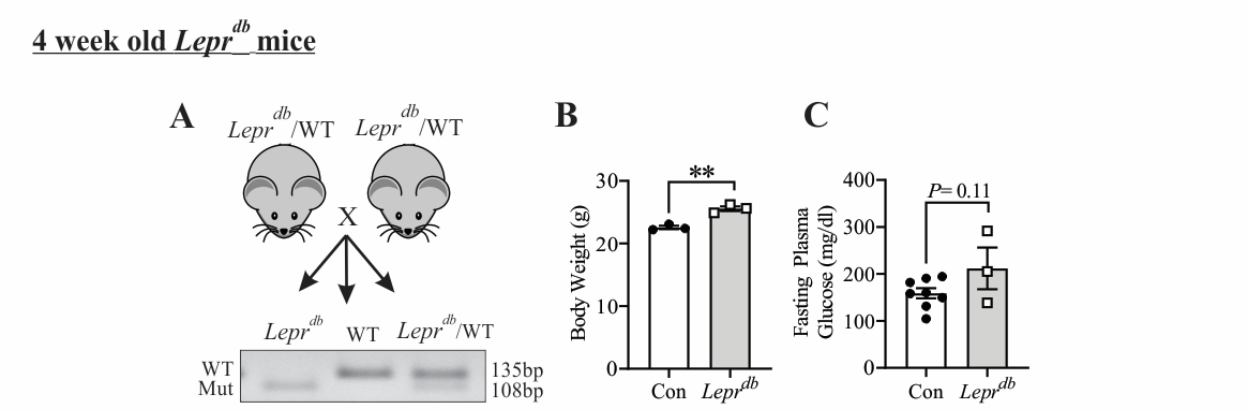

Figure 2.1: Characterization of 4-week old *Lepr*^{db} cohort.
A) PCR genotyping to detect wildtype (WT) and mutant (Mut) alleles within the leptin receptor gene. B) Body weights C) and plasma glucose levels assessed after 4 hours of fasting. $^{**}P < 0.01$; unpaired student's t-test.

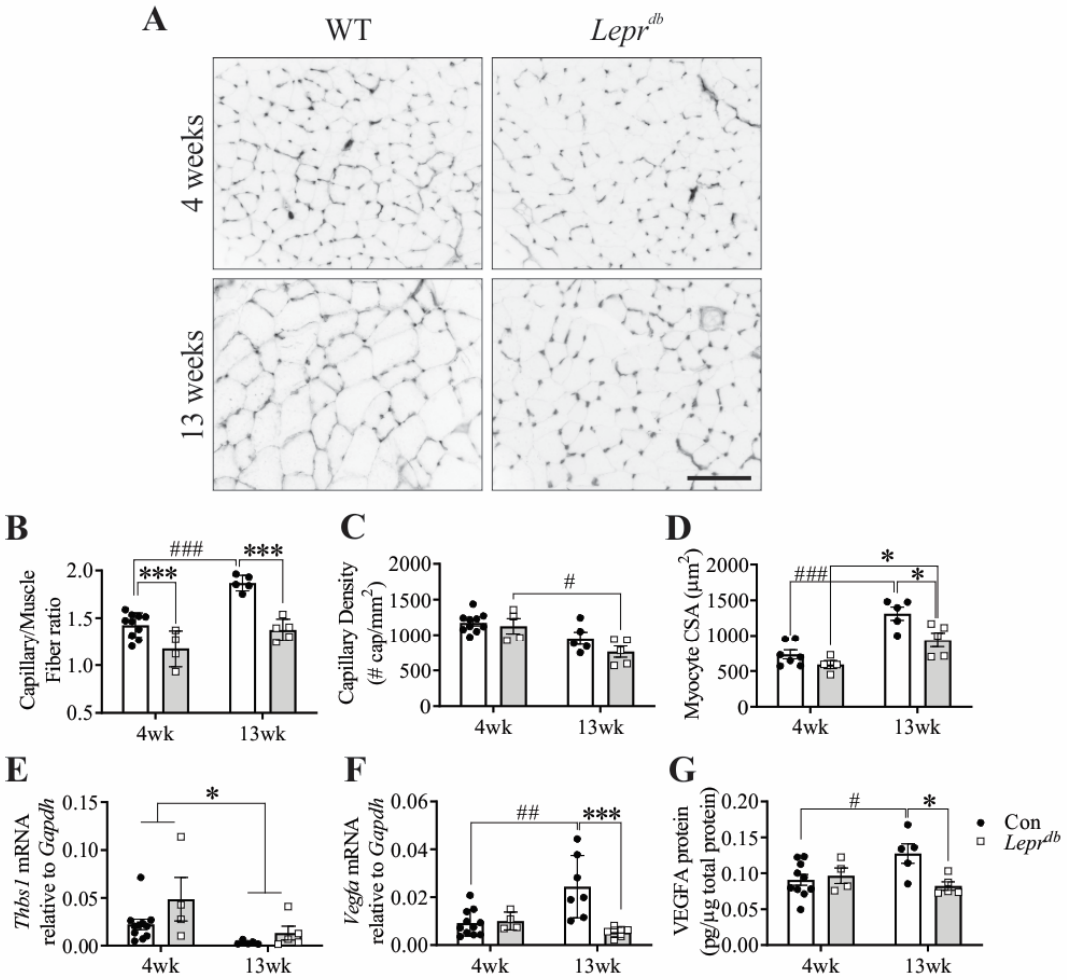

Figure 2.2: Skeletal muscle characteristics of *Lepr*^{db} mice at 4 and 13 weeks of age.
A) Representative images of the plantaris muscle stained with G. *simplicifolia* lectin-FITC to visualize capillaries. Grayscale images were inverted to enhance visualization of capillaries. Scale bar = 100 μm. Quantifications of B) capillary/muscle fiber ratio, C) capillary density and D) myocyte cross-sectional area (CSA) were performed from at least 3 independent fields of view per mouse. E) Thbs1 and F) *Vegfa* mRNA in the gastrocnemius muscle was assessed by real-time quantitative PCR relative to *Gapdh* and expressed as $2^{-\Delta Ct}$. G) VEGF-A protein levels were assessed by ELISA using gastrocnemius muscle homogenates. $^{*}P < 0.05$, and $^{***}P < 0.001$ vs. age-matched control (Con) mice. $\#P < 0.05$, $\#\#P < 0.01$, and $\#\#\#P < 0.001$ vs. corresponding 4-week old mice; two-way ANOVA with Tukey post-hoc analysis.

Leptin Increases VEGFA mRNA Levels in Murine and Human Skeletal Muscle Cells

The observed reduction of VEGF-A levels in the skeletal muscle of leptin resistant mice suggested a regulatory influence of leptin on VEGF-A levels within skeletal muscle. To directly assess the influence of leptin on muscle VEGF-A levels, in vitro experiments were performed using skeletal muscle cells, as these cells constitute ~90% of VEGF-A production within skeletal muscle (Olfert

et al., 2009). Leptin treatment (100nM) significantly increased VEGF-A transcripts not only in murine C2C12 myoblasts (Fig. 2.3A) but also, in primary human myoblasts (Fig. 2.3B) and differentiated human myotubes (Fig. 2.3C), demonstrating that leptin is a positive regulator of VEGF-A levels in skeletal myocytes. In C2C12 myoblasts, this effect of leptin was blunted by inhibition of either PI3K (Ly294002) or Jak2 (AG-490) (Fig. 2.3A).

Because leptin signalling converges with the insulin signalling pathway, and insulin has also been implicated in the regulation of VEGF-A gene expression in several cell types (Lu et al., 1999; Olfert et al., 2009; Takahashi et al., 2002), we investigated whether disruptions to insulin signalling in *Lepr*^{db} mice might also regulate VEGF-A levels within skeletal muscle. *Ex-vivo* insulin stimulation of the *extensor hallucis proprius* (EHP) muscle in the 13-week *Lepr*^{db} cohort revealed that insulin-induced phosphorylation of Akt was impaired significantly relative to control mice (Fig. 2.3G), indicating reduced myocyte insulin sensitivity in *Lepr*^{db} relative to control mice. In C2C12 myoblasts (Fig. 2.3D), as well as human myoblasts (Fig. 2.3E) and differentiated myotubes (Fig. 2.3F), *Vegfa* transcripts were significantly increased in C2C12 myoblasts (Fig. 2.3D), as well as in human myoblasts (Fig. 2.3E) and differentiated myotubes (Fig. 2.3F) after 4-hours of insulin treatment. Together, these data indicate that skeletal myocyte insulin sensitivity may also contribute to reduced skeletal muscle VEGF-A levels in *Lepr*^{db} mice.

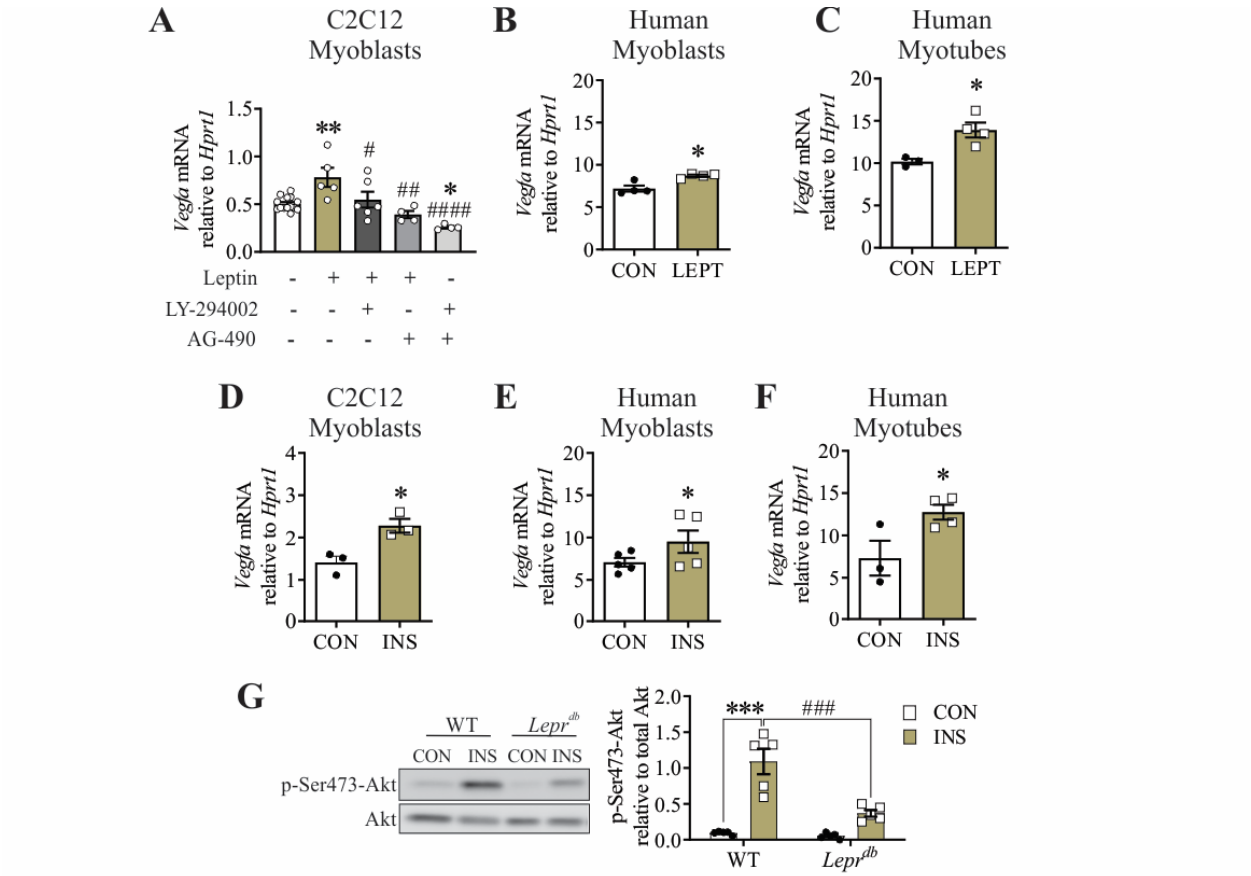

Figure 2.3: Leptin increases *Vegfa* mRNA expression in murine and human skeletal muscle cells.

A-F) In leptin (A-C) and insulin (INS) (D-F) treated C2C12 myoblasts (A,D) primary human myoblasts (B,E) and differentiated human myotubes (C, F). *Vegfa* mRNA levels were assessed by quantitative PCR relative to *Hprt1* and expressed as $2^{-\Delta Ct}$. Inhibitors for PI3K (LY-294002) and Jak2 (AG-490) were used in leptin treated C2C12 myoblasts. $^{*}P < 0.05$ vs. unstimulated Control (Con) group; unpaired student's t-test. G) Extensor hallucis proprius muscles were isolated from WT and Leprdb mice and analyzed for insulin sensitivity. pSer473-Akt was assessed following ex-vivo incubation with insulin and normalized to total Akt levels. $^{***}P < 0.001$ vs. respective WT mice. $^{###}P < 0.001$ vs. insulin stimulated muscle, two-way ANOVA with Tukey post hoc analysis.

Myocyte-Specific Leptin Resistance is Associated with Reduced Skeletal Muscle Capillarity

To determine whether skeletal myocyte specific leptin signalling is physiologically relevant for skeletal muscle capillarity, mice with myocyte specific depletion of the long leptin receptor isoform (MCKCre+;LepRb$^{fl/fl}$) were generated and compared to age-matched control (MCKCre-;LepRb$^{fl/fl}$) littermates, henceforth referred to as MLepRb- and MLepRb+ mice, respectively. Myocyte specificity of recombinase activity was confirmed by PCR genotyping, demonstrating

the expected excision of exon 17 in skeletal muscle but not in the mouse ear or adipose tissue (Fig. 2.4A). Consistent with being leptin resistant, MLepRb- mice displayed higher protein levels of the leptin receptor at baseline compared to MLepRb+ mice (Fig. 2.4B). At 12 weeks, MLepRb- and MLepRb+ mice had similar body weights (n=2-4, Fig. 2.4C) and fasting plasma glucose levels (Fig. 2.4D). *Vegfa* mRNA levels did not differ between MLepRb- and MLepRb+ mice at baseline (Fig.2.4E). However, *ex-vivo* leptin stimulation of skeletal muscle elicited an increase in *Vegfa* mRNA levels in MLepRb+ but not MLepRb- mice (n=2-3, Fig. 2.4F). No difference in skeletal myocyte insulin sensitivity was evident between MLepRb- and MLepRb+ mice (Fig, 2.4G).

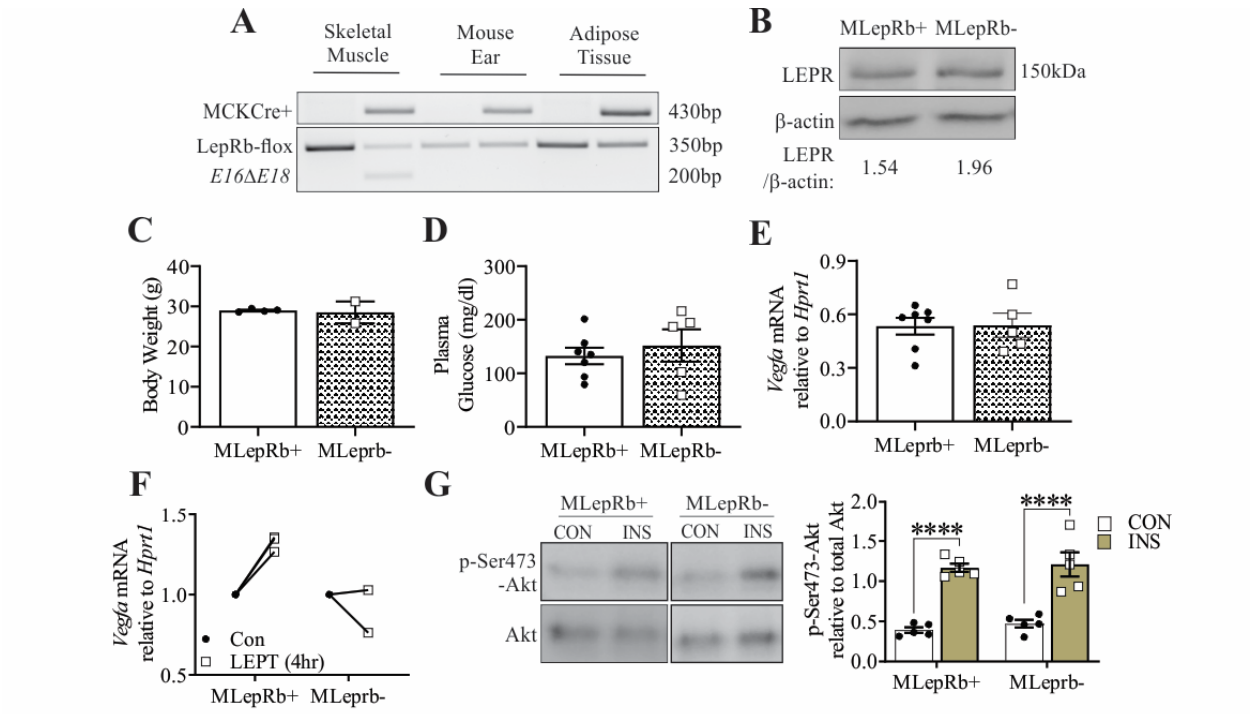

Figure 2.4: Characterization of myocyte-specific leptin-resistant (MLepRb+) mice.
A) PCR genotyping to detect floxed and exon-17 depleted (E16Δ18) leptin receptor alleles in multiple organs from muscle creatine kinase (MCK) Cre- and Cre+ mice. B) Representative western blot of the leptin receptor protein skeletal muscle homogenates relative to β-actin. C) Body weight and D) Plasma glucose levels were assessed in mature (12-weeks old) MLepRb- and MLepRb+ mice. *Vegfa* mRNA levels were assessed in skeletal muscle at E) baseline (gastrocnemius muscle) and F) following 4-hours of ex-vivo leptin stimulation (soleus) muscle. G) pSer473-Akt was assessed in control (CON) and insulin (INS) stimulated (*ex-vivo*) EDL muscles and normalized to total Akt levels. ****$P < 0.0001$ vs. MLepRb+ mice. ###$P < 0.001$ vs. insulin stimulated muscle, two-way ANOVA with Tukey post hoc analysis.

Histological assessment of the EDL muscle (Fig. 2.5A) revealed a modest but significant reduction (11%) of C:F in male MLepRb- mice (Fig. 2.5B), however CD was unaltered (Fig. 2.5C). In females, MLepRb- mice demonstrated a tendency for a reduction of both C:F (*P*=0.09, Fig. 2.5D) and CD (P=0.07, Fig. 2.5E). Together, these data suggest that leptin resistance induces capillary rarefaction by restricting leptin-induced myocyte VEGF-A production.

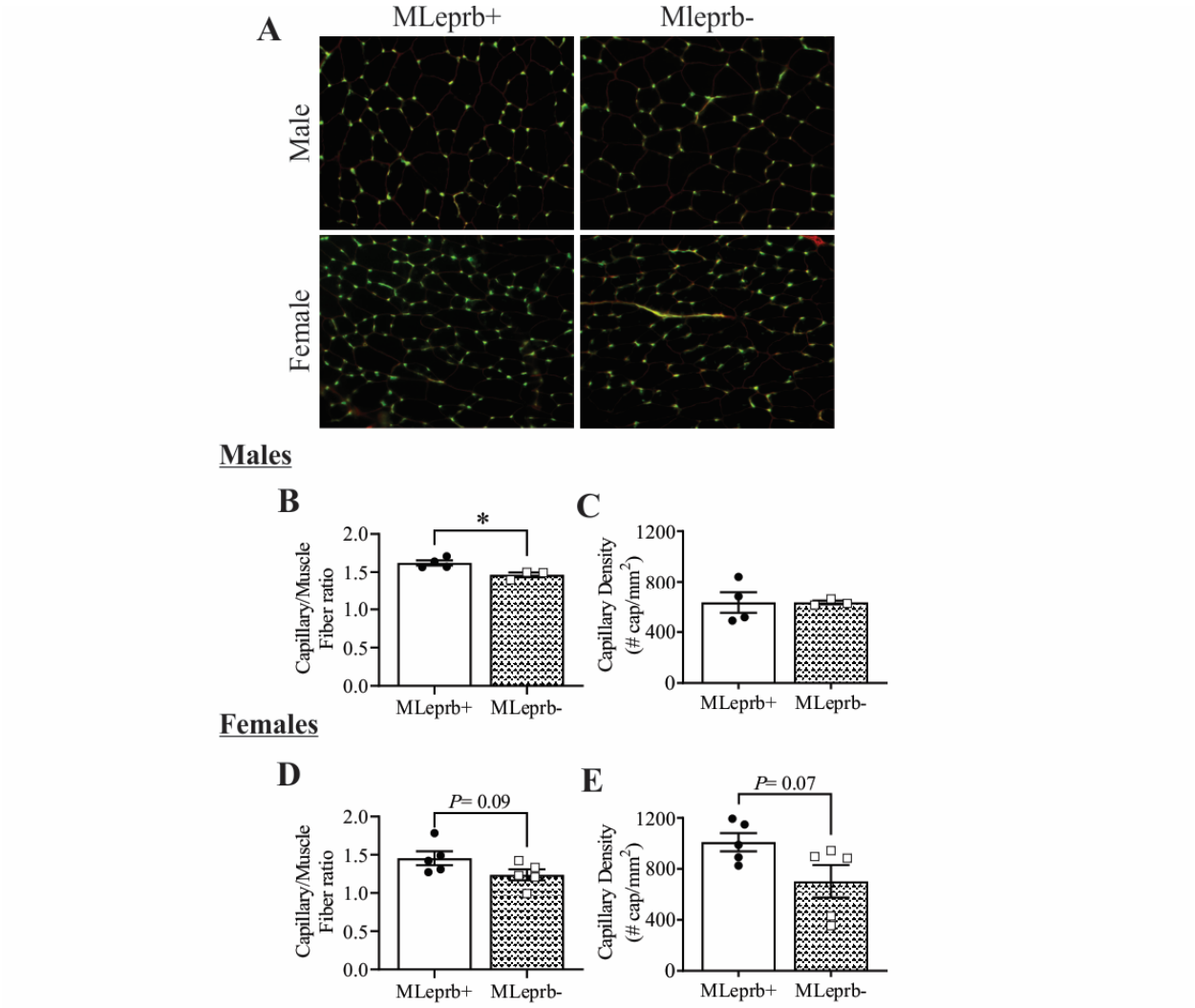

Figure 2.5: Skeletal muscle capillarization in MLepRb mice.
A) Representative images of EDL muscles from MLepRb+ and MLepRb- mice stained with G. *simplicifolia* lectin-FITC to visualize capillaries. Scale bar = 100 µm. B-E) Capillary/muscle fiber (B,D) and capillary density (C,E) were assessed in male (B,C) and female (D,E) mice from independent fields of view encompassing the entire muscle. *$P <$ 0.05 vs. MLepRb+ mice; unpaired student's t-test.

Increased Skeletal Muscle Capillarity in EDL but not Plantaris Muscles from High-fat Fed Mice

To specifically assess the effect of metabolic dysfunction (i.e. in leptin sensitive animals) on skeletal muscle capillarity, high fat (HF)-feeding was used to induce metabolic impairments in male FVB/N mice. Expectedly, HF-fed mice consumed more calories (Fig. 2.6A) and gained significantly more weight (Fig. 2.6B) over the 16-week diet period compared to normal chow (NC) counterparts. Metabolic assessments were performed over the course of the diet-period to track the progression of metabolic dysfunction in HF-fed mice. A tendency for increased fasting glucose was evident in HF fed mice as early as 6 weeks of diet but was significantly elevated only after 16 weeks (Fig. 2.6C).

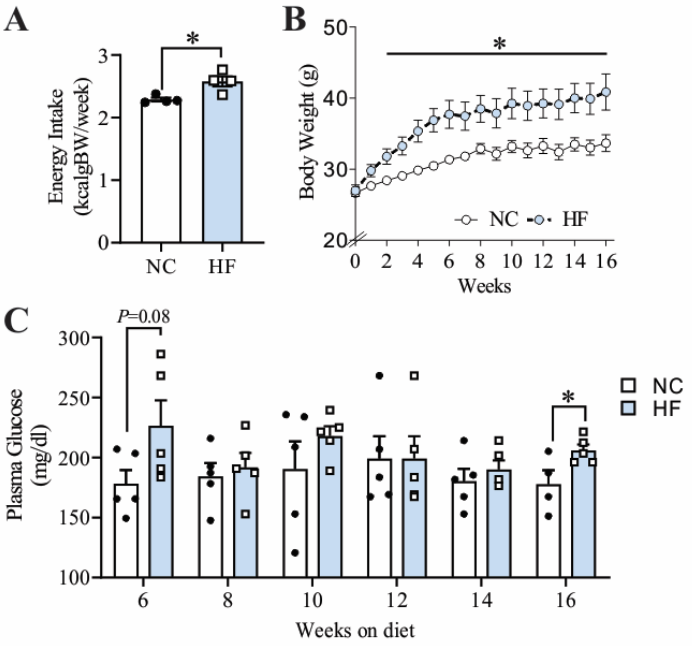

Figure 2.6: Mouse model of diet-induced obesity.
Male WT FVB/N mice were fed a normal chow (NC) or high fat (HF) diet for 16-weeks. A) Average energy intake, B) Body weight C) and fasting (4hr) plasma glucose levels during the diet period was assessed. *$P < 0.05$ vs. corresponding NC group; unpaired student's t-test.

Insulin resistance, indicated by insulin tolerance tests (ITT), was evident in HF-fed mice after 10, 12 and 14 (P=0.06) weeks of diet but returned back to basal levels by week 16 (Fig. 2.7A-F). No differences in plasma glucose clearance was observed between HF- and NC-fed mice during a glucose tolerance test (GTT, Fig. 2.7G). Furthermore, myocyte-specific insulin responsiveness did not differ between NC- and HF-fed mice (Fig. 2.7H)

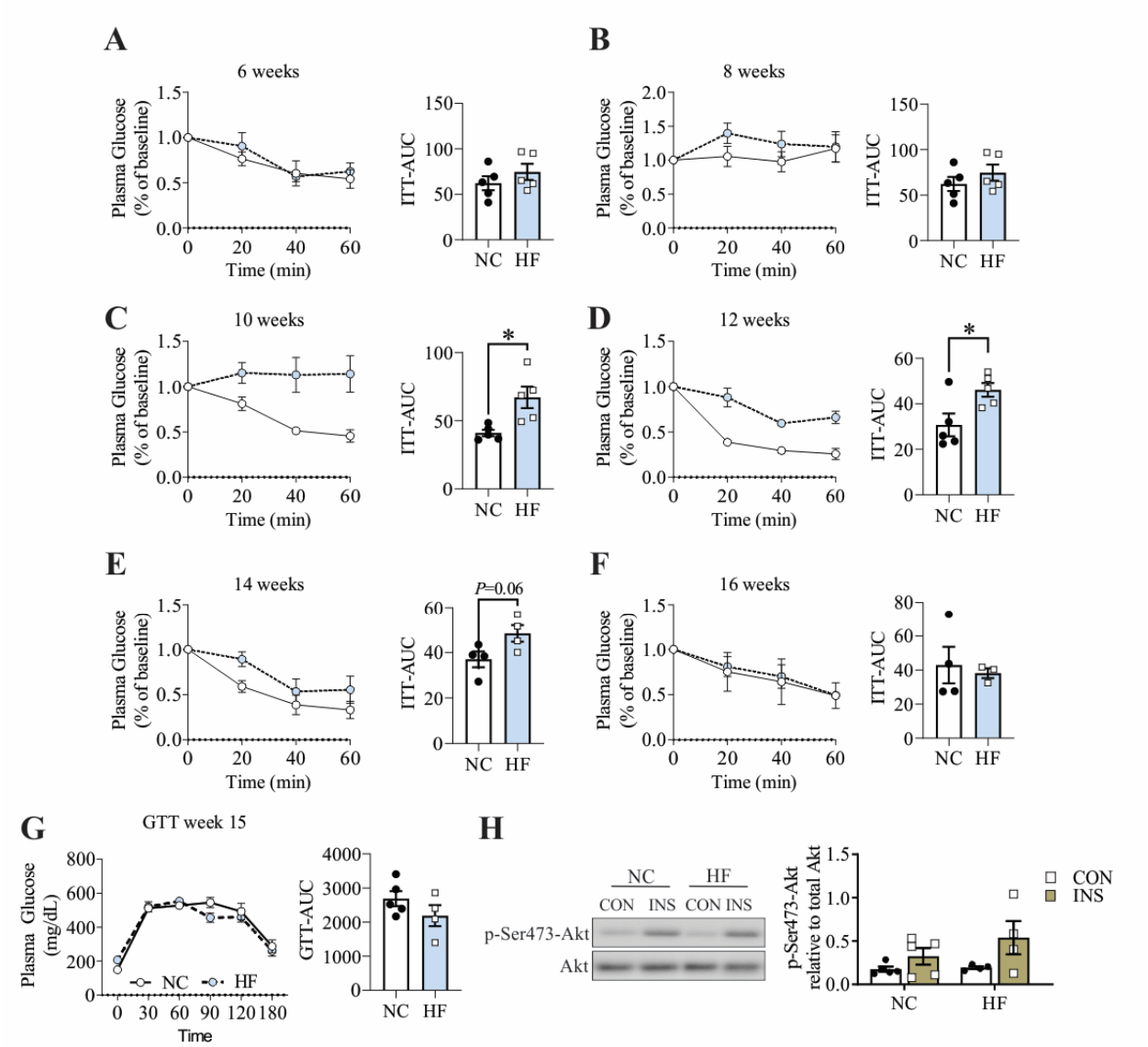

Figure 2.7: Assessments of insulin sensitivity and glucose tolerance in diet-fed mice.
Line graphs and corresponding area under the curve (AUC) of insulin tolerance tests (ITT) performed after A) 6, B) 8, C) 10, D) 12, E) 14, F) and 16 weeks of diet. G) Line graph and AUC of glucose tolerance test performed after 15 weeks of diet ; H) pSer473-Akt was assessed in extensor hallucis proprius muscles incubated *ex-vivo* with insulin and normalized to total Akt levels. Two-way ANOVA indicates a main effect of insulin on pSer473-Akt levels (P< 0.05). *$P < 0.05$ vs. corresponding NC group; unpaired student's t-test.

At the end of the 16-week diet period, both C:F and CD were unaltered in the plantaris muscle of HF-fed mice (Fig. 2.8A-C). In contrast, C:F and CD were significantly elevated in HF-fed mice when assessed in the EDL muscle (Fig. 2.8 A,D,E), suggesting muscle specific differences. This pattern of HF-diet induced capillary remodelling was associated with elevated VEGF-A protein (Fig. 2.8F) and *Leptin* mRNA (Fig. 2.8G) levels. In contrast, skeletal muscle mRNA expression of anti-angiogenic factors *Foxo1* and *Thbs1* were unaltered by diet induced metabolic dysfunction (Fig. 2.8H-I). Together, this data indicate that high-fat feeding is a pro-angiogenic stimulus in skeletal muscle.

2.5 **Discussion**

In this study, we demonstrate that leptin-signalling deficiency and metabolic dysfunction elicit independent and opposite capillary remodelling responses within skeletal muscle. Leptin resistance was associated with a reduction of skeletal muscle capillarity and impaired angiogenic response during normal developmental maturation in the post-weaning period. In contrast, metabolic dysfunction induced by HF-diet promoted a pro-angiogenic skeletal muscle environment. Furthermore, leptin was demonstrated to function as a positive regulator of VEGF-A production in both murine and human skeletal myocytes. These findings challenge the prevailing theory that metabolic dysfunction induces capillary rarefaction within skeletal muscle and provide novel evidence that leptin is a physiological regulator of skeletal muscle capillarity and angiogenesis.

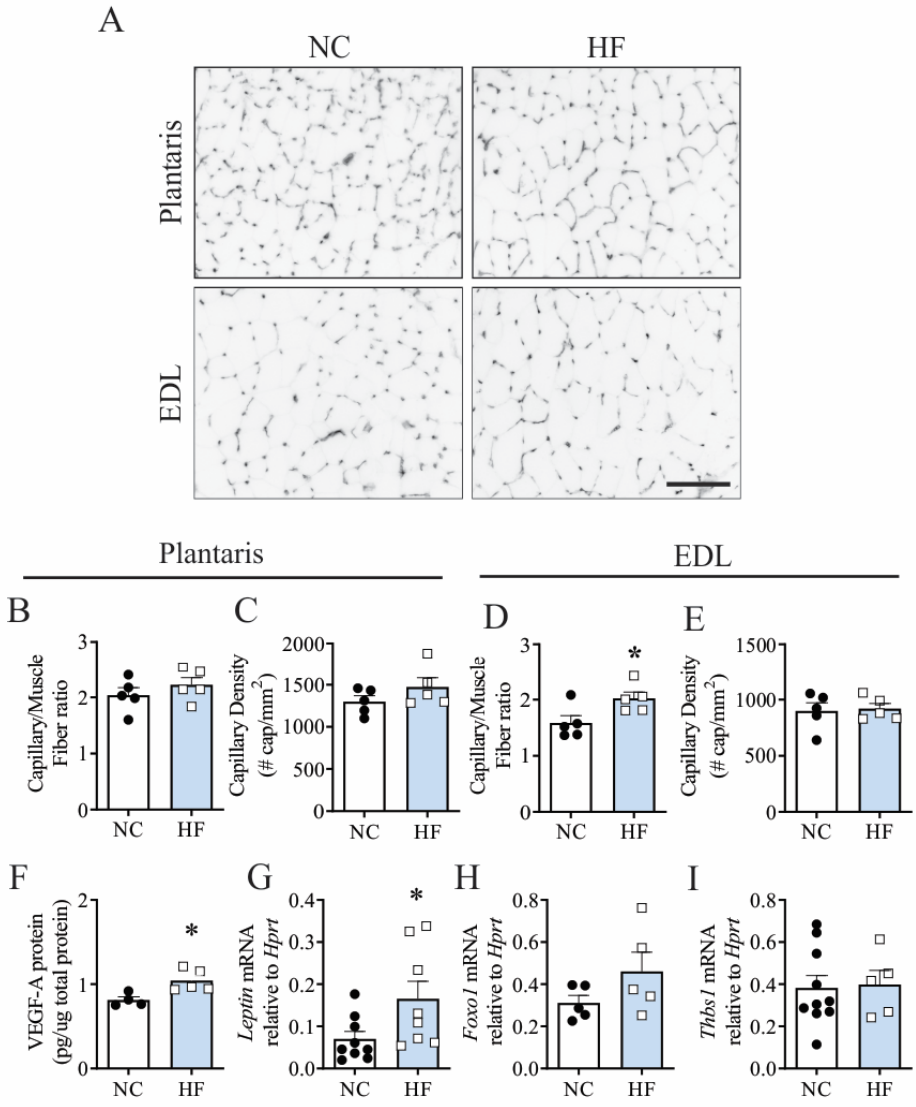

Figure 2.8: HF-feeding promotes angiogenesis within skeletal muscle.
A) Representative images of the plantaris and extensor digitorum longus (EDL) muscles stained with G. *simplicifolia* lectin-FITC to visualize capillaries. Scale bar = 100 μm. B-E) capillary/muscle fiber (B,D) and capillary density (C,E) were assessed in the plantaris (B,C) and EDL (D,E) muscles from at least 3 independent fields of view per mouse. In gastrocnemius muscle homogenates F) protein levels of VEGF-A were assessed by ELISA as well as mRNA levels of G) *Leptin* H) *Foxo1* and I) *Thbs1* by real-time quantitative PCR relative to *Hprt1* and expressed as $2^{-\Delta Ct}$. *$P < 0.05$ vs. NC mice; unpaired t-test.

A common explanation for lower skeletal muscle capillarity associated with leptin-deficiency models of obesity is that capillary rarefaction occurs as a result of chronic metabolic dysfunction that is characteristic of leptin deficiency (Frisbee, 2007). These inferences are often based on cross-sectional data collected from a single cohort of adult mice and overlook microvascular remodelling

events that may occur in the absence of leptin signalling. In the current study, *Lepr*^{db} mice exhibited a substantially (18%) lower C:F before a sustained period of metabolic dysfunction, suggesting that the lower capillary number associated with leptin signalling deficiency occurs independently of metabolic impairments. Capillary number (C:F) was unaltered in *Lepr*^{db} mice between 4 and 13 weeks. In contrast, control mice exhibited an increase in capillary number over the same time period, in parallel with age-associated myocyte hypertrophy. These findings indicate that the lower capillary density in mature *Lepr*^{db} mice cannot be explained by capillary rarefaction. Rather, our data are consistent with the idea that reduced skeletal muscle capillarity in *Lepr*^{db} mice is a direct consequence of leptin resistance and an uncoupling of capillary growth from myocyte hypertrophy during normal developmental maturation. In fact, based on the growing number of studies that have shown a positive correlation between skeletal muscle capillarity and insulin sensitivity (Lillioja et al., 1987; Prior et al., 2015), the present findings support the concept that reduced skeletal muscle capillarity contributes to the development of metabolic dysfunction in *Lepr*^{db} mice.

Leptin receptors are also expressed on endothelial cells and leptin has been shown to directly enhance endothelial cell survival, proliferation, migration, and the formation of capillary networks in various *in-vitro* and *in-vivo* angiogenesis assays (Artwohl et al., 2002; Bouloumié et al., 1998; Garonna et al., 2011; Manjunathan and Ragunathan, 2015; Park et al., 2001; Schäfer et al., 2004; Sierra-Honigmann et al., 1998). The observed reduction of skeletal muscle capillarity in MLepRb-mice suggests that myocyte leptin signalling is important for the maintenance of skeletal muscle capillary homeostasis. Considering the critical role of VEGF-A in skeletal muscle angiogenesis (Gorman et al., 2014; Olfert et al., 2009; Uchida et al., 2015), the observed failure of *Lepr*^{db} mice to increase VEGF-A in skeletal muscle undoubtedly contributed to the poor angiogenic capacity observed in these mice. Our results implicate myocyte leptin resistance as the underlying cause of

suppressed VEGF-A production, since recombinant leptin induced VEGF-A expression in cultured murine myoblasts and primary human myocytes. This finding is consistent with prior reports that leptin is a direct regulator of VEGF-A production in tumors (Gonzalez et al., 2006; Yang et al., 2014). VEGF-A production in murine and human myocyte cultures was also positively regulated by treatment with insulin. This is noteworthy considering that leptin has been shown to sensitize insulin signalling (Yau et al., 2014) and *Lepr*^{db} mice exhibited impaired skeletal myocyte insulin sensitivity. Thus, convergence between leptin and insulin signalling may contribute to the overall reduction in VEGF-A levels in the skeletal muscle of mature *Lepr*^{db} mice. Notably, MLepRb- mice had normal insulin sensitivity indicating that myocyte leptin resistance alone is insufficient to induce insulin resistance. Overall, these findings demonstrate that leptin functions as a pro-angiogenic factor within skeletal muscle by promoting VEGF-A production in skeletal myocytes.

Prolonged HF-feeding did not alter the sensitivity of skeletal myocytes to insulin, despite the onset of systemic insulin resistance. Considering that insulin sensitivity is determined primarily by skeletal muscle, our data suggests that impairments in vascular delivery of insulin to skeletal myocytes contributed to the reduced systemic insulin sensitivity observed in HF-fed mice. Indeed, several studies have shown that endothelial dysfunction is an early occurrence in the progression of obesity that contributes to the onset of peripheral insulin resistance, independent of changes to myocyte insulin sensitivity (Karaca et al., 2014; Kim et al., 2008; Kubota et al., 2011; Zhao et al., 2015). Intriguingly, reduced peripheral insulin sensitivity in HF-fed mice appeared to be reversed after 16 weeks of diet. Based on our data, it is tempting to speculate that the observed angiogenesis in HF-fed mice, which would increase the surface area available for insulin transport within skeletal muscle, was a physiological adaptation that restored skeletal muscle insulin sensitivity by

week 16. However, angiogenesis was only assessed after 16 weeks in the current study, making it difficult to establish a causal relationship.

A similar increase in skeletal muscle capillarity was reported in another study that demonstrated increased skeletal muscle capillarization after 19 weeks of HF-diet (Silvennoinen et al., 2013). In their study, Silvennoinen et al. postulated that increased capillarization is a physiological adaptation that enhances oxygen supply to support HF diet-induced increases in skeletal muscle oxidative capacity (Silvennoinen et al., 2013). Intriguingly, in the current study, HF-diet induced angiogenesis was observed in the EDL but not in the plantaris muscle. In rats, comparative assessments of fibre type composition have demonstrated a greater proportion of glycolytic fibres in the EDL compared to the plantaris muscle (Cornachione et al., 2011; Toth et al., 2006). In line with this, diet-fed mice in the current study had lower basal levels of capillarization in the EDL relative to the plantaris muscle. Thus, it is plausible that the EDL muscle, being more glycolytic, has a greater potential to increase oxidative metabolism and therefore more susceptible to HF diet-induced changes in skeletal muscle oxidative capacity. VEGF-A protein levels were significantly elevated with HF-feeding and likely contributed to HF diet-induced angiogenesis. Based on the findings in the current paper, it is plausible that obesity-related increases in leptin levels, promoted VEGF-A production by skeletal myocytes. Notably, skeletal muscle uptake of circulating leptin has been shown to be relatively low (Hill et al., 1998; McMurtry et al., 2004). In this study, we demonstrated that leptin transcripts are detectable within skeletal muscle and increase with HF-diet. Thus, paracrine leptin signalling may be more important for skeletal myocyte VEGF-A production in the context of HF-feeding. However, the cellular source and regulation of leptin production within skeletal muscle are still unknown.

In conclusion, the current study identifies leptin as a stimulus for VEGF-A production by skeletal myocytes and demonstrates a novel role for myocyte leptin signalling in the physiological regulation of skeletal muscle capillary homeostasis and angiogenesis. Furthermore, in contrast to the widely accepted concept of obesity-induced capillary rarefaction, the HF diet-induced angiogenesis observed in the current study is consistent with the idea that structural adaptations within the skeletal muscle capillary network mitigate the progression of metabolic dysfunction during obesity. The extent to which myocyte-leptin signalling contributes to physiological capillary remodelling in obesity remains to be elucidated. However, our findings caution against the interpretation of peripheral consequences of leptin- and leptin receptor deficiency in rodents as driven solely by systemic metabolic disturbances.

Chapter 3:

Nutrient-Excess Induces Leptin Production By PDGFRβ+ Perivascular Cells in Skeletal Muscle: Implications for Capillary Remodeling.

3.1 Contributions:

I was involved in the development of the conceptual and experimental framework used in the current study. My specific contributions to experiments included the generation and propagation of transgenic mouse models, administration of diets, isolation of individual cell populations from skeletal muscle, as well as biochemical and histological assessments. Additional contributions were made by fellow lab members and collaborators: Andrew Ng quantified microvascular remodelling in NG2-DsRed mice (Fig. 3.6D-G). Anna Strömberg assessed *LEPTIN* mRNA levels in human muscle and endothelial cells (results mentioned in text). Thomas Gustafsson provided human muscle tissue used for histological assessments (Fig. 3.1-3.4).

3.2 Published Data:

Nwadozi, E. [1], Ng, A. [1], Strömberg, A. [2,3], Liu, H.-Y. [1], Olsson, K. [2,3], Gustafsson, T. [2,3], and Haas, T.L. [1] (2019). Leptin is a physiological regulator of skeletal muscle angiogenesis and is locally produced by PDGFRα and PDGFRβ expressing perivascular cells. Angiogenesis 22, 103–115.

- Figures: 3.1-3.4, 3.5C-J

[1]School of Kinesiology and Health Science, Faculty of Health, York University, Toronto, Canada; [2]Department of Laboratory Medicine, Clinical Physiology, Karolinska Institutet, Stockholm, Sweden; [3]Department of Clinical Physiology, Karolinska University Hospital, Stockholm, Sweden

3.3 **Chapter Summary**

Background/Rationale

In the previous chapter, I demonstrated that leptin is a physiological regulator of capillary homeostasis within skeletal muscle by acting directly on skeletal myocytes to promote VEGF-A production. Although leptin functions are normally attributed to circulating levels secreted by adipose tissue (Kershaw and Flier, 2004), previous studies have demonstrated that leptin uptake into skeletal muscle is low relative to other leptin-sensitive tissues (Hill et al., 1998; McMurtry et al., 2004). Evidence for local leptin production was first provided by Wang et al. in 1998, demonstrating that the expression of leptin transcripts can be induced within skeletal muscle in proportion with nutrient availability (Wang et al., 1998). Consistent with their findings, I have shown that levels of leptin transcripts within skeletal muscle are elevated with HF-feeding in mice and in human subjects with higher body fat percentage (Nwadozi et al., 2019), indicating that paracrine leptin signalling within skeletal muscle is relevant in the context of obesity. Surprisingly, since the original discovery of locally-produced leptin in skeletal muscle over 20 years ago, the cellular source and regulation of leptin-production within skeletal muscle remains poorly understood. The presence of ectopic fat depots within skeletal muscle has been shown to increase in proportion with high-fat diet in both rodents and humans (Buettner et al., 2007; Kiens et al., 1987). Thus, I hypothesized that intramuscular adipocytes are local sources of leptin within skeletal muscle and that leptin synthesis would increase with expansion of intramuscular fat depots and in response to nutrient excess.

Objectives

1) Identify leptin producing cell populations within skeletal muscle.

2) Investigate the influence of nutrient excess on leptin synthesis in leptin-producing cells within skeletal muscle.

Experimental Approach

Leptin producing cells were identified by co-localizing leptin positive immunoreactivity with various cell types (i.e. adipocytes, myocytes and stromal cell populations) within skeletal muscle. Nutrient overload was induced by 2-weeks of high-fat diet, to increase circulating levels of nutrients (i.e. fatty acids, glucose) without the development of chronic metabolic impairments. Leptin-producing cells were isolated from skeletal muscle using antibody-coupled magnetic beads and the influence of nutrient overload on leptin gene expression in these cells was assessed.

For detailed methods, refer to Chapter #7, including methods pertaining to immunohistological staining (#7.3.2.2a), antibody-based isolation of cell fragments from skeletal muscle (#7.2.6) and the propagation of NG2DsRed transgenic mice (#7.2.1)

3.4 Results

Leptin-positive Immunoreactivity Within Skeletal Muscle is Localized to the Perivascular Space.

Leptin transcripts were either absent or detected in negligible amounts (Ct > 35) in C2C12 myoblasts as well as primary human myoblasts and differentiated myotubes, indicating that leptin production does not originate from satellite cells or skeletal myocytes. Immunohistological staining of mouse and human skeletal muscles was used as a tool to gain further insight into the cellular localization of leptin within skeletal muscle. Leptin staining was first performed using adipose tissue sections as a positive control. Within adipose tissue, leptin-positive immunoreactivity was localized to the thin cytoplasmic rim of individual adipocytes and to discrete entities in the interstitial space (Fig. 3.1A). Similarly, in mouse skeletal muscle leptin immunoreactivity was detected faintly within the peri-myocyte interstitium and distinctly in focal interstitial sites that appeared more numerous and intense with high-fat (HF) feeding (Fig. 3.1A). To evaluate potential co-localization of leptin immunoreactivity and skeletal muscle-resident adipocytes, BODIPY was utilized to demarcate lipid-laden cells. Surprisingly, there were no identifiable BODIPY-positive interstitial cells observed in murine muscle sections, and a complete lack of overlap between BODIPY staining and leptin immunoreactivity (Fig. 3.1B). Human muscle biopsies were characterized by the substantial presence of intra-myocyte lipid droplets. However, similar to mouse muscles, there were no identifiable BODIPY-positive interstitial cells and no overlap between BODIPY staining and leptin-positive immunoreactivity (Fig. 3.1B).

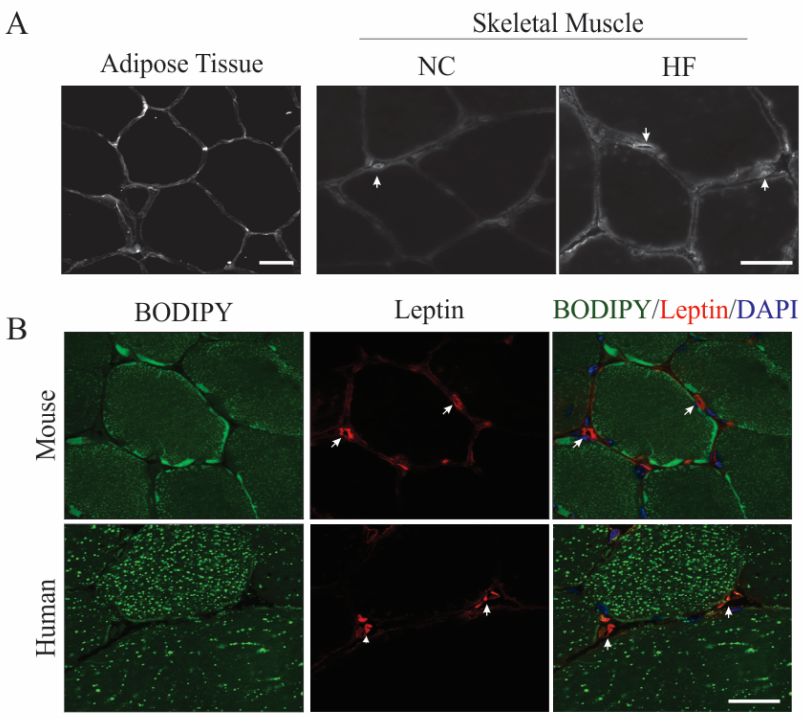

Figure 3.1: Cellular localization of leptin within skeletal muscle.
A) Leptin-positive immunoreactivity (arrows) in adipose tissue sections (positive control) and soleus muscle sections from NC- and HF-fed mice. B) Co-staining for BODIPY (to detect lipids) and leptin in murine soleus muscle and human biopsy sections. Scale bar = 20μm.

Co-localization with capillary structures was next examined. The majority of leptin immunoreactivity co-localized with lectin-positive capillaries in both mouse and human muscles (Fig. 3.2A). In microvascular fragments isolated from murine skeletal muscle, *leptin* transcripts were detected and increased with 9 weeks of HF feeding (Fig. 3.2B). However, neither cultured murine skeletal muscle endothelial cells nor human umbilical vein endothelial cells had detectable levels of *Leptin* mRNA (Ct > 35). Together, these data indicate that perivascular cells in close proximity to capillaries provide a local source of leptin within skeletal muscles.

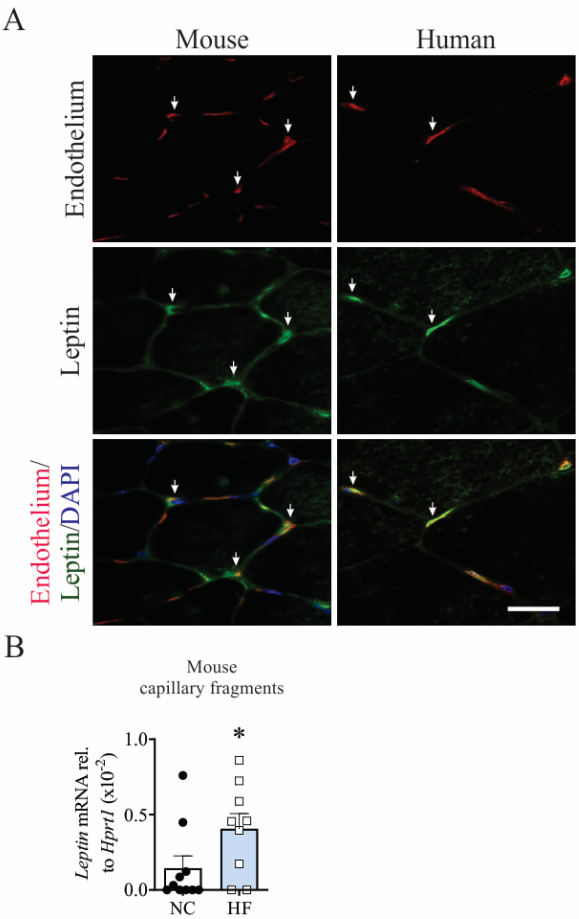

Figure 3.2: Leptin is produced in skeletal muscle capillary fragments.
A) Histological assessment of mouse and human muscle sections demonstrating overlap between leptin immunoreactivity and lectin-positive (capillary) staining (arrows). Scale bar = 20μm. B) *Leptin* mRNA levels were assessed in capillary fragments isolated from skeletal muscles of NC- and HF-fed mice by quantitative PCR relative to *Hprt1* and expressed as $2^{-\Delta Ct.}$ *$P < 0.05$ vs. NC mice.

PDGFRα+ and PDGFRβ+ Perivascular Cells Colocalize with Leptin-positive Immunoreactivity Within Skeletal Muscle

The absence of identifiable adipocytes led us to consider adipogenic precursor cells as potential leptin producing cells within skeletal muscle. PDGFRα- and PDGFRβ-expressing cells are an overlapping population of cells that are abundant in the perivascular space and exhibit adipogenic potential *in-vivo* (Birbrair et al., 2013a; Uezumi et al., 2010), leading us to investigate them as potential sources of leptin within skeletal muscle. In both murine and human skeletal muscles, PDGFRα immunoreactivity was detectable at discrete locations in the skeletal muscle interstitium

and importantly, in close proximity to capillaries (Fig. 3.3A). The majority of PDGFRα staining demonstrated overlap with leptin immunoreactivity (Fig. 3.3B). This overlap was evident particularly around capillaries, but also occasionally in cells within the skeletal muscle interstitium. PDGFRβ immunoreactivity was associated exclusively with microvessels (Fig. 3.4A), and co-localized prominently with leptin immunoreactivity in both mouse and human muscles (Fig. 3.4B). Together, these data implicate adipogenic (PDGFRα+ and PDGFRβ+) cells in the perivascular space as leptin producing cells within skeletal muscle.

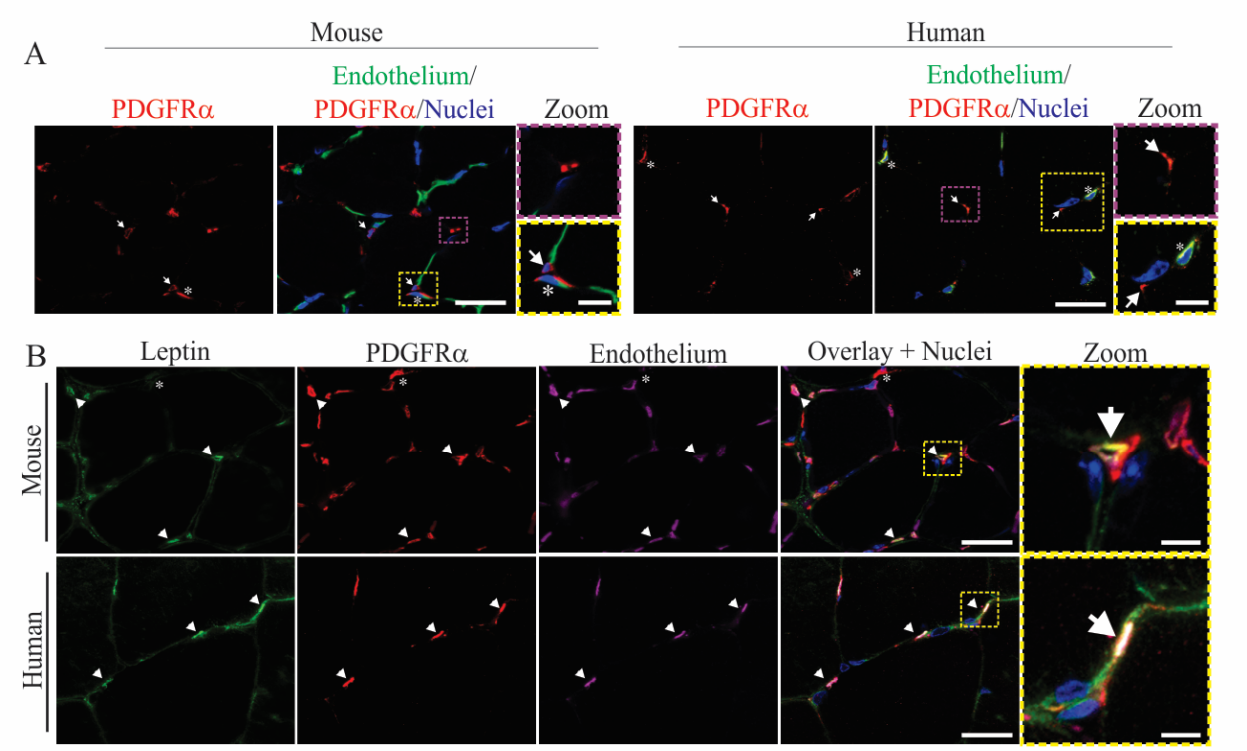

Figure 3.3: Co-localization of PDGFRα and leptin immunoreactivity.
A) Immunostaining for PDGFRα and lectin (capillaries) in mouse and human skeletal muscle in order to determine the cellular localization of PDGFRα+ cells. PDGFRα+ cells were identifiable in the interstitium (arrows) and associated with lectin + capillaries (asterisks). B) Co-staining for leptin, PDGFRα, lectin and DAPI demonstrating overlap between leptin and a subset of PDGFRα+ cells (arrows) in both mouse and human muscles. Scale bar = 20μm (5μm for zoomed images).

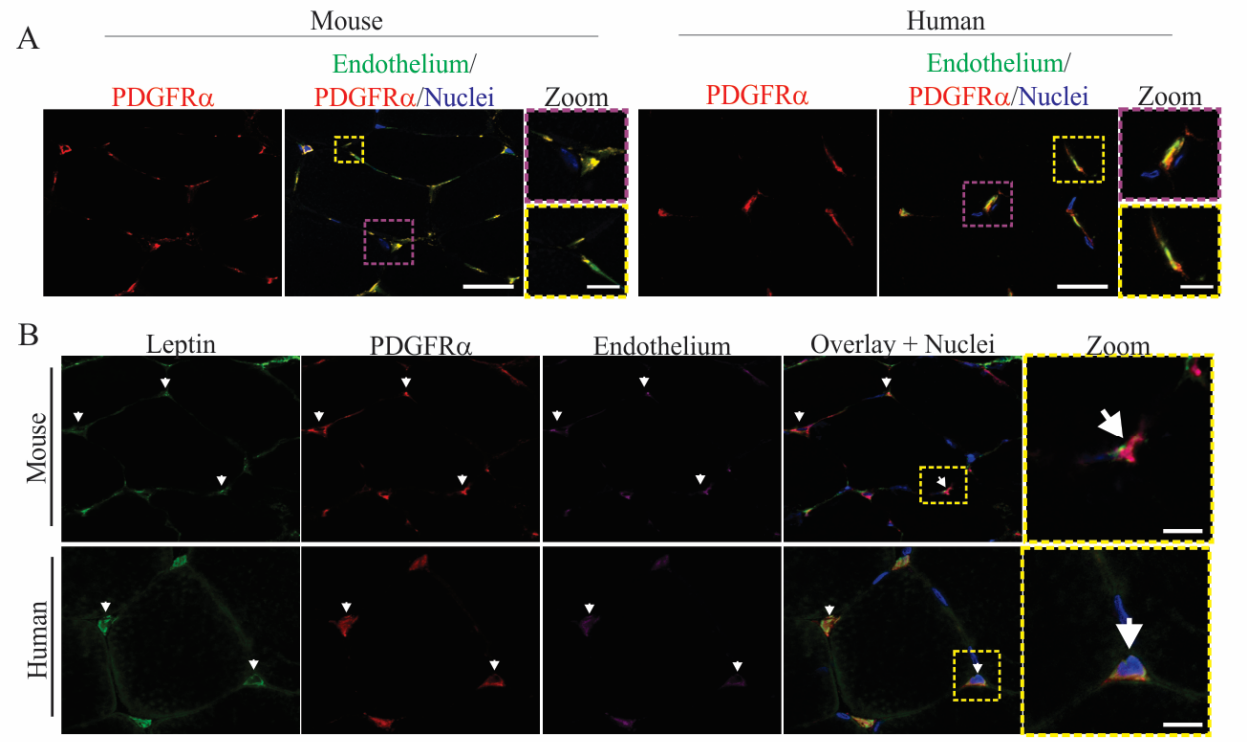

Figure 3.4: Co-localization of PDGFRβ and leptin immunoreactivity.
A) Immunostaining for PDGFRβ and lectin (capillaries) in mouse and human skeletal muscle demonstrating the perivascular localization of PDGFRβ+ cells. B) Leptin, PDGFRβ, lectin and DAPI demonstrating overlap between leptin and pericapillary PDGFRβ+ cells (arrows) in both mouse and human skeletal muscle. Scale bar = 20μm (5μm for zoomed images).

Nutrient Excess Promotes Leptin Synthesis in Murine PDGFRβ+ Cells Concomitant with Commitment to a Preadipocyte Lineage.

To test the hypothesis that nutrient excess promotes leptin synthesis within skeletal muscle, a group of male C57BL6/J mice were fed a NC or HF diet for 2 weeks to increases nutrient availability without inducing metabolic changes associated with chronic HF-feeding. 2 weeks of HF-diet was associated with a modest (~1.7g) increase in body weight and higher (54%) resting plasma glucose levels relative to NC-fed mice (Fig. 3.5A,B). Multiple cell populations were isolated following collagenase digest of skeletal muscles to assess the influence of nutrient excess on leptin synthesis within skeletal muscle (illustrated in Fig. 3.5C,F). *Leptin* transcripts were detected in the digested muscle fraction (containing all cellular constituents) and was enriched in isolated capillary fragments (Fig. 3.5D). Importantly, capillary fragments expressed both *Pdgfra* and *Pdgfrb*

transcripts (Fig. 3.5E), confirming the presence of these cell populations in our preparation. Individual populations of PDGFRα+ and PDGFRβ+ cells were isolated following a longer collagenase digest to generate a single-cell suspension (Fig. 3.5F) and *Leptin* mRNA levels assessed. Whereas PDGFRα+ cells from all NC-fed mice expressed *Leptin* mRNA, only 1 out of 5 NC-fed mice had detectable levels of *Leptin* transcripts in isolated PDGFRβ+ cells (Fig. 3.5G). Interestingly, in response to HF-diet, expression of *Leptin* transcripts was induced in PDGFRβ+ cells but remained unaltered in the PDGFRα+ fraction (Fig. 3.5G).

To further characterize the identity and adipogenic commitment of PDGFRα+ and PDGFRβ+ cells, we assessed several additional markers. PDGFRα+ and PDGFRβ+ cells expressed similar levels of the gene product *Cspg4* (Fig. 3.5H), which encodes the pericyte marker NG2. Next, we assessed various markers of adipogenesis to determine whether HF-induced leptin synthesis was associated with shifts in the adipogenic state of cells. Both PDGFRα+ and PDGFRβ+ cells had detectable mRNA levels of the preadipocyte commitment factor, zinc finger protein 423 (*Zfp423*) and Ccaat enhancer binding protein alpha (*Cebpa*), whereas mRNA encoding the mature adipocyte marker peroxisome proliferator-activated receptor γ (*Pparg*) was undetectable (Fig. 3.5I-J). Notably, HF-feeding further increased levels of *Zfp423* transcripts in isolated PDGFRβ+, but not PDGFRα+ cells (Fig. 3.5J), implicating HF diet as a trigger for a population of PDGFRβ+ cells to undergo preadipocyte commitment in mice.

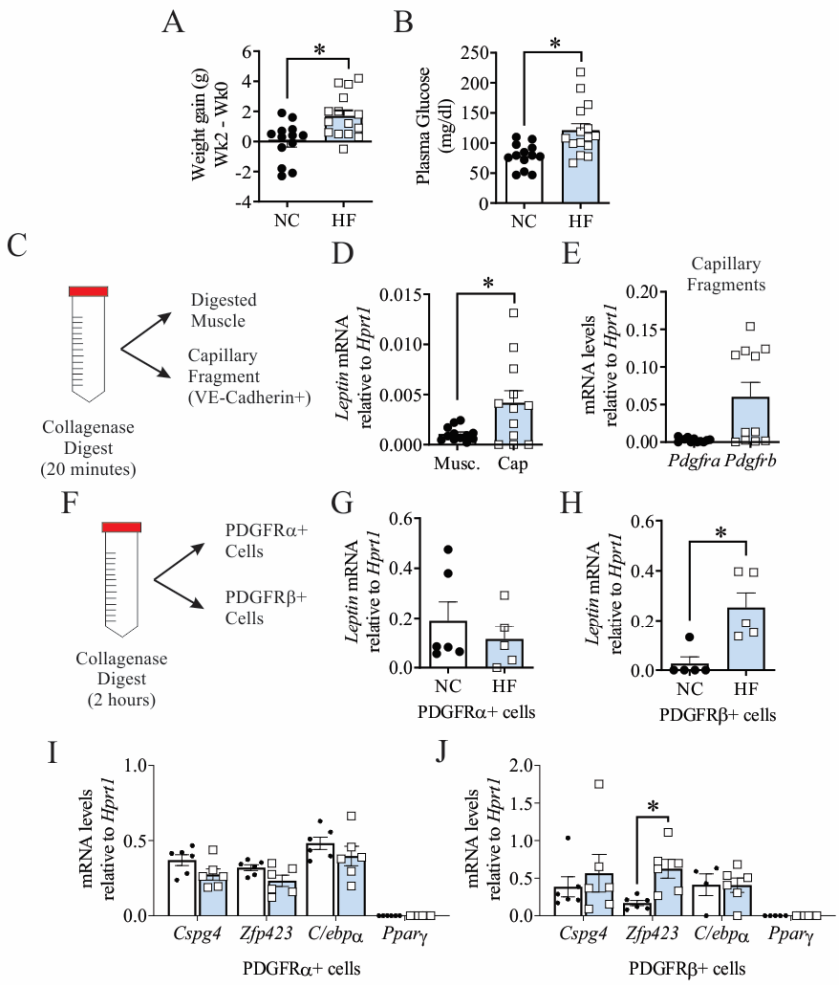

Figure 3.5: PDGFRα+ and PDGFRβ+ perivascular cells are leptin producing within skeletal muscle.

A) Weight gain B) and plasma glucose in mice fed a NC- or HF-diet for 2 weeks to induce nutrient excess. Isolation of various cell fractions was performed using skeletal muscles from NC- and HF- fed mice C) Following a brief collagenase digest, capillary fragments were isolated from the entire muscle digest using VE-Cadherin (VECAD) conjugated magnetic beads D) and *Leptin* mRNA was measured demonstrating an enrichment of *Leptin* transcripts in the isolated capillary fragments. E) Relative levels of *Pdgfra* and *Pdgfrb* mRNA were assessed in capillary fragments. F) Following a longer digest, *Leptin* mRNA was assessed in G) PDGFRα+ H) and PDGFRb+ cells isolated using antibody coupled magnetic beads. Transcript identifiers of pericytes and adipocyte lineage were quantified in the I) PDGFRα+ J) and PDGFRβ+ cells. mRNA levels are expressed as $2^{-\Delta Ct.}$ $*P < 0.05$ vs. NC mice.

Nutrient Excess is Associated with Reduced Pericyte Coverage of the Skeletal Muscle Microvasculature.

Pericytes (PDGFRβ+) ensure the stability and quiescence of capillary networks leading us to examine how increased leptin production and the preadipocyte phenotype shift observed with nutrient excess would influence pericyte-capillary interactions. Transgenic mice expressing

nuclear-localized DsRed (a red fluorescent protein) under the control of the pericyte-specific NG2 (*Cspg4*) promoter/enhancer (NG2DsRed mice) were fed a high fat diet for 2 weeks. In PDGFRβ+ cells isolated from NG2DsRed mice, *Leptin* and *Zfp423* mRNA levels were increased following 2 weeks of HF-diet (Fig. 3.6A,B) confirming that a similar induction of preadipocyte commitment was achieved in NG2DsRed mice. Nutrient excess was associated with a reduction of pericyte density within the skeletal muscle microvasculature (Fig. 3.6C-D) but did not affect pericyte coverage of the capillary surface (Fig. 3.6E), microvascular area (Fig. 3.6F) or capillary diameter (Fig. 3.6G). Markers of proliferation (*Ki67*) and basement membrane remodelling (*Mmp2*, *Mmp9*), which are early indicators of angiogenesis in pericytes, were unaltered at the mRNA level in PDGFRβ+ cells (Fig. 3.6H-J). Interestingly, angiopoietin-2 (*Angpt2*) mRNA levels demonstrated a tendency (P=0.06) to increase in capillary fragments isolated from HF-fed mice (Fig. 3.6K), consistent with the dissolution of endothelial-pericyte contacts. Together, these data suggest that nutrient excess promotes the dissociation of pericytes from the capillary wall in skeletal muscle, which may be permissive for capillary remodelling to occur.

3.5 **Discussion**

In this study, PDGFRα+ and PDGFRβ+ cells were identified as local sources of leptin in murine skeletal muscle. Nutrient excess induced leptin production in PDGFRβ+ cells, concomitant with preadipocyte lineage commitment and decreased pericyte density within skeletal muscle capillaries. Together, these findings implicate PDGFRβ+ cells as components of a local nutrient sensing network that may regulate capillary remodelling in skeletal muscle.

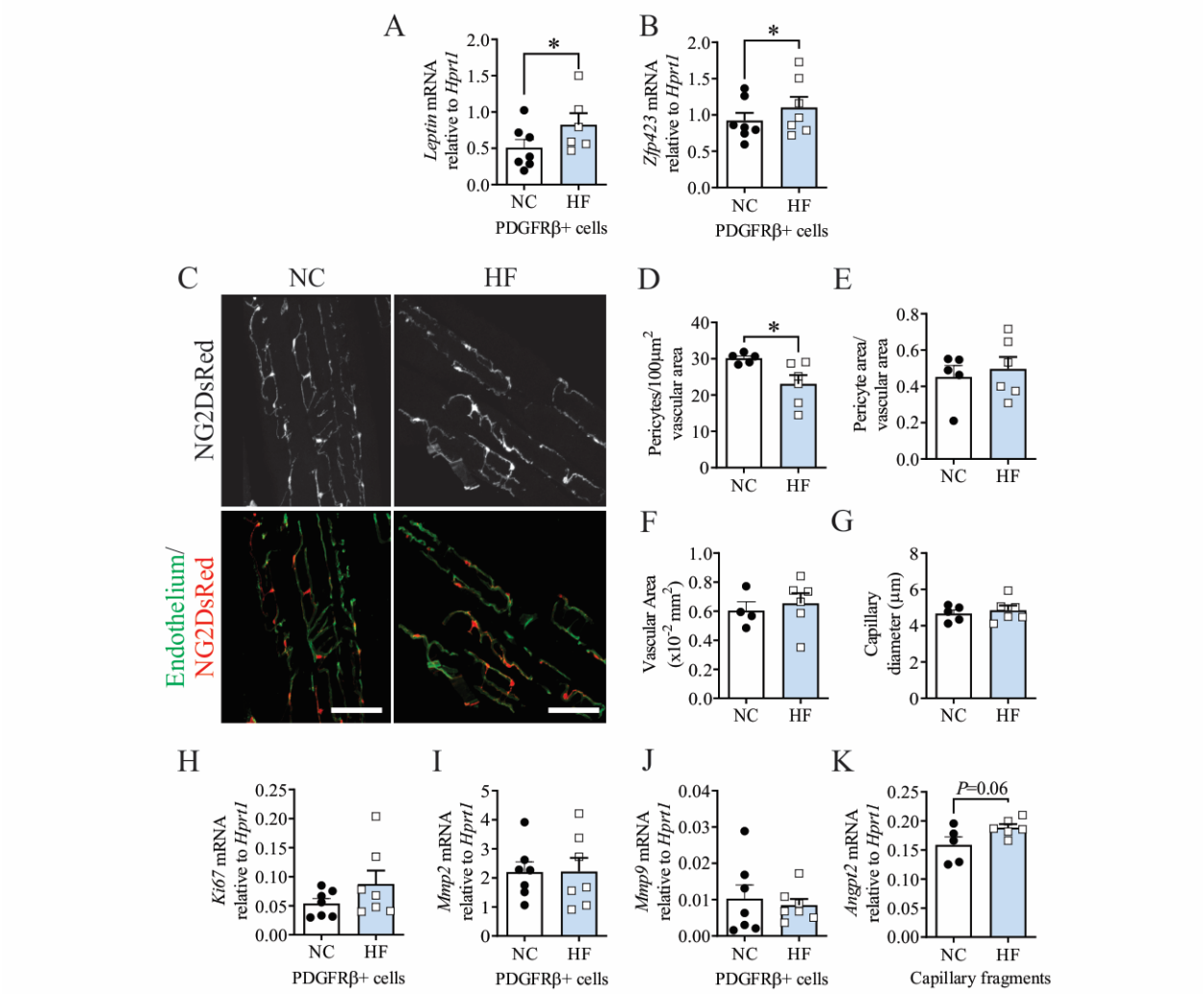

Figure 3.6: Microvascular remodeling in NC- and HF-fed mice.
NG2DsRed mice were fed NC- or HF-diet for 2 weeks to assess microvascular remodeling in response to nutrient excess. A) *Leptin* and B) *Znf423* mRNA levels were assessed in isolated PDGFRβ+ cells. C) Visualization of pericytes (NG2DsRed+, arrows) and capillaries in skeletal muscle (scale bar = 25μm) and associated quantifications for D) pericyte density, E) pericyte coverage, F) vascular area G) and capillary diameter. Relative mRNA levels of H) *Ki67*, I) *Mmp2*, J) *Mmp9* were assessed in isolated PDGFRβ+ cells and K) *Angpt2* levels assessed in capillary fragments. mRNA levels are expressed as $2^{-\Delta Ct}$. *$P < 0.05$ vs. NC mice.

Identification of the cellular source of leptin within skeletal muscle is important to be able to establish a foundation for mapping its potential paracrine signalling pathways. PDGFRα and PDGFRβ cell surface markers are typical (but not exclusive) of interstitial cells that exhibit adipogenic capacity (i.e., fibro-adipocyte precursors) and pericytes, respectively (Birbrair et al., 2013a; Gong et al., 1997). Notably, the pattern of PDGFRβ immunoreactivity in both mouse and

human skeletal muscle appeared most consistent with that of capillary-associated pericytes, while PDGFRα reactivity was found in association with capillaries as well as at non-capillary locations. Interestingly, a subset of pericytes possessing adipogenic potential also expresses PDGFRα (Birbrair et al., 2013a), which is consistent with the detection of pericyte marker *Cspg4* in both PDGFRα+ and PDGFRβ+ populations. This suggests that leptin-producing pericytes may be both PDGFRα+ and PDGFRβ+, but the antibody-based selection method used in the current study to isolate these cells did not resolve the extent of co-expression of PDGFRα and PDGFRβ. Thus, the available data lead us to conclude that local leptin production within skeletal muscle originates dominantly from a population of pericytes, although a contribution of interstitial PDGFRα+ cells cannot be excluded.

Skeletal muscle pericytes exhibit multipotent capacity to differentiate into several lineages including adipocytes (Birbrair et al., 2013a). Although mature adipocytes are the predominant source of leptin, the absence of *Pparγ* transcripts in isolated PDGFRβ+ cells preclude the possibility of terminal differentiation of pericytes in response to nutrient excess, considering Pparγ is indispensable for adipogenesis (Rosen et al., 2002). Furthermore, in histological analyses, there were no ectopic adipose depots visible within skeletal muscle. Leptin can also be produced in adipogenic precursor cells (Noer et al., 2006). In PDGFRβ+ cells, *Leptin* transcripts were elevated with a short-term HF-diet, coinciding with an increased expression of *Zfp423,* implying that nutrient excess provokes adipocyte commitment within the pericyte population. Thus, local leptin production within skeletal muscle seems to be closely linked to adipogenic potential rather than terminal differentiation of precursor cells. The responsiveness of PDGFRβ+ but not PDGFRα+ cells may be facilitated by their perivascular localization, as they are situated in a privileged position for exposure to nutrients as they are transported across the capillary to the skeletal

myocytes. Taking these observations into consideration, increased leptin production by pericytes in response to HF-feeding may serve as a mechanism to communicate systemic nutrient status within skeletal muscle in order to coordinate a tissue-level response to nutrient excess.

Pericyte coverage ensures the quiescence and stability of capillary networks and is inversely related with endothelial cell proliferation (Tilton et al., 1985) and susceptibility to undergo remodelling (Cai et al., 2012; Feldman et al., 1978). In the current study, vascular pericyte density was reduced after just 2 weeks of high-fat diet. The exact mechanism for the observed pericyte loss was not resolved in the current study but may involve hyperglycaemia induced apoptosis or migration of pericytes from the perivascular space similar to reports of pericyte "dropout" in proliferative diabetic retinopathy (Beltramo and Porta, 2013). In diabetic retinopathy, elevated levels of Angpt2 were shown to be critical for pericyte loss (Hammes et al., 2004). Consistent with this idea, we observed a tendency for Angpt2 levels to increase within capillary fragments following 2 weeks of HF-diet, suggesting that Angpt2 may also have contributed to pericyte loss in skeletal muscle. Alternatively, it is possible that pericytes are retained on perivascular space with nutrient excess but lose their pericyte identity (gene expression profile and function) overtime as they transition into committed preadipocytes.

Reduced pericyte coverage is destabilizing for capillary networks and renders them more susceptible to stimuli in their microenvironment (Ramsauer and D'Amore, 2002). Considering our previous observations, which showed that HF-feeding promotes a pro-angiogenic skeletal muscle microenvironment (i.e. increased leptin and VEGF-A levels, chapter #2, Fig. 8F-G), It is plausible that pericyte loss, induced as a result of nutrient excess in the current study, is permissive for the expansion of the skeletal muscle capillary network. However, neither vascular area nor capillary diameter was increased, indicating that capillary expansion had not occurred at the 2-week time-

point used in the current study. The lack of capillary remodelling may be explained by the relatively short duration of the diet administered, which may have been insufficient to allow for capillary remodelling. Interestingly, the relative surface area of pericytes was unaltered despite reduced pericyte density, suggesting that the remaining pericytes compensated for pericyte loss by increasing their coverage of the vasculature to maintain vascular stability. As a next step, it will be interesting to consider the interplay between pericyte density and capillary remodelling with longer diet durations.

In conclusion, the current study identifies pericytes and interstitial fibro-adipogenic precursor cells as local sources of leptin within skeletal muscle and points to pericytes as plausible "nutrient-sensors" within skeletal muscle. Considering leptin's role as a rheostat for energy homeostasis, local leptin production may serve as an intrinsic mechanism that facilitates intercellular communication of systemic energy status and draws attention to the physiological relevance of leptin paracrine actions within skeletal muscle. Finally, this study provides novel evidence that the loss of pericyte coverage/identity is an early occurrence in the pathogenesis of obesity that may prime skeletal muscle capillaries to respond to the pro-angiogenic skeletal muscle microenvironment generated by HF-diet.

Investigations into the intracellular mechanisms that link nutrient excess with leptin expression are currently underway in human cells. Preliminary results demonstrating a potential role for Zfp423 in the regulation of leptin gene expression are summarized in Appendix A.

Chapter 4:

Endothelial FoxO proteins Impair Insulin Sensitivity and Restrain Muscle angiogenesis in response to a high-fat diet.

4.1 Contributions:

I was involved in the development of the conceptual and experimental framework used in the current study. My specific contributions to experiments included the propagation of transgenic mouse models, administration of diets, metabolic testing, cell culture studies as well as well as biochemical and histological assessments. Additional contributions were made by fellow lab members and collaborators: Emilie Roudier was involved in developing the conceptual and theoretical framework, generation of transgenic mice and performed Foxo1 immunostaining in the plantaris muscle (Fig. 4.3D). Eric Rullman performed bioinformatics assessments featured in Fig 4.7-4.8 and Tables 4.1-4.4. Sujeenthar Tharmalingam was involved in the optimization of capillary fragment isolation (Fig. 4.1A,B). Hsin-yi Liu performed mRNA assessments (Fig. 4.6B,C).

4.2 Published Data:

All data in this chapter have previously been published:

***Nwadozi, E.[1]**, *Roudier, E. [1], Rullman, E. [2], Tharmalingam, S. [1], Liu, H.-Y. [1], Gustafsson, T. [2,3], and Haas, T.L[1]. (2016). Endothelial FoxO proteins impair insulin sensitivity and restrain muscle angiogenesis in response to a high-fat diet. FASEB J. *30*, 3039–3052.

[1]School of Kinesiology and Health Science, Faculty of Health, York University, Toronto, Canada; [2]Department of Laboratory Medicine, Clinical Physiology, Karolinska Institutet, Stockholm, Sweden; and [3]Department of Clinical Physiology, Karolinska University Hospital, Stockholm, Sweden.

***Equal contributions**

4.3 **Chapter Summary**

Background/Rationale

In the preceding chapters, I demonstrated that excessive intake of nutrients is associated with the up-regulation of pro-angiogenic factors such as leptin and VEGF-A within skeletal muscle. Intriguingly, despite the generation of a pro-angiogenic skeletal muscle environment as early as 2 weeks of HF-diet, only a modest expansion of the capillary network was observed in the EDL muscle but not plantaris muscles after prolonged (16 weeks) administration of a HF-diet. One possible explanation is that a parallel increase of anti-angiogenic factors within the endothelium in response to HF-feeding counteracts the influence of pro-angiogenic factors. However, the role that these anti-angiogenic factors play in the context of obesity-induced capillary remodelling in skeletal muscle has yet to be explored.

Our lab has shown that inducible deletion of endothelial FoxO proteins enhanced capillary growth in response to exercise or muscle ischemia (Roudier et al., 2013; Slopack et al., 2014) demonstrating that Foxo transcription factors are potent anti-angiogenic factors within skeletal muscle. Several lines of evidence indicate that vascular FoxO proteins play a pathological role in the context of metabolic disorders. In cultured endothelial cells, elevated glucose was shown to promote FoxO1 transcriptional activity, leading to increased LDL oxidation and development of endothelial dysfunction (Tanaka et al., 2009). Furthermore, increased endothelial Foxo1 was associated with reduced insulin sensitivity and endothelial dysfunction in the adipose tissue of obese individuals (Karki et al., 2015). Together, these observations suggest that endothelial FoxO proteins are activated in obesity; however, it remains unknown whether their activation promotes dysfunction within the skeletal muscle vascular niche. I hypothesized that prolonged high fat (HF)

feeding would increase the expression of FoxO proteins within the endothelium, which acts as a brake to the angiogenic process in response to HF-feeding.

Objectives

1) Investigate the impact of HF-diet on the expression of FoxO proteins within endothelial cells

2) Determine the impact of endothelial-directed depletion of FoxO proteins on HF-induced angiogenesis and peripheral insulin responsiveness following a prolonged administration of a HF-diet.

3) Assess the skeletal muscle transcriptome downstream of endothelial Foxo signalling to identify Foxo dependent genes, pathways and biological functions that are altered in HF-fed mice.

Experimental Approach

Transgenic mice with an inducible endothelium-directed depletion of FoxO proteins were fed a NC- or HF-diet for a total of 8 or 16 weeks. After 8-weeks of diet, in-vivo (vascular dependent) and ex-vivo (vascular-independent) stimulation of skeletal muscle was used to assess myocyte specific insulin responsiveness. Peripheral insulin sensitivity and skeletal muscle capillarity (in the plantaris muscle) was assessed after 16-weeks of diet. Skeletal muscle transcriptome was assessed in RNA extracted from plantaris muscles of HF-fed mice after 16 weeks to identify signalling pathways within muscle that mediate the Foxo response.

For detailed methods, refer to Chapter #7, including methods pertaining to the generation of endothelial Foxo1/3/4 deficient ($Foxo^{\Delta}$) mice (#7.2.1), Cell culture experiments (#7.4.2), *in-vivo* and *ex-vivo* stimulation of skeletal muscles (#7.2.4), immune cell infiltration into skeletal muscle (#7.3.2.3) and transcriptome analyses of skeletal muscles from HF-fed mice (#7.6).

4.4 Results

Endothelial Foxo1 Expression is Increased by Diet-Induced Obesity and is Associated with Reduced Insulin Sensitivity

To define the levels of Foxo1 and Foxo3 within the endothelial compartment, capillary fragments were isolated from the skeletal muscle of male FVB/N mice that were previously fed a NC and HF diet for 16 weeks (Chapter #2). Foxo1 protein levels increased substantially in the capillary fragments from HF- compared to NC-fed mice, whereas Foxo3 protein was not detectable (Fig. 4.1A, B). Endothelial Foxo1 expression correlated inversely with insulin sensitivity (as assessed by the ITT in Chapter #2, Fig. 7) after 14 weeks of diet (Pearson's r = -0.77; $P = 0.04$; Fig. 4.1C). The relative expression of Foxo1 and Foxo3 proteins also was assessed in whole-muscle homogenates but was not affected by HF feeding (Foxo1: 1.0 ± 0.1 NC vs. 0.9 ± 0.13 HF; Foxo3a: 1.0 ± 0.2 NC vs. 0.8 ± 0.3 HF; $P>0.05$, n=5, unpaired Student's t test). Foxo1 immunostaining was detectable in HF-fed mice, colocalizing dominantly with capillaries but also with nonvascular cells (Fig. 4.1D). Together, these results indicate that the HF diet–induced increase in Foxo1 occurs in the endothelial compartment within skeletal muscle and that higher levels of endothelial Foxo1 correlate with reduced insulin sensitivity.

To identify potential stimuli that lead to elevated Foxo1 in endothelial cells, we cultured microvascular endothelial cells in the presence of factors known to be increased by an HF-diet. The saturated fatty acid palmitate (200 mM), which is the major fatty acid present in the HF-diet, caused an increase in endothelial cell Foxo1 protein (Fig. 4.2A). The cytokines TNFα and IL6 are both elevated in obese individuals (Arner et al., 2010; Gustafson et al., 2007; Hotamisligil et al., 1995). IL-6 (10 or 20 ng/ml) exerted no effect whereas TNFα (1 ng/ml) induced a substantial increase in Foxo1 protein (Fig. 4.2B, C). These data suggest that circulating fatty acids and the

proinflammatory cytokine TNFα may promote the accumulation of endothelial Foxo1 protein in HF-fed mice.

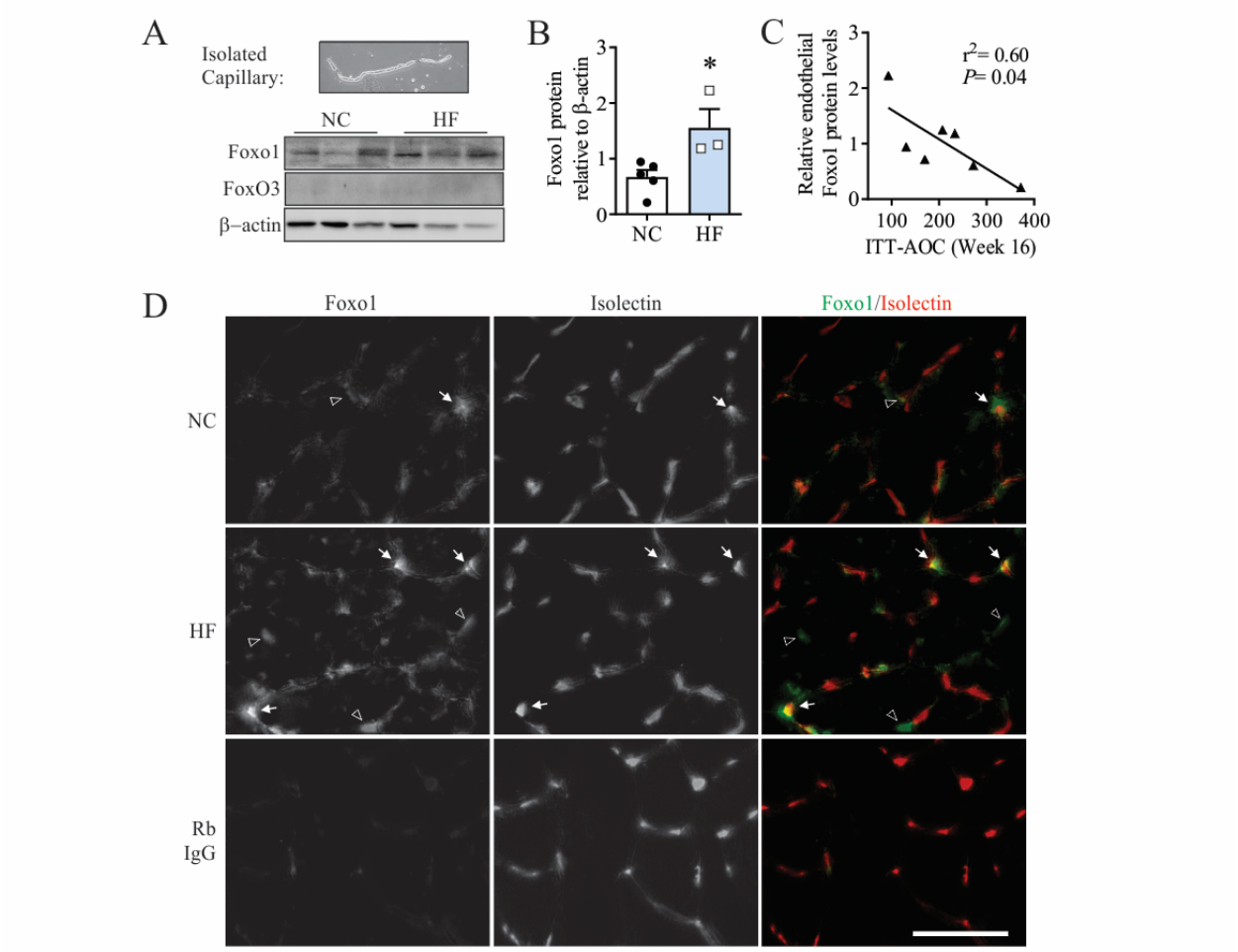

Figure 4.1: Diet-induced obesity increases the expression of FOXO1 in the endothelium of WT FVB/n mice.

A) Capillary segments were isolated from the muscles of NC and HF-fed mice at 16 weeks and used to assess Foxo1 and Foxo3 protein levels by Western blot. B) Quantification of Foxo1 protein levels in isolated capillaries. C) Linear regression of 16-week ITT-AOC (from chapter #2) and endothelial Foxo1 expression (B) in NC and HF animals. *$P<$ 0.05 vs. the NC group; unpaired Student's t-test. D) Immunostaining for Foxo1 (green) co-stained with isolectin (red) to delineate blood vessels. Arrows: Foxo1+ capillaries. Open arrowheads: Foxo1+ immune reactivity in extravascular cells. Normal rabbit (Rb) IgG was used as a negative control. Scale bar= 50μm

Endothelium-Directed Foxo Depletion Protects Against the Development of HF Diet-Induced Impairments in Peripheral Insulin Sensitivity

To ascertain the contribution of endothelial FoxO proteins to the metabolic phenotype of HF-fed mice, we used a mouse model of inducible, endothelial cell–directed depletion of all 3 FoxO

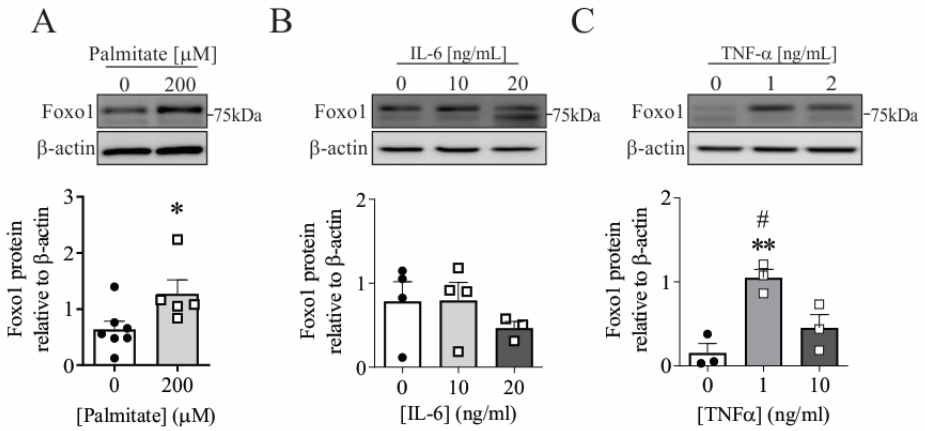

Figure 4.2: Endothelial Foxo1 is increased by palmitate and TNFα.
Cultured murine microvascular endothelial cells were treated with A) palmitate for 48-hours, B) IL-6, or C) TNFα and cellular extracts were analyzed by western blot. Foxo1 protein level (~70 and 78 kDa bands) was quantified relative to β-actin. **P*< 0.05 vs. palmitate control, unpaired Student's t-test; ***P*< 0.01 vs. TNFα control, one-way ANOVA with Bonferroni post hoc test.

proteins found in the endothelium (Foxo1/3/4), in which endothelial Foxo1 and Foxo3 proteins are reduced by approximately 70 to 80%, but FoxO expression within skeletal myocytes is unaffected (Paik et al., 2007; Roudier et al., 2013; Slopack et al., 2014). The excised Foxo1 allele (190 bp PCR product) was detectable within Cre+ ($Foxo^{\Delta}$) mice, whereas only the floxed Foxo1 allele was detectable in Cre- ($Foxo^{L/L}$) mice (Fig. 4.3A). Skeletal muscle endothelial cells extracted from $Foxo^{\Delta}$ mice exhibited ~80% reduction in Foxo1 protein compared to cells from $Foxo^{L/L}$ mice (Fig. 4.3B). In HF-fed mice, a detectable increase in Foxo1 (P<0.05) but not Foxo3 (P= 0.09) protein levels was evident in skeletal muscle homogenates (Fig. 4.3C). Expectedly, Foxo1 and Foxo3 protein levels were reduced by ~30% in skeletal muscle homogenates of $Foxo^{\Delta}$ mice compared to control littermates, reflecting the expected contribution of endothelial FoxO proteins to total Foxo levels within the whole muscle (Fig. 4.3C). Similarly, a reduction in capillary-associated Foxo1 immunoreactivity also was detectable within muscles of HF-$Foxo^{\Delta}$ compared to HF-$Foxo^{L/L}$ mice (Fig. 4.3D). HF-fed mice gained more weight than their NC-fed counterparts during the 16-week diet. However, HF-$Foxo^{\Delta}$ mice gained significantly less weight (Fig. 4.3E) and exhibited enhanced

peripheral insulin sensitivity compared to HF-Foxo$^{L/L}$ mice (Fig 4.3F,G). These results demonstrate that endothelial-directed Foxo depletion protects mice from weight gain and the development of peripheral insulin resistance during long-term consumption of an HF diet.

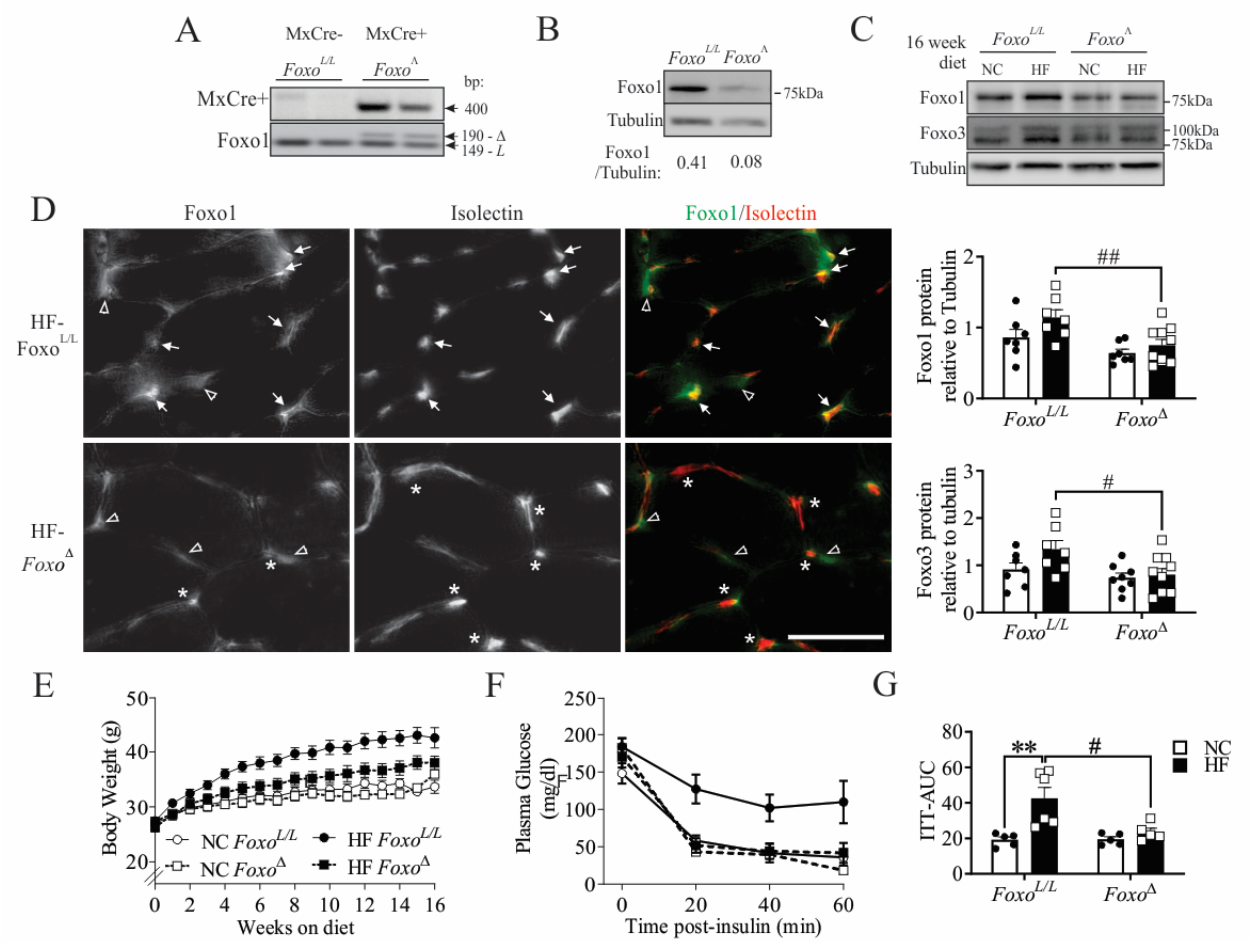

Figure 4.3: Endothelium-directed Foxo deletion protects mice from the development of an obese phenotype.

A) PCR genotyping was used to identify the floxed (*L*) and deleted (D) Foxo1 alleles in muscle from MxCre- and MxCre+ mice. B) Representative western blot of Foxo1 protein (relative to tubulin) in endothelial cells extracted from Foxo$^{L/L}$ and Foxo$^{\Delta}$ mice. C) Representative western blots and quantification of Foxo1 and Foxo3 protein levels (relative to tubulin) within gastrocnemius muscle homogenates from NC- or HF-fed Foxo$^{L/L}$ and Foxo$^{\Delta}$ mice after 16 weeks of diet (n= 7–10). Two-way ANOVA indicated a main effect of diet ($P< 0.05$) on Foxo1 levels only and main effects of diet on both Foxo1 ($P<0.01$) and Foxo3 ($P<0.05$) levels. #$P< 0.05$ and ##$P< 0.01$ vs. NC-Foxo$^{L/L}$ group, with Bonferroni post hoc analysis. D) Immunostaining for Foxo1 in muscle from HF-Foxo$^{L/L}$ and HF-Foxo$^{\Delta}$ mice, co-stained with isolectin to indicate blood vessels. Arrows: Foxo1+ capillaries. Open arrowheads: Foxo1+ immune-reactivity in extravascular cells. Asterisks: capillaries with minimal Foxo1 reactivity in Foxo$^{\Delta}$ samples. Scale bar = 25μm. E) Body weights over the duration of the diet. F, G) Insulin tolerance test (ITT) was conducted after 4-hours of fasting. Data are displayed as a line graph (F) and the corresponding area under the curve (AUC) (G). A significant interaction was found between diet and genotype, $P= 0.009$. **$P< 0.01$ compared to the corresponding NC group. #$P< 0.05$ compared to NC-Foxo$^{L/L}$, with Bonferroni *post hoc* analysis.

Endothelium-Directed Foxo Depletion Enhances Vascular Dependent Skeletal Muscle Insulin Sensitivity

To explore whether the enhanced insulin tolerance observed in HF-Foxo$^{\Delta}$ mice was a function of changes to the skeletal muscle microvascular network, we compared insulin-induced phosphorylation of Akt in a second cohort of mice that were fed NC or HF diet for 8 wk. At this time point, HF-Foxo$^{L/L}$ mice exhibited significantly reduced peripheral insulin sensitivity, whereas HF-Foxo$^{\Delta}$ mice retained an ITT response similar to that of the NC groups (Fig. 4.4A, B), as had been observed after 16 weeks on the diet. *In-vivo* and *ex-vivo* insulin stimulation of skeletal muscle was compared as a tool to segregate the contributions of vascular delivery of insulin vs. skeletal myocyte insulin receptor activation, respectively. *In-vivo* delivery of insulin resulted in substantially greater phosphorylation of Akt (at both Ser473 and Thr308) within the muscle of HF-Foxo$^{\Delta}$ compared to HF-Foxo$^{L/L}$ mice (Fig. 4.4C, E). In contrast, no difference in the Akt phosphorylation of muscles from HF-Foxo$^{\Delta}$ and HF-Foxo$^{L/L}$ mice was detected with *ex-vivo* insulin stimulation (Fig. 4.4D, F), suggesting that enhanced vascular delivery of insulin to skeletal muscles underlies the improved peripheral insulin responsiveness observed in HF-Foxo$^{\Delta}$ mice.

Next, we assessed the impact of the 16-week HF-diet on skeletal muscle arteriole density and capillarization in Foxo$^{L/L}$ and Foxo$^{\Delta}$ mice. The density of SMA+ vessels having a diameter of <20μm was unaffected by diet or genotype (Fig. 4.5B). Endothelial Foxo depletion elicited a 20% increase in C:F ratio in plantaris muscles from HF- but not NC-fed mice (Fig. 4.5C), indicating that FoxO proteins repress obesity-induced angiogenesis within skeletal muscle. Together, these findings support the hypothesis that improvements in skeletal muscle microvascular density and/or function underlie the enhanced insulin sensitivity detected in HF- Foxo$^{\Delta}$ mice.

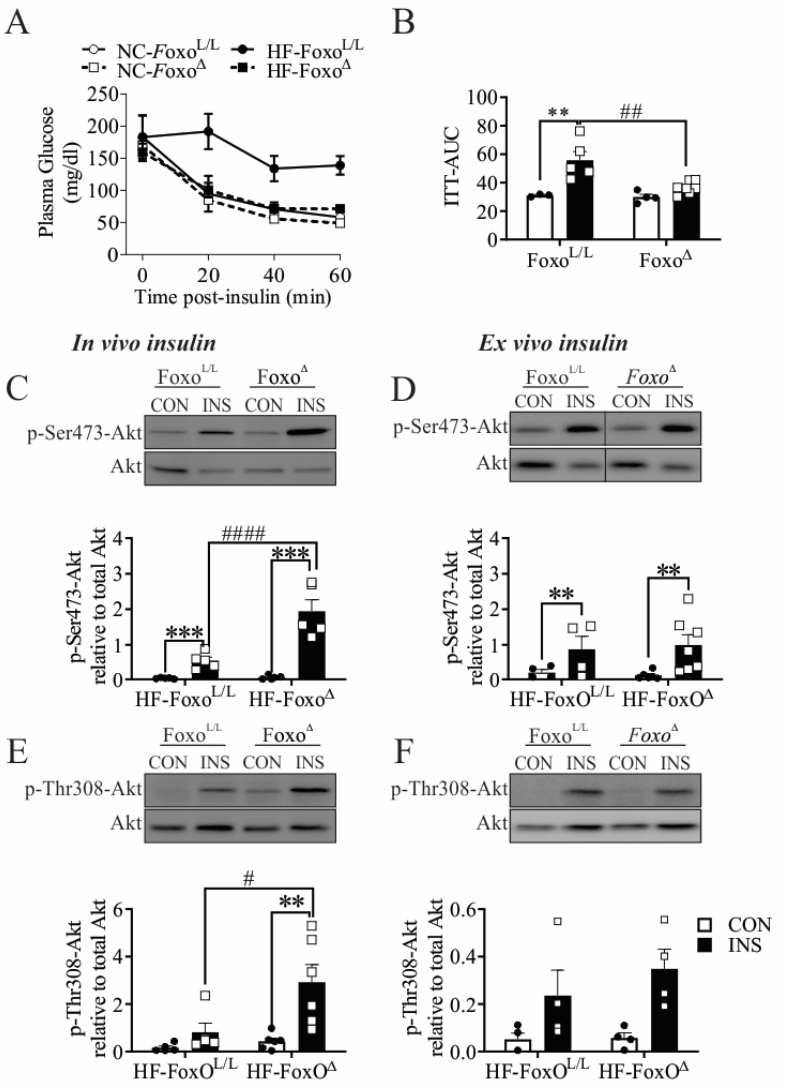

Figure 4.4: Increased vascular-dependent insulin sensitivity in muscle of HF-Foxo^{D} mice (2nd cohort; 8-week diet).

ITT data displayed as A) a line graph B) and the corresponding AUC graph. C) p-Ser473-Akt and D) p-Thr308-Akt (E) were assessed in EDL muscle before and after *in-vivo* insulin injection. D, F) p-Ser473-Akt (D) and p-Thr308-Akt (F) were assessed in *extensor hallucis proprius* muscles incubated *ex-vivo* in the absence or presence of insulin. Results are normalized to total Akt levels. Vertical line indicates that lanes are not contiguous. ***P*< 0.01 and ****P*< 0.001 relative to matched non-stimulated (CON) muscle. #*P*< 0.05, ##*P*< 0.01 vs. insulin (INS)-stimulated Foxo$^{L/L}$ mice, with Bonferroni *post-hoc* analysis.

Lack of Detectable Immune Cell Infiltration in Skeletal Muscle of HF-Foxo$^{L/L}$ and HF-Foxo$^{\Delta}$ Mice

Chronic low-grade inflammation is thought to be a contributing factor in the development of insulin resistance in obese individuals (Esser et al., 2014; Gustafson et al., 2007). Inflammatory

cell infiltrates were not apparent within plantaris muscle cross-sections from HF-Foxo$^{L/L}$ or -Foxo$^{\Delta}$ mice (Fig. 4.6A, top row). Macrophage staining (F4/80) detected sparsely localized positive reactivity in all experimental groups (Fig. 4.6A, bottom 3 rows). We assessed mRNA levels of several immune cell markers. The T-helper 17 marker *Rorc* mRNA levels was did not change with diet or genotype (Fig. 4.6B). Neutrophil elastase (*Elane*) mRNA was undetectable. The global monocytic/neutrophil marker *Itgam* was unaffected by genotype or diet. These findings indicate that there is minimal infiltration of immune cells in response to an HF-diet in either Foxo$^{L/L}$ or Foxo$^{\Delta}$ mice.

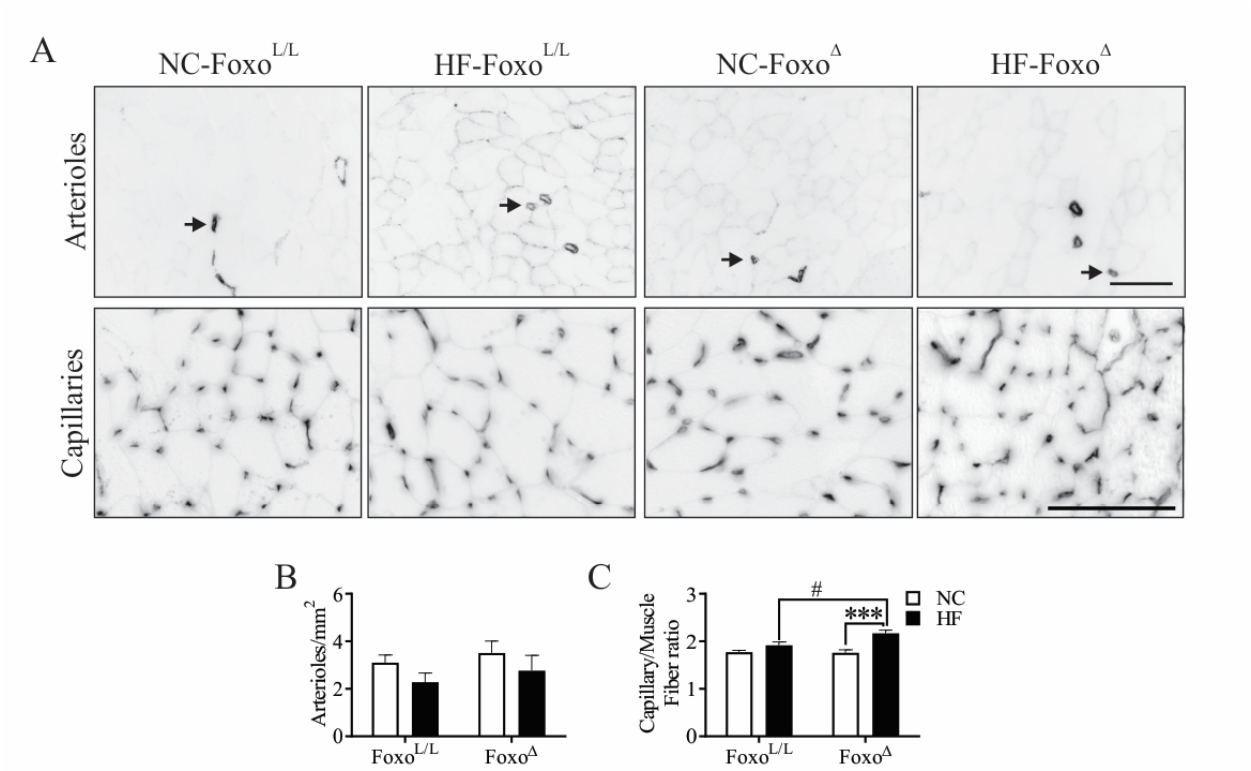

Figure 4.5: High-fat induces induces angiogenesis in Foxo$^{\Delta}$ mice.

A) Images of plantaris muscles stained with Cy3-anti-αSMA and *simplicifolia* lectin-FITC to visualize arterioles and capillaries, respectively. Scale bar= 100μm. Arrows: representative arterioles with diameter <20μm. Grayscale images were inverted to enhance visualization of vessels. B) Arteriole density C) and capillary/muscle fibre (C:F) ratios were calculated from 3–6 independent fields of view per mouse. Diet exerted a main effect on C:F ratio (P= 0.0003). ***P< 0.001 vs. corresponding NC group; #P< 0.05 vs. corresponding Foxo$^{L/L}$ group, with Bonferroni *post hoc* analysis.

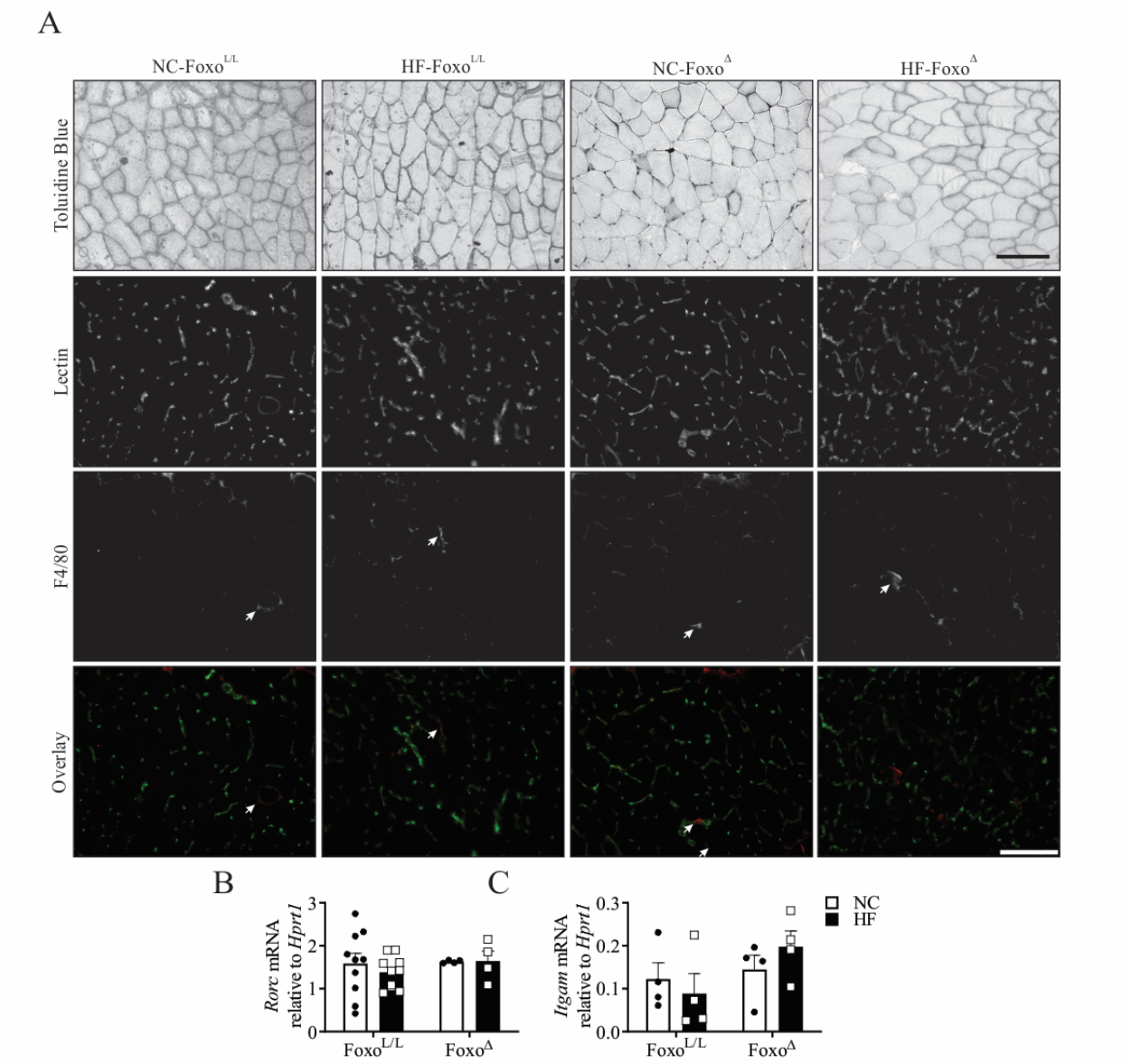

Figure 4.6: High fat diet is not associated with skeletal muscle immune cell infiltration.
A) Plantaris muscle sections were stained with toluidine blue to visualize basic muscle morphology (top row). Staining for capillaries (lectin; green) and macrophages (F4/80; red) and a merged image (overlay) are shown. Arrows: positive F4/80 staining. Scale bar= 100μm. B) *Rorc* and C) *Itgam* mRNA in the gastrocnemius muscle of NC or HF-fed Foxo$^{L/L}$ and Foxo$^{\Delta}$ mice, as assessed by real-time quantitative PCR. Values were normalized to *Hprt1* and expressed as $2^{-\Delta Ct}$.

Transcriptome Analysis of Skeletal Muscles from HF-Foxo$^{L/L}$ and HF-Foxo$^{\Delta}$ mice

To identify plausible signalling pathways that may be altered as a consequence of endothelial Foxo depletion, the gene expression profiles of plantaris muscle from HF-Foxo$^{L/L}$ and HF-Foxo$^{\Delta}$ mice were explored by microarray analysis. A total of 88 genes were significantly down-regulated,

whereas 280 probe sets were significantly up-regulated in the Foxo$^{\Delta}$ group at a confidence level of $P < 0.1$. A list of the top 100 differentially expressed genes (based on adjusted *P* value) are listed in Table 4.1. Gene ontology analysis revealed 24 significantly up-regulated pathways and functions within the up-regulated genes and 1 pathway among the downregulated genes (Table 4.2). The top-ranking up-regulated ontologies in the muscles from Foxo$^{\Delta}$ mice were related mainly to cell migration and adhesion. Ingenuity Pathway Analysis (IPA) of both up- and down-regulated genes was used to identify activated canonical pathways, functions and potential upstream regulators in Foxo$^{\Delta}$ mice. The top activated and inhibited functions (based on adjusted *P* value) in Foxo$^{\Delta}$ mice and associated genes, as determined by IPA analysis are listed in Table 4.3, with "migration of cells" being the most up-regulated function (z score= 5.4, *P*= 5E-19). "Angiogenesis" (z score = 3.6; *P*= 4E-15;) and "fatty acid metabolism" (z score = 3.8; *P*= 4E-5) are functions that were also robustly activated in the muscles of Foxo$^{\Delta}$ mice the top differentially expressed genes within these functions are illustrated in Fig. 4.7A and Fig. 4.7B, respectively. In contrast, the function with the most negative z score (predicting inhibition) was "inflammation" (z score = -2.4,P = 2.9E-9; Fig. 4.7C). To assess macrophage polarization, we examined the enrichment of genes associated with the M1 (pro-inflammatory) and M2 (anti-inflammatory) macrophage phenotypes in HF-Foxo$^{L/L}$ and -Foxo$^{\Delta}$ mice. M2 markers were highly enriched among genes up-regulated in Foxo$^{\Delta}$ mice (enrichment score 4.7; P = 4.5E-10), whereas M1 markers were enriched among down-regulated genes (enrichment score 1.9; P = 0.004; Fig. 4.8A), indicating that endothelial Foxo depletion is associated with an anti-inflammatory skeletal muscle environment after HF-feeding. Finally, we used the upstream regulator analysis as a tool to assist in identifying intermediary effectors of the Foxo$^{\Delta}$ phenotype. The most robustly "activated"

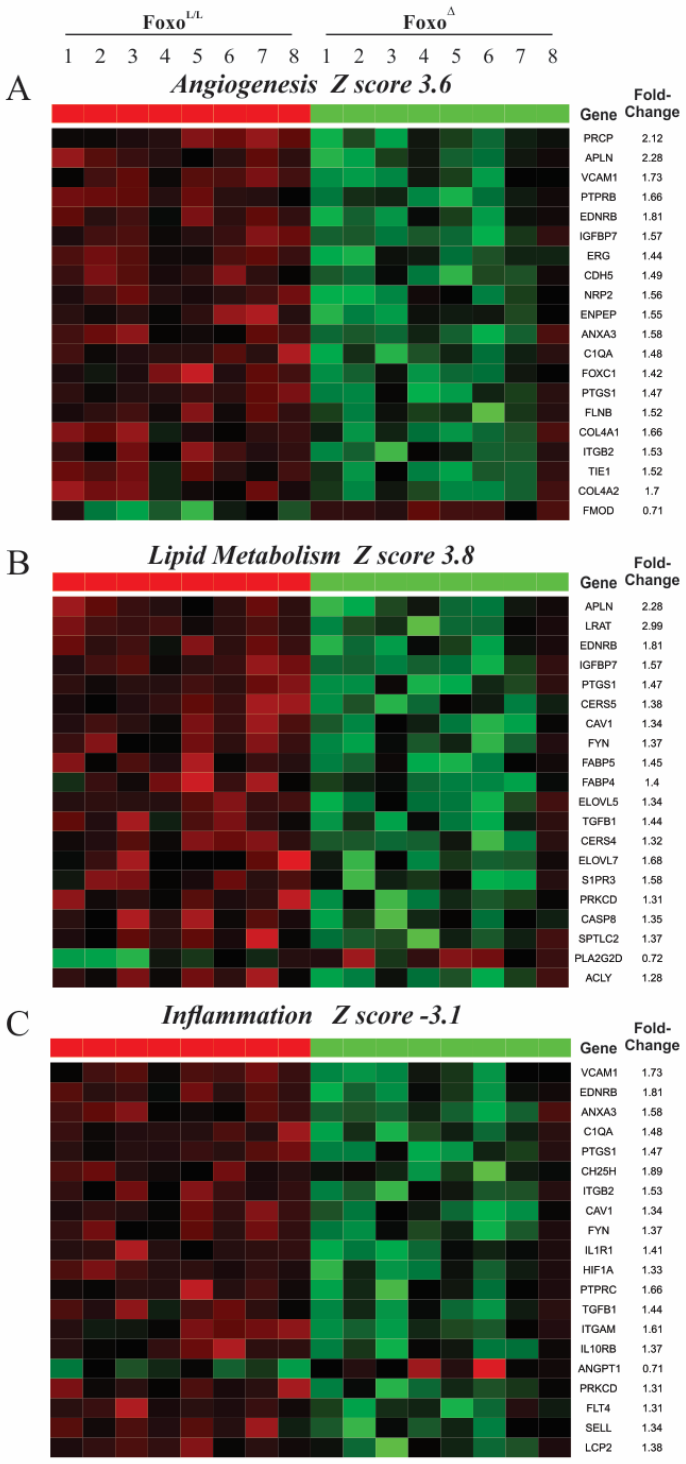

Figure 4.7: Differential expression of genes associated with angiogenesis, lipid metabolism, and inflammation in HF-fed Foxo$^{\Delta}$ vs. Foxo$^{L/L}$ mice.

Heatmaps and hierarchical clustering of the top 20 most significantly differentially expressed genes within each of the functional categories: A) Angiogenesis B) lipid metabolism (both predicted to be activated) and C) inflammation of body cavity (predicted as inhibited). Color is based on log2 normalized expression values, with higher and lower expression in Foxo$^{\Delta}$ vs. Foxo$^{L/L}$ indicated by green and red, respectively (n = 8). Genes are organized by *P* value (highest to lowest significance).

upstream regulator was the TGFβ1 network (z score = 4.5; *P*= 5E-15; Fig. 5.8B). Summaries of the predicted functions and are provided in Table 4.4.

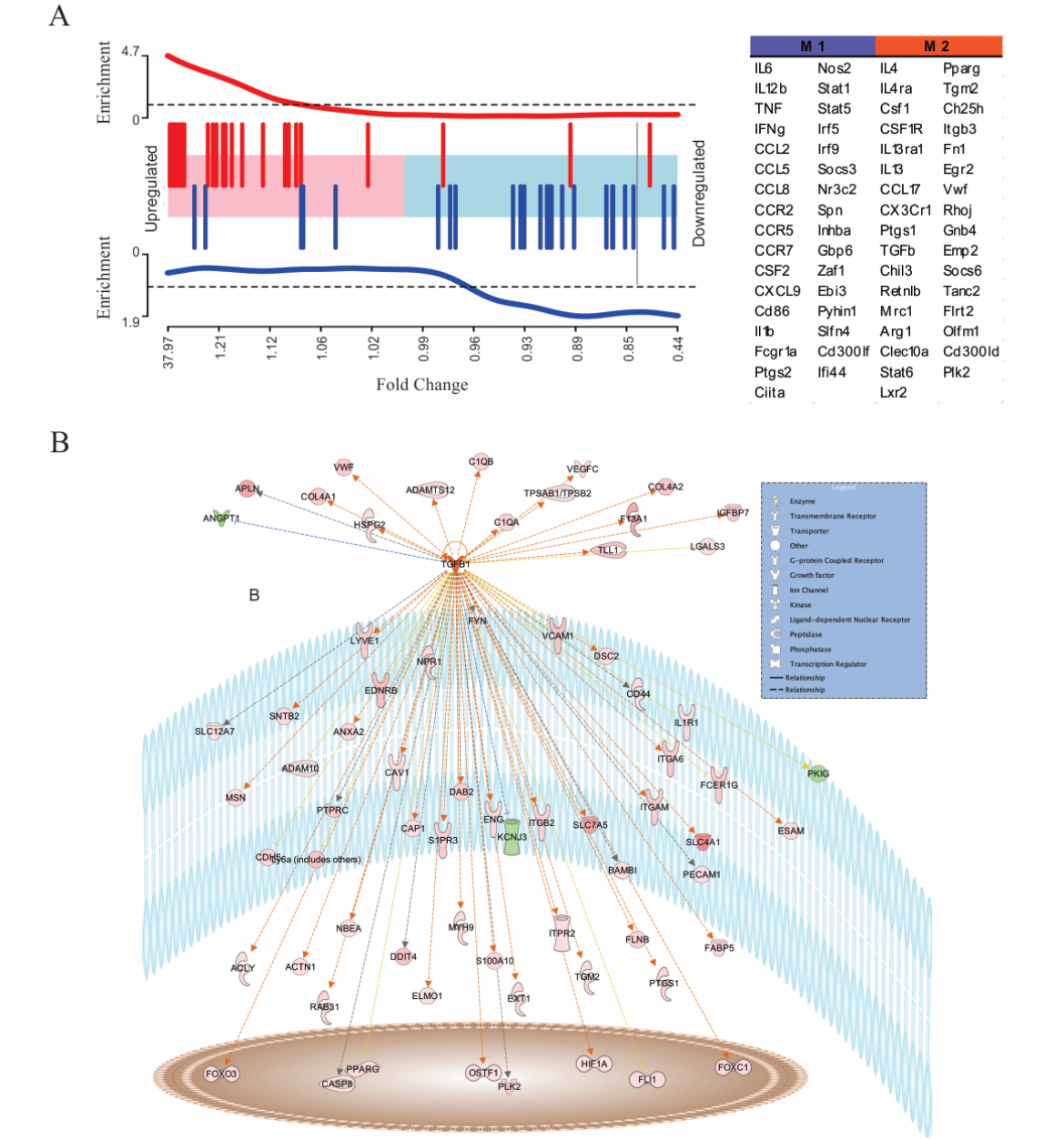

Figure 4.8: Indicators of M2 polarization and a potential role of TGFβ1 as an upstream regulator within muscle of HF-Foxo$^{\Delta}$ mice.

A) Barcode plot (left) showing M1 (blue bars) and M2 (red bars) signature genes (as listed in the table) based on their average fold-change in HF-Foxo$^{\Delta}$ vs. Foxo$^{L/L}$ mice. Up- and down-regulation of genes is highlighted by red and blue shading, respectively. M2 genes were highly enriched among up-regulated genes (P = 4.5E-10), whereas M1 markers were marginally enriched among genes down-regulated in Foxo$^{\Delta}$ mice (P = 0.004). B) The most robustly activated up-stream regulator in Foxo$^{\Delta}$ compared with Foxo$^{L/L}$ mice was the TGFβ1 network (z score= 4.5; P= 5E-15). The intensity of the node color indicates the degree of up- or down-regulation of a given gene (red and green, respectively).

Table 4.1: Top 100 differentially expressed genes in HF-Foxo$^{\Delta}$ vs. HF-Foxo$^{L/L}$

Gene Name	Log Ratio FC	Adj. p-value
Hsd3b6	5.247	6.68E-07
Usp24	-1.032	6.82E-07
Enpp6	1.722	1.07E-05
Prkaa2	-0.932	1.07E-05
Slco1a4	1.619	3.15E-05
Gm10021	1.322	7.49E-05
Fabp5	1.108	1.09E-04
Cd209a	-1.009	1.96E-04
Plk2	0.722	3.87E-04
G630055G22Rik	0.925	8.29E-04
S100a9	1.382	9.04E-04
Prcp	1.087	9.52E-04
Gpr126	0.930	9.98E-04
Ttc4	-0.636	1.17E-03
Apln	1.186	2.89E-03
Lrat	1.579	2.97E-03
Trp53i11	1.238	2.97E-03
Trpm3	0.632	2.97E-03
Emr4	0.854	3.10E-03
Tll1	0.837	3.10E-03
Vcam1	0.793	3.32E-03
Lyve1	0.715	3.32E-03
Syne1	0.676	3.52E-03
Slc16a4	0.874	4.64E-03
Adamts9	1.021	4.76E-03
Phxr4	0.798	4.76E-03
Vsig4	1.166	4.89E-03
Ptprb	0.735	4.89E-03
Clec14a	0.761	5.70E-03
Ednrb	0.854	5.93E-03
Igfbp7	0.655	6.64E-03
Itga6	0.745	8.47E-03
Erg	0.523	9.72E-03
Tfpi2	0.602	1.09E-02
Epb4.1l4a	0.593	1.27E-02
Cdh5	0.575	1.27E-02
Ppap2b	-0.547	1.27E-02
Cdr2	-0.881	1.27E-02
Kera	-1.190	1.41E-02
Nrp2	0.637	1.52E-02
Stfa2l1	1.609	1.54E-02
Enpep	0.634	1.68E-02
Apol11b	2.868	1.73E-02
S100a8	1.278	1.73E-02
Mir466h	-0.616	1.73E-02
Trim59	1.787	2.07E-02
Nepn	0.844	2.14E-02
Pip4k2a	0.839	2.14E-02
Pkhd1l1	0.752	2.14E-02
F13a1	1.102	2.21E-02

Gene Name	Log Ratio FC	Adj. p-value
Olfr584	-0.682	2.21E-02
Anxa3	0.658	2.21E-02
Fli1	0.479	2.55E-02
Gm3591	0.530	2.66E-02
Shank3	0.513	2.66E-02
Retnla	0.837	2.71E-02
C1qa	0.564	2.71E-02
Gpr165	0.718	2.78E-02
Gm3993	0.676	2.78E-02
Cfl1	0.659	2.78E-02
Rapgef5	0.565	2.78E-02
Ptgs1	0.560	2.78E-02
Fcna	0.546	2.78E-02
Foxc1	0.510	2.78E-02
Ext1	0.486	2.78E-02
Zfp773	-0.571	2.78E-02
AI464131	-0.621	2.78E-02
Gm3453	0.719	2.83E-02
Cers5	0.466	2.83E-02
Asap1	0.398	2.83E-02
Vwf	0.698	2.85E-02
Flnb	0.605	2.85E-02
Clec4n	1.035	2.91E-02
Cp	0.753	2.91E-02
Csgalnact1	0.500	2.91E-02
Plscr2	0.599	2.93E-02
Ch25h	0.922	3.11E-02
Taf1d	0.653	3.11E-02
Prkch	0.610	3.11E-02
Fyb	0.596	3.13E-02
Gm5797	0.596	3.13E-02
Flrt2	0.581	3.13E-02
Iqgap1	0.530	3.13E-02
Acot11	-0.499	3.13E-02
Bambi	0.461	3.35E-02
Col4a1	0.732	3.52E-02
Rpl3	0.631	3.60E-02
Col4a2	0.768	3.67E-02
Itgb2	0.614	3.67E-02
Tie1	0.600	3.67E-02
Cav1	0.421	3.70E-02
Acap2	0.403	3.70E-02
Fmod	-0.491	3.70E-02
Mir23b	0.669	3.91E-02
Emcn	0.554	3.91E-02
Chst2	0.540	3.91E-02
Fabp5	0.533	3.91E-02
Npr1	0.531	3.91E-02
Fyn	0.457	3.91E-02
Sh2d4a	-0.439	3.91E-02

Table 4.2: GSEA of genes upregulated in HF-Foxo$^{\Delta}$ vs. HF-Foxo$^{L/L}$

Upregulated in HF-Foxo$^{\Delta}$

Database (ID)	Functional Annotation	# of genes	*P*-Value	Fold Enrichment
GOTERM_BP_FAT (GO:0007155)	Cell adhesion	24	2.68E-07	3.52
GOTERM_BP_FAT (GO:0022610)	Biological adhesion	24	2.76E-07	3.52
GOTERM_BP_FAT (GO:0016477)	Cell migration	15	1.24E-06	5.15
KEGG_PATHWAY (mmu04670)	Leukocyte transendothelial migration	12	2.24E-06	6.29
GOTERM_BP_FAT (GO:0001568)	Blood vessel development	15	1.51E-06	5.06
GOTERM_BP_FAT (GO:0001944)	Vasculature development	15	2.01E-06	4.94
GOTERM_BP_FAT (GO:0048514)	Blood vessel morphogenesis	13	4.97E-06	5.41
KEGG_PATHWAY (mmu04510)	Focal adhesion	14	1.19E-05	4.41
GOTERM_BP_FAT (GO:0051674)	Localization of cell	15	8.81E-06	4.35
GOTERM_BP_FAT (GO:0048870)	Cell motility	15	8.81E-06	4.35
KEGG_PATHWAY (mmu04514)	Cell adhesion molecules (CAMs)	12	2.71E-05	4.86
KEGG_PATHWAY (mmu04530)	Tight junction	11	4.73E-05	5.08
GOTERM_BP_FAT (GO:0001525)	Angiogenesis	10	3.31E-05	6.19
GOTERM_BP_FAT (GO:0006928)	Cell motion	16	3.82E-05	3.59
GOTERM_BP_FAT (GO:0001775)	Cell activation	13	4.37E-05	4.35
GOTERM_BP_FAT (GO:0030029)	Actin filament-based process	11	5.42E-05	5.15
GOTERM_BP_FAT (GO:0045321)	Leukocyte activation	12	7.03E-05	4.51
GOTERM_BP_FAT (GO:0032844)	Regulation of homeostatic process	7	8.24E-05	9.61
KEGG_PATHWAY (mmu04810)	Regulation of actin cytoskeleton	13	1.42E-04	3.74
GOTERM_BP_FAT (GO:0016337)	Cell-cell adhesion	12	1.37E-04	4.19
GOTERM_BP_FAT (GO:0032943)	Mononuclear cell proliferation	6	1.60E-04	11.49
GOTERM_BP_FAT (GO:0070661)	Leukocyte proliferation	6	1.60E-04	11.49
GOTERM_BP_FAT (GO:0060537)	Muscle tissue development	9	2.42E-04	5.45
GOTERM_BP_FAT (GO0009611)	Response to wounding	14	2.99E-04	3.32

Downregulated in HF-Foxo$^{\Delta}$

Database (ID)	Functional Annotation	# of genes	*P*-Value	Fold Enrichment
KEGG_PATHWAY (mmu00565)	Ether lipid metabolism	3	0.0064107	23.42

Table 4.3: Selected functions that are represented within the set of differentially expressed genes

Functions Predicted to be Activated in HF-Foxo$^{\Delta}$

Disease or Function	*P*-Value	Activation z-score	Example of Genes in Dataset (total #)
Migration of cells	5.27E-19	5.41	ACTN4, ADAM10, ASAP1, COL4A1, CORO1B, DOCK1, ECSCR, EPHB4, FLNB, FLRT2, FMOD, IQGAP1, ITGA6, MMP8, MSN, SKAP2, STC1, TFPI2 (**103**)
Angiogenesis	4.30E-15	3.61	ADAMTS12, ANGPT1, CAV1, CDH5, ENG, EPHB4, FLT4, HIF1A, IGFBP7, NOSTRIN, NRP2, S1PR3, TGFB1, TIE1 (**56**)
Leukocyte migration	3.02E-13	4.73	ADAM10, CD44, DOCK1, ENG, ESAM, FYB, FYN, ITGAM, ITGB2, LCP1, LGALS3, Ly6a, PECAM1, SELL,VCAM1 (**56**)
Engulfment of cells	5.06E-09	3.93	ANXA3, C1QA, CD44, ELMO1, FCER1G, FYN, IQGAP1, ITGB2, LGALS3, PLD4, SHANK3, SIGLEC1 (**29**)
Lymph-angiogenesis	1.13E-06	1.05	ANGPT1, FLT4, FOXC1, LYVE1, NRP2, TIE1, VEGFC (**9**)
Synthesis of lipid	1.58E-06	2.78	CERS5, CH25H, DEGS1, ELOVL7, FABP5, HSD3B1, LRAT, PIP4K2A, PLA2G2D, PRKAA2, PTGS1, SPTLC2 (**37**)
Fatty acid metabolism	3.63E-05	3.81	ACLY, ACSL5, DEGS1, ELOVL7, FABP4&5, IGFBP7, LRAT, PLA2G2D, PPARG, PRKCD, PTGS1 (**28**)

Functions Predicted to be Inhibited in HF-Foxo$^{\Delta}$

Disease or Function	*P*-value	Activation z-score	Example of Genes in Dataset (total #)
Inflammation of body region	2.92E-09	-2.41	ANXA3, C1QA, EDNRB, IL10RB, IL1R1, IRAK4, ITGAM, LCP2, MMP8, PTGS1, SELL, TGFB1, VCAM1 (**36**)
Bleeding	2.98E-09	-3.21	COL4A1, ECSCR, F13A1, FLRT2, PRKAA2, PTGS1, TGFB1, TIE1, TLL1, VWF (**31**)
Organismal death	1.59E-06	-6.94	CASP8, DAB2, DDX17, DNAJA3, FOXO3, ITGA6, ITPR2, PLK2, RASA3, SLC4A1, SYNE1, TLL1, TSHZ3, UTRN (**90**)
Blood pressure	5.21E-05	-1.17	APLN, CAV1, EDNRB, NPR1, Pln, PPARG, PRKAA2, PTGS1, SNTB2, STC1, TAC3, TGFB1 (**18**)

Data were generated using the Ingenuity Pathway Analysis "Diseases and Functions" tool.

Table 4.4: Selected upstream regulators of the differentially expressed gene set

Upstream Biological Regulators Predicted to be Activated

Upstream Regulator	Established Functions	z-score	p-value of overlap
TGFB1	Promotes vascular stability and extracellular matrix synthesis; immunomodulation	4.47	5.65E-15
ERG	Promotes endothelial migration, regulates angiogenesis and vascular stability	3.62	5.07E-10
IL1B	Pro-inflammatory cytokine; promotes the release of secondary inflammatory mediators	4.23	3.93E-06
CTNNB1	Pro-proliferative transcriptional co-activator within the Wnt pathway	2.31	9.22E-06
VEGF	Growth factor that promotes endothelial cell permeability, nitric oxide production and angiogenesis	2.15	9.32E-06
IL4	Promotes M2 macrophage phenotype; anti-inflammatory	3.74	3.24E-04

Upstream Biological Regulators Predicted to be Inhibited

Upstream Regulator	Established Functions	z-score	p-value of overlap
α-catenin	Component of adherens junctions: regulates permeability and leukocyte extravasation	-3.26	6.18E-06
COL18A1	Proteoglycan; Regulates leukocyte extravasation; Proteolysis generates anti-angiogenic endostatin	-2.81	9.91E-05

Data were generated using the Ingenuity Pathway Analysis "Diseases and Functions" tool.

4.5 **Discussion**

In this study, we provide novel evidence implicating the angiostatic function of endothelial FoxO proteins in the pathogenesis of metabolic dysfunction. Foxo1 protein levels increased within the endothelial compartment in response to HF-feeding. Depletion of endothelial Foxo gene products was permissive for capillary expansion and prevented impairments to peripheral insulin sensitivity associated with HF-feeding. This phenotype shift was supported robustly by the prominence of genes associated with the promotion of angiogenesis among those differentially expressed in muscle from HF-Foxo$^{\Delta}$ vs. HF-Foxo$^{L/L}$ mice. Furthermore, endothelial Foxo depletion was characterized by a gene signature consistent with increased lipid metabolism and generation of an anti-inflammatory environment within skeletal muscle.

To the best of our knowledge, this report is the first to isolate capillary fragments from the skeletal muscle of HF-fed mice and provided us with the unique opportunity to specifically assess changes within the endothelial compartment. The observed up-regulation of Foxo1 in the capillaries of HF-fed mice provided evidence that FoxO proteins may contribute to the microvascular pathologies associated with insulin resistance. Previous studies have suggested that endothelial Foxo1 protein levels increase as a consequence of hyperglycaemia-induced oxidative stress (Tanaka et al., 2009) and insulin resistance (Karki et al., 2015; Tanaka et al., 2009), linked with reduced activation of Akt, a negative regulator of Foxo1 expression and activity (van den Berg and Burgering, 2011). In this study, we demonstrated that Foxo1 protein levels can be increased in cultured endothelial cells by exposure to either the saturated fatty acid palmitate or to the circulating inflammatory cytokine TNFα, both of which are characteristically elevated in obesity and diabetes (Aroor et al., 2013). Thus, our data identify Foxo1 as a novel downstream effector of fatty acid and inflammatory pathways within the endothelium.

Functional assessments of insulin sensitivity also reveal that the up-regulation of FoxO proteins within the vascular niche exacerbates the progression of insulin resistance in response to HF-feeding (Karki et al., 2015; Tsuchiya and Accili, 2013). Here, we demonstrate that endothelium directed depletion of FoxO proteins enhances peripheral insulin sensitivity. Cre-mediated recombination of FoxO proteins was driven by the Mx1 promoter to ensure endothelial specificity (Paik et al., 2007; Roudier et al., 2013; Slopack et al., 2014). A recognized limitation of this promoter is the off-target induction of cre-expression in hepatocytes (Kühn et al., 1995; Paik et al., 2007), which could suppress gluconeogenesis downstream of Foxo1 signalling leading to basal hypoglycaemia (Matsumoto et al., 2007; Tikhanovich et al., 2013). However, hepatocyte-specific deletion of Foxo1 has been previously shown to have no influence on peripheral insulin responsiveness or glucose uptake (Matsumoto et al., 2007). This finding suggests that the enhanced peripheral insulin responsiveness observed in Foxo$^{\Delta}$ mice is not due to reduced Foxo levels within the liver. In fact, our results demonstrate preserved insulin responsiveness in skeletal muscles from HF-Foxo$^{\Delta}$ mice which undoubtedly contributed to enhanced peripheral insulin sensitivity relative to Foxo$^{L/L}$ controls. Interestingly, vascular delivery and not myocyte sensitivity was enhanced by Foxo depletion suggesting that positive adaptations within the skeletal muscle vascular niche underlie the enhanced skeletal muscle insulin sensitivity in HF- Foxo$^{\Delta}$ mice.

HF-Foxo$^{\Delta}$ mice exhibited a 13% increase in muscle capillarity compared to the HF-Foxo$^{L/L}$ mice suggesting that FoxO proteins establish an anti-angiogenic skeletal muscle microenvironment in the context of obesity. This expansion of the capillary network, and thus, endothelial surface area, within skeletal muscle of HF-Foxo$^{\Delta}$ mice may contribute to increased transport of insulin across the capillary endothelium. Intriguingly, even though 16 weeks of HF-diet induced an increase in endothelial Foxo1 expression, there was no reduction in muscle C:F ratio in Foxo$^{L/L}$ mice. This

implies the coexistence of proangiogenic signals that negated the influence of Foxo1. Consistent with this idea, we also detected increased levels of VEGF-A in wildtype mice placed on a similar 16-week diet (as described in Chapter #2, Fig. 8F) similar to that previously reported by Silvennoinen et al. (Silvennoinen et al., 2013). In the current study, the unmasking of a pro-angiogenic phenotype in HF-fed mice after endothelial Foxo depletion was reflected strongly in the over-representation of cell migration and angiogenesis related genes within skeletal muscle. In addition to the structural changes, functional adaptations within the skeletal muscle vascular niche may also contribute to enhanced peripheral insulin sensitivity in HF-Foxo$^{\Delta}$ mice. Pharmacological inhibition of Foxo1 was shown to restore insulin-induced activation of endothelial nitric oxide synthase (eNOS) in endothelial cells isolated from obese individuals (Karki et al., 2015), indicating a reversal of endothelial dysfunction. Thus, although the current investigation did not include assessments of blood flow, it is likely that enhanced peripheral insulin responsiveness in HF-Foxo$^{\Delta}$ mice also reflects augmented delivery of insulin to skeletal myocytes. Together, these data reinforce the growing understanding that a positive correlation exists between skeletal muscle capillarity and insulin sensitivity (Hedman et al., 2000; Lillioja et al., 1987).

Inflammation is recognized as a significant contributing factor to the development of insulin resistance in individuals with obesity (Aroor et al., 2013; Gustafson et al., 2007). Assessments of the skeletal muscle transcriptome revealed a significant inhibition of the "Inflammation" in HF-fed HF-Foxo$^{\Delta}$ mice. This result is consistent with a prior study in which depletion of endothelial FoxO proteins was reported to induce an anti-inflammatory macrovascular phenotype within the aorta of HF-fed mice (Tsuchiya et al., 2012). Infiltration of immune cells was not prominent within the muscle of HF-fed mice in the current study. However, enrichment in genes associated with M2 polarization was detected in HF-Foxo$^{\Delta}$ compared to HF-Foxo$^{L/L}$ mice, consistent with the

induction of an anti-inflammatory skeletal muscle environment. In adipose tissue endothelial cells, enhanced endothelial insulin sensitivity in obese mice has been linked with a shift in macrophage phenotype (Sun et al., 2016). Thus, it is plausible that the shift in macrophage phenotype observed in the current study occurs secondary to Foxo dependent changes in endothelial cell function.

The elevated circulating levels of fatty acids present in individuals with obesity and diabetes can induce a proinflammatory phenotype within peripheral tissues (Bilan et al., 2009; Pillon et al., 2015; Steinberg et al., 2000). Lipotoxicity associated with the ectopic deposition of fatty acids exacerbates this inflammatory state and skeletal muscle insulin resistance (Lee et al., 2006; Pan et al., 1997). Numerous genes related to lipid metabolism were differentially expressed, including fatty acid binding protein-4, which functions to enhance the trans-endothelial transport and metabolism of lipids (Iso et al., 2013). Overall, the function "fatty acid metabolism" was predicted to be activated in HF-Foxo$^{\Delta}$ mice, which may reduce lipotoxicity in these mice. Thus, the modulation of M2 polarization and lipid metabolism pathways in HF-Foxo$^{\Delta}$ mice may contribute to improved metabolic phenotype by protecting them from the inflammation and lipotoxicity typically associated with prolonged HF-feeding.

The exact cellular signals leading to the extensive changes in gene expression within the skeletal muscle of HF-Foxo$^{\Delta}$ remain to be clarified. The upstream regulator analysis suggests that cross-talk between TGFβ1 signalling and Foxo contributes to the observed reprogramming of gene expression, in HF-Foxo$^{\Delta}$ mice. Considering that FoxO proteins act as effectors of the canonical TGFβ signal pathway (Seoane et al., 2004), it is possible that reduction of endothelial FoxO proteins substantially alters the TGFβ-dependent transcriptome to evoke the observed pro-angiogenic, anti-inflammatory and lipid metabolism phenotypes observed in HF-Foxo$^{\Delta}$ mice.

In conclusion, this study provided novel evidence that endothelial Foxo1 acts as a brake on the angiogenic process and contributes to the progression metabolic dysfunction. Expansion of the skeletal muscle capillary bed in concert with modulation of cellular processes such as lipid metabolism and repression of inflammation may be fundamental determinants of the beneficial effects induced by a reduction in endothelial FoxO proteins. Moreover, these results illustrate a potential mechanism by which microangiopathy and the progression to tissue ischemia may be initiated during the development of type 2 diabetes. Overall, these findings provide mechanistic insight into the functional role of FoxO proteins in regulating endothelial cell phenotype and highlight the importance of the microvascular niche in modulating the development of metabolic disturbances.

Chapter 5:

High-fat diet pre-conditioning improves microvascular remodeling during regeneration of ischemic mouse skeletal muscle

5.1 Contributions:

I was involved in the development of the conceptual and experimental framework used in the current study. My specific contributions to experiments included administration of high-fat diets, metabolic testing, ligation surgeries/laser doppler imaging, isolation of capillary fragments and histological assessments of microvascular remodelling post-ischemia. Additional contributions were made by fellow lab members and collaborators: Matthew DeCiantis performed some histological assessments (Fig. 5.1G-H, 5.2B-C, 5.6C-G), RNA analyses in skeletal muscle homogenates (Fig. 5.2D-E, 5.4D-E) and assisted with assessments of perfusion recovery (Fig. 5.3). Martina Rudnicki performed qPCR analyses in capillary fragments (Fig. 5.2F-H, 5.4F) and assisted with Ki67 immunostaining and subsequent quantification of proliferating cells (Fig. 5.4G-H). Alexandru Pulbere assisted with histological quantifications of myocyte regeneration and microvascular remodelling (Fig. 5.1E-F, 5.5A-D, 5.6A-B). Stephanie Milkovich and Chris Ellis were responsible for performed hemodynamic assessments performed at the University of Western Ontario. Since I was not directly involved in the assessment of hemodynamics which were performed using a separate age-matched cohort of mice, I did not include these data in the main body of my thesis but have included them in Appendix B for reference.

5.2 Published Data:

All data in this chapter have previously been published:

***Nwadozi, E.** [1], *Rudnicki, M. [1], *DeCiantis[1], M., Milkovich, S. [2], Pulbere[1], A., Roudier, E. [1], Birot, O. [1], Gustafsson, T. [3,4], Ellis, C.G. [2], and Haas, T.L. [1] (2020). High fat diet pre-conditioning improves microvascular remodeling during regeneration of ischemic mouse skeletal muscle. Acta Physiol. doi:10.1111/apha.13449.

[1]School of Kinesiology and Health Science, Faculty of Health, York University, Toronto, Canada; [2]Department of Medical Biophysics, University of Western Ontario, London, ON. Canada. [3]Department of Laboratory Medicine, Clinical Physiology, Karolinska Institutet, Stockholm, Sweden; [4]Department of Clinical Physiology, Karolinska University Hospital, Stockholm, Sweden

***Equal contributions**

5.3 **Chapter Summary**

Background/Rationale

Having investigated the coordination of capillary remodelling during the progression of obesity, my next aim was to examine how microvascular remodelling contributes to cardiovascular complications that arise due to prolonged/unresolved obesity. Specifically, I focused on peripheral artery disease (PAD) since the severity of the disease is largely dependent on microvascular remodelling processes within skeletal muscle. Insulin resistance and type-2 diabetes increase the incidence and severity of PAD, in part, due to the development of microangiopathies (i.e. endothelial dysfunction). In the preceding chapters, I demonstrated that HF-feeding is associated the expansion of the skeletal muscle capillary network despite the upregulation of both pro- and anti-angiogenic stimuli. Here, I asked whether positive microvascular adaptations prior to the onset of ischemia could influence post-ischemia skeletal muscle recovery in a mouse model of PAD. I hypothesized that HF pre-conditioning in mice would enhance microvascular expansion, post-ischemia perfusion recovery and muscle regeneration.

Objectives

1) Assess the influence of HF pre-conditioning on hemodynamic, structural and functional adaptations within skeletal muscle

2) Compare microvascular remodelling responses, perfusion recovery and muscle regeneration between NC- and HF-fed mice in early (4 days) and regenerating (14 days) phases following the induction of ischemia.

Experimental Approach

HF pre-conditioning was achieved by administering a HF diet for a total of 9 weeks to establish metabolic dysfunction and elicit adaptations within the microvasculature. Skeletal muscle ischemia was induced by unilateral ligation of the common femoral artery and post-ischemia recovery was tracked over 14 days while mice were still maintained on their respective diets. Hemodynamic assessments were assessed by intravital microscopy. Perfusion recovery was tracked by laser doppler imaging. Capillary and arteriole remodelling within EDL muscles were used as indicators of microvascular remodelling. Myocyte regeneration, fibrosis and adipose tissue accumulation within skeletal muscle was used to assess tissue regeneration.

For detailed methods, refer to Chapter #7, including methods pertaining to the HF-preconditioning of C57BL6/J mice (#7.2.1), femoral artery ligation surgery (7.2.5), isolation of microvascular fragments (7.2.6) as well as histological assessments of microvascular remodeling (#7.3.2.1), vascular cell proliferation (#7.3.2.2c), cellular infiltration into skeletal muscle (#7.3.2.3) and skeletal muscle regeneration (#7.3.2.4).

5.4 **Results**

Influence of HF-Diet Pre-Conditioning on Metabolic, Structural and Capillary Haemodynamic Characteristics Within Skeletal Muscle

Male C57BL/6J mice were randomized into a NC- or HF-diet for a total of 9 weeks to elicit a pre-conditioning response. HF pre-conditioning was associated with a greater body weight gain (Fig. 5.1A), elevated fasting plasma glucose levels (Fig. 5.1B) and impaired insulin sensitivity (Fig. 5.1C,D) after 7 weeks of diet. NC- and HF-fed mice displayed similar skeletal myofiber cross-sectional areas within the extensor digitorum longus (EDL) muscle (Fig. 5.1E,F). However, high succinate dehydrogenase (SDH) activity, indicative of increased oxidative potential, was detectable in a greater proportion of the muscle of HF- compared to NC-fed mice (Fig. 6.1G,H).

Capillary network organization, visualized by intravital microscopy, was equivalent between NC- and HF-fed mice (Fig. 5.2A). These mature networks were characterized by dominantly long capillary segments oriented parallel to the muscle fibres, with few interconnecting transverse segments. Neither capillary diameters (4.4± 0.05 vs 4.2± 0.06 μm) nor capillary haematocrit (21.2± 0.8% vs 19.4± 1.3%, NC vs HF) was affected by diet. Transit rates (velocities) of red blood cells (RBC) through capillaries were greater in HF- relative to NC-fed mice, which were accompanied by higher RBC supply rates and RBC oxygen saturations in the HF diet-fed mice (Fig. 5.2B-D). The significantly higher RBC supply rate and oxygen saturation resulted in a substantially higher mean oxygen supply in the HF group (Fig. 5.2E). Together, these data indicate that HF diet pre-conditioning induced metabolic and hemodynamic adaptations within skeletal muscle consistent with an increased capacity for oxygen delivery.

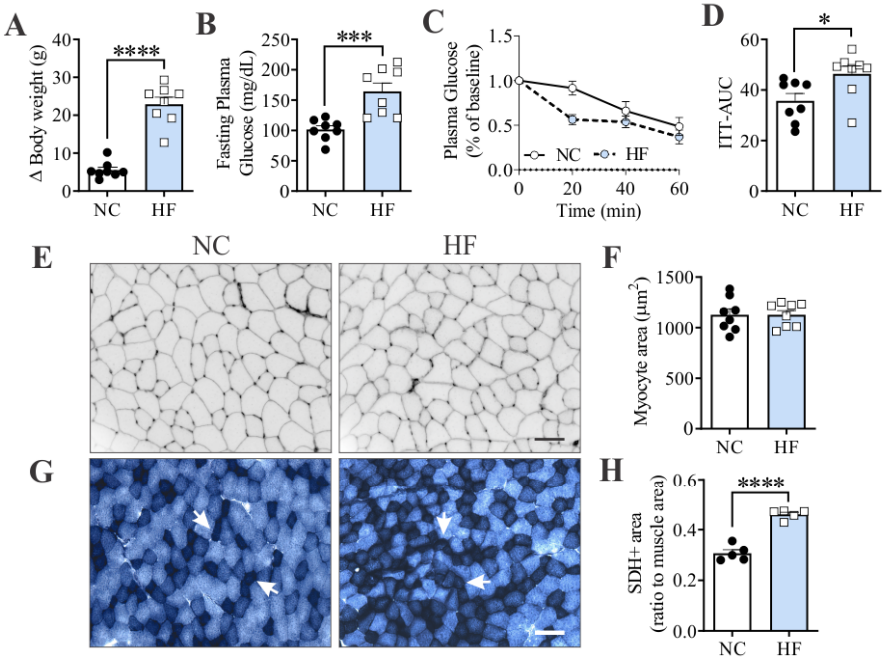

Figure 5.1

Muscle characteristics after 9-weeks of NC or HF diet.
Male C57Bl/6J mice were fed NC or HF diets beginning at 6 weeks of age. After 7 weeks of diet, A) body weight gain B) and fasting (4hr) blood glucose levels were assessed. An insulin tolerance test (ITT) was performed at the same time-point, represented as C) a line graph and corresponding D) area under the curve (AUC) graph. E) EDL muscle cross sections were stained with wheat germ agglutinin (WGA) to delineate myocyte membranes. F) Myocyte cross-sectional areas were measured from three independent fields of view per animal. G) Succinate Dehydrogenase (SDH) was detected using a colorimetric enzyme activity assay. H) The relative proportion of oxidative fibres was quantified by calculating the fractional area of muscle containing intermediate/high levels of SDH activity (indicated by white arrows). Scale bars= 50μm. *$P < .05$, ***$P < .001$ and ****$P < .000$ vs. NC-fed mice; Student's t test.

Muscle Damage and the Initiation of Vascular Remodelling in the Early Phase of Ischemia

Unilateral ligation of the common femoral artery induced an immediate severe (~90%) reduction of paw blood flow as assessed by laser doppler imaging. After 4 days, representing the early stages of post-ischemia recovery, both diet groups demonstrated modest improvements in paw blood flow (~25% that of the contralateral limb; Fig. 5.3A). Within ischemic skeletal muscles, a marked infiltration of immune cells (Fig. 5.3B,C) and significant reduction in the mRNA levels of adult fast myosin (*Myh2*; Fig 5.3D) was evident in both NC- and HF-fed mice, indicative of substantive muscle damage. Lower post-ligation levels of *Vegfa* mRNA were detected within ischemic

muscles independent of diet (Fig. 5.3E), which may also reflect the extent of myocyte damage, considering skeletal myocytes are the predominant source of VEGF-A within skeletal muscle.

To examine the influence of HF-diet on microvascular cells in the early phase of ischemia recovery, we assessed indicators of endothelial cell survival and activation in isolated capillary fragments. mRNA level of *Vegfa*, considered to play an autocrine survival role in endothelial cells (Lee et al., 2007), was not altered by ischemia but exhibited a tendency to increase with HF-diet (P= 0.07; Fig. 5.3F). HF-diet was associated with an increase in *Foxo1* mRNA level only in the non-ischemic limb (Fig. 5.3G). In addition, a diet-independent increase in *Ki67* mRNA was detected in isolated capillary fragments (Fig. 5.3H), indicating the initiation of endothelial cell proliferation within the ischemic muscles of both NC- and HF-fed mice at this time point.

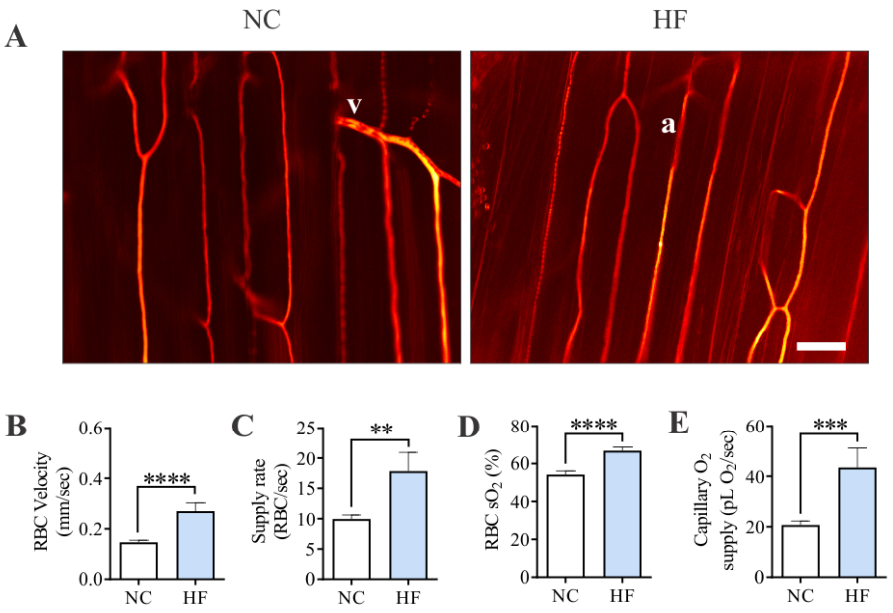

Figure 5.2

Capillary hemodynamics after 8 weeks of NC or HF diet.
Male C57Bl/6J mice were fed NC or HF diets for a total of 8 weeks. (A-E) Intravital microscopy of EDL muscles was used to collect baseline data for capillary hemodynamics. A) Representative optical density images are shown (E) to illustrate typical capillary network structures. Red/yellow colours indicate capillaries with moving red blood cells (RBCs). "a" and "v" designates arteriole and venule, respectively. B) RBC velocity, C) capillary supply rate D) and RBC oxygen saturations were assessed from video images. E) Capillary O2 supply was calculated from supply rate and oxygen saturation data. Scale bar= 50µm. $^{**}P < .01$, $^{***}P < .001$ and $^{****}P < .0001$ vs NC-fed mice; Student's t test.

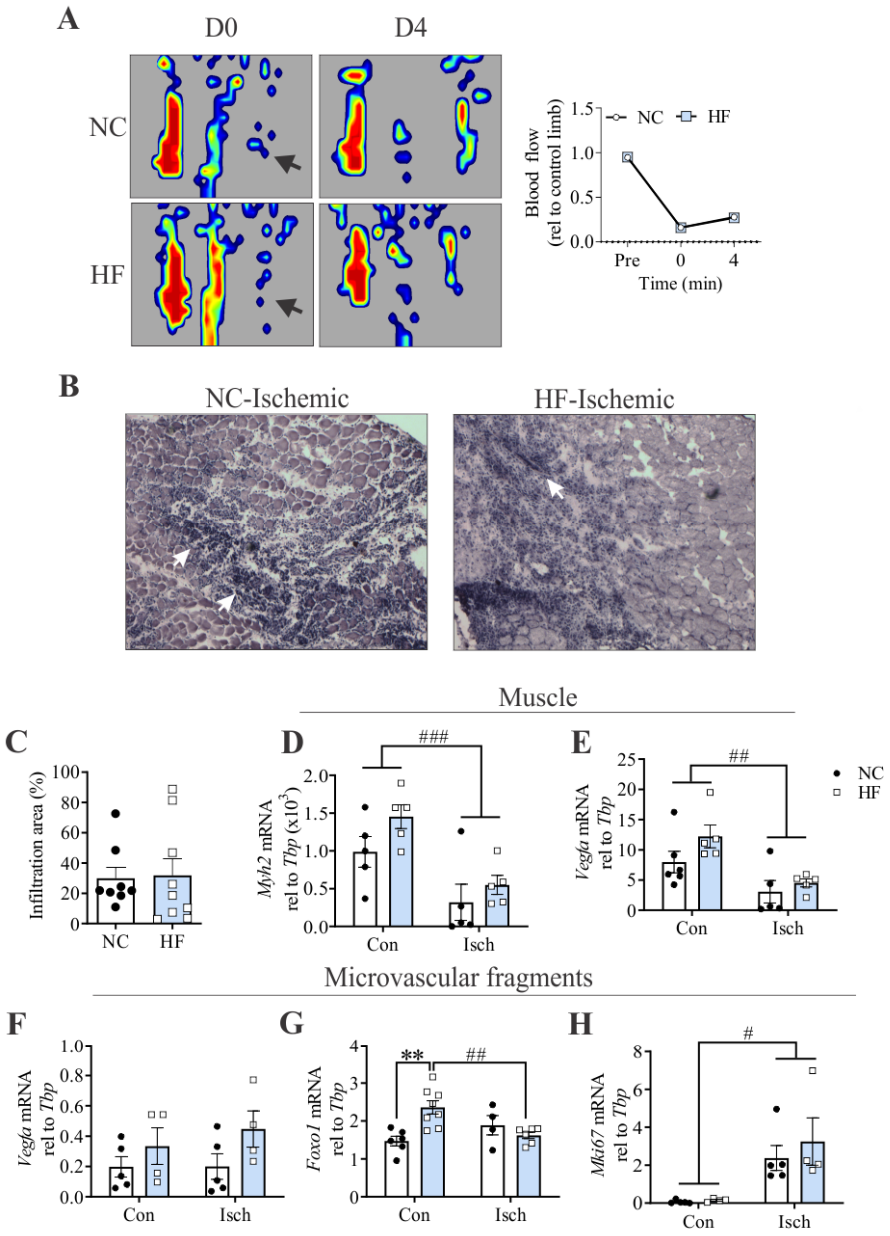

Figure 5.3

Blood flow recovery and muscle characteristics 4 days post-ligation.
Laser Doppler imaging was used to assess paw blood flow in the ligated and contralateral non-ligated leg at baseline (Pre), immediately following ligation (day 0) and at 4 days post-ligation. A) Representative images are shown for the days 0 and 4 time points, with black arrows indicating the ligated limb. Paw blood flow in the ligated limb was quantified and represented as a ratio to that of the control limb. B) Haematoxylin and Eosin (H&E) of the EDL muscle was used to demarcate regions of immune cell infiltration (arrows) post-ligation. C) These regions were quantified as a percentage of cross-sectional muscle area. mRNA levels of D) adult myosin heavy chain (*Myh2*) E) and *Vegfa* were analysed in plantaris muscles of control (Con) and ischemic (Isch) limbs. (F-H) Microvascular fragments isolated from control and ligated limb muscles were assessed for F) *Vegfa*, G) *Foxo1* (H) and *Mki67* mRNA. **P*<0.05 vs. respective NC mice. #*P* < .05, ##*P* < .01 and ###*P* < .001 vs control limbs; two-way ANOVA with Bonferroni post-hoc test.

Capillary Hemodynamics and Oxygen Delivery Capacity Increased in Regenerating Muscle of HF Diet-Fed Mice

Intravital imaging was utilized to visualize the intact capillary network structure, hemodynamics and oxygen delivery capacity of regenerating EDL muscles at 14 days post-ligation. Capillary network remodelling was evident in both diet groups, resulting in more capillary loop structures and transversely oriented short capillary segments than was seen in control muscles (Fig. 5.4A). RBC velocity and supply rates within individual capillary segments were modestly but significantly elevated in HF vs NC diet-fed mice (Fig 5.4B,C). Capillary haematocrit did not differ between groups (26.0 ± 0.7% vs 28.1 ± 0.8%, NC vs HF). Although RBC oxygen saturation levels were not different between diet groups (Fig 5.4D), capillary O2 supply was significantly higher in the HF-fed group (Fig 5.4E). In sum, these data indicate greater recovery of blood flow, both globally and at the capillary level, in regenerating muscles of HF-fed mice.

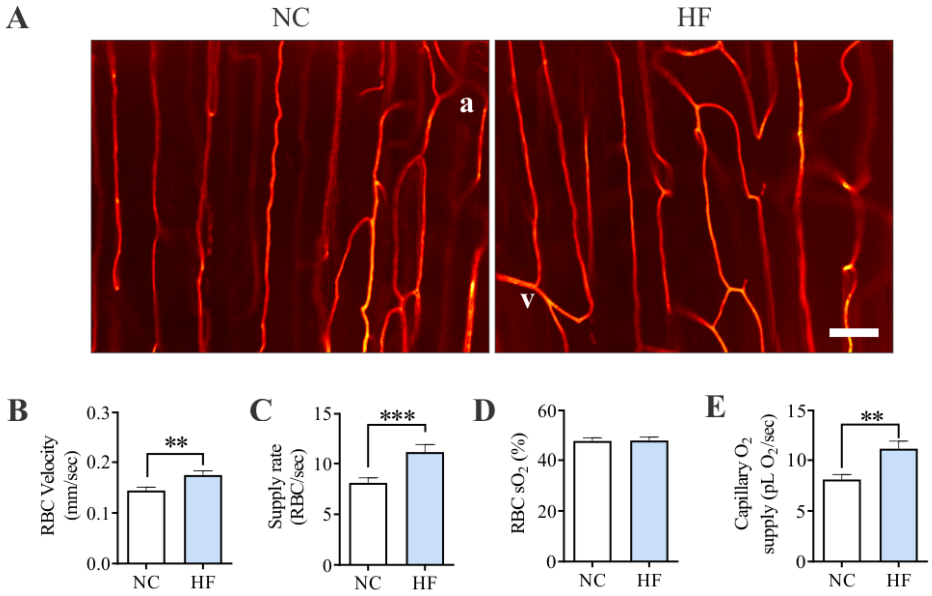

Figure 5.4

Capillary hemodynamics recover better in HF-fed regenerating muscles.
Representative optical density images are shown A) to illustrate typical capillary network structures of the EDL muscle 14 days after ligation. Red/yellow colours indicate capillaries with moving red blood cells (RBCs). a, v designates arteriole and venule, respectively. B) RBC velocity, C) capillary supply rate and D) RBC oxygen saturations were assessed from video images. E) Capillary O2 supply (E) was calculated from supply rate and RBC O2 saturation values. White and blue bars represent NC and HF diet conditions respectively. Scale bar = 50µm. $^{**}P < .01$ and $^{***}P < .001$ vs NC, respectively, Student's t test.

HF Diet Pre-Conditioning Augments Post-Ischemia Blood Flow Recovery, Angiogenesis and Arteriolarization

In a second cohort of age-matched NC- and HF -fed mice, blood flow recovery up to 14 days post-ligation was assessed by laser doppler imaging. In NC- and HF-fed mice, paw blood flow improved from 0 to 4 days post-ligation but no significant recovery beyond that time point was detected with NC feeding (Fig. 5.5A,B). At 14 days, paw blood flow in HF-fed mice was significantly higher than that of NC-fed mice (Fig 5.5A,B). Since the paw (comprised largely skin and tendons) (Wong et al., 2006) is a region with minimal metabolic activity, limb blood flow was also assessed in this cohort as an indicator of bulk flow to muscle and skin of the leg. At days 4 and 7, perfusion in the ligated limbs of HF-fed mice was significantly greater than that of NC-fed mice and this tendency was maintained at day 14 (P= 0.09; Fig. 5.5C,D).

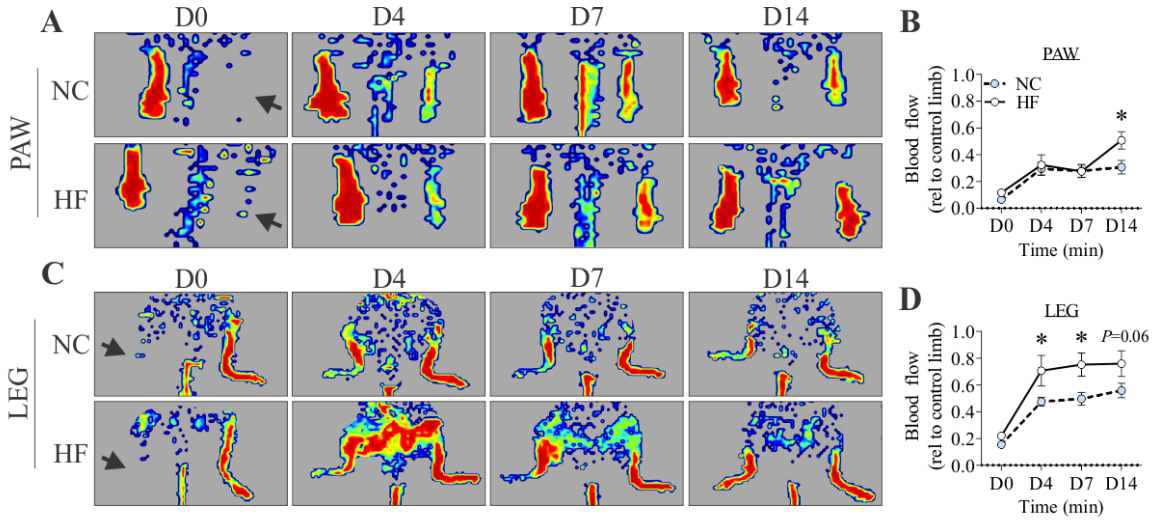

Figure 5.5

Blood flow recovery in ligated limbs at 14 days post-ligation.
Representative laser Doppler images for the A) dorsal paw C) and hindlimb regions at days (D) 0, 4, 7 and 14 post-ligation. Black arrows indicate the position of the ligated limb in each set of images. Quantification of these recordings was represented as a perfusion ratio between the ligated and contralateral non-ligated limb (B, D). *P < .05, vs respective NC mice, two-way ANOVA with Bonferroni post-hoc test.

Histological analysis was used to further investigate microvascular remodelling in the regenerating EDL muscle. Representative images of capillaries in control and regenerating EDL muscles 14 days post-ligation is shown (Fig. 5.6A). Capillary density was elevated in HF fed mice only ($P <$ .001; Fig. 5.6B). However, we considered that the high number of transverse capillaries may result in the under-representation of capillary content when expressed as capillary density, thus we also calculated the microvascular area relative to muscle cross-sectional area. Microvascular area was elevated in the regenerating muscles in both diet groups compared to control muscles, but HF-fed mice exhibited substantially higher microvascular areas compared to NC-fed mice (Fig 5.6C). Consistent with the morphological evidence of capillary growth, substantial increases in mRNA for *Pecam1* (endothelial cell marker) and *Efnb2,* an endothelial regulator of sprouting angiogenesis (Wang et al., 2010) were detected in the regenerating skeletal muscle of mice from both diets (Fig 5.6D,E). Interestingly, at this time point, *Ki67* mRNA remained moderately elevated in microvascular fragments from the ligated limb of NC- but not HF-fed mice (Fig 5.6F), suggesting ongoing vascular cell proliferation in the NC-fed mice. Immunostaining for Ki67 (Fig 5.6G) revealed that >75% of microvessel-associated Ki67+ cells in both diet groups were endothelial, based on overlap with lectin staining (Fig 5.6H).

Smooth muscle actin (SMA) staining of the EDL muscle identified arteriolar and venular microvessels and a population of small SMA+ vessels having a diameter < 10μm, which we defined as SMA+ capillaries (Honkura et al., 2018; Thurston et al., 1998) and may represent newly formed arterioles (Peirce and Skalak, 2003; Skalak et al., 1998) (Fig. 5.7A). The number of SMA+ capillaries was elevated in the regenerating muscle of both diet groups, but a substantially greater number was detected in HF-fed mice (Fig 5.7B). Thus, regenerating muscles from HF diet-fed mice were characterized by both angiogenesis and the formation of small arterioles from existing

capillaries (arteriolarization). HF mice also exhibited an increase in the total number of larger SMA+ microvessels (arterioles, venules; >10 μm diameter) within the regenerating muscle, as compared to NC-fed mice (Fig 5.7C). The average diameter of these larger microvessels (>10 μm) was unaltered by ischemia or diet (Fig 5.7D). Thus, regenerating muscles from HF-diet fed mice were characterized by both capillary growth and increased numbers of small arterioles.

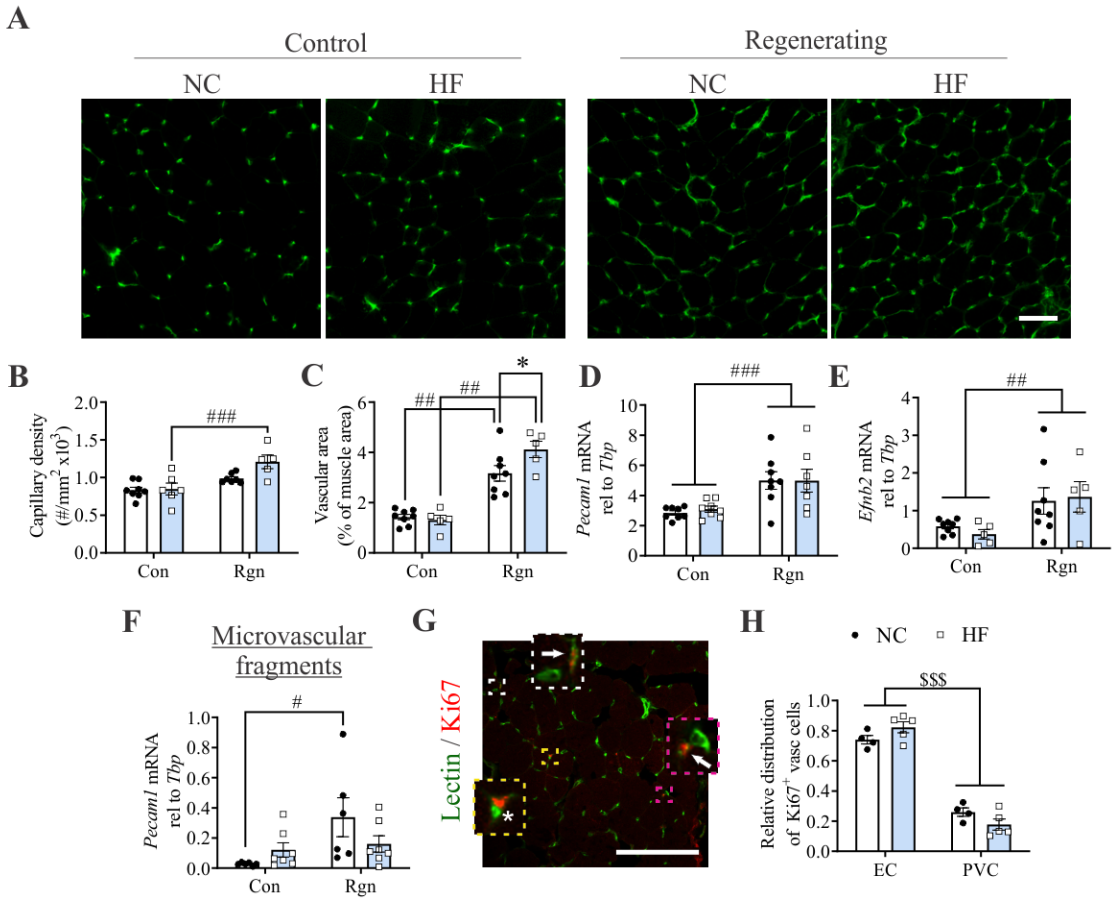

Figure 5.6

Greater capillary growth in regenerating muscle from HF-fed mice at 14 days post-ligation.
A) Representative images of *Griffonia simplicifolia* lectin-FITC stained (to detect capillaries) control and regenerating EDL cross sections of diet-fed mice 14 days post-ligation. B) Capillary density C) and vascular area was calculated from up to 3 independent fields of view. mRNA levels of D) *Pecam1* and E) *Efnb2* were assessed in control (Con) and regenerating (Rgn) plantaris muscles as molecular markers of angiogenesis. F) *Mki67* mRNA was measured in isolated microvascular fragments from control and regenerating hindlimb muscles, as an indicator of vascular proliferation. In regenerating EDL muscles, G) proliferating (Ki67+) endothelial (EC, white arrow) and perivascular (PVC, asterisk) cells were detected by immunofluorescence H) and quantified relative to the total number of Ki67+ nuclei in the vascular compartment (H). Scale bars= 100μm. ##P < .01 and ###P < .001 vs respective control limbs; *$$$P*<0.001 vs. EC group; two-way ANOVA with Bonferroni post-hoc test.

HF Diet Pre-Conditioning Reduces Fibrosis and Adipocyte Accumulation in Regenerating Skeletal Muscle

To determine whether enhanced vascularization and perfusion recovery in HF diet-fed mice were associated with improved muscle recovery, we assessed several indicators of muscle regeneration at 14 days post-ligation. At this time point, there was no difference between diet groups in myocyte cross-sectional areas (Fig 5.8A,B), indicating a similar extent of recovery amongst the regenerated myocytes. Interestingly, adipocyte accumulation in the skeletal muscle interstitium was greater in regenerating muscles from NC- compared to HF-fed mice (Fig. 5.8C,D). Further, picrosirius red staining revealed a greater deposition of fibrillar collagen within the regenerating muscle of NC- compared to HF-fed mice (Fig. 5.8E,F), which corresponded with elevated levels of *Cola1* mRNA in NC-fed mice (Fig. 5.8G). Together, these data indicate that HF diet pre-conditioning mitigates ischemia-induced ectopic fat accumulation and fibrosis within skeletal muscle.

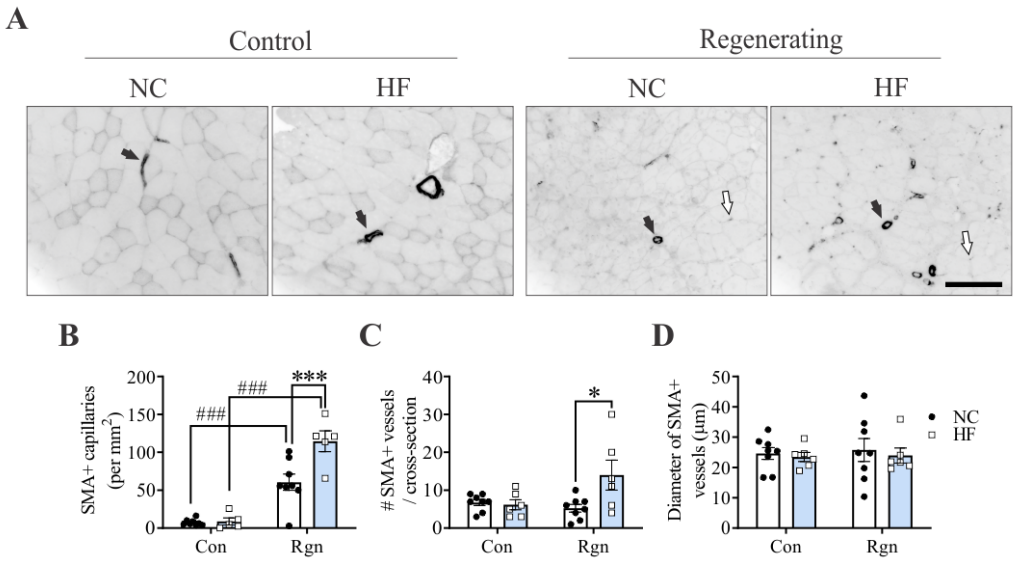

Figure 5.7

Higher arteriole numbers in HF diet-fed regenerating muscles 14 days post-ligation.
A) Cy3-anti-αSMA staining was used to visualize arterioles in control (Con) and regenerating (Rgn) EDL muscle cross-sections. Grayscale images were inverted to improve staining visibility. B) SMA+ capillaries (<10µm in diameter, indicated by white arrows), C) arteriole (>10µm in diameter, indicated by black arrows) density D) and diameter were quantified. Scale bars= 100µm. **P*<0.05, ****P*<0.001 vs. respective NC mice. ###*P* < .001 vs respective control limbs; two-way ANOVA with Bonferroni post-hoc test.

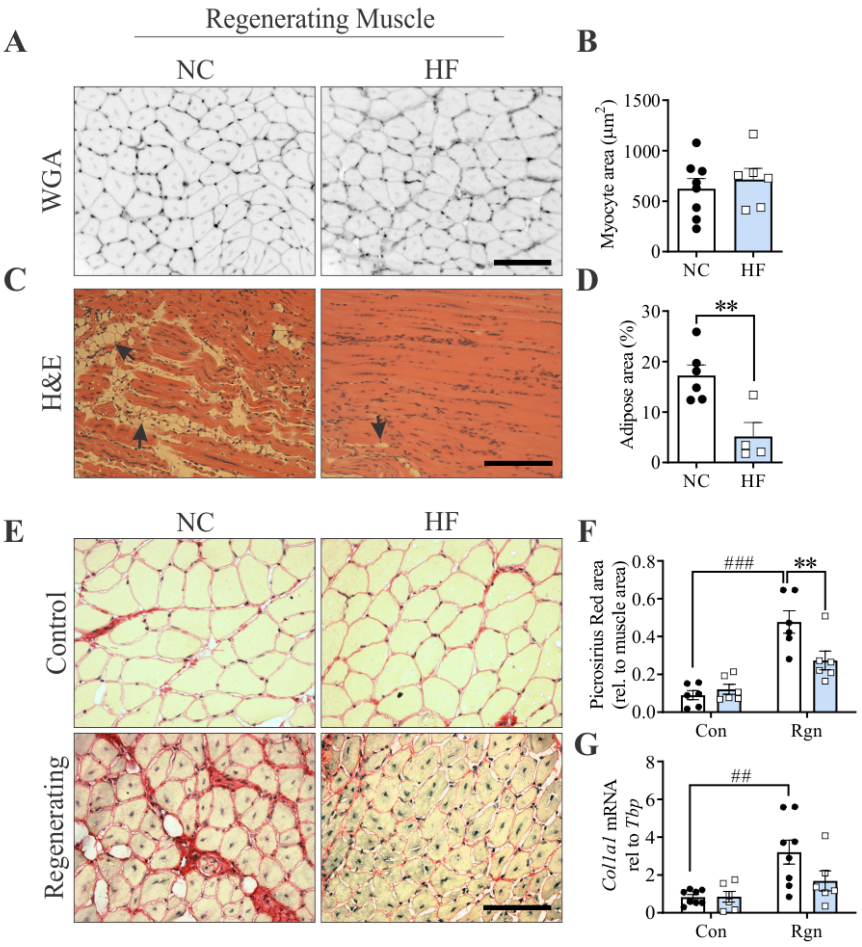

Figure 5.8

Less adipocyte accumulation and fibrosis in HF-fed muscles 14 days post-ligation.
A) WGA staining was used to detect myofibre membranes in the regenerating EDL muscle from NC- and HF-fed mice at 14 days post-ligation. Grayscale images were inverted to improve visibility of staining. B) Myocyte cross-sectional areas were assessed from three fields of view per animal. C) Adipocyte regions were visualized in H&E stained longitudinal sections from regenerating limbs. Arrows point to adipocytes. D) The relative adipocyte area (%) was quantified. E) Picrosirius red staining to detect fibrillar collagen was performed in control and regenerating EDL muscles and F) relative area within the muscle quantified as an indicator of fibrosis. G) mRNA levels of Col1a1 was also assessed as a molecular marker of fibrosis. Scale bars= 100 µm. $^{**}P<0.01$ vs. respective NC mice. $^{\#\#}P< 0.01$, $^{\#\#\#}P < .001$ vs. respective control limbs; two-way ANOVA with Bonferroni post-hoc test.

5.5 **Discussion**

In this study, we found that a HF-diet pre-conditioning enhances post-ischemia skeletal muscle recovery. Diet pre-conditioning was shown to 1) accelerate perfusion recovery, 2) enhance angiogenesis and arteriolarization and 3) reduce fat accumulation and fibrosis within regenerating muscles. Together, these findings support the idea that positive adaptations to a fat-enriched diet can be beneficial for muscle regeneration.

Diet-preconditioning elicited structural and functional adaptations within skeletal muscle that increased the oxidative metabolic capacity prior to the ischemic insult. The increased oxidative potential observed in the myocytes is consistent with previous reports that showed elevated mitochondrial capacity previously shown in skeletal muscles of mice fed a HF-diet (Thomas et al., 2014; Turner et al., 2007). In the current study, we show that hemodynamic adaptations support this phenotype shift by enhancing capillary oxygen supply within skeletal muscle. Increased RBC velocity observed under basal conditions could not be explained by changes in haematocrit, capillary diameter or vascular remodelling, providing indirect evidence that HF diet promoted vasodilation within intact muscle under resting conditions. Higher RBC velocities would result in elevated shear stress in the capillaries of HF-fed mice, resulting in enhanced endothelial cell survival and function following exposure to ischemia, since shear stress is well established to promote protective signalling that evokes a healthy endothelial cell phenotype (Chistiakov et al., 2017; Zhou et al., 2014).

Successful recovery from an ischemic insult requires the coordinated expansion of arterial and capillary networks to restore bulk flow and distribution of blood, respectively. Our data show that diet pre-conditioning resulted in greater perfusion recovery in HF-fed mice and this was associated with enhanced angiogenesis and arteriolarization despite a similar induction of endothelial cell

proliferation between NC- and HF-fed mice in the early phase of ischemia recovery. We observed a decrease in *Vegfa* mRNA levels within ischemic skeletal muscles, likely due to extensive myocyte damage that resulted from ischemia (Olfert et al., 2009). In contrast, *Vegfa* mRNA levels showed a tendency to increase when assessed in capillary fragments isolated from ischemic skeletal muscles. However, endothelial-derived VEGF-A is more important for endothelial survival and insufficient for vascular remodelling (Gerber et al., 1998). Thus, our data do not support a role for VEGF-A as the trigger for post-ischemia vascular remodelling. Downregulation of *Foxo1* mRNA within microvascular endothelial cells may have facilitated enhanced vascular remodelling in the skeletal muscles of HF-fed mice by relieving the angiostatic signals associated with this transcriptional regulator (Wilhelm et al., 2016). HF-induced increases in capillary Foxo1 protein levels was previously shown (Chapter #4, Fig. 1B) whereas capillary-level assessment of Foxo1 in ischemic muscle has not previously been reported. It is possible that the inflammatory microenvironment present following induction of ischemia counteracted the HF-induced increase in *Foxo1* mRNA (Ludikhuize et al., 2007). Resolving the contributions of specific signalling pathways to the enhanced vascular remodelling response in HF-diet pre-conditioned mice requires further investigation.

The regenerating muscles from HF diet-fed mice also exhibited evidence of more arteriolarization when compared to NC diet-fed counterparts, based on a greater density of SMA+ microvessels at 14 days post-ligation. Capillary hemodynamic assessments were congruent with this conclusion. Particularly, the higher RBC velocities and supply rates within individual capillaries in the regenerating EDL of HF diet-fed mice, despite the more extensive capillary network in these muscles, could be achieved only if the capillary network was supplied with higher total blood flow. The increased density of arterioles, as detected by histology, would facilitate this greater blood

supply to the capillaries. Vasodilation was not assessed in the current study, but it may have contributed to the more rapid recovery of limb blood flow in HF diet-fed mice (which was significantly greater as early as 4 days post-ligation) as well as to the observed patterns of capillary hemodynamics in regenerating muscle at the 14-day time point. Notably, the microvascular remodelling within the regenerating muscle of HF diet-fed mice enabled better recovery of oxygen delivery capacity per capillary compared to NC diet-fed mice.

Diet pre-conditioning also reduced interstitial fibrosis and adipocyte accumulation in regenerating skeletal muscles. This finding is important considering the prominence of these features in the ischemic myopathy that is prevalent in PAD patients (Pipinos et al., 2007, 2008). Post-ischemia fibrosis and ectopic fat accumulation involve fibro-adipogenic progenitors (FAP) that differentiate into collagen-secreting fibroblasts and/or adipocytes (Biferali et al., 2019; Judson et al., 2013; Uezumi et al., 2010, 2011). Shear-stress induced release of nitric oxide may inhibit FAP adipogenesis by repressing the transcriptional activity of PPARγ, the master regulator of adipogenesis (Cordani et al., 2014). Interestingly, previous reports have shown that nutrient availability can influence the process of FAP differentiation (Marinkovic et al., 2019; Mogi et al., 2016; Radley-Crabb et al., 2011; Teng and Huang, 2019). Thus, altered fatty acid availability in HF-fed mice may have influenced the differentiation potential of FAPs. Further investigations are required to delineate the causal relationship between diet pre-conditioning and muscle regeneration following ischemic damage.

Based on our findings, we propose that adaptive responses triggered locally within the microvasculature and skeletal myocytes by HF pre-conditioning facilitated the observed post-ischemia vascular remodelling and muscle regeneration responses. An alternative possibility is that the caloric (and fat) content of the NC diet was inadequate to support the energy-intensive

processes associated with tissue regeneration. Furthermore, the size of adipose depots at the time of ischemic injury may have impacted the outcomes both by establishing the amount of available energy reserve and by acting as a source of factors that regulate vascular remodelling (Chen et al., 2018). Furthermore, it is possible that the initial physiological adaptations in response to HF-feeding are temporary and can eventually become overwhelmed by chronic exposure to HF-induced stressors, resulting in accumulation of intramuscular triglycerides and development of inflammation and fibrosis. This transition is likely influenced by age, genetics, diet composition and duration.

In conclusion, the current study provides evidence to support a novel perspective that HF-induced adaptations poise skeletal muscle to undergo enhanced post-ischemia vascularization, resulting in enhanced perfusion recovery and as a consequence, reduced fibrosis and lipid accumulation. Future studies to elucidate molecular pathways that link HF-diet preconditioning with enhanced vascular remodelling and tissue regeneration are important and may uncover novel therapeutic targets for the repair of ischemic muscle in conditions such as PAD.

Ongoing investigations into the role(s) of endothelial FoxO proteins in the regulation of post-ischemia skeletal muscle recovery are currently underway and my preliminary findings are summarized in Appendix C.

Chapter 6: Concluding Remarks

6.1 Perspectives

The prevalence of obesity has been on a steep incline over the last 4 decades and according to prospective global estimates, over 1 billion individuals will be obese by the year 2030 if current trends continue unabated (Kelly et al., 2008). Obesity represents a major public health challenge and economic burden because it substantially increases an individual's risk for developing diseases such as type-2 diabetes, cardiovascular disease, cancer, musculoskeletal disorders and neurodegenerative conditions (Anandacoomarasamy et al., 2008; Anstey et al., 2011; Chooi et al., 2019; Kim and Basu, 2016; Lauby-Secretan et al., 2016). Not surprisingly, considerable efforts have been made to develop effective preventative and therapeutic strategies against obesity-related diseases. However, these efforts have had limited long-term success to date (Blüher, 2019).

Fundamentally, obesity arises due to an imbalance between energy intake and disposal. The latter involves several organ systems that act in concert to regulate the uptake, breakdown and storage of energy substrates in order to maintain metabolic homeostasis. Ultimately, the metabolic function of these organs hinges on the supply of energy substrates and regulatory hormones within the tissue microenvironment. Thus, the vasculature is arguably the most critical determinant of energy homeostasis and should be at the forefront of research efforts focused on developing novel therapeutic strategies against obesity-related diseases.

A considerable body of experimental and clinical vascular-centric research into obesity has demonstrated an undisputed link between endothelial dysfunction and the development of obesity-related diseases (Bakker et al., 2009; Jager et al., 2000; Rattigan et al., 2007; Serné et al., 2001). However, to date, very few studies have investigated the influence of obesity on capillary number and the consequences of microvascular remodeling on clinical sequalae that arise secondary to

obesity. My dissertation set out to address this knowledge gap by defining the molecular control of capillary remodeling in obesity. Specifically, my research work focused on skeletal muscle because it comprises a large portion (40%) of total body mass, is the primary determinant of peripheral insulin resistance and glucose disposal and is one of the few tissues capable of undergoing post-natal capillary remodeling.

Based on the discordance in capillary remodeling responses between genetic (leptin- and leptin receptor-resistant rodents) and physiological models of obesity, I first investigated a potential role for leptin, an adipokine that is elevated in obesity, in the physiological regulation of skeletal muscle capillary homeostasis. Then, considering the well-documented metabolic and angiostatic influences of FoxO proteins, I hypothesized that the negative influence of these proteins on skeletal muscle capillarity would contribute to the progression of metabolic dysfunction in obesity. This led to investigations of obesity-induced capillary remodeling in transgenic mice deficient for all 3 FoxO proteins within the endothelium. Finally, I investigated whether microvascular adaptations to obesity could impact perfusion recovery and skeletal muscle regeneration in a mouse model of peripheral artery disease, providing clinical insight into the therapeutic benefits of vascular-centric therapies against obesity-induced pathologies (Key findings from this dissertation are illustrated in Fig. 6.1). This work has contributed valuable insights towards our understanding of the progression of obesity and the potential therapeutic benefit of vascular-centric therapies, which will be discussed in detail below.

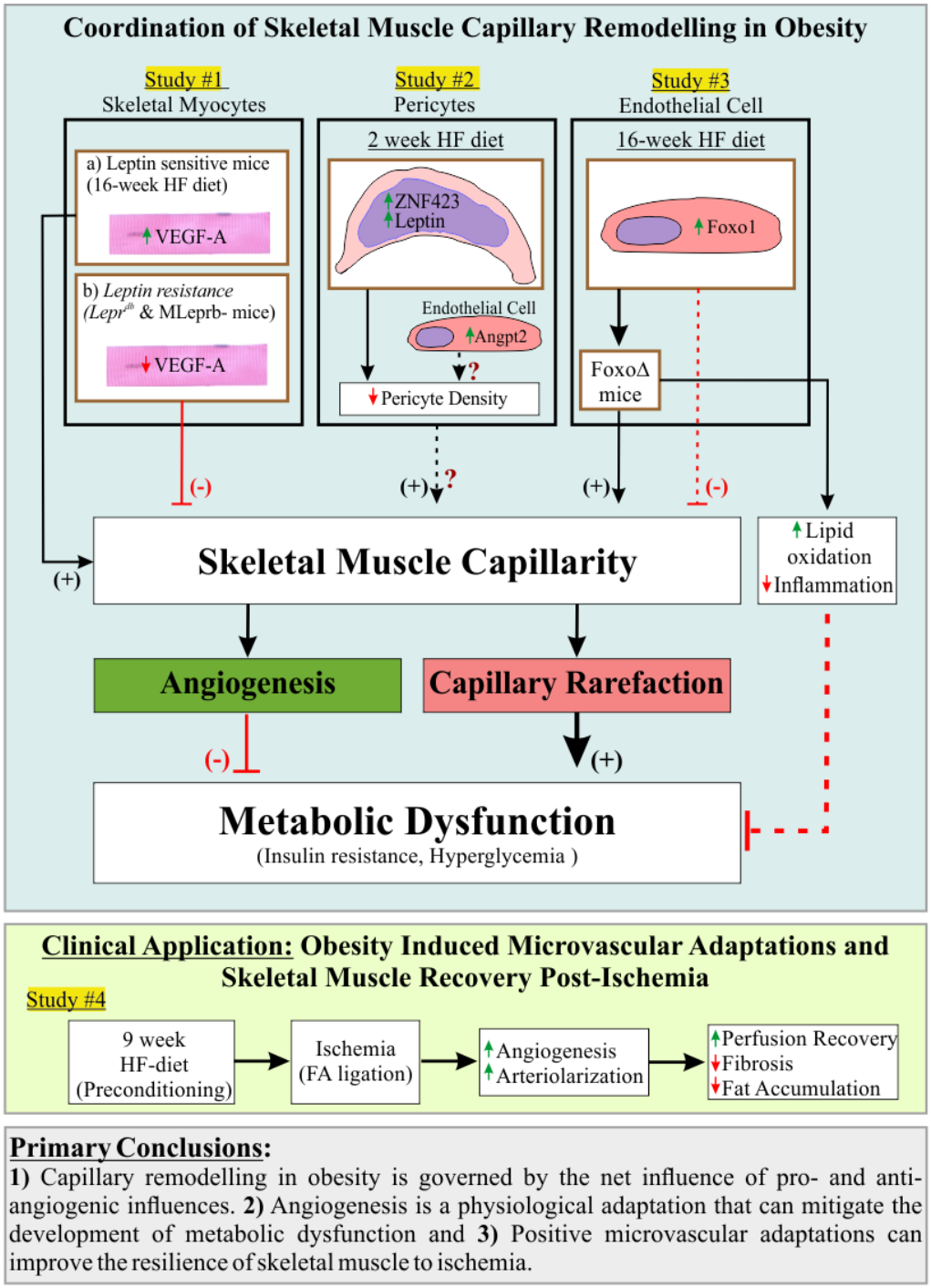

Figure 6.1: Summary of Key Findings (solid lines) and Inferences (dotted lines) made in the current dissertation. Prolonged administration of a high-fat (HF) diet was associated with increased levels of VEGF-A and angiogenesis within skeletal muscle **(Study #1a)**. Leptin resistance was associated with reduced skeletal muscle VEGF-A levels and impaired post-natal angiogenesis. **(Study #1b)** Nutrient overload provoked pericytes to adopt a preadipocyte phenotype and was associated with reduced pericyte density, both of which may promote angiogenesis **(Study #2).** Foxo$^{\Delta}$ mice exhibited enhanced angiogenesis, an over-representation of lipid metabolism and anti-inflammatory genes, and did not develop metabolic dysfunction following 16-weeks of HF-feeding **(Study #3)**. HF-preconditioning was associated with enhanced microvascular remodelling, perfusion recovery and tissue regeneration following femoral artery (FA) ligation to induce ischemia **(Study #4)** . (+) and (-) denote a positive and negative effect, respectively.

6.2 Novel Contributions to the Field

The current dissertation elucidates novel concepts that advance our current understanding about the pathogenesis of obesity and illuminates several intriguing avenues for further research

6.2.1 Angiogenesis is a Physiological Adaptation to Obesity that Contributes to the Preservation of Metabolic Homeostasis

The most significant contribution of my research work is the idea that obesity induces angiogenesis within skeletal muscle. This remodelling response was shown to be a necessary adaptation to mitigate the onset of metabolic dysfunction, similar to metabolic adaptations (i.e. increased fat oxidation) that have been shown to occur within myocytes (Lundsgaard et al., 2019). A significant barrier that has limited our understanding of capillary remodelling in obesity is the often-contradictory response observed between diet-induced and genetic leptin-signalling deficiency models of obesity. Here, I unveiled a substantial limitation in the use of genetic models of obesity by demonstrating unequivocally that leptin resistance alters skeletal muscle capillarity independent of obesity. As such, the dominant 'obesity-induced capillary rarefaction' theory, developed primarily using genetic models, is comparatively non-physiological due to the confounding influence of leptin resistance. Thus, my findings establish a novel paradigm whereby angiogenesis is a physiological adaptation during obesity that preserves metabolic homeostasis.

From a therapeutic sandpoint, this finding is important because it demonstrate the potential that stimulating skeletal muscle angiogenesis has as an effective mitigating strategy against the development of insulin resistance and type-2 diabetes. Furthermore, I showed that HF-preconditioning enhanced the capacity for skeletal muscle to undergo microvascular remodelling under ischemic conditions, leading to enhanced perfusion recovery and tissue regeneration, despite the concomitant presence of metabolic dysfunction. Thus, generating a skeletal muscle

environment conducive for microvascular growth enhanced the resilience of skeletal muscle to ischemic stress and may be a viable strategy against cardiovascular complications and other clinical sequalae of obesity.

The regulation of this capillary adaptation likely involved intricate intercellular coordination between pericytes, endothelial cells and myocytes, that modified the expression of angiogenic factors (i.e. VEGF-A, FoxO) and pericyte-endothelial interactions to facilitate microvascular growth in response to an appropriate trigger (i.e. chronic nutrient overload, ischemia). Interestingly, endothelial cell depletion of FoxO proteins elicited a gene signature consistent with enhanced lipid metabolism and the generation of an anti-inflammatory phenotype, indicating a broader influence of endothelial cells beyond its role in microvascular remodelling. This endothelium-dependent response was predicted to occur downstream of the TGFβ1 signalling pathway, demonstrating potential crosstalk between TGFβ1 signalling and endothelial FoxO proteins in modulating the skeletal muscle microenvironment in obesity.

6.2.2 Potential Role of Pericytes as Energy-Sensing Cells That Coordinate Myocyte and Microvascular Adaptations Within Skeletal Muscle

Most intriguing from these investigations, was the novel observation that nutrient overload provoked preadipocyte lineage commitment amongst skeletal muscle pericytes, demonstrating that a physiological stimulus such as nutrient overload can disrupt pericyte stemness and potentially alter their identity. In the current study, we found that nutrient overload resulted in the induction of leptin synthesis within the pericyte cell population. Considering leptin role as a rheostat for energy homeostasis, I propose a novel role for pericytes as local “energy-sensors” within skeletal muscle that couple circulating levels of nutrients with paracrine signals to promote adaptations such as angiogenesis (Artwohl et al., 2002; Bouloumié et al., 1998; Garonna et al., 2011) and

enhanced fatty acid oxidation (Dyck, 2009). This energy-sensing role of pericytes may serve as a feed-forward mechanism that elicits changes within skeletal muscle to facilitate the disposal of excess nutrients. Moreover, pericytes are multipotent progenitors and it is possible that multi-lineage differentiation or lack thereof contributed to the improved microvascular remodelling and muscle regeneration responses observed in the ischemic muscles from HF-preconditioned mice. Although these considerations were beyond the scope of the current dissertation, my findings lay the foundation for clinically-relevant research investigating the relationship between pericyte plasticity and skeletal muscle adaptations during the clinical progression of obesity.

6.3 **Study Limitations**

1. The conclusion drawn from the current dissertation, which postulates that obesity promotes adaptive angiogenesis within skeletal muscle to preserve metabolic homeostasis, is based on studies performed on relatively young mice (i.e. HF-diet administered beginning at ~6 weeks of age). Considering that the capacity of skeletal muscle to undergo angiogenesis declines with age (Ambrose, 2015), my hypothesis can only be applied with confidence to young and relatively healthy populations. However, the global prevalence of obesity is markedly greater in middle-aged and old cohorts (i.e. >35 years of age) (Hodges et al., 2018). Thus, future studies are required to test the validity of my theory in older populations.

2. As previously mentioned, a known limitation of the Mx1-Cre driver, which was used for inducible depletion of endothelial FoxO proteins in chapter 4, is the simultaneous induction of Cre expression in other tissues including hepatocytes and immune cells (Kühn et al., 1995). While depletion of FoxO proteins in hepatocytes likely did not have and influence on peripheral insulin sensitivity, we cannot completely exclude the influence liver Foxo depletion on other systemic indicators of metabolic homeostasis (i.e. fasting glucose levels) (Matsumoto et al., 2007). However, our lab has since generated a different mouse model of inducible endothelial Foxo1 depletion using the endothelial-specific PDGFB promoter to drive Cre expression. Using this model, we have since observed a similar influence of endothelial Foxo1 depletion on fasting glucose levels (Rudnicki et al., 2018). Thus, I am confident in the validity of my conclusions.

6.4 **Future Work**

The role(s) that pericytes play in skeletal muscle adaptations to both nutrient overload and ischemia is also an area of interest for future studies. Specifically, the mechanisms by which leptin influence myocyte and endothelial cell functions within skeletal muscle. These investigations would involve an unbiased assessment of the pericyte secretome following exposure to nutrient overload (i.e. palmitate, glucose) or hypoxic conditions (simulating ischemia), to identify novel proteins (i.e. beyond leptin) that may influence skeletal muscle function. The specific roles of the identified proteins can then be validated in transgenic mice deficient for these pericyte-secreted proteins. In the context of ischemia, the contribution of pericytes to the tissue regeneration response can further be assessed by lineage tracing studies to determine whether pericytes contribute to arterialization, fibrosis and adipocyte accumulation post-ischemia.

Also, to further investigate the therapeutic potential of vasculo-centric therapies against the clinical progression of obesity, expansion of the capillary network could be achieved pharmacologically (i.e. VEGF-A, prazosin, Foxo inhibitors) after the development of obesity-induced metabolic dysfunction and indicators of metabolic homeostasis (i.e. insulin/glucose tolerance) and post-ischemia skeletal muscle regeneration (i.e. perfusion recovery, microvascular remodelling, tissue regeneration) assessed.

Chapter 7: Materials & Methods

7.1 Human Studies

Human studies were approved by the Regional Ethics Review Board in Stockholm (Dnr2006/1232-31/1, 2010/786-31/3, Dnr2012/173-31/3, DNR2012/753-31/2) and performed in accordance with the 1964 Helsinki declaration. Histological assessments of human skeletal muscles (Chapter #3) were made in biopsies from 3 healthy non-smoking young men collected using the percutaneous needle technique, cleaned of connective tissue and frozen in liquid nitrogen cooled isopentane as previously described (Strömberg et al., 2017). Mean (range) age, height, and weight of volunteers were 25 (24–27) year, 179 (173–187)cm, and 73 (70–74) kg, respectively. Informed written consent was obtained from all participants following explanation of the experimental procedures.

7.2 Animal Studies

All animal studies were approved by the York University Committee on Animal Care (#2017-19R3, #2017-20R3) and performed in accordance with the American Physiological Society's guiding principles in the care and use of animal models and the University of Western Ontario Animal Care and Use Committee (#2016-045; for intravital microscopy studies [Chapter #5]). Mice were housed under a 12:12 h light/dark cycle with free access to food and water. Tissue collection was conducted under isofluorane anesthesia and mice were euthanized by exsanguination.

7.2.1 **Transgenic Mouse Models**

Chapter #2

Leptin Receptor Mutant (Lepr^{db}) Mice

Male homozygous leptin receptor mutants on a C57BL/6J background (B6.BKS(D)-*Leprdb/J*; referred to as *Lepr^{db}*) and age-matched wild-type C57BL/6J mice were purchased from The Jackson Laboratories (Bar Harbor, ME, USA) and used for experiments at 13 weeks of age. Four-week-old *Lepr^{db}* mice were generated by crossing *Lepr^{db}/Lepr+* mice and genotype was confirmed by PCR analysis (http://www.jax.org).

Myocyte-Specific Leptin Receptor Knockout Mice (MLepRb-)

Age- and gender-matched skeletal myocyte specific leptin resistant mice were generated by crossing mice in which Cre recombinase is expressed under control of the muscle creatine kinase promoter (MCKCre; #006475, The Jackson Laboratories, Bar Harbor, ME, USA)(Brüning et al., 1998) with mice harbouring loxP sites flanking exon 17 of the leptin receptor gene (LepR$^{fl/fl}$ mice; A kind gift from Dr. Martin Myers, originally generated in the lab of Dr. Streamson Chua (McMinn et al., 2004) that is critical for intracellular signalling. The MLepRb genotype (Chapter #2, Fig. 4A) was confirmed by PCR analysis of DNA extracted from ear punches, skeletal muscle and adipose tissue using the following forward (5'AATGAAAAAGTTGTTTTGGGACGA 3') and reverse (5'CAGGCTTCAGAACATGAACACAACAAC 3') primers

NG2DsRed Mice

Hemizygous NG2DsRed mice [stock Tg(Cspg4-DsRed.T1)1Akik/J] expressing a red fluorescent protein variant (DsRed) under the control of the neural/glial antigen-2 (NG2, gene name: Cspg4) promoter (Zhu et al., 2008) were purchased from Jackson Labs (#008241) and crossed to generate mice NG2DsRed-positive and non-carrier (control) mice used in the current study.

Chapter #4

Endothelial Foxo1/3/4 deficient mice

Male FVB/N mice harbouring an endothelial directed deletion of Foxo1/3/4 ($Mx1Cre^{+}$;$Foxo1,3,4^{L/L}$) and corresponding age-matched $Mx1Cre^{-}$;$Foxo1,3,4^{L/L}$ littermates (referred to as $Foxo^{\Delta}$ and $Foxo^{L/L}$, respectively) (Paik et al., 2007) were used for studies. At 4 weeks of age, mice received 3 separate injections of polyinosine:cytosine (500mg/injection *i.p.*; InvivoGen, San Diego, CA, USA) to transiently induce Cre expression. $Foxo^{\Delta}$ exhibit a 70–80% reduction of Foxo1 and Foxo3 but undetectable levels of Foxo4 within the endothelium (Paik et al., 2007; Roudier et al., 2013).

Chapter #5

C57BL/6J mice

Male C57BL/6J mice from Jackson Labs, pre-conditioned with NC or HF diets consisting of 10% and 60% kcals from fat (#D12450B, #D12492, Research Diets) beginning at 6 weeks of age, were received at 13 weeks of age and used in experiments at 14 weeks of age, after 8 weeks of diet. One group of mice was used directly for intravital microscopy assessments to assess diet effects while the remaining mice underwent femoral artery ligation (as described in chapter #7.2.5). A subset of the mice, received at 5 weeks old, were diet preconditioned at York University, so that body weights could be recorded through-out the 8-week diet.

7.2.2 **Administration of High-Fat Diet**

For diet comparisons, mice were randomized into normal chow (NC) and high-fat (HF) diet groups beginning at approximately 6-8 weeks of age and for a total of 2, 9 and 16 weeks as indicated in the specific studies. In chapters 2 and 4, diets had a protein: fat: carbohydrate composition of 16:11:73 %kcal (NC) and 17:58:25 %kcal (HF) (#D12329 and #D12331, respectively). In

Chapters 3 and 5, diet protein: fat: carbohydrate composition was 20:10:70 %kcal (NC) and 20:60:20 %kcal (HF) (#D12450J and #D12429, respectively; Research Diets, Inc., New Brunswick, NJ, USA). Diets were administered *ad libitum* and, in some studies, body and food weight were recorded weekly.

7.2.3 **Metabolic Testing**

Insulin tolerance tests (ITT)

ITTs were conducted after a 4-hour fast period. Blood glucose was measured by glucometer (Aviva Accu-Chek; Roche Diagnostics, Indianapolis, IN, USA) at 0, 20, 40- and 60-minutes following insulin injection (0.75U/kg; Humalog) into the intraperitoneal cavity.

Glucose tolerance test (GTT)

GTT was performed following an overnight (~16 hour) fast and blood glucose at 0, 30, 60, 90, 120- and 180-minutes following glucose injection (1.75g/kg, *i.p.*).

7.2.4 ***In-vivo* and *Ex-vivo* stimulation of mouse skeletal muscles**

Insulin

Skeletal muscles were analyzed to assess vascular dependent and independent myocyte insulin sensitivity, respectively. For *in-vivo analysis*, mice were maintained under isoflurane anaesthesia; 1 extensor digitorum longus (EDL) muscle was removed and snap frozen. Mice were then injected with 0.12U insulin (*i.p.*) and after 15 min, the contralateral EDL was removed and snap frozen. For *ex-vivo* analysis, *extensor hallucis proprius* (EHP) muscles were removed from both legs, preincubated in HEPES-saline buffer, then stimulated either with fresh HEPES-saline buffer (control) or insulin (25mU/mL; Humalog; Lilly, Scarborough, ON, Canada) for 30 mins at 37°C.

Muscles were subsequently snap frozen in liquid nitrogen. Protein analyses (described later) was then performed to assess insulin-induced activation of Akt.

Leptin

Ex-vivo stimulation of the EDL muscle with leptin was used to assess leptin-responsiveness in MLepRb mice (Chapter #2, Figure 4F). Muscles were removed from both legs and stimulated either DMEM (1g/L glucose, control) or recombinant leptin (498-OB-01M; R&D Systems, Minneapolis, MN, USA) for 4-hours at 37°C.

7.2.5 Mouse Model of Femoral Artery Ligation

Unilateral ligation of the common femoral artery was conducted by isolating the femoral artery immediately distal to its exit from the abdominal wall, tying it with a double-knot (6-0 suture) and closing the skin with sutures (5-0). Mice received buprenorphine (0.05 mg/kg, s.c.) for pain relief and ampicillin (20mg/kg in drinking water for 4 days) to prevent infection.

Hindlimb and paw blood flow was assessed prior to and immediately post-ligation surgery (day 0), then subsequently on days 4, 7 and 14 by laser doppler imaging (Perimed, Stockholm, Sweden), with mice under light isoflurane anaesthesia and positioned on a warming pad. Relative blood flow was expressed as a perfusion ratio of the ligated limb (paw) and the corresponding region in the contralateral non-ligated leg (Mandel et al., 2017). At days 4- or 14- post-ligation, mice were euthanized while under isoflurane inhalation anaesthesia and hindlimb muscles were excised from both ligated and non-ligated legs for subsequent protein, RNA and histological analyses. Several hindlimb muscles were also used to isolate capillary fragments, as described below.

7.2.6 **Isolation of Cell Fragments from Mouse Skeletal Muscle**

Microvascular fragments

Chapter #4

NC and HF WT FVB/N mice underwent cardiac perfusion of polystyrene magnetic beads (8.0 3 107 beads/mouse; PM-50-10; Spherotech, Lake Forest, IL,USA). These beads (5–6μm diameter) lodge within the capillaries, enabling magnetic collection of the capillaries (Takemoto et al., 2002). Hindlimb muscles were minced and digested with 0.2% collagenase type II (17101-015; Thermo Fisher Scientific Life Sciences, Burlington, ON, Canada) and subsequently, magnetic separation was used to collect bead-filled capillary segments. Protein was extracted and analyzed by Western blot.

Chapters #3 and #5

Microvascular fragments were isolated from skeletal muscles from NC-/HF-fed mice (2 or 9 weeks, Chapter #3) and from control/ligated hindlimbs (Chapter #5). Muscles were separately minced then enzymatically dissociated by agitation in 0.2% (w/v) Collagenase Type II (LS004177; Worthington Biochemical Corp., Lakewood, NJ, USA) for 30 minutes at 37°C. Following centrifugation and washes to neutralize collagenase activity, the cell suspension was incubated with CD144 (#555289, BD Biosciences, San Jose, USA) coupled to Dynabeads (#14311D, ThermoFisher Scientific, Mississauga, Canada) for 1 hour at 4°C to enable coating of microvascular fragments with beads. Afterwards, microvascular fragments were selected with a magnet, washed twice with PBS, and immediately lysed with TRIzol (#15596026, ThermoFisher Scientific) for RNA analyses.

PDGFRα+ and PDGFRβ+ cells

Chapter #3

In mice fed a NC- or HF-diet for 2 weeks, PDGFRα+ and PDGFRβ+ cells were isolated using dynabeads conjugated to CD140a (#135902) and CD140b (#136002, BioLegend) antibodies, respectively, following collagenase digest (2-hours) and filtration through a 100-μm cell strainer. All antibody incubations were performed at 4 °C for 20 min and selection performed using a magnet. Isolated cellular fractions were immediately lysed with Trizol, for RNA analyses.

7.3 Histological Assessments

7.3.1 Cryopreservation of Skeletal Muscles

For transverse sections, plantaris, *extensor digitorum longus* (EDL) and soleus muscles were excised, embedded in optimal cutting temperature (OCT) compound and immediately frozen by immersing OCT-embedded tissues in cooled isopentane then liquid nitrogen before storing at -80°C. For longitudinal sections (used in Chapter #3, Fig. 6C), EDL muscles were excised into a paraformaldehyde (3.7%) solution (1 hour) and infiltrated with 2 changes (15% and 30%) of sucrose prior to cryopreservation. In human studies (Chapter #3), vastus lateralis biopsies were obtained using the percutaneous needle biopsy technique and immediately underwent cryopreservation. 10μm thick transverse muscle slices (from muscle mid-belly) and 20μm thick longitudinal slices were prepared and used in staining protocols described below.

7.3.2 Staining Protocols

7.3.2.1 Capillarity, arterioles and myocyte cross-sectional area (Chapter #2, #3, #4 and #5)

Capillaries, arterioles, and the connective tissue surrounding myocytes were detected in plantaris and EDL cryosections using *Griffonia simplicifolia isolectin* B4 (1:100; Vector Laboratories,

Burlington, ON, Canada), Cy3-anti-α-smooth muscle actin (SMA) antibody (1:300; C6198; Sigma-Aldrich, Oakville, ON, Canada) and wheat germ agglutinin (WGA)-CF350 (#29021-1; Biotium) respectively. For transverse sections, digital images were captured using an Axiovert 200 M microscope (x10x or ×20 objective; Zeiss, Oberkochen, Germany) equipped with a digital CCD camera and Metamorph software. For longitudinal sections (Chapter #3, Figure 6C), images were captured with a Zeiss LSM700 inverted confocal microscope equipped with a PLAN-Apochromat 20×/0.8 M27 objective and are presented as maximal intensity projections. Morphometric assessments of capillaries, arterioles and myocyte cross-sectional area were made by a blinded observer (using Metamorph or ImageJ Software) from at least 2 non-overlapping fields of view per muscle, encompassing most of the muscle area.

7.3.2.2 Intracellular localization of Leptin, Foxo1 and Ki67 (Chapter #3, #4 and #5)

For intracellular visualization of proteins, transverse skeletal muscle cryosections were fixed in paraformaldehyde for 15 minutes, then blocked/permeabilized in blocking buffer (5% donkey/goat serum + 0.05% Triton X-100 in PBS) for 30 minutes prior to incubation with primary (2-hours at room temperature or overnight at 4°C) and secondary (1-hour at room temperature) antibodies, as described below. Specificity of secondary antibodies was confirmed with secondary only negative controls for all staining protocols.

a) Cellular localization of leptin (Chapter #3) was visualized in mouse soleus muscles or vastus lateralis human biopsies using a rabbit anti-leptin antibody (1:200, #16227, Abcam) diluted in blocking buffer and co-stained with the following goat antibodies: anti-mouse PDGFRα (1:100, #AF1026), anti-mouse PDGFRβ (1: 100, #AF1042), anti-human PDGFRα (1:100, #AF-307-NA), or anti-human PDGFRβ (1:100, #AF385, R&D systems). Intramuscular lipids were detected with Alexa Fluor488 BODIPY (0.25μg/mL, #D3922, ThermoFisher Scientific)

and capillaries were visualized in mouse and human sections using Dylight 649-Simplicifolia isolectin B4 (1:50, #DL-1208) and *Ulex Europaeus Agglutinin* (1:50, #DL-1068, Vector Laboratories), respectively. Alexa Fluor488 donkey anti-rabbit (#705-165-147) and Cy3 conjugated donkey anti-goat (#711-545-152) cross-adsorbed secondary antibodies (1:400; Jackson Immunoresearch) were used as appropriate. All images were captured with a Zeiss LSM700 inverted confocal microscope equipped with either the EC PLAN-Neofluar 40×/1.30 Oil M27 or Plan-Apochromat 63×/1.40 Oil DIC M27 objectives with identical gain and exposure settings across samples.

b) Foxo1+ capillaries (Chapter #4) were detected by co-staining isolectin (rhodamine G. *simplicifolia isolectin* B4; 1:100; Vector Laboratories) with rabbit anti-Foxo1 (1:50; PLA0084-100; Sigma-Aldrich) or normal rabbit IgG (cat no. 2729; Cell Signalling Technology) and Alexa Fluor488 goat anti-rabbit IgG (1:300; A11008; Thermo Fisher Scientific Life Sciences).

c) To detect vascular cell proliferation (Chapter #5), EDL muscle sections were incubated overnight with rabbit anti-ki67 antibody (1:100, #16667, Abcam), followed by Alexa Fluor647 goat anti-rabbit (1:400; Jackson Immunoresearch, #111-607-008), DAPI (Vector Laboratories, H-1200) and FITC-*Griffonia simplicifolia* lectin I (GSL) (#FL-1101; Vector Laboratories, Inc). Images were captured with a Zeiss LSM700 inverted confocal microscope, using the EC PLAN-Neofluar 40x/1.30 Oil or Plan-Apochromat 63x/1.40 Oil DIC objectives.

7.3.2.3 Cellular Infiltration into skeletal muscle (Chapter #4 and #5)

Cellular infiltration into skeletal muscle of NC- and HF-fed was assessed by toluidine Blue (Chapter 4) and Haematoxylin and Eosin (H&E, Chapter 5) to visualize basic muscle morphology. For toluidine blue (chapter #4), transverse plantaris cryosections from NC- and HF-fed $FOXO^{L/L}$ and $FOXO^{\Delta}$ mice were fixed in 3.7% paraformaldehyde and incubated in toluidine blue solution

(10 mg ⁄ mL toluidine blue in 70% ethanol, diluted 1:10 in 1% NaCl) for 20 minutes. Sections were rinsed with PBS and mounted with AquaPerm media (Fisher Scientific, Whitby, ON, Canada).

Haematoxylin & Eosin staining (chapter #5) was performed on transverse EDL cryosections 4-days post-ligation surgery according to manufacturer's instructions (Mayer's Haematoxylin: #26306-01; Eosin Y: #26051-10, Electron Microscopy Sciences). Images were captured on an inverted Olympus microscope (Toluidine blue- 20x; H&E- 4x) using a digital colour CCD camera (Hitachi; Applied Biosystems, Burlington, ON, Canada). H&E images were stitched (Image J) and nuclei-dense areas of infiltration were traced and quantified relative to muscle cross-sectional area.

7.3.2.4 Skeletal Muscle regeneration (Chapter #5).

a) Fibrosis within Ischemic Skeletal Muscle

Picrosirius red staining [0.06% w/v Direct Red 80 (#365548-5G; Sigma-Aldrich) in picric acid] (Hadi et al., 2011) was used to detect fibrillar collagen within EDL muscle cross-sections 14-days after the ligation surgery (Chapter #5). 2-3 fields of view per muscle were captured on an inverted Olympus microscope (10x) using a digital colour CCD camera (Hitachi; Applied Biosystems, Burlington, ON, Canada). Colour-thresholding on the red (fibrotic) stain was used to quantify fibrotic area relative to muscle cross-sectional area (Image J).

b) Adipose Tissue Accumulation in Ischemic Skeletal Muscle

To assess adipose tissue accumulation within ischemic skeletal muscle (Chapter #5), regenerating EDL muscles were immersed in 3.7% formaldehyde and paraffin embedded. Longitudinal sections (6 µm thick) were prepared and stained with H&E (The Centre for Phenogenomics; Toronto,

Canada). The region of muscle occupied by adipocytes was quantified relative to the total area of the muscle tissue using Image J.

7.4 **Cell Culture**

Leptin and Insulin Treatment of Mouse and Human Skeletal Muscle Cells

C2C12 myoblasts were cultured on gelatin-coated flasks with DMEM (11960-044; Invitrogen) supplemented with 10% fetal bovine serum (Invitrogen, Burlington, ON, Canada), 50 μg/mL penicillin/streptomycin, 1% Glutamax (35050-061, Invitrogen), and 1 mM sodium pyruvate (Invitrogen). C2C12 myoblasts were seeded to confluence on 12-well tissue culture dishes and treated for 4 h with either 100 nM recombinant leptin (#498-OB-01M; R&D Systems) or 25 mU/mL insulin (Humalog), then processed for RNA analysis. For leptin treatments, cells were first pre-treated with inhibitors for PI3K (LY-294002, #440202) and JAK2 (AG-490, #658411) at concentrations of 10mM and 25mm, respectively (Calbiochem).

Human myoblasts were isolated from healthy individuals as previously described (Strömberg et al., 2016) and cultured on collagen-coated flasks with proliferation media consisting of DMEM/F-12 (11330-032; GIBCO) supplemented with 20% FBS, 50 μg/mL penicillin/streptomycin, and 1 mM sodium pyruvate. Human myotubes were differentiated in a 12-well tissue culture dish by seeding myoblasts to ~ 50% confluency and switching to differentiation media (containing only 2% FBS) for 5 days before leptin (100 nM) and insulin (25 mU/mL) treatments and RNA analysis. Human umbilical vein endothelial cells (HUVECs) (C-003-5C; Life Technologies, Carlsbad, CA) were cultured in Medium 200 (M200) supplemented with low-serum growth supplement and 1% antibiotic–antimycotic (Life Technologies).

TNFα, IL-6 and Palmitate Treatment of Skeletal Muscle Microvascular Endothelial Cells (Chapter #4)

Mouse skeletal muscle microvascular endothelial cells were isolated as previously described (Han et al., 2003) and cultured in gelatin-coated flasks with DMEM (11960-044; Invitrogen) supplemented with 10% fetal bovine serum (Invitrogen, Burlington, ON, Canada), 50 μg/mL penicillin/streptomycin, 1% Glutamax (35050-061, Invitrogen), and 1 mM sodium pyruvate (Invitrogen). Cells were plated to confluence in a 6-well tissue culture dish and treated overnight with recombinant TNF-a or IL-6 (PHC3015 and PHC0064, respectively; Thermo Fisher Scientific Life Sciences) or with albumin conjugated palmitate (Pillon et al., 2015) for 48-hours.

7.5 RNA Analysis

RNA extraction was performed on the following tissues as follows: Skeletal muscle: Total RNA from mouse gastrocnemius (Chapters #2, #3 and #4) and plantaris (Chapter #5) muscles was extracted using the RNeasy Fibrous Tissue Mini Kit (Qiagen, Inc. Toronto, ON, Canada). In human biopsies (Chapter #2), total RNA was extracted using TRIzol and alcohol precipitation (Invitrogen, Carlsbad, CA). Cellular Fragments: Total RNA was isolated from capillary fragments using TRIzol and alcohol precipitation. For PDGFRα+ and PDGFRβ+ cells (Chapter #3), isolated fractions were lysed in TRIzol and RNA purified using the RNeasy Micro Kit Qiagen, Inc. Toronto, ON, Canada). Cell culture experiments: For cell culture experiments using mouse cells, RNA extraction performed using Cells-to-cDNA II lysis buffer ThermoFisher Scientific, Burlington, ON, Canada. For human studies, RNA extraction was performed by lysis in TRIzol and alcohol precipitation (Invitrogen, Carlsbad, CA).

RNA concentrations were quantified spectrophotometrically by absorbance at 260 nm. ~150ng of total RNA was reverse transcribed using M-MLV reverse transcriptase (Mouse: #M0253, New

England Biolabs; Human biopsies: #28025021 Applied Biosystems, Carlsbad, CA). cDNA was analysed by Taqman real-time quantitative polymerase chain reaction (qPCR) using Taqman primer/probes (Listed in Table 1) and Mastermix (#4444963; ThermoFisher Scientific). Transcript levels are presented as $2^{-\Delta Ct}$.

7.6 **Transcriptome Analyses of HF-Foxo$^{L/L}$ and HF-Foxo$^{\Delta}$ Mouse Muscles (Chapter #4)**

Gene expression in the muscle of HF-Foxo$^{L/L}$ and HF-Foxo$^{\Delta}$ mice was analyzed on the MouseGene 2.0 platform at the Centre for Applied Genomics (The Hospital for Sick Children, Toronto, ON, Canada). Total RNA was isolated from plantaris muscles (n = 8/group) by RNeasy Fibrous Tissue Mini Kit (Qiagen, Inc.) and was quantified and quality checked on the BioAnalyzer System (Agilent Technologies, Santa Clara, CA, USA). Quality control and normalization were ensured with the AffyPLM and Oligo packages from Bioconductor on the R platform (http://www.bioconductor.org). All samples passed quality control, as assessed by mean-expression, normalized unscaled standard errors, run length encoding, and principal component analysis of raw expression values. Robust multiarray average (RMA) was used for normalization. Raw data and RMA-normalized expression values are publicly available [Gene Expression Omnibus no. GSE72576; National Institutes of Health (NIH), Bethesda, MD, USA] (https://www.ncbi.nlm.nih.cove/geo/). Annotation and filtering were performed with the mogene20sttranscriptcluster.db and Genefilter packages from Bioconductor. Probe sets were filtered by quantile, excluding those with an interquartile range below 0.5 from further analysis. Differential expression of probe sets was analyzed using the Linear Models for Microarray Data (LIMMA) package (Bioconductor), with the Bayesian adjusted $P < 0.1$.

Significantly up- and down-regulated probe-sets were analyzed for overrepresentation of gene ontologies by using the web-based Database for Annotation, Visualization, and Integrated

Discovery (DAVID) v6.7 (NIH National Institute of Allergy and Infectious Diseases) (https://david.ncifcrf.gov). Probe sets with a false-discovery rate (FDR) of ≤5% were analyzed for significant overlap with biologic functions and KEGG pathways (collaborative effort by University of Tokyo and University of Kyoto, Japan) (http://www.genome.jp/kegg/pathway.html). To correct for possible selection bias of genes, we used only probe sets found in the LIMMA analysis as background (Dennis et al., 2003). Ontologies overlapping with an FDR of ≤1% were categorized as significant. The web-based bioinformatics tool, Ingenuity pathway analysis (IPA; Qiagen) (http://www.ingenuity.com) was used to detect networks of genes and to identify associated functions. The Diseases and Functions tool was used to identify potential activated/inhibited signalling pathways. The Upstream Analysis tool was used to identify molecules that potentially explain the observed changes in gene expression (Krämer et al., 2014). For illustrative purposes, genes related to several functions of interest were visualized by using the heatmap function on the R platform. The z score of the $\log_2$ expression values of each observation was calculated and colour coded as red or green to represent expression levels above or below the mean, respectively. HF-Foxo$^{\Delta}$ mice were tested for enrichment of M1 and M2 marker genes by using a Wilcoxon gene set enrichment test, and the results were visualized by a barcode plot (Michaud et al., 2008). M1 and M2 genes were compiled from frequently used markers and from genes identified as differentially expressed in a transcriptome analysis of murine macrophages (Jablonski et al., 2015; Lawrence and Natoli, 2011; Mauer et al., 2014).

7.7 **Protein Analyses**

Western Blot

Protein extractions were performed using radioimmunoprecipitation assay (RIPA) lysis buffer supplemented with cOmplete protease inhibitor cocktail and PhosStop phosphatase inhibitor

tablets (Roche, Indianapolis IN). Muscle lysis was performed using the Retsch MM400 tissue lyser (Retsch GmbH, Haan, Germany)

20µg of protein per sample, as determined by BCA assay (Pierce, Fisher Thermo Scientific), was denatured and equivalent amounts of protein were separated using SDS-PAGE, then transferred to polyvinylidene difluoride membranes (Immobilon P; Fisher Thermo Scientific). A full list of primary and secondary antibodies used for western blots are provided in Table 2. Membranes were developed using enhanced chemiluminescence and densitometry analysis was performed with ImageJ Analysis Software (NIH).

Enzyme-Linked Immunosorbent Assay (ELISA)

ELISA was used to assess VEGFA protein levels in gastrocnemius muscle homogenates from mice fed a NC- or HF-diet for 16 weeks (Fig. 3.8). Protein was extracted in PBS using the Retsch MM400 tissue lyser (Retsch GmbH, Haan, Germany). 100ug of protein per sample was assessed using mouse VEGFA ELISA plates (DY493-05; R&D Systems, Minneapolis, MN, USA) according to manufacturer's directions.

7.8 **Statistical Analysis**

Data are presented as mean ± SEM. A two-tailed students t-test, one-way ANOVA or two-way ANOVA with Tukey or Bonferroni post-hoc tests was used as appropriate to analyse datasets (Prism 8; Graphpad software Inc; La Jolla, CA, USA). In all cases, $P< 0.05$ was considered statistically significant.

Table 7.1: Taqman primer sets	
Gene Name	**Probe Set ID**
Angpt2	Mm00545822_m1
Cebpa	Mm00514283_s1
Col1a1	Mm00801666_g1
Cspg4	Mm00507257_m1
Efnb2	Mm01215897_m1
Elane	Mm00469310_m1
Foxo1	Mm00490671_m1
Hprt1	Mm00446968_m1
Itgam	Mm00434455_m1
Leptin	Mm00434759_m1
Mki67	Mm01278617_m1
Mmp2	Mm00439498_m1
Mmp9	Mm00442991_m1
Myh2	Mm01332564_m1
Pdgfra	Mm00440701_m1
Pdgfrb	Mm00435546_m1
Pecam1	Mm00476712_m1
Pparg	Mm00440940_m1
Rorc	Mm01261022_m1
Tbp	Mm00446973_m1
Thbs1	Mm00449032_m1
Vegfa	Mm00437306_m1
Zfp423	Mm01246261_m1

Table 7.2: Antibodies used for western blotting	
Primary Antibodies (dilution)	**Company (Catalog #)**
α/β-tubulin (1:1000)	CST (#2148)
β-actin (1:5000)	Santa Cruz (#sc47778)
Akt (1:1000)	CST (#9272)
Phospho-Akt (s473; 1:1000)	CST (#4058)
Phospho-Akt (Thr308; 1:1000)	CST (#9275)
Foxo1 (1:750)	CST (#2880)
Foxo3 (1:1000)	CST (#2497)
Anti-Leptin Receptor Antibody (1:2000)	Abcam (#ab5593)
Secondary Antibodies (dilution)	**Company (Catalog #)**
Goat anti-rabbit IgG (1:400)	Jackson ImmunoResearch (#111-035-003)
Goat anti-mouse IgG (1:400)	Jackson ImmunoResearch (#115-035-003)

Appendix A: Nutrient-Overload Induced Leptin Production Within Skeletal Muscle: Potential Role for ZNF423

Contributions:

I was involved in the development of the conceptual and experimental approach for this study and performed most of the experiments described herein. Dr. Michael Melin collected biopsy samples. Johan Boström (SciLifeLabs) captured images and generated the analysis pipeline (Cell Profiler) used for the high-throughput immunocytochemical analysis (Fig. 1). This work was performed partly in Stockholm, Sweden at the Karolisnka University Hospital (Dr. Thomas Gustafsson) and at the Science for Life laboratories (SciLifeLabs; Dr. Mikael Altun) as part of the Michael Smith Foreign Study Supplement to my CIHR doctoral award.

Unpublished Data

Chapter Summary

Background/Rationale

In Chapter 4, I showed that nutrient excess (generated by 2 weeks of HF-feeding) induced leptin synthesis in the pericyte (PDGFRβ+ cells) population within skeletal muscle. This was associated elevated levels of *Zfp423* mRNA amongst the pericyte population indicating a shift towards a preadipocyte phenotype. To further elucidate the molecular regulation of induced pericyte leptin synthesis in response to nutrient excess, the purpose of the current study is to investigate a potential role for ZNF423 (human ZFP423 homolog) in the regulation of leptin synthesis in pericytes isolated from human skeletal muscle. I hypothesize that ZNF423 is a positive transcriptional regulator leptin synthesis in pericytes. Because pericytes are multipotent progenitor cells, the following investigation considered adipogenic (PDGFRα^{high}) and non-adipogenic (PDGFRα^{low}) pericytes separately.

Objectives

1) Isolate adipogenic and non-adipogenic pericytes from human skeletal muscle.

2) In isolated pericyte subsets:
    a. Assess the influence of specific nutrients (i.e. fatty acids, glucose) and hormones (i.e. insulin) on leptin synthesis
    b. Investigate the potential transcriptional regulation of leptin by ZNF423

Experimental Approach

Adipogenic (PDGFRβ+PDGFRα^{high}) and non-adipogenic (PDGFRβ+PDGFRα^{low}) pericyte subsets were isolated by flow activated cell sorting (FACS) using human *vastus lateralis* biopsy samples obtained by the percutaneous needle biopsy technique from 2 healthy male subjects. Because the yield of cells from a single biopsy sample was expected to be low, I first propagated

the unsorted cell population over 2 passages to maximize the yield of pericytes prior to FACS. Preliminary assessments were first made in unsorted cells to optimize experimental protocols (i.e. treatment dose) to be used in sorted cells. Short (24hr, 72hr) and Long (2 week) treatment durations were used to determine whether induced leptin induction is an acute event or requires chronic/repeated exposure to nutrient excess. Finally, potential transcriptional regulation of the leptin gene by ZNF423 will be assessed by examining 1) direct ZNF423 binding to leptin promoter regions by the Chromatin Immunoprecipitation (ChIP) technique and 2) assessing leptin production in sorted cells with lentiviral-mediated depletion of ZNF423.

Preliminary findings

Characterization of Cell Populations in Cultured Cells from Human Skeletal Muscle.

Collagenase digest yielded a total of ~675,000 heterogenous cells from a single human biopsy sample. To characterize the various cell populations, high throughput immunocytochemical analyses of plated cells was performed using markers of cell populations known to reside within skeletal muscle (App. A Fig. 1 A-B). The proportion of adherent cells that express cell surface markers at a mean intensity greater than negative controls (dotted lines) was assessed. 99.7% of cells were positive for TE-7, a marker for mesodermal-derived fibrous stroma and widely used as a fibroblast marker (Haynes et al., 1984). However, TE-7+ cells within skeletal muscle have also been shown to undergo adipogenic differentiation (Agley et al., 2013) suggesting that TE-7+ cells encompass fibro-adipogenic precursors (FAPs). Furthermore, TE-7+ staining was previously shown to stain fibroblast-like cells in the perivascular space (Goodpaster et al., 2008), indicating that TE-7+ cells may also include pericytes. 8.7% of adherent cells were positive for the endothelial cell marker vascular cell adhesion molecule (VCAM1), 0.24% for the hematopoietic stem cell marker CD34 and 71.9% for adipogenic precursor cell marker PDGFRα (App. A Fig. 1B), which has also been shown to detect FAPs within skeletal muscle (Birbrair et al., 2014a). Additional surface markers for macrophages (CD68), endothelial cells (VEGFR2) and satellite cells (CD56) were not detectable in adherent cells. These findings indicate a preponderance of interstitial fibroblast-like (TE-7+) adipogenic precursor (PDGFRα+) cells amongst the adherent cell population. Importantly, the wide distribution of intensities amongst TE-7+ and PDGFRα+ cells indicated the presence of a heterogenous population of cells that express varying levels of these markers. Flow cytometry was used to characterize the proportion of cells that express PDGFRβ+. Approximately 88% of the adherent cells were PDGFRβ+ (App. A Fig. 1C) and

exhibited a broad distribution of staining intensities, representing various PDGFRβ+ cell populations. Together, these data indicate that the adherent cells are comprised of a heterogenous populations of stromal cells that include various pericyte subsets.

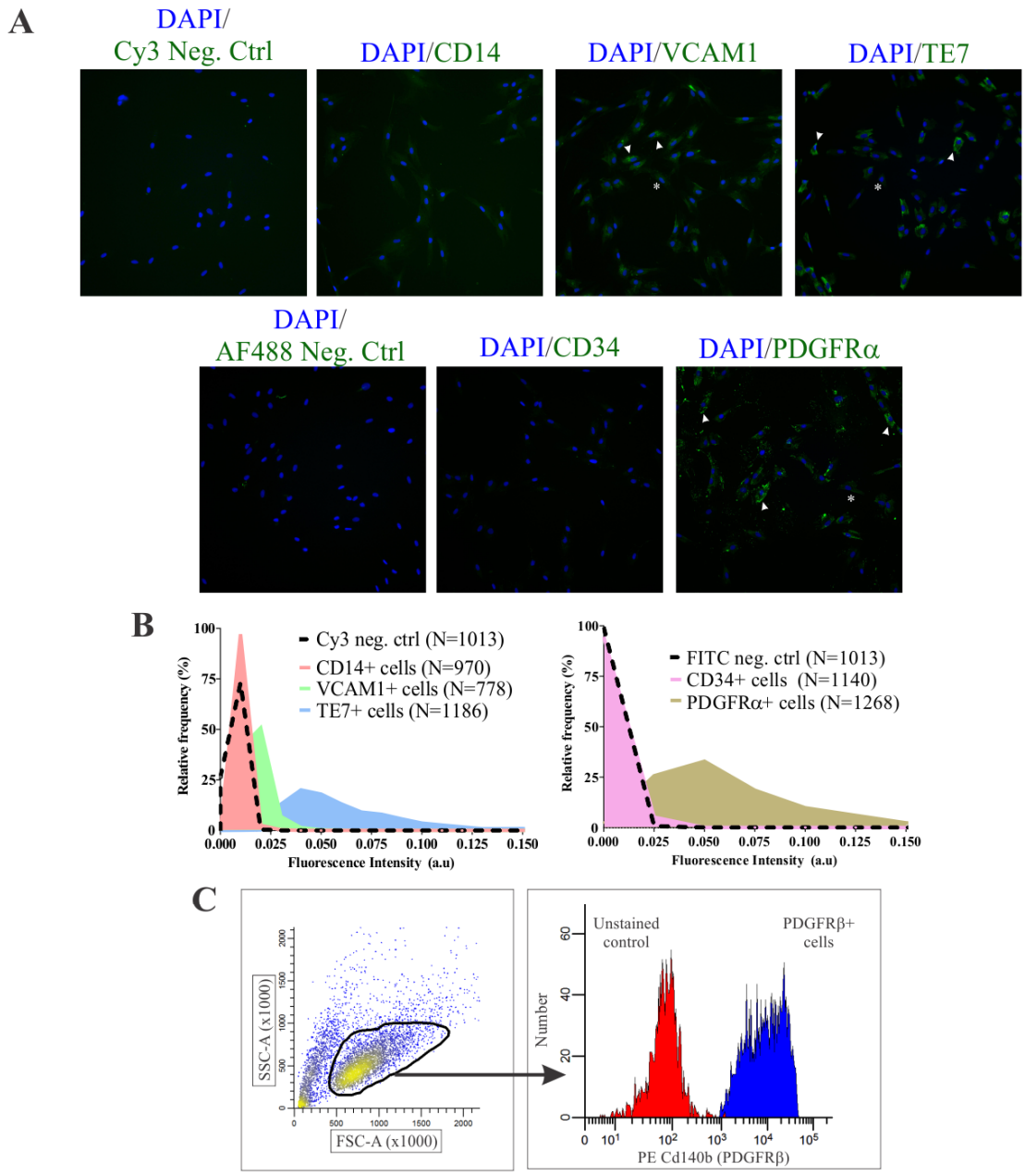

Figure 1:Characterization of unsorted plastic-adherent cell populations from skeletal muscle biopsy.

Immunocytochemical (ICC) staining for cell specific markers was performed on adherent cells to characterize specific cell populations. A) Representative images of ICC staining. Arrows and asterisks indicate positively and negatively stained cells, respectively. B) Frequency distribution of cellular fluoresence intensities was assessed for each antibody performed. Approximately 800-1300 individual data points (cells) are included for each distribution, as indicated. C) Fow cytometry was used to assess the relative abundance of PDGFRβ+ cells.

Additive Influence of Chronic Glucose Overload and Palmitate Treatment on the Induction of Leptin Synthesis in Adherent Cells

To examine the influence of nutrient excess on leptin synthesis, adherent cells were exposed to various conditions to mimic the microenvironment generated by HF-feeding. Adherent cells were propagated in alpha minimum essential medium (αMEM) which contains physiological levels of glucose (5.5mM) and was used to simulate basal conditions. Dulbecco's modified Eagle's medium (DMEM) which contains supraphysiological levels of glucose (25mM) was used as a condition of glucose overload. Under basal conditions, *LEPTIN* mRNA was undetectable in adherent cells (App. A, Fig. 2A). However, *LEPTIN* mRNA expression was induced in these cells after chronic (2 weeks) but not acute (24, 72 hours) exposure to glucose overload and was further elevated with the addition of the saturate fatty acid palmitate (App. A, Fig. 2A), at a concentration typical of obese individuals (Pillon et al., 2015).

To investigate whether the observed induction of *LEPTIN* mRNA expression was associated with a shift in the cellular phenotype, markers of adipogenic differentiation were assessed in adherent cells exposed to glucose overload and palmitate. In mice, ZNF423 has been identified as a transcriptional regulator of preadipocyte determination in progenitor cells (Gupta et al., 2010) and was considered as an early marker of adipogenic differentiation in the current study. CEBPα and PPARγ are well-established to function cooperatively in order to induce adipocyte-specific genes that establish the mature adipocyte phenotype and were thus considered as late markers of adipogenesis (MacDougald and Lane, 1995; Morrison and Farmer, 2000). All 3 adipogenic genes were detectable at the mRNA level in adherent cells. *ZNF423* and *PPARγ* but not *CEBPα* mRNA levels were elevated with chronic glucose overload (App. A, Fig. 2B-D). However, palmitate did not influence the expression of adipogenic genes during the course of glucose overload (App. A,

Fig. 2B-D). Taken together, these data indicate that elevated levels of both glucose and fatty acids coordinate the induction of leptin expression following chronic/repeated exposure to nutrient overload.

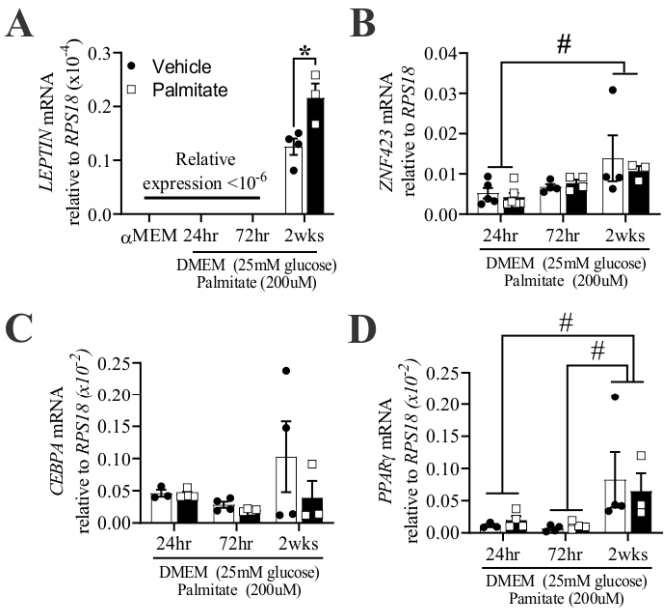

Figure 2: Nutrient overload induces leptin synthesis in unsorted plastic-adherent cells.
Unsorted plastic-adherent cells were maintained in alpha minimal essential medium (αMEM) containing a physiological (5mM) concentration of glucose and representing the basal state. Nutrient overload was induced by culturing cells in high (25mM) glucose dulbecco's modified eagles media (DMEM) and palmitate for 24hrs, 72hrs or for 2 weeks. mRNA levels of A) *LEPTIN* B) *ZNF423* C) *CEBPA* and D) *PPARγ* was assessed in cells subjected to basal and/or nutrient overload conditions. **P*<0.05, unpaired students t-test; #*P*<0.05, Two-way ANOVA.

Nuclear ZNF423 protein levels coincide with increased leptin protein expression in adherent cells expose to glucose overload and palmitate

Having observed that the induction of leptin expression coincides with a shift towards a preadipocyte phenotype (Chapter 3, Fig. 2A-D), my next aim was to investigate a potential role for ZNF423 in the transcriptional regulation of leptin gene expression. Using the LASAGNA-Search 2.0 platform (https://biogrid-lasagna.engr.uconn.edu/lasagna_search/index.php), several potential bindings sites for ZNF423 were identified at a *P*-value <0.05 (Table A.1), consistent with idea that ZNF423 is involved in the transcriptional regulation of the leptin gene. Next, we asked whether chronic glucose overload and palmitate treatments could influence the translocation of

ZNF423 into the nucleus. Immunocytochemical staining of adherent cells that demonstrated increased localization of ZNF423 positive reactivity in the nucleus after just 48 hours of glucose overload and palmitate treatment (App. A, Fig. 3A). Cytoplasmic and nuclear protein fractions from adherent cells revealed 2 distinct bands at ~120kDA and ~150kDA, respectively (App. A, Fig. 3B) (predicted molecular weight = 145). Thus, we quantified these bands separately to assess nuclear and cytoplasmic ZNF423 protein expression levels. After 2 weeks of glucose overload and palmitate treatment, nuclear levels of ZNF423 proteins were significantly elevated, but cytoplasmic levels remained unaltered (App. A, Fig. 3C-E), indicating an increased presence of ZNF423 protein in the nucleus. Increased nuclear ZNF423 protein levels coincided with a parallel increase in leptin protein levels (App. A, Fig. 3F) and a significant positive linear relationship (r=0.63) between nuclear ZNF423 levels and leptin protein expression (App. A, Fig. 3G). Together, these data suggest potential involvement of ZNF423 in the transcriptional regulation of leptin in response to nutrient overload.

Table A.1: Predicted ZNF423 binding sites on human leptin promoter

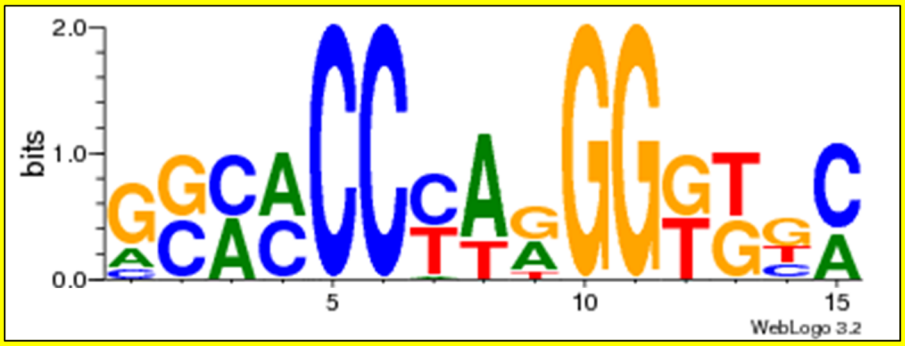

Zfp423 Sequence Logo (JASPAR ID: MA0116.1)

Predicted Binding Sequence	Position relative to TSS (bp)	Binding Specificity Score	*P*-value
CGCACCCTTGGGTAC	-233	7.01	0.0004
GCCCCTCAGGGTAGC	-336	3.27	0.00173
GGCCCGCAGTGTGCA	-295	1.25	0.00375

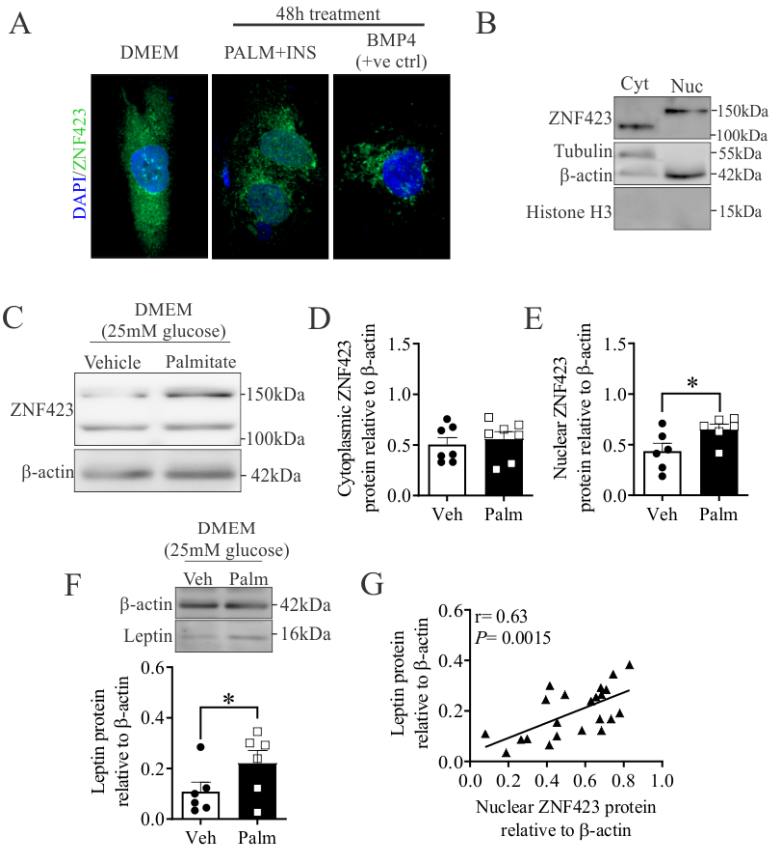

Figure 3: Nutrient overload promotes nuclear translocation of ZNF423 in plastic-adherent cells.
A) ZNF423 staining of plastic-adherent cells treated with Palmitate and Insulin for 48 hours. B) ZNF423 Western blot of cytoplasmic and nuclear fractions isolated from plastic adherent cells clearly demonstrating to distinct bands representing cytoplasmic (~120kDa) and nuclear (~150kDa) localized ZNF423. C-E) In cells exposed to nutrient overload for 2 weeks (high glucose+ palmitate), western blot was performed to assess protein levels of cytoplasmic (D) and nuclear (E) ZNF423. F) Leptin protein levels was also assesse in cells exposed to 2 weeks of nutrient overload. G) Linear regression of nuclear ZNF423 and leptin levels in plastic adherent cells. *$P < .05$, Student's t test.

Isolation of adipogenic and non-adipogenic pericytes by FACS

After 2 passages to increase cell yield, adherent cells were stained with stained with anti-CD140a (PDGFRα) and anti-CD140b (PDGFRβ) antibodies and adipogenic ($PDGFR\beta^{high}PDGFR\alpha^{high}$) and non-adipogenic ($PDGFR\beta^{high}PDGFR\alpha^{low}$) pericyte subsets isolated by FACS (App. A, Fig. 4). These cells will be used in subsequent experiments investigating the nutrient-sensing capacity of pericytes and to further elucidate the role of ZNF423 in the transcriptional regulation of leptin expression in adipogenic and non-adipogenic pericyte subsets.

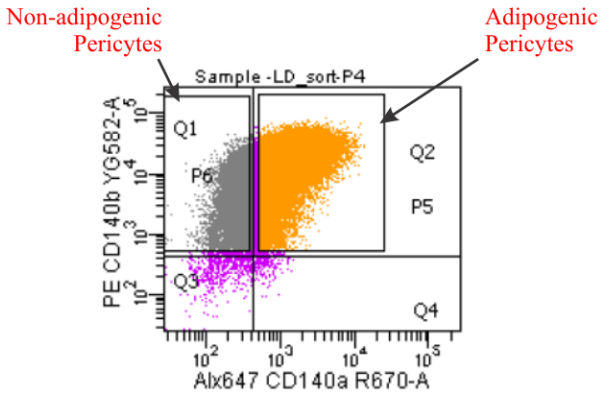

Figure 4: Fluorescence activated cell sorting (FACS) of non-adipogenic and adipogenic pericytes.

A) FACS plot illustrating the non-adipogenic (PDGFRβ+PDGFRα^{low}) and (PDGFRβ+PDGFRα^{high}) populations that were isolated from plastic-adherent cells.

Appendix B: Endothelial-specific Foxo1,3 depletion enhances post-ischemia perfusion recovery in HF-fed mice.

Contributions:

I was involved in the development of the conceptual and experimental approach for this study, generation and propagation of transgenic mouse models, as well as the collection of all preliminary findings presented herein.

Unpublished Data

Chapter Summary

Background/Rationale

The incidence and prognosis of peripheral artery disease (PAD) is worsened by the presence concurrent Type-2 diabetes (Katwal and Dokun, 2011). In two separate studies, our lab has demonstrated that endothelial FoxO proteins repress skeletal muscle capillary growth in the contexts of peripheral insulin resistance (Chapter 5) (Nwadozi et al., 2016) and ischemia (Roudier et al., 2013). The purpose of the current investigation is to determine whether concurrent insulin resistance and ischemia synergistically elevate endothelial FoxO proteins, which in turn will affect skeletal muscle capillary remodelling, perfusion recovery and ischemic muscle damage. I hypothesized that both Foxo1 and Foxo3 increase with concurrent insulin resistance and muscle ischemia and that endothelial-specific depletion of these factors would protect against ischemic muscle damage. Because only Foxo1 levels were found to be increased in the skeletal muscle with both ischemia and metabolic dysfunction (Nwadozi et al., 2016; Roudier et al., 2013), I assessed the contribution of Foxo1 alone as well as the combined role of both Foxo1 and Foxo3.

Objectives

1) Develop mouse models of endothelial-specific Foxo1 and Foxo1/3 depletion
2) Assess role(s) of endothelial FoxO proteins on perfusion recovery, vascular remodelling and muscle regeneration in a mouse model of concurrent insulin resistance and PAD

Experimental Approach

Prolonged HF-feeding will be used to induce insulin resistance in mice. To overcome the protective influence of endothelial Foxo depletion against the development of insulin resistance in HF-fed mice (as shown in Chapter 4), Foxo depletion was induced after the development of insulin resistance (assessed by ITT). Perfusion recovery will be assessed over a 14-day period at

which point skeletal muscle tissue was extracted for assessments of vascular remodelling and tissue regeneration.

Preliminary findings

Mouse Model of Endothelial Foxo1 and Foxo1/3 Depletion.

Endothelial specific Foxo1 and Foxo1/3 depleted mice were generated by first segregating the floxed sites in Foxo1/3/4$^{L/L}$ mice (used in Chapter 4) via breeding with wild-type mice (FVB/N background). Foxo1^{tm1Rdp} and Foxo1/3^{tm1Rdp} (Foxo1$^{L/L}$ and Foxo1/3$^{L/L}$, respectively) progeny were then crossed with mice that express cre recombinase under the control of a tamoxifen inducible PDGFB promoter [Tg (PdgfbiCreERT2)1Frut, henceforth referred to as PDGFBiCre^{ERT2} (Claxton et al., 2008). This generated PDGFB-iCre^{ERT2+} or PDGFB-iCre^{ERT2-}; Foxo1$^{L/L}$ and Foxo1,3$^{L/L}$ mice. To assess the efficacy of the depletion, a series of tamoxifen injections (3mg x 5 consecutive days *i.p.*) was administered to induce the depletion in PDGFB-iCre^{ERT2+} mice (generating Foxo1$^{\Delta}$ and Foxo1/3$^{\Delta}$ mice, respectively). Similar injections were administered to age-matched PDGFB-iCre^{ERT2-} mice (generating Foxo1$^{L/L}$ and Foxo1/3$^{L/L}$ mice, respectively). Foxo1$^{L/L}$ and Foxo1/3$^{L/L}$ mice were pooled to generate 1 control group. A 62% reduction in *Foxo1* mRNA (App. B, Fig. 1A) and protein (App. B, Fig. 1B) levels was evident in isolated capillary fragments from Foxo1 deficient mice relative to control mice.

Perfusion Recovery in Foxo-Deficient Mice with Concurrent PAD and Insulin Resistance

A schematic of my experimental model is presented in (App. B, Fig. 1C). To overcome the protective influence of endothelial Foxo depletion against the development of insulin resistance in HF-fed mice PDGFB-iCre^{ERT2+} and PDGFB-iCre^{ERT2-}; Foxo1$^{L/L}$ and Foxo1,3$^{L/L}$ mice were first fed a HF diet to induce insulin resistance prior to the induction of Foxo depletion. After 14 weeks, HF-fed mice exhibited elevated levels of fasting glucose (App. B, Fig. 1D) and impaired peripheral

insulin sensitivity assessed by an insulin tolerance test (App. B, Fig. 1E,F). A considerable amount of heterogeneity was evident in the insulin responsiveness of HF-fed mice (App. B, Fig. 1F), thus, only mice with impaired insulin sensitivity relative to age-matched controls were selected to proceed in the experimental protocol. Depletion of endothelial FoxO proteins was induced in selected mice during their 15^{th} week on the diet by administration of tamoxifen (3mg/day, *i.p.*) for 5 consecutive days. After 16 weeks of diet, control and Foxo-deficient mice were subjected to unilateral ligation of the common femoral artery to induce a ~90% reduction of blood flow to the lower limb and perfusion recovery assessed over a 14-day period (App. B, Fig. 1G). Preliminary results suggest that both Foxo1$^{\Delta}$ (n=1, ns) and Foxo1/3$^{\Delta}$ (n=5) mice exhibited enhanced perfusion recovery at Day 11 compared to control mice. However, at Day 14 post-ligation, there were no differences observed in perfusion recovery.

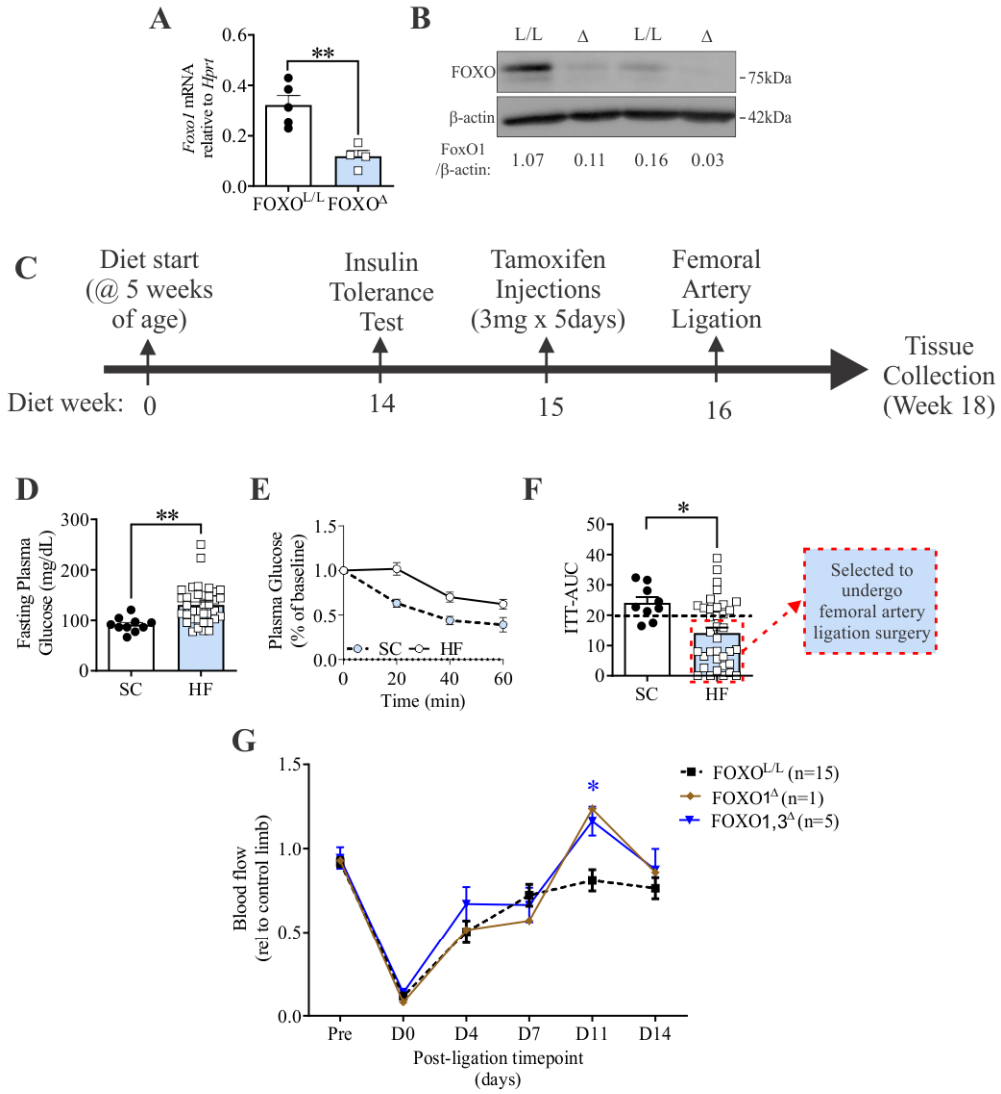

Figure 1.

Endothelial-specific Foxo1/3 depletion enhances post-ischemia perfusion recovery in HF-fed mice.
The efficacy of Foxo depletion was assessed in tamoxifen-injected PDGFB-iCre^{ERT2+} and PDGFB-iCre^{ERT2-}; Foxo1$^{L/L}$ and Foxo1,3$^{L/L}$. Foxo1 A) mRNA and B) protein levels, as well as C) Foxo3 mRNA levels were assessed in capillary fragments isolated from skeletal muscle. D) Schematic representation of the experimental protocol used in the current study. After 14 weeks of HF diet, E) Fasting (4hr) glucose levels were assessed. An insulin tolerance test was performed at the same timepoint, represented as a F) line graph and G) area under the curve (AUC) graph. Following induction of FOXO depletion (during week 15), unilateral ligation of the common femoral artery was performed to induce hindlimb ischemia and perfusion recovery assessed by laser doppler imaging. H) Paw blood flow in the ligated limb was quantified and expressed as a ratio to the control limb. *P<0.05, **P< 0.01 vs. respective control groups; unpaired student's t-test.

Reference List

Adams, J.C., and Lawler, J. (2011). The thrombospondins. Cold Spring Harb. Perspect. Biol. *3*, a009712.

Agley, C.C., Rowlerson, A.M., Velloso, C.P., Lazarus, N.R., and Harridge, S.D.R. (2013). Human skeletal muscle fibroblasts, but not myogenic cells, readily undergo adipogenic differentiation. J. Cell Sci. *126*, 5610–5625.

Akerstrom, T., Laub, L., Vedel, K., Brand, C.L., Pedersen, B.K., Lindqvist, A.K., Wojtaszewski, J.F.P., and Hellsten, Y. (2014). Increased skeletal muscle capillarization enhances insulin sensitivity. Am. J. Physiol. Endocrinol. Metab. *307*, E1105-1116.

Alarcon-Martinez, L., Yilmaz-Ozcan, S., Yemisci, M., Schallek, J., Kılıç, K., Villafranca-Baughman, D., Can, A., Di Polo, A., and Dalkara, T. (2019). Retinal ischemia induces α-SMA-mediated capillary pericyte contraction coincident with perivascular glycogen depletion. Acta Neuropathol. Commun. *7*, 134.

Ambrose, C. (2015). Muscle weakness during aging: a deficiency state involving declining angiogenesis. Ageing Res. Rev. *23*, 139–153.

Anandacoomarasamy, A., Caterson, I., Sambrook, P., Fransen, M., and March, L. (2008). The impact of obesity on the musculoskeletal system. Int. J. Obes. 2005 *32*, 211–222.

Angleys, H., and Østergaard, L. (2020). Krogh's capillary recruitment hypothesis, 100 years on: Is the opening of previously closed capillaries necessary to ensure muscle oxygenation during exercise? Am. J. Physiol. Heart Circ. Physiol. *318*, H425–H447.

Annex, B.H. (2013). Therapeutic angiogenesis for critical limb ischaemia. Nat. Rev. Cardiol. *10*, 387–396.

Anstey, K.J., Cherbuin, N., Budge, M., and Young, J. (2011). Body mass index in midlife and late-life as a risk factor for dementia: a meta-analysis of prospective studies. Obes. Rev. Off. J. Int. Assoc. Study Obes. *12*, e426-437.

Armulik, A., Abramsson, A., and Betsholtz, C. (2005). Endothelial/pericyte interactions. Circ. Res. *97*, 512–523.

Armulik, A., Genové, G., and Betsholtz, C. (2011). Pericytes: developmental, physiological, and pathological perspectives, problems, and promises. Dev. Cell *21*, 193–215.

Arner, E., Rydén, M., and Arner, P. (2010). Tumor necrosis factor alpha and regulation of adipose tissue. N. Engl. J. Med. *362*, 1151–1153.

Aroor, A.R., McKarns, S., Demarco, V.G., Jia, G., and Sowers, J.R. (2013). Maladaptive immune and inflammatory pathways lead to cardiovascular insulin resistance. Metabolism. *62*, 1543–1552.

Artwohl, M., Roden, M., Hölzenbein, T., Freudenthaler, A., Waldhäusl, W., and Baumgartner-Parzer, S.M. (2002). Modulation by leptin of proliferation and apoptosis in vascular endothelial cells. Int. J. Obes. Relat. Metab. Disord. J. Int. Assoc. Study Obes. *26*, 577–580.

Augustin, H.G., and Koh, G.Y. (2017). Organotypic vasculature: From descriptive heterogeneity to functional pathophysiology. Science *357*.

Azizi, P.M., Zyla, R.E., Guan, S., Wang, C., Liu, J., Bolz, S.-S., Heit, B., Klip, A., and Lee, W.L. (2015). Clathrin-dependent entry and vesicle-mediated exocytosis define insulin transcytosis across microvascular endothelial cells. Mol. Biol. Cell *26*, 740–750.

Baenziger, N.L., Brodie, G.N., and Majerus, P.W. (1971). A thrombin-sensitive protein of human platelet membranes. Proc. Natl. Acad. Sci. U. S. A. *68*, 240–243.

Bakker, W., Eringa, E.C., Sipkema, P., and van Hinsbergh, V.W.M. (2009). Endothelial dysfunction and diabetes: roles of hyperglycemia, impaired insulin signaling and obesity. Cell Tissue Res. *335*, 165–189.

Bao, P., Kodra, A., Tomic-Canic, M., Golinko, M.S., Ehrlich, H.P., and Brem, H. (2009). The role of vascular endothelial growth factor in wound healing. J. Surg. Res. *153*, 347–358.

Barron, L., Gharib, S.A., and Duffield, J.S. (2016). Lung Pericytes and Resident Fibroblasts: Busy Multitaskers. Am. J. Pathol. *186*, 2519–2531.

Beltramo, E., and Porta, M. (2013). Pericyte loss in diabetic retinopathy: mechanisms and consequences. Curr. Med. Chem. *20*, 3218–3225.

Benjamin, L.E., Hemo, I., and Keshet, E. (1998). A plasticity window for blood vessel remodelling is defined by pericyte coverage of the preformed endothelial network and is regulated by PDGF-B and VEGF. Dev. Camb. Engl. *125*, 1591–1598.

van den Berg, M.C.W., and Burgering, B.M.T. (2011). Integrating opposing signals toward Forkhead box O. Antioxid. Redox Signal. *14*, 607–621.

Bergers, G., and Song, S. (2005). The role of pericytes in blood-vessel formation and maintenance. Neuro-Oncol. *7*, 452–464.

Biferali, B., Proietti, D., Mozzetta, C., and Madaro, L. (2019). Fibro-Adipogenic Progenitors Cross-Talk in Skeletal Muscle: The Social Network. Front. Physiol. *10*, 1074.

Bilan, P.J., Samokhvalov, V., Koshkina, A., Schertzer, J.D., Samaan, M.C., and Klip, A. (2009). Direct and macrophage-mediated actions of fatty acids causing insulin resistance in muscle cells. Arch. Physiol. Biochem. *115*, 176–190.

Birbrair, A., Zhang, T., Wang, Z.-M., Messi, M.L., Enikolopov, G.N., Mintz, A., and Delbono, O. (2013a). Role of pericytes in skeletal muscle regeneration and fat accumulation. Stem Cells Dev. *22*, 2298–2314.

Birbrair, A., Zhang, T., Wang, Z.-M., Messi, M.L., Enikolopov, G.N., Mintz, A., and Delbono, O. (2013b). Skeletal muscle pericyte subtypes differ in their differentiation potential. Stem Cell Res. *10*, 67–84.

Birbrair, A., Zhang, T., Wang, Z.-M., Messi, M.L., Mintz, A., and Delbono, O. (2013c). Type-1 pericytes participate in fibrous tissue deposition in aged skeletal muscle. Am. J. Physiol. Cell Physiol. *305*, C1098-1113.

Birbrair, A., Zhang, T., Wang, Z.-M., Messi, M.L., Mintz, A., and Delbono, O. (2014a). Pericytes: multitasking cells in the regeneration of injured, diseased, and aged skeletal muscle. Front. Aging Neurosci. *6*, 245.

Birbrair, A., Zhang, T., Wang, Z.-M., Messi, M.L., Olson, J.D., Mintz, A., and Delbono, O. (2014b). Type-2 pericytes participate in normal and tumoral angiogenesis. Am. J. Physiol. Cell Physiol. *307*, C25-38.

Birbrair, A., Borges, I. da T., Gilson Sena, I.F., Almeida, G.G., da Silva Meirelles, L., Gonçalves, R., Mintz, A., and Delbono, O. (2017). How Plastic Are Pericytes? Stem Cells Dev. *26*, 1013–1019.

Bjørbaek, C., Elmquist, J.K., Michl, P., Ahima, R.S., van Bueren, A., McCall, A.L., and Flier, J.S. (1998). Expression of leptin receptor isoforms in rat brain microvessels. Endocrinology *139*, 3485–3491.

Blüher, M. (2019). Obesity: global epidemiology and pathogenesis. Nat. Rev. Endocrinol. *15*, 288–298.

Bonaca, M.P., and Creager, M.A. (2015). Pharmacological treatment and current management of peripheral artery disease. Circ. Res. *116*, 1579–1598.

Bonner, J.S., Lantier, L., Hasenour, C.M., James, F.D., Bracy, D.P., and Wasserman, D.H. (2013). Muscle-specific vascular endothelial growth factor deletion induces muscle capillary rarefaction creating muscle insulin resistance. Diabetes *62*, 572–580.

Bonora, E., Formentini, G., Calcaterra, F., Lombardi, S., Marini, F., Zenari, L., Saggiani, F., Poli, M., Perbellini, S., Raffaelli, A., et al. (2002). HOMA-estimated insulin resistance is an independent predictor of cardiovascular disease in type 2 diabetic subjects: prospective data from the Verona Diabetes Complications Study. Diabetes Care *25*, 1135–1141.

Bouloumié, A., Drexler, H.C., Lafontan, M., and Busse, R. (1998). Leptin, the product of Ob gene, promotes angiogenesis. Circ. Res. *83*, 1059–1066.

Britton, K.A., Mukamal, K.J., Ix, J.H., Siscovick, D.S., Newman, A.B., de Boer, I.H., Thacker, E.L., Biggs, M.L., Gaziano, J.M., and Djoussé, L. (2012). Insulin resistance and incident peripheral artery disease in the Cardiovascular Health Study. Vasc. Med. Lond. Engl. *17*, 85–93.

Bruce, A.C., and Peirce, S.M. (2012). Exogenous thrombin delivery promotes collateral capillary arterialization and tissue reperfusion in the murine spinotrapezius muscle ischemia model. Microcirc. N. Y. N 1994 *19*, 143–154.

Brudno, Y., Ennett-Shepard, A.B., Chen, R.R., Aizenberg, M., and Mooney, D.J. (2013). Enhancing microvascular formation and vessel maturation through temporal control over multiple pro-angiogenic and pro-maturation factors. Biomaterials *34*, 9201–9209.

Brüning, J.C., Michael, M.D., Winnay, J.N., Hayashi, T., Hörsch, D., Accili, D., Goodyear, L.J., and Kahn, C.R. (1998). A muscle-specific insulin receptor knockout exhibits features of the metabolic syndrome of NIDDM without altering glucose tolerance. Mol. Cell *2*, 559–569.

Bruns, R.R., and Palade, G.E. (1968). Studies on blood capillaries. I. General organization of blood capillaries in muscle. J. Cell Biol. *37*, 244–276.

Buettner, R., Schölmerich, J., and Bollheimer, L.C. (2007). High-fat diets: modeling the metabolic disorders of human obesity in rodents. Obes. Silver Spring Md *15*, 798–808.

Cai, J., Ruan, Q., Chen, Z.J., and Han, S. (2012). Connection of pericyte-angiopoietin-Tie-2 system in diabetic retinopathy: friend or foe? Future Med. Chem. *4*, 2163–2176.

Cao, R., Brakenhielm, E., Wahlestedt, C., Thyberg, J., and Cao, Y. (2001). Leptin induces vascular permeability and synergistically stimulates angiogenesis with FGF-2 and VEGF. Proc. Natl. Acad. Sci. U. S. A. *98*, 6390–6395.

Carmeliet, P., and Jain, R.K. (2011). Molecular mechanisms and clinical applications of angiogenesis. Nature *473*, 298–307.

Chadderdon, S.M., Belcik, J.T., Bader, L., Peters, D.M., Kievit, P., Alkayed, N.J., Kaul, S., Grove, K.L., and Lindner, J.R. (2016). Temporal Changes in Skeletal Muscle Capillary Responses and Endothelial-Derived Vasodilators in Obesity-Related Insulin Resistance. Diabetes *65*, 2249–2257.

Chen, I.I., Prewitt, R.L., and Dowell, R.F. (1981). Microvascular rarefaction in spontaneously hypertensive rat cremaster muscle. Am. J. Physiol. *241*, H306-310.

Chen, L., Wang, L., Li, Y., Wuang, L., Liu, Y., Pang, N., Luo, Y., He, J., Zhang, L., Chen, N., et al. (2018). Transplantation of Normal Adipose Tissue Improves Blood Flow and Reduces Inflammation in High Fat Fed Mice With Hindlimb Ischemia. Front. Physiol. *9*, 197.

Cherwek, D.H., Hopkins, M.B., Thompson, M.J., Annex, B.H., and Taylor, D.A. (2000). Fiber type-specific differential expression of angiogenic factors in response to chronic hindlimb ischemia. Am. J. Physiol. Heart Circ. Physiol. *279*, H932-938.

Chistiakov, D.A., Orekhov, A.N., and Bobryshev, Y.V. (2017). Effects of shear stress on endothelial cells: go with the flow. Acta Physiol. Oxf. Engl. *219*, 382–408.

Chiu, J.D., Richey, J.M., Harrison, L.N., Zuniga, E., Kolka, C.M., Kirkman, E., Ellmerer, M., and Bergman, R.N. (2008). Direct administration of insulin into skeletal muscle reveals that the

transport of insulin across the capillary endothelium limits the time course of insulin to activate glucose disposal. Diabetes *57*, 828–835.

Chooi, Y.C., Ding, C., and Magkos, F. (2019). The epidemiology of obesity. Metabolism. *92*, 6–10.

Clark, M.G., Wallis, M.G., Barrett, E.J., Vincent, M.A., Richards, S.M., Clerk, L.H., and Rattigan, S. (2003). Blood flow and muscle metabolism: a focus on insulin action. Am. J. Physiol. Endocrinol. Metab. *284*, E241-258.

Claxton, S., Kostourou, V., Jadeja, S., Chambon, P., Hodivala-Dilke, K., and Fruttiger, M. (2008). Efficient, inducible Cre-recombinase activation in vascular endothelium. Genes. N. Y. N 2000 *46*, 74–80.

Clerk, L.H., Vincent, M.A., Jahn, L.A., Liu, Z., Lindner, J.R., and Barrett, E.J. (2006). Obesity blunts insulin-mediated microvascular recruitment in human forearm muscle. Diabetes *55*, 1436–1442.

Conte, M.S., Bradbury, A.W., Kolh, P., White, J.V., Dick, F., Fitridge, R., Mills, J.L., Ricco, J.-B., Suresh, K.R., Murad, M.H., et al. (2019). Global vascular guidelines on the management of chronic limb-threatening ischemia. J. Vasc. Surg. *69*, 3S-125S.e40.

Cooke, J.P., and Losordo, D.W. (2015). Modulating the vascular response to limb ischemia: angiogenic and cell therapies. Circ. Res. *116*, 1561–1578.

Cordani, N., Pisa, V., Pozzi, L., Sciorati, C., and Clementi, E. (2014). Nitric oxide controls fat deposition in dystrophic skeletal muscle by regulating fibro-adipogenic precursor differentiation. Stem Cells Dayt. Ohio *32*, 874–885.

Cornachione, A.S., Benedini-Elias, P.C.O., Polizello, J.C., Carvalho, L.C., and Mattiello-Sverzut, A.C. (2011). Characterization of fiber types in different muscles of the hindlimb in female weanling and adult Wistar rats. Acta Histochem. Cytochem. *44*, 43–50.

Couffinhal, T., Silver, M., Zheng, L.P., Kearney, M., Witzenbichler, B., and Isner, J.M. (1998). Mouse model of angiogenesis. Am. J. Pathol. *152*, 1667–1679.

Crisan, M., Yap, S., Casteilla, L., Chen, C.-W., Corselli, M., Park, T.S., Andriolo, G., Sun, B., Zheng, B., Zhang, L., et al. (2008). A perivascular origin for mesenchymal stem cells in multiple human organs. Cell Stem Cell *3*, 301–313.

DeFronzo, R.A., Gunnarsson, R., Björkman, O., Olsson, M., and Wahren, J. (1985). Effects of insulin on peripheral and splanchnic glucose metabolism in noninsulin-dependent (type II) diabetes mellitus. J. Clin. Invest. *76*, 149–155.

Dellavalle, A., Maroli, G., Covarello, D., Azzoni, E., Innocenzi, A., Perani, L., Antonini, S., Sambasivan, R., Brunelli, S., Tajbakhsh, S., et al. (2011). Pericytes resident in postnatal skeletal muscle differentiate into muscle fibres and generate satellite cells. Nat. Commun. *2*, 499.

Dennis, G., Sherman, B.T., Hosack, D.A., Yang, J., Gao, W., Lane, H.C., and Lempicki, R.A. (2003). DAVID: Database for Annotation, Visualization, and Integrated Discovery. Genome Biol. *4*, P3.

Dharaneeswaran, H., Abid, M.R., Yuan, L., Dupuis, D., Beeler, D., Spokes, K.C., Janes, L., Sciuto, T., Kang, P.M., Jaminet, S.-C.S., et al. (2014). FOXO1-mediated activation of Akt plays a critical role in vascular homeostasis. Circ. Res. *115*, 238–251.

Díaz-Flores, L., Gutiérrez, R., Varela, H., Rancel, N., and Valladares, F. (1991). Microvascular pericytes: a review of their morphological and functional characteristics. Histol. Histopathol. *6*, 269–286.

van Dijk, C.G.M., Nieuweboer, F.E., Pei, J.Y., Xu, Y.J., Burgisser, P., van Mulligen, E., el Azzouzi, H., Duncker, D.J., Verhaar, M.C., and Cheng, C. (2015). The complex mural cell: pericyte function in health and disease. Int. J. Cardiol. *190*, 75–89.

Djonov, V., Andres, A.C., and Ziemiecki, A. (2001). Vascular remodelling during the normal and malignant life cycle of the mammary gland. Microsc. Res. Tech. *52*, 182–189.

Durbeej, M. (2010). Laminins. Cell Tissue Res. *339*, 259–268.

Dyck, D.J. (2009). Adipokines as regulators of muscle metabolism and insulin sensitivity. Appl. Physiol. Nutr. Metab. Physiol. Appl. Nutr. Metab. *34*, 396–402.

Egginton, S. (2009). Invited review: activity-induced angiogenesis. Pflugers Arch. *457*, 963–977.

Ejaz, S., Chekarova, I., Ejaz, A., Sohail, A., and Lim, C.W. (2008). Importance of pericytes and mechanisms of pericyte loss during diabetes retinopathy. Diabetes Obes. Metab. *10*, 53–63.

Ellis, C.G., Wrigley, S.M., and Groom, A.C. (1994). Heterogeneity of red blood cell perfusion in capillary networks supplied by a single arteriole in resting skeletal muscle. Circ. Res. *75*, 357–368.

Emanueli, C., Caporali, A., Krankel, N., Cristofaro, B., Van Linthout, S., and Madeddu, P. (2007). Type-2 diabetic Lepr(db/db) mice show a defective microvascular phenotype under basal conditions and an impaired response to angiogenesis gene therapy in the setting of limb ischemia. Front. Biosci. J. Virtual Libr. *12*, 2003–2012.

Eriksson, K.F., Saltin, B., and Lindgärde, F. (1994). Increased skeletal muscle capillary density precedes diabetes development in men with impaired glucose tolerance. A 15-year follow-up. Diabetes *43*, 805–808.

Esser, N., Legrand-Poels, S., Piette, J., Scheen, A.J., and Paquot, N. (2014). Inflammation as a link between obesity, metabolic syndrome and type 2 diabetes. Diabetes Res. Clin. Pract. *105*, 141–150.

Faber, J.E., Chilian, W.M., Deindl, E., van Royen, N., and Simons, M. (2014). A brief etymology of the collateral circulation. Arterioscler. Thromb. Vasc. Biol. *34*, 1854–1859.

Feldman, P.S., Shneidman, D., and Kaplan, C. (1978). Ultrastructure of infantile hemangioendothelioma of the liver. Cancer *42*, 521–527.

Fernández-Klett, F., Offenhauser, N., Dirnagl, U., Priller, J., and Lindauer, U. (2010). Pericytes in capillaries are contractile in vivo, but arterioles mediate functional hyperemia in the mouse brain. Proc. Natl. Acad. Sci. U. S. A. *107*, 22290–22295.

Fischer, H., Gustafsson, T., Sundberg, C.J., Norrbom, J., Ekman, M., Johansson, O., and Jansson, E. (2006). Fatty acid binding protein 4 in human skeletal muscle. Biochem. Biophys. Res. Commun. *346*, 125–130.

Fowkes, F.G.R., Aboyans, V., Fowkes, F.J.I., McDermott, M.M., Sampson, U.K.A., and Criqui, M.H. (2017). Peripheral artery disease: epidemiology and global perspectives. Nat. Rev. Cardiol. *14*, 156–170.

Francischetti, E.A., Tibirica, E., da Silva, E.G., Rodrigues, E., Celoria, B.M., and de Abreu, V.G. (2011). Skin capillary density and microvascular reactivity in obese subjects with and without metabolic syndrome. Microvasc. Res. *81*, 325–330.

Franco, C.A., Jones, M.L., Bernabeu, M.O., Geudens, I., Mathivet, T., Rosa, A., Lopes, F.M., Lima, A.P., Ragab, A., Collins, R.T., et al. (2015). Dynamic endothelial cell rearrangements drive developmental vessel regression. PLoS Biol. *13*, e1002125.

Freidenberg, G.R., Suter, S.L., Henry, R.R., Reichart, D., and Olefsky, J.M. (1991). In vivo stimulation of the insulin receptor kinase in human skeletal muscle. Correlation with insulin-stimulated glucose disposal during euglycemic clamp studies. J. Clin. Invest. *87*, 2222–2229.

Freidenberg, G.R., Suter, S., Henry, R.R., Nolan, J., Reichart, D., and Olefsky, J.M. (1994). Delayed onset of insulin activation of the insulin receptor kinase in vivo in human skeletal muscle. Diabetes *43*, 118–126.

Frisbee, J.C. (2007). Obesity, insulin resistance, and microvessel density. Microcirc. N. Y. N 1994 *14*, 289–298.

Furuyama, T., Kitayama, K., Shimoda, Y., Ogawa, M., Sone, K., Yoshida-Araki, K., Hisatsune, H., Nishikawa, S., Nakayama, K., Nakayama, K., et al. (2004). Abnormal angiogenesis in Foxo1 (Fkhr)-deficient mice. J. Biol. Chem. *279*, 34741–34749.

Garonna, E., Botham, K.M., Birdsey, G.M., Randi, A.M., Gonzalez-Perez, R.R., and Wheeler-Jones, C.P.D. (2011). Vascular endothelial growth factor receptor-2 couples cyclo-oxygenase-2 with pro-angiogenic actions of leptin on human endothelial cells. PloS One *6*, e18823.

Gaudreault, N., Scriven, D.R.L., Laher, I., and Moore, E.D.W. (2008). Subcellular characterization of glucose uptake in coronary endothelial cells. Microvasc. Res. *75*, 73–82.

Gee, E., Milkiewicz, M., and Haas, T.L. (2010). p38 MAPK activity is stimulated by vascular endothelial growth factor receptor 2 activation and is essential for shear stress-induced angiogenesis. J. Cell. Physiol. *222*, 120–126.

Geevarghese, A., and Herman, I.M. (2014). Pericyte-endothelial crosstalk: implications and opportunities for advanced cellular therapies. Transl. Res. J. Lab. Clin. Med. *163*, 296–306.

Gerber, H.P., McMurtrey, A., Kowalski, J., Yan, M., Keyt, B.A., Dixit, V., and Ferrara, N. (1998). Vascular endothelial growth factor regulates endothelial cell survival through the phosphatidylinositol 3'-kinase/Akt signal transduction pathway. Requirement for Flk-1/KDR activation. J. Biol. Chem. *273*, 30336–30343.

Gerhardt, H., Wolburg, H., and Redies, C. (2000). N-cadherin mediates pericytic-endothelial interaction during brain angiogenesis in the chicken. Dev. Dyn. Off. Publ. Am. Assoc. Anat. *218*, 472–479.

Geudens, I., and Gerhardt, H. (2011). Coordinating cell behaviour during blood vessel formation. Dev. Camb. Engl. *138*, 4569–4583.

Gianni-Barrera, R., Trani, M., Reginato, S., and Banfi, A. (2011). To sprout or to split? VEGF, Notch and vascular morphogenesis. Biochem. Soc. Trans. *39*, 1644–1648.

Gianni-Barrera, R., Butschkau, A., Uccelli, A., Certelli, A., Valente, P., Bartolomeo, M., Groppa, E., Burger, M.G., Hlushchuk, R., Heberer, M., et al. (2018). PDGF-BB regulates splitting angiogenesis in skeletal muscle by limiting VEGF-induced endothelial proliferation. Angiogenesis *21*, 883–900.

Golub, A.S., and Pittman, R.N. (2013). Bang-bang model for regulation of local blood flow. Microcirc. N. Y. N 1994 *20*, 455–483.

Gong, D.W., He, Y., Karas, M., and Reitman, M. (1997). Uncoupling protein-3 is a mediator of thermogenesis regulated by thyroid hormone, beta3-adrenergic agonists, and leptin. J. Biol. Chem. *272*, 24129–24132.

Gonzalez, R.R., Cherfils, S., Escobar, M., Yoo, J.H., Carino, C., Styer, A.K., Sullivan, B.T., Sakamoto, H., Olawaiye, A., Serikawa, T., et al. (2006). Leptin signaling promotes the growth of mammary tumors and increases the expression of vascular endothelial growth factor (VEGF) and its receptor type two (VEGF-R2). J. Biol. Chem. *281*, 26320–26328.

Good, D.J., Polverini, P.J., Rastinejad, F., Le Beau, M.M., Lemons, R.S., Frazier, W.A., and Bouck, N.P. (1990). A tumor suppressor-dependent inhibitor of angiogenesis is immunologically and functionally indistinguishable from a fragment of thrombospondin. Proc. Natl. Acad. Sci. U. S. A. *87*, 6624–6628.

Goodpaster, T., Legesse-Miller, A., Hameed, M.R., Aisner, S.C., Randolph-Habecker, J., and Coller, H.A. (2008). An immunohistochemical method for identifying fibroblasts in formalin-fixed, paraffin-embedded tissue. J. Histochem. Cytochem. Off. J. Histochem. Soc. *56*, 347–358.

Gorman, J.L., Liu, S.T.K., Slopack, D., Shariati, K., Hasanee, A., Olenich, S., Olfert, I.M., and Haas, T.L. (2014). Angiotensin II evokes angiogenic signals within skeletal muscle through co-ordinated effects on skeletal myocytes and endothelial cells. PloS One *9*, e85537.

Greenaway, J., Lawler, J., Moorehead, R., Bornstein, P., Lamarre, J., and Petrik, J. (2007). Thrombospondin-1 inhibits VEGF levels in the ovary directly by binding and internalization via the low density lipoprotein receptor-related protein-1 (LRP-1). J. Cell. Physiol. *210*, 807–818.

Groen, B.B.L., Hamer, H.M., Snijders, T., van Kranenburg, J., Frijns, D., Vink, H., and van Loon, L.J.C. (2014). Skeletal muscle capillary density and microvascular function are compromised with aging and type 2 diabetes. J. Appl. Physiol. Bethesda Md 1985 *116*, 998–1005.

Grotte, G. (1956). Passage of dextran molecules across the blood-lymph barrier. Acta Chir. Scand. Suppl. *211*, 1–84.

Guillot, M., Charles, A.-L., Chamaraux-Tran, T.N., Bouitbir, J., Meyer, A., Zoll, J., Schneider, F., and Geny, B. (2014). Oxidative stress precedes skeletal muscle mitochondrial dysfunction during experimental aortic cross-clamping but is not associated with early lung, heart, brain, liver, or kidney mitochondrial impairment. J. Vasc. Surg. *60*, 1043-1051.e5.

Guimarães-Camboa, N., Cattaneo, P., Sun, Y., Moore-Morris, T., Gu, Y., Dalton, N.D., Rockenstein, E., Masliah, E., Peterson, K.L., Stallcup, W.B., et al. (2017). Pericytes of Multiple Organs Do Not Behave as Mesenchymal Stem Cells In Vivo. Cell Stem Cell *20*, 345-359.e5.

Gupta, K., Gupta, P., Wild, R., Ramakrishnan, S., and Hebbel, R.P. (1999). Binding and displacement of vascular endothelial growth factor (VEGF) by thrombospondin: effect on human microvascular endothelial cell proliferation and angiogenesis. Angiogenesis *3*, 147–158.

Gupta, R.K., Arany, Z., Seale, P., Mepani, R.J., Ye, L., Conroe, H.M., Roby, Y.A., Kulaga, H., Reed, R.R., and Spiegelman, B.M. (2010). Transcriptional control of preadipocyte determination by Zfp423. Nature *464*, 619–623.

Gustafson, B., Hammarstedt, A., Andersson, C.X., and Smith, U. (2007). Inflamed adipose tissue: a culprit underlying the metabolic syndrome and atherosclerosis. Arterioscler. Thromb. Vasc. Biol. *27*, 2276–2283.

Gustafsson, T., Ameln, H., Fischer, H., Sundberg, C.J., Timmons, J.A., and Jansson, E. (2005). VEGF-A splice variants and related receptor expression in human skeletal muscle following submaximal exercise. J. Appl. Physiol. Bethesda Md 1985 *98*, 2137–2146.

Haas, T.L., and Nwadozi, E. (2015). Regulation of skeletal muscle capillary growth in exercise and disease. Appl. Physiol. Nutr. Metab. Physiol. Appl. Nutr. Metab. *40*, 1221–1232.

Hadi, A.M., Mouchaers, K.T.B., Schalij, I., Grunberg, K., Meijer, G.A., Vonk-Noordegraaf, A., van der Laarse, W.J., and Beliën, J.A.M. (2011). Rapid quantification of myocardial fibrosis: a new macro-based automated analysis. Cell. Oncol. Dordr. *34*, 343–354.

Haghighat, L., Ionescu, C.N., Regan, C.J., Altin, S.E., Attaran, R.R., and Mena-Hurtado, C.I. (2019). Review of the Current Basic Science Strategies to Treat Critical Limb Ischemia. Vasc. Endovascular Surg. *53*, 316–324.

Hamilton, N.B., Attwell, D., and Hall, C.N. (2010). Pericyte-mediated regulation of capillary diameter: a component of neurovascular coupling in health and disease. Front. Neuroenergetics *2*.

Hammes, H.-P., Lin, J., Wagner, P., Feng, Y., Vom Hagen, F., Krzizok, T., Renner, O., Breier, G., Brownlee, M., and Deutsch, U. (2004). Angiopoietin-2 causes pericyte dropout in the normal retina: evidence for involvement in diabetic retinopathy. Diabetes *53*, 1104–1110.

Han, K.A., Patel, Y., Lteif, A.A., Chisholm, R., and Mather, K.J. (2011). Contributions of dysglycaemia, obesity, and insulin resistance to impaired endothelium-dependent vasodilation in humans. Diabetes Metab. Res. Rev. *27*, 354–361.

Han, X., Boyd, P.J., Colgan, S., Madri, J.A., and Haas, T.L. (2003). Transcriptional up-regulation of endothelial cell matrix metalloproteinase-2 in response to extracellular cues involves GATA-2. J. Biol. Chem. *278*, 47785–47791.

Harmon, C.M., and Abumrad, N.A. (1993). Binding of sulfosuccinimidyl fatty acids to adipocyte membrane proteins: isolation and amino-terminal sequence of an 88-kD protein implicated in transport of long-chain fatty acids. J. Membr. Biol. *133*, 43–49.

Hayden, M.R., Yang, Y., Habibi, J., Bagree, S.V., and Sowers, J.R. (2010). Pericytopathy: oxidative stress and impaired cellular longevity in the pancreas and skeletal muscle in metabolic syndrome and type 2 diabetes. Oxid. Med. Cell. Longev. *3*, 290–303.

Haynes, B.F., Scearce, R.M., Lobach, D.F., and Hensley, L.L. (1984). Phenotypic characterization and ontogeny of mesodermal-derived and endocrine epithelial components of the human thymic microenvironment. J. Exp. Med. *159*, 1149–1168.

He, L., Vanlandewijck, M., Mäe, M.A., Andrae, J., Ando, K., Del Gaudio, F., Nahar, K., Lebouvier, T., Laviña, B., Gouveia, L., et al. (2018). Single-cell RNA sequencing of mouse brain and lung vascular and vessel-associated cell types. Sci. Data *5*, 180160.

Hedman, A., Berglund, L., Essén-Gustavsson, B., Reneland, R., and Lithell, H. (2000). Relationships between muscle morphology and insulin sensitivity are improved after adjustment for intra-individual variability in 70-year-old men. Acta Physiol. Scand. *169*, 125–132.

Hellsten, Y., Rufener, N., Nielsen, J.J., Høier, B., Krustrup, P., and Bangsbo, J. (2008). Passive leg movement enhances interstitial VEGF protein, endothelial cell proliferation, and eNOS mRNA content in human skeletal muscle. Am. J. Physiol. Regul. Integr. Comp. Physiol. *294*, R975-982.

Herzog, B., Pellet-Many, C., Britton, G., Hartzoulakis, B., and Zachary, I.C. (2011). VEGF binding to NRP1 is essential for VEGF stimulation of endothelial cell migration, complex formation between NRP1 and VEGFR2, and signaling via FAK Tyr407 phosphorylation. Mol. Biol. Cell *22*, 2766–2776.

Hileman, S.M., Tornøe, J., Flier, J.S., and Bjørbaek, C. (2000). Transcellular transport of leptin by the short leptin receptor isoform ObRa in Madin-Darby Canine Kidney cells. Endocrinology *141*, 1955–1961.

Hileman, S.M., Pierroz, D.D., Masuzaki, H., Bjørbaek, C., El-Haschimi, K., Banks, W.A., and Flier, J.S. (2002). Characterizaton of short isoforms of the leptin receptor in rat cerebral microvessels and of brain uptake of leptin in mouse models of obesity. Endocrinology *143*, 775–783.

Hill, R.A., Margetic, S., Pegg, G.G., and Gazzola, C. (1998). Leptin: its pharmacokinetics and tissue distribution. Int. J. Obes. Relat. Metab. Disord. J. Int. Assoc. Study Obes. *22*, 765–770.

Hill, R.A., Tong, L., Yuan, P., Murikinati, S., Gupta, S., and Grutzendler, J. (2015). Regional Blood Flow in the Normal and Ischemic Brain Is Controlled by Arteriolar Smooth Muscle Cell Contractility and Not by Capillary Pericytes. Neuron *87*, 95–110.

Hlushchuk, R., Riesterer, O., Baum, O., Wood, J., Gruber, G., Pruschy, M., and Djonov, V. (2008). Tumor recovery by angiogenic switch from sprouting to intussusceptive angiogenesis after treatment with PTK787/ZK222584 or ionizing radiation. Am. J. Pathol. *173*, 1173–1185.

Hodges, N.A., Suarez-Martinez, A.D., and Murfee, W.L. (2018). Understanding angiogenesis during aging: opportunities for discoveries and new models. J. Appl. Physiol. Bethesda Md 1985 *125*, 1843–1850.

Hoefer, I.E., van Royen, N., Buschmann, I.R., Piek, J.J., and Schaper, W. (2001). Time course of arteriogenesis following femoral artery occlusion in the rabbit. Cardiovasc. Res. *49*, 609–617.

Hoekman, M.F.M., Jacobs, F.M.J., Smidt, M.P., and Burbach, J.P.H. (2006). Spatial and temporal expression of FoxO transcription factors in the developing and adult murine brain. Gene Expr. Patterns GEP *6*, 134–140.

Hoier, B., and Hellsten, Y. (2014). Exercise-induced capillary growth in human skeletal muscle and the dynamics of VEGF. Microcirc. N. Y. N 1994 *21*, 301–314.

Høier, B., Olsen, K., Nyberg, M., Bangsbo, J., and Hellsten, Y. (2010). Contraction-induced secretion of VEGF from skeletal muscle cells is mediated by adenosine. Am. J. Physiol. Heart Circ. Physiol. *299*, H857-862.

Hoier, B., Walker, M., Passos, M., Walker, P.J., Green, A., Bangsbo, J., Askew, C.D., and Hellsten, Y. (2013). Angiogenic response to passive movement and active exercise in individuals with peripheral arterial disease. J. Appl. Physiol. Bethesda Md 1985 *115*, 1777–1787.

Honkura, N., Richards, M., Laviña, B., Sáinz-Jaspeado, M., Betsholtz, C., and Claesson-Welsh, L. (2018). Intravital imaging-based analysis tools for vessel identification and assessment of concurrent dynamic vascular events. Nat. Commun. *9*, 2746.

Hosaka, T., Biggs, W.H., Tieu, D., Boyer, A.D., Varki, N.M., Cavenee, W.K., and Arden, K.C. (2004). Disruption of forkhead transcription factor (FOXO) family members in mice reveals their functional diversification. Proc. Natl. Acad. Sci. U. S. A. *101*, 2975–2980.

Hotamisligil, G.S., and Bernlohr, D.A. (2015). Metabolic functions of FABPs--mechanisms and therapeutic implications. Nat. Rev. Endocrinol. *11*, 592–605.

Hotamisligil, G.S., Arner, P., Caro, J.F., Atkinson, R.L., and Spiegelman, B.M. (1995). Increased adipose tissue expression of tumor necrosis factor-alpha in human obesity and insulin resistance. J. Clin. Invest. *95*, 2409–2415.

Iso, T., Maeda, K., Hanaoka, H., Suga, T., Goto, K., Syamsunarno, M.R.A.A., Hishiki, T., Nagahata, Y., Matsui, H., Arai, M., et al. (2013). Capillary endothelial fatty acid binding proteins 4 and 5 play a critical role in fatty acid uptake in heart and skeletal muscle. Arterioscler. Thromb. Vasc. Biol. *33*, 2549–2557.

Jablonski, K.A., Amici, S.A., Webb, L.M., Ruiz-Rosado, J. de D., Popovich, P.G., Partida-Sanchez, S., and Guerau-de-Arellano, M. (2015). Novel Markers to Delineate Murine M1 and M2 Macrophages. PloS One *10*, e0145342.

Jacobs, F.M.J., van der Heide, L.P., Wijchers, P.J.E.C., Burbach, J.P.H., Hoekman, M.F.M., and Smidt, M.P. (2003). FoxO6, a novel member of the FoxO class of transcription factors with distinct shuttling dynamics. J. Biol. Chem. *278*, 35959–35967.

Jager, A., van Hinsbergh, V.W., Kostense, P.J., Emeis, J.J., Nijpels, G., Dekker, J.M., Heine, R.J., Bouter, L.M., and Stehouwer, C.D. (2000). Increased levels of soluble vascular cell adhesion molecule 1 are associated with risk of cardiovascular mortality in type 2 diabetes: the Hoorn study. Diabetes *49*, 485–491.

Ji, Y., Chen, S., Xiang, B., Li, Y., Li, L., and Wang, Q. (2016). Jagged1/Notch3 Signaling Modulates Hemangioma-Derived Pericyte Proliferation and Maturation. Cell. Physiol. Biochem. Int. J. Exp. Cell. Physiol. Biochem. Pharmacol. *40*, 895–907.

de Jongh, R.T., Serné, E.H., Ijzerman, R.G., de Vries, G., and Stehouwer, C.D.A. (2004a). Free fatty acid levels modulate microvascular function: relevance for obesity-associated insulin resistance, hypertension, and microangiopathy. Diabetes *53*, 2873–2882.

de Jongh, R.T., Serné, E.H., IJzerman, R.G., de Vries, G., and Stehouwer, C.D.A. (2004b). Impaired microvascular function in obesity: implications for obesity-associated microangiopathy, hypertension, and insulin resistance. Circulation *109*, 2529–2535.

de Jongh, R.T., Serné, E.H., IJzerman, R.G., Jørstad, H.T., and Stehouwer, C.D.A. (2008). Impaired local microvascular vasodilatory effects of insulin and reduced skin microvascular vasomotion in obese women. Microvasc. Res. *75*, 256–262.

Jonk, A.M., Houben, A.J.H.M., de Jongh, R.T., Serné, E.H., Schaper, N.C., and Stehouwer, C.D.A. (2007). Microvascular dysfunction in obesity: a potential mechanism in the pathogenesis of obesity-associated insulin resistance and hypertension. Physiol. Bethesda Md *22*, 252–260.

Jonk, A.M., Houben, A.J., Schaper, N.C., de Leeuw, P.W., Serné, E.H., Smulders, Y.M., and Stehouwer, C.D. (2011a). Meal-related increases in microvascular vasomotion are impaired in obese individuals: a potential mechanism in the pathogenesis of obesity-related insulin resistance. Diabetes Care *34 Suppl 2*, S342-348.

Jonk, A.M., Houben, A.J., Schaper, N.C., de Leeuw, P.W., Serné, E.H., Smulders, Y.M., and Stehouwer, C.D. (2011b). Obesity is associated with impaired endothelial function in the postprandial state. Microvasc. Res. *82*, 423–429.

Jude, E.B., Eleftheriadou, I., and Tentolouris, N. (2010). Peripheral arterial disease in diabetes--a review. Diabet. Med. J. Br. Diabet. Assoc. *27*, 4–14.

Judson, R.N., Zhang, R.-H., and Rossi, F.M.A. (2013). Tissue-resident mesenchymal stem/progenitor cells in skeletal muscle: collaborators or saboteurs? FEBS J. *280*, 4100–4108.

Kaestner, K.H., Knochel, W., and Martinez, D.E. (2000). Unified nomenclature for the winged helix/forkhead transcription factors. Genes Dev. *14*, 142–146.

Karaca, Ü., Schram, M.T., Houben, A.J.H.M., Muris, D.M.J., and Stehouwer, C.D.A. (2014). Microvascular dysfunction as a link between obesity, insulin resistance and hypertension. Diabetes Res. Clin. Pract. *103*, 382–387.

Karki, S., Farb, M.G., Ngo, D.T.M., Myers, S., Puri, V., Hamburg, N.M., Carmine, B., Hess, D.T., and Gokce, N. (2015). Forkhead Box O-1 Modulation Improves Endothelial Insulin Resistance in Human Obesity. Arterioscler. Thromb. Vasc. Biol. *35*, 1498–1506.

Katwal, A.B., and Dokun, A.O. (2011). Peripheral arterial disease in diabetes: is there a role for genetics? Curr. Diab. Rep. *11*, 218–225.

Kazantzis, M., and Stahl, A. (2012). Fatty acid transport proteins, implications in physiology and disease. Biochim. Biophys. Acta *1821*, 852–857.

Kelly, T., Yang, W., Chen, C.-S., Reynolds, K., and He, J. (2008). Global burden of obesity in 2005 and projections to 2030. Int. J. Obes. 2005 *32*, 1431–1437.

Kershaw, E.E., and Flier, J.S. (2004). Adipose tissue as an endocrine organ. J. Clin. Endocrinol. Metab. *89*, 2548–2556.

Keske, M.A., Dwyer, R.M., Russell, R.D., Blackwood, S.J., Brown, A.A., Hu, D., Premilovac, D., Richards, S.M., and Rattigan, S. (2017). Regulation of microvascular flow and metabolism: An overview. Clin. Exp. Pharmacol. Physiol. *44*, 143–149.

Kiens, B., Essen-Gustavsson, B., Gad, P., and Lithell, H. (1987). Lipoprotein lipase activity and intramuscular triglyceride stores after long-term high-fat and high-carbohydrate diets in physically trained men. Clin. Physiol. Oxf. Engl. *7*, 1–9.

Kim, D.D., and Basu, A. (2016). Estimating the Medical Care Costs of Obesity in the United States: Systematic Review, Meta-Analysis, and Empirical Analysis. Value Health J. Int. Soc. Pharmacoeconomics Outcomes Res. *19*, 602–613.

Kim, F., Pham, M., Maloney, E., Rizzo, N.O., Morton, G.J., Wisse, B.E., Kirk, E.A., Chait, A., and Schwartz, M.W. (2008). Vascular inflammation, insulin resistance, and reduced nitric oxide

production precede the onset of peripheral insulin resistance. Arterioscler. Thromb. Vasc. Biol. *28*, 1982–1988.

Kim, J., Montagnani, M., Koh, K.K., and Quon, M.J. (2006). Reciprocal relationships between insulin resistance and endothelial dysfunction: molecular and pathophysiological mechanisms. Circulation *113*, 1888–1904.

Kirton, J.P., Crofts, N.J., George, S.J., Brennan, K., and Canfield, A.E. (2007). Wnt/beta-catenin signaling stimulates chondrogenic and inhibits adipogenic differentiation of pericytes: potential relevance to vascular disease? Circ. Res. *101*, 581–589.

Kisler, K., Nelson, A.R., Rege, S.V., Ramanathan, A., Wang, Y., Ahuja, A., Lazic, D., Tsai, P.S., Zhao, Z., Zhou, Y., et al. (2017). Pericyte degeneration leads to neurovascular uncoupling and limits oxygen supply to brain. Nat. Neurosci. *20*, 406–416.

Kofler, N.M., Cuervo, H., Uh, M.K., Murtomäki, A., and Kitajewski, J. (2015). Combined deficiency of Notch1 and Notch3 causes pericyte dysfunction, models CADASIL, and results in arteriovenous malformations. Sci. Rep. *5*, 16449.

Konishi, M., Sakaguchi, M., Lockhart, S.M., Cai, W., Li, M.E., Homan, E.P., Rask-Madsen, C., and Kahn, C.R. (2017). Endothelial insulin receptors differentially control insulin signaling kinetics in peripheral tissues and brain of mice. Proc. Natl. Acad. Sci. U. S. A. *114*, E8478–E8487.

Korn, C., and Augustin, H.G. (2015). Mechanisms of Vessel Pruning and Regression. Dev. Cell *34*, 5–17.

Korthuis, R.J. (2011). Skeletal Muscle Circulation (San Rafael (CA): Morgan & Claypool Life Sciences).

Krämer, A., Green, J., Pollard, J., and Tugendreich, S. (2014). Causal analysis approaches in Ingenuity Pathway Analysis. Bioinforma. Oxf. Engl. *30*, 523–530.

Krock, B.L., Skuli, N., and Simon, M.C. (2011). Hypoxia-induced angiogenesis: good and evil. Genes Cancer *2*, 1117–1133.

Krogh, A. (1919a). The number and distribution of capillaries in muscles with calculations of the oxygen pressure head necessary for supplying the tissue. J. Physiol. *52*, 409–415.

Krogh, A. (1919b). The supply of oxygen to the tissues and the regulation of the capillary circulation. J. Physiol. *52*, 457–474.

Kubota, T., Kubota, N., Kumagai, H., Yamaguchi, S., Kozono, H., Takahashi, T., Inoue, M., Itoh, S., Takamoto, I., Sasako, T., et al. (2011). Impaired insulin signaling in endothelial cells reduces insulin-induced glucose uptake by skeletal muscle. Cell Metab. *13*, 294–307.

Kühn, R., Schwenk, F., Aguet, M., and Rajewsky, K. (1995). Inducible gene targeting in mice. Science *269*, 1427–1429.

Kusuhara, S., Fukushima, Y., Ogura, S., Inoue, N., and Uemura, A. (2018). Pathophysiology of Diabetic Retinopathy: The Old and the New. Diabetes Metab. J. *42*, 364–376.

Lauby-Secretan, B., Scoccianti, C., Loomis, D., Grosse, Y., Bianchini, F., Straif, K., and International Agency for Research on Cancer Handbook Working Group (2016). Body Fatness and Cancer--Viewpoint of the IARC Working Group. N. Engl. J. Med. *375*, 794–798.

Lawler, P.R., and Lawler, J. (2012). Molecular basis for the regulation of angiogenesis by thrombospondin-1 and -2. Cold Spring Harb. Perspect. Med. *2*, a006627.

Lawler, J.W., Slayter, H.S., and Coligan, J.E. (1978). Isolation and characterization of a high molecular weight glycoprotein from human blood platelets. J. Biol. Chem. *253*, 8609–8616.

Lawrence, T., and Natoli, G. (2011). Transcriptional regulation of macrophage polarization: enabling diversity with identity. Nat. Rev. Immunol. *11*, 750–761.

Lederman, R.J., Mendelsohn, F.O., Anderson, R.D., Saucedo, J.F., Tenaglia, A.N., Hermiller, J.B., Hillegass, W.B., Rocha-Singh, K., Moon, T.E., Whitehouse, M.J., et al. (2002). Therapeutic angiogenesis with recombinant fibroblast growth factor-2 for intermittent claudication (the TRAFFIC study): a randomised trial. Lancet Lond. Engl. *359*, 2053–2058.

Lee, G.H., Proenca, R., Montez, J.M., Carroll, K.M., Darvishzadeh, J.G., Lee, J.I., and Friedman, J.M. (1996). Abnormal splicing of the leptin receptor in diabetic mice. Nature *379*, 632–635.

Lee, J.S., Pinnamaneni, S.K., Eo, S.J., Cho, I.H., Pyo, J.H., Kim, C.K., Sinclair, A.J., Febbraio, M.A., and Watt, M.J. (2006). Saturated, but not n-6 polyunsaturated, fatty acids induce insulin resistance: role of intramuscular accumulation of lipid metabolites. J. Appl. Physiol. Bethesda Md 1985 *100*, 1467–1474.

Lee, S., Chen, T.T., Barber, C.L., Jordan, M.C., Murdock, J., Desai, S., Ferrara, N., Nagy, A., Roos, K.P., and Iruela-Arispe, M.L. (2007). Autocrine VEGF signaling is required for vascular homeostasis. Cell *130*, 691–703.

Liapaki, I., Anagnostoulis, S., Karayiannakis, A., Korkolis, D., Labropoulou, M., Matarasso, A., and Simopoulos, C. (2008). Burn wound angiogenesis is increased by exogenously administered recombinant leptin in rats. Acta Cir. Bras. *23*, 118–124.

Lillioja, S., and Bogardus, C. (1988). Insulin resistance in Pima Indians. A combined effect of genetic predisposition and obesity-related skeletal muscle cell hypertrophy. Acta Med. Scand. Suppl. *723*, 103–119.

Lillioja, S., Young, A.A., Culter, C.L., Ivy, J.L., Abbott, W.G., Zawadzki, J.K., Yki-Järvinen, H., Christin, L., Secomb, T.W., and Bogardus, C. (1987). Skeletal muscle capillary density and fiber type are possible determinants of in vivo insulin resistance in man. J. Clin. Invest. *80*, 415–424.

Lindahl, P., Johansson, B.R., Levéen, P., and Betsholtz, C. (1997). Pericyte loss and microaneurysm formation in PDGF-B-deficient mice. Science *277*, 242–245.

Liu, L., Karkanias, G.B., Morales, J.C., Hawkins, M., Barzilai, N., Wang, J., and Rossetti, L. (1998). Intracerebroventricular leptin regulates hepatic but not peripheral glucose fluxes. J. Biol. Chem. *273*, 31160–31167.

Longland, C.J. (1953). The collateral circulation of the limb; Arris and Gale lecture delivered at the Royal College of Surgeons of England on 4th February, 1953. Ann. R. Coll. Surg. Engl. *13*, 161–176.

Lu, M., Amano, S., Miyamoto, K., Garland, R., Keough, K., Qin, W., and Adamis, A.P. (1999). Insulin-induced vascular endothelial growth factor expression in retina. Invest. Ophthalmol. Vis. Sci. *40*, 3281–3286.

Ludikhuize, J., de Launay, D., Groot, D., Smeets, T.J.M., Vinkenoog, M., Sanders, M.E., Tas, S.W., Tak, P.P., and Reedquist, K.A. (2007). Inhibition of forkhead box class O family member transcription factors in rheumatoid synovial tissue. Arthritis Rheum. *56*, 2180–2191.

Lundsgaard, A.-M., Holm, J.B., Sjøberg, K.A., Bojsen-Møller, K.N., Myrmel, L.S., Fjære, E., Jensen, B.A.H., Nicolaisen, T.S., Hingst, J.R., Hansen, S.L., et al. (2019). Mechanisms Preserving Insulin Action during High Dietary Fat Intake. Cell Metab. *29*, 50-63.e4.

Mac Gabhann, F., and Peirce, S.M. (2010). Collateral capillary arterialization following arteriolar ligation in murine skeletal muscle. Microcirc. N. Y. N 1994 *17*, 333–347.

MacDougald, O.A., and Lane, M.D. (1995). Transcriptional regulation of gene expression during adipocyte differentiation. Annu. Rev. Biochem. *64*, 345–373.

Maisonpierre, P.C., Suri, C., Jones, P.F., Bartunkova, S., Wiegand, S.J., Radziejewski, C., Compton, D., McClain, J., Aldrich, T.H., Papadopoulos, N., et al. (1997). Angiopoietin-2, a natural antagonist for Tie2 that disrupts in vivo angiogenesis. Science *277*, 55–60.

Majumdar, S., Genders, A.J., Inyard, A.C., Frison, V., and Barrett, E.J. (2012). Insulin entry into muscle involves a saturable process in the vascular endothelium. Diabetologia *55*, 450–456.

Makanya, A.N., Hlushchuk, R., Baum, O., Velinov, N., Ochs, M., and Djonov, V. (2007). Microvascular endowment in the developing chicken embryo lung. Am. J. Physiol. Lung Cell. Mol. Physiol. *292*, L1136-1146.

Makanya, A.N., Hlushchuk, R., and Djonov, V.G. (2009). Intussusceptive angiogenesis and its role in vascular morphogenesis, patterning, and remodeling. Angiogenesis *12*, 113–123.

Malek, M.H., and Olfert, I.M. (2009). Global deletion of thrombospondin-1 increases cardiac and skeletal muscle capillarity and exercise capacity in mice. Exp. Physiol. *94*, 749–760.

Mandel, E.R., Uchida, C., Nwadozi, E., Makki, A., and Haas, T.L. (2017). Tissue Inhibitor of Metalloproteinase 1 Influences Vascular Adaptations to Chronic Alterations in Blood Flow. J. Cell. Physiol. *232*, 831–841.

Manjunathan, R., and Ragunathan, M. (2015). In ovo administration of human recombinant leptin shows dose dependent angiogenic effect on chicken chorioallantoic membrane. Biol. Res. *48*, 29.

Maresh, G.A., Maness, L.M., Zadina, J.E., and Kastin, A.J. (2001). In vitro demonstration of a saturable transport system for leptin across the blood-brain barrier. Life Sci. *69*, 67–73.

Marinkovic, M., Fuoco, C., Sacco, F., Cerquone Perpetuini, A., Giuliani, G., Micarelli, E., Pavlidou, T., Petrilli, L.L., Reggio, A., Riccio, F., et al. (2019). Fibro-adipogenic progenitors of dystrophic mice are insensitive to NOTCH regulation of adipogenesis. Life Sci. Alliance *2*.

Matsumoto, M., Pocai, A., Rossetti, L., Depinho, R.A., and Accili, D. (2007). Impaired regulation of hepatic glucose production in mice lacking the forkhead transcription factor Foxo1 in liver. Cell Metab. *6*, 208–216.

Mauer, J., Chaurasia, B., Goldau, J., Vogt, M.C., Ruud, J., Nguyen, K.D., Theurich, S., Hausen, A.C., Schmitz, J., Brönneke, H.S., et al. (2014). Signaling by IL-6 promotes alternative activation of macrophages to limit endotoxemia and obesity-associated resistance to insulin. Nat. Immunol. *15*, 423–430.

Maxhimer, J.B., Soto-Pantoja, D.R., Ridnour, L.A., Shih, H.B., Degraff, W.G., Tsokos, M., Wink, D.A., Isenberg, J.S., and Roberts, D.D. (2009). Radioprotection in normal tissue and delayed tumor growth by blockade of CD47 signaling. Sci. Transl. Med. *1*, 3ra7.

McMinn, J.E., Liu, S.-M., Dragatsis, I., Dietrich, P., Ludwig, T., Eiden, S., and Chua, S.C. (2004). An allelic series for the leptin receptor gene generated by CRE and FLP recombinase. Mamm. Genome Off. J. Int. Mamm. Genome Soc. *15*, 677–685.

McMurtry, J.P., Ashwell, C.M., Brocht, D.M., and Caperna, T.J. (2004). Plasma clearance and tissue distribution of radiolabeled leptin in the chicken. Comp. Biochem. Physiol. A. Mol. Integr. Physiol. *138*, 27–32.

Michaud, J., Simpson, K.M., Escher, R., Buchet-Poyau, K., Beissbarth, T., Carmichael, C., Ritchie, M.E., Schütz, F., Cannon, P., Liu, M., et al. (2008). Integrative analysis of RUNX1 downstream pathways and target genes. BMC Genomics *9*, 363.

Michel, C.C., and Curry, F.E. (1999). Microvascular permeability. Physiol. Rev. *79*, 703–761.

Miles, P.D., Levisetti, M., Reichart, D., Khoursheed, M., Moossa, A.R., and Olefsky, J.M. (1995). Kinetics of insulin action in vivo. Identification of rate-limiting steps. Diabetes *44*, 947–953.

Milkiewicz, M., Hudlicka, O., Shiner, R., Egginton, S., and Brown, M.D. (2006). Vascular endothelial growth factor mRNA and protein do not change in parallel during non-inflammatory skeletal muscle ischaemia in rat. J. Physiol. *577*, 671–678.

Milkiewicz, M., Mohammadzadeh, F., Ispanovic, E., Gee, E., and Haas, T.L. (2007). Static strain stimulates expression of matrix metalloproteinase-2 and VEGF in microvascular endothelium via JNK- and ERK-dependent pathways. J. Cell. Biochem. *100*, 750–761.

Milkiewicz, M., Roudier, E., Doyle, J.L., Trifonova, A., Birot, O., and Haas, T.L. (2011). Identification of a mechanism underlying regulation of the anti-angiogenic forkhead transcription factor FoxO1 in cultured endothelial cells and ischemic muscle. Am. J. Pathol. *178*, 935–944.

Mogi, M., Kohara, K., Nakaoka, H., Kan-No, H., Tsukuda, K., Wang, X.-L., Chisaka, T., Bai, H.-Y., Shan, B.-S., Kukida, M., et al. (2016). Diabetic mice exhibited a peculiar alteration in body composition with exaggerated ectopic fat deposition after muscle injury due to anomalous cell differentiation. J. Cachexia Sarcopenia Muscle *7*, 213–224.

Morrison, R.F., and Farmer, S.R. (2000). Hormonal signaling and transcriptional control of adipocyte differentiation. J. Nutr. *130*, 3116S-3121S.

Morton, G.J., Gelling, R.W., Niswender, K.D., Morrison, C.D., Rhodes, C.J., and Schwartz, M.W. (2005). Leptin regulates insulin sensitivity via phosphatidylinositol-3-OH kinase signaling in mediobasal hypothalamic neurons. Cell Metab. *2*, 411–420.

Müller, M., Holmäng, A., Andersson, O.K., Eichler, H.G., and Lönnroth, P. (1996). Measurement of interstitial muscle glucose and lactate concentrations during an oral glucose tolerance test. Am. J. Physiol. *271*, E1003-1007.

Muoio, D.M., and Lynis Dohm, G. (2002). Peripheral metabolic actions of leptin. Best Pract. Res. Clin. Endocrinol. Metab. *16*, 653–666.

Murakami, S., Fujino, H., Takeda, I., Momota, R., Kumagishi, K., and Ohtsuka, A. (2010). Comparison of capillary architecture between slow and fast muscles in rats using a confocal laser scanning microscope. Acta Med. Okayama *64*, 11–18.

Murakami, S., Fujita, N., Kondo, H., Takeda, I., Momota, R., Ohtsuka, A., and Fujino, H. (2012). Abnormalities in the fiber composition and capillary architecture in the soleus muscle of type 2 diabetic Goto-Kakizaki rats. ScientificWorldJournal *2012*, 680189.

Muris, D.M.J., Houben, A.J.H.M., Schram, M.T., and Stehouwer, C.D.A. (2012). Microvascular dysfunction is associated with a higher incidence of type 2 diabetes mellitus: a systematic review and meta-analysis. Arterioscler. Thromb. Vasc. Biol. *32*, 3082–3094.

Nascimento, A.R., Machado, M., de Jesus, N., Gomes, F., Lessa, M.A., Bonomo, I.T., and Tibiriçá, E. (2013). Structural and functional microvascular alterations in a rat model of metabolic syndrome induced by a high-fat diet. Obes. Silver Spring Md *21*, 2046–2054.

Navarro, R., Compte, M., Álvarez-Vallina, L., and Sanz, L. (2016). Immune Regulation by Pericytes: Modulating Innate and Adaptive Immunity. Front. Immunol. *7*, 480.

Nehls, V., Denzer, K., and Drenckhahn, D. (1992). Pericyte involvement in capillary sprouting during angiogenesis in situ. Cell Tissue Res. *270*, 469–474.

Neufeld, G., Cohen, T., Gitay-Goren, H., Poltorak, Z., Tessler, S., Sharon, R., Gengrinovitch, S., and Levi, B.Z. (1996). Similarities and differences between the vascular endothelial growth factor (VEGF) splice variants. Cancer Metastasis Rev. *15*, 153–158.

Noer, A., Sørensen, A.L., Boquest, A.C., and Collas, P. (2006). Stable CpG hypomethylation of adipogenic promoters in freshly isolated, cultured, and differentiated mesenchymal stem cells from adipose tissue. Mol. Biol. Cell *17*, 3543–3556.

Nwadozi, E., Roudier, E., Rullman, E., Tharmalingam, S., Liu, H.-Y., Gustafsson, T., and Haas, T.L. (2016). Endothelial FoxO proteins impair insulin sensitivity and restrain muscle angiogenesis in response to a high-fat diet. FASEB J. Off. Publ. Fed. Am. Soc. Exp. Biol. *30*, 3039–3052.

Nwadozi, E., Ng, A., Strömberg, A., Liu, H.-Y., Olsson, K., Gustafsson, T., and Haas, T.L. (2019). Leptin is a physiological regulator of skeletal muscle angiogenesis and is locally produced by PDGFRα and PDGFRβ expressing perivascular cells. Angiogenesis *22*, 103–115.

Nwadozi, E., Rudnicki, M., and Haas, T.L. (2020). Metabolic Coordination of Pericyte Phenotypes: Therapeutic Implications. Front. Cell Dev. Biol. *8*, 77.

Oellerich, M.F., and Potente, M. (2012). FOXOs and sirtuins in vascular growth, maintenance, and aging. Circ. Res. *110*, 1238–1251.

Olfert, I.M. (2016). Physiological Capillary Regression is not Dependent on Reducing VEGF Expression. Microcirc. N. Y. N 1994 *23*, 146–156.

Olfert, I.M., Howlett, R.A., Tang, K., Dalton, N.D., Gu, Y., Peterson, K.L., Wagner, P.D., and Breen, E.C. (2009). Muscle-specific VEGF deficiency greatly reduces exercise endurance in mice. J. Physiol. *587*, 1755–1767.

Olfert, I.M., Howlett, R.A., Wagner, P.D., and Breen, E.C. (2010). Myocyte vascular endothelial growth factor is required for exercise-induced skeletal muscle angiogenesis. Am. J. Physiol. Regul. Integr. Comp. Physiol. *299*, R1059-1067.

Oliva, A., Fariña, J., and Llabrés, M. (2000). Development of two high-performance liquid chromatographic methods for the analysis and characterization of insulin and its degradation products in pharmaceutical preparations. J. Chromatogr. B. Biomed. Sci. App. *749*, 25–34.

Olsson, A.-K., Dimberg, A., Kreuger, J., and Claesson-Welsh, L. (2006). VEGF receptor signalling - in control of vascular function. Nat. Rev. Mol. Cell Biol. *7*, 359–371.

Paik, J.-H., Kollipara, R., Chu, G., Ji, H., Xiao, Y., Ding, Z., Miao, L., Tothova, Z., Horner, J.W., Carrasco, D.R., et al. (2007). FoxOs are lineage-restricted redundant tumor suppressors and regulate endothelial cell homeostasis. Cell *128*, 309–323.

Pan, D.A., Lillioja, S., Kriketos, A.D., Milner, M.R., Baur, L.A., Bogardus, C., Jenkins, A.B., and Storlien, L.H. (1997). Skeletal muscle triglyceride levels are inversely related to insulin action. Diabetes *46*, 983–988.

Papapetropoulos, A., Fulton, D., Mahboubi, K., Kalb, R.G., O'Connor, D.S., Li, F., Altieri, D.C., and Sessa, W.C. (2000). Angiopoietin-1 inhibits endothelial cell apoptosis via the Akt/survivin pathway. J. Biol. Chem. *275*, 9102–9105.

Pappenheimer, J.R., Renkin, E.M., and Borrero, L.M. (1951). Filtration, diffusion and molecular sieving through peripheral capillary membranes; a contribution to the pore theory of capillary permeability. Am. J. Physiol. *167*, 13–46.

Park, H.Y., Kwon, H.M., Lim, H.J., Hong, B.K., Lee, J.Y., Park, B.E., Jang, Y., Cho, S.Y., and Kim, H.S. (2001). Potential role of leptin in angiogenesis: leptin induces endothelial cell proliferation and expression of matrix metalloproteinases in vivo and in vitro. Exp. Mol. Med. *33*, 95–102.

Peirce, S.M., and Skalak, T.C. (2003). Microvascular remodeling: a complex continuum spanning angiogenesis to arteriogenesis. Microcirc. N. Y. N 1994 *10*, 99–111.

Pi, X., Xie, L., and Patterson, C. (2018). Emerging Roles of Vascular Endothelium in Metabolic Homeostasis. Circ. Res. *123*, 477–494.

Pierantozzi, E., Vezzani, B., Badin, M., Curina, C., Severi, F.M., Petraglia, F., Randazzo, D., Rossi, D., and Sorrentino, V. (2016). Tissue-Specific Cultured Human Pericytes: Perivascular Cells from Smooth Muscle Tissue Have Restricted Mesodermal Differentiation Ability. Stem Cells Dev. *25*, 674–686.

Pillon, N.J., Azizi, P.M., Li, Y.E., Liu, J., Wang, C., Chan, K.L., Hopperton, K.E., Bazinet, R.P., Heit, B., Bilan, P.J., et al. (2015). Palmitate-induced inflammatory pathways in human adipose microvascular endothelial cells promote monocyte adhesion and impair insulin transcytosis. Am. J. Physiol. Endocrinol. Metab. *309*, E35-44.

Pipinos, I.I., Judge, A.R., Selsby, J.T., Zhu, Z., Swanson, S.A., Nella, A.A., and Dodd, S.L. (2007). The myopathy of peripheral arterial occlusive disease: part 1. Functional and histomorphological changes and evidence for mitochondrial dysfunction. Vasc. Endovascular Surg. *41*, 481–489.

Pipinos, I.I., Judge, A.R., Selsby, J.T., Zhu, Z., Swanson, S.A., Nella, A.A., and Dodd, S.L. (2008). The myopathy of peripheral arterial occlusive disease: Part 2. Oxidative stress, neuropathy, and shift in muscle fiber type. Vasc. Endovascular Surg. *42*, 101–112.

Poole, D.C., Copp, S.W., Hirai, D.M., and Musch, T.I. (2011). Dynamics of muscle microcirculatory and blood-myocyte O(2) flux during contractions. Acta Physiol. Oxf. Engl. *202*, 293–310.

Poole, D.C., Copp, S.W., Ferguson, S.K., and Musch, T.I. (2013). Skeletal muscle capillary function: contemporary observations and novel hypotheses. Exp. Physiol. *98*, 1645–1658.

Potente, M., Urbich, C., Sasaki, K., Hofmann, W.K., Heeschen, C., Aicher, A., Kollipara, R., DePinho, R.A., Zeiher, A.M., and Dimmeler, S. (2005). Involvement of Foxo transcription factors in angiogenesis and postnatal neovascularization. J. Clin. Invest. *115*, 2382–2392.

Potenza, M.A., Addabbo, F., and Montagnani, M. (2009). Vascular actions of insulin with implications for endothelial dysfunction. Am. J. Physiol. Endocrinol. Metab. *297*, E568-577.

Powell, R.J., Simons, M., Mendelsohn, F.O., Daniel, G., Henry, T.D., Koga, M., Morishita, R., and Annex, B.H. (2008). Results of a double-blind, placebo-controlled study to assess the safety of intramuscular injection of hepatocyte growth factor plasmid to improve limb perfusion in patients with critical limb ischemia. Circulation *118*, 58–65.

Prior, S.J., Goldberg, A.P., Ortmeyer, H.K., Chin, E.R., Chen, D., Blumenthal, J.B., and Ryan, A.S. (2015). Increased Skeletal Muscle Capillarization Independently Enhances Insulin Sensitivity in Older Adults After Exercise Training and Detraining. Diabetes *64*, 3386–3395.

Pugh, C.W., and Ratcliffe, P.J. (2003). Regulation of angiogenesis by hypoxia: role of the HIF system. Nat. Med. *9*, 677–684.

Pugsley, M.K., and Tabrizchi, R. (2000). The vascular system. An overview of structure and function. J. Pharmacol. Toxicol. Methods *44*, 333–340.

Radley-Crabb, H.G., Fiorotto, M.L., and Grounds, M.D. (2011). The different impact of a high fat diet on dystrophic mdx and control C57Bl/10 mice. PLoS Curr. *3*, RRN1276.

Ramsauer, M., and D'Amore, P.A. (2002). Getting Tie(2)d up in angiogenesis. J. Clin. Invest. *110*, 1615–1617.

Rattigan, S., Bussey, C.T., Ross, R.M., and Richards, S.M. (2007). Obesity, insulin resistance, and capillary recruitment. Microcirc. N. Y. N 1994 *14*, 299–309.

Ren, B., Yee, K.O., Lawler, J., and Khosravi-Far, R. (2006). Regulation of tumor angiogenesis by thrombospondin-1. Biochim. Biophys. Acta *1765*, 178–188.

Reynolds, L.E., D'Amico, G., Lechertier, T., Papachristodoulou, A., Muñoz-Félix, J.M., De Arcangelis, A., Baker, M., Serrels, B., and Hodivala-Dilke, K.M. (2017). Dual role of pericyte α6β1-integrin in tumour blood vessels. J. Cell Sci. *130*, 1583–1595.

Ribatti, D., Nico, B., and Crivellato, E. (2011). The role of pericytes in angiogenesis. Int. J. Dev. Biol. *55*, 261–268.

Rippe, B., Rosengren, B.-I., Carlsson, O., and Venturoli, D. (2002). Transendothelial transport: the vesicle controversy. J. Vasc. Res. *39*, 375–390.

Rivilis, I., Milkiewicz, M., Boyd, P., Goldstein, J., Brown, M.D., Egginton, S., Hansen, F.M., Hudlicka, O., and Haas, T.L. (2002). Differential involvement of MMP-2 and VEGF during muscle stretch- versus shear stress-induced angiogenesis. Am. J. Physiol. Heart Circ. Physiol. *283*, H1430-1438.

Robinson, R.S., Woad, K.J., Hammond, A.J., Laird, M., Hunter, M.G., and Mann, G.E. (2009). Angiogenesis and vascular function in the ovary. Reprod. Camb. Engl. *138*, 869–881.

Rodriguez-Manzaneque, J.C., Lane, T.F., Ortega, M.A., Hynes, R.O., Lawler, J., and Iruela-Arispe, M.L. (2001). Thrombospondin-1 suppresses spontaneous tumor growth and inhibits

activation of matrix metalloproteinase-9 and mobilization of vascular endothelial growth factor. Proc. Natl. Acad. Sci. U. S. A. *98*, 12485–12490.

Rosen, E.D., Hsu, C.-H., Wang, X., Sakai, S., Freeman, M.W., Gonzalez, F.J., and Spiegelman, B.M. (2002). C/EBPalpha induces adipogenesis through PPARgamma: a unified pathway. Genes Dev. *16*, 22–26.

Roudier, E., Milkiewicz, M., Birot, O., Slopack, D., Montelius, A., Gustafsson, T., Paik, J.H., DePinho, R.A., Casale, G.P., Pipinos, I.I., et al. (2013). Endothelial FoxO1 is an intrinsic regulator of thrombospondin 1 expression that restrains angiogenesis in ischemic muscle. Angiogenesis *16*, 759–772.

Rudnicki, M., Abdifarkosh, G., Nwadozi, E., Ramos, S.V., Makki, A., Sepa-Kishi, D.M., Ceddia, R.B., Perry, C.G., Roudier, E., and Haas, T.L. (2018). Endothelial-specific FoxO1 depletion prevents obesity-related disorders by increasing vascular metabolism and growth. ELife *7*.

Sargiannidou, I., Zhou, J., and Tuszynski, G.P. (2001). The role of thrombospondin-1 in tumor progression. Exp. Biol. Med. Maywood NJ *226*, 726–733.

Saunders, W.B., Bohnsack, B.L., Faske, J.B., Anthis, N.J., Bayless, K.J., Hirschi, K.K., and Davis, G.E. (2006). Coregulation of vascular tube stabilization by endothelial cell TIMP-2 and pericyte TIMP-3. J. Cell Biol. *175*, 179–191.

Schäfer, K., Halle, M., Goeschen, C., Dellas, C., Pynn, M., Loskutoff, D.J., and Konstantinides, S. (2004). Leptin promotes vascular remodeling and neointimal growth in mice. Arterioscler. Thromb. Vasc. Biol. *24*, 112–117.

Schiekofer, S., Galasso, G., Sato, K., Kraus, B.J., and Walsh, K. (2005). Impaired revascularization in a mouse model of type 2 diabetes is associated with dysregulation of a complex angiogenic-regulatory network. Arterioscler. Thromb. Vasc. Biol. *25*, 1603–1609.

Schlatter, P., König, M.F., Karlsson, L.M., and Burri, P.H. (1997). Quantitative study of intussusceptive capillary growth in the chorioallantoic membrane (CAM) of the chicken embryo. Microvasc. Res. *54*, 65–73.

Seoane, J., Le, H.-V., Shen, L., Anderson, S.A., and Massagué, J. (2004). Integration of Smad and forkhead pathways in the control of neuroepithelial and glioblastoma cell proliferation. Cell *117*, 211–223.

Serné, E.H., Gans, R.O., ter Maaten, J.C., Tangelder, G.J., Donker, A.J., and Stehouwer, C.D. (2001). Impaired skin capillary recruitment in essential hypertension is caused by both functional and structural capillary rarefaction. Hypertens. Dallas Tex 1979 *38*, 238–242.

Shikatani, E.A., Trifonova, A., Mandel, E.R., Liu, S.T.K., Roudier, E., Krylova, A., Szigiato, A., Beaudry, J., Riddell, M.C., and Haas, T.L. (2012). Inhibition of proliferation, migration and proteolysis contribute to corticosterone-mediated inhibition of angiogenesis. PloS One *7*, e46625.

Siedlecki, J., Asani, B., Wertheimer, C., Hillenmayer, A., Ohlmann, A., Priglinger, C., Priglinger, S., Wolf, A., and Eibl-Lindner, K. (2018). Combined VEGF/PDGF inhibition using axitinib induces αSMA expression and a pro-fibrotic phenotype in human pericytes. Graefes Arch. Clin. Exp. Ophthalmol. Albrecht Von Graefes Arch. Klin. Exp. Ophthalmol. *256*, 1141–1149.

Sierra-Honigmann, M.R., Nath, A.K., Murakami, C., García-Cardeña, G., Papapetropoulos, A., Sessa, W.C., Madge, L.A., Schechner, J.S., Schwabb, M.B., Polverini, P.J., et al. (1998). Biological action of leptin as an angiogenic factor. Science *281*, 1683–1686.

da Silva Meirelles, L., Caplan, A.I., and Nardi, N.B. (2008). In search of the in vivo identity of mesenchymal stem cells. Stem Cells Dayt. Ohio *26*, 2287–2299.

Silvennoinen, M., Rinnankoski-Tuikka, R., Vuento, M., Hulmi, J.J., Torvinen, S., Lehti, M., Kivelä, R., and Kainulainen, H. (2013). High-fat feeding induces angiogenesis in skeletal muscle and activates angiogenic pathways in capillaries. Angiogenesis *16*, 297–307.

Silvestre, J.-S., Smadja, D.M., and Lévy, B.I. (2013). Postischemic revascularization: from cellular and molecular mechanisms to clinical applications. Physiol. Rev. *93*, 1743–1802.

Simons, M., Gordon, E., and Claesson-Welsh, L. (2016). Mechanisms and regulation of endothelial VEGF receptor signalling. Nat. Rev. Mol. Cell Biol. *17*, 611–625.

Skalak, T.C., Price, R.J., and Zeller, P.J. (1998). Where do new arterioles come from? Mechanical forces and microvessel adaptation. Microcirc. N. Y. N 1994 *5*, 91–94.

Slopack, D., Roudier, E., Liu, S.T.K., Nwadozi, E., Birot, O., and Haas, T.L. (2014). Forkhead BoxO transcription factors restrain exercise-induced angiogenesis: FoxO proteins delay exercise-driven angiogenesis. J. Physiol. *592*, 4069–4082.

Soker, S., Takashima, S., Miao, H.Q., Neufeld, G., and Klagsbrun, M. (1998). Neuropilin-1 is expressed by endothelial and tumor cells as an isoform-specific receptor for vascular endothelial growth factor. Cell *92*, 735–745.

Soker, S., Miao, H.-Q., Nomi, M., Takashima, S., and Klagsbrun, M. (2002). VEGF165 mediates formation of complexes containing VEGFR-2 and neuropilin-1 that enhance VEGF165-receptor binding. J. Cell. Biochem. *85*, 357–368.

Solomon, T.P.J., Haus, J.M., Li, Y., and Kirwan, J.P. (2011). Progressive hyperglycemia across the glucose tolerance continuum in older obese adults is related to skeletal muscle capillarization and nitric oxide bioavailability. J. Clin. Endocrinol. Metab. *96*, 1377–1384.

Stapor, P.C., Sweat, R.S., Dashti, D.C., Betancourt, A.M., and Murfee, W.L. (2014). Pericyte dynamics during angiogenesis: new insights from new identities. J. Vasc. Res. *51*, 163–174.

Steinberg, H.O., Paradisi, G., Hook, G., Crowder, K., Cronin, J., and Baron, A.D. (2000). Free fatty acid elevation impairs insulin-mediated vasodilation and nitric oxide production. Diabetes *49*, 1231–1238.

Strömberg, A., Olsson, K., Dijksterhuis, J.P., Rullman, E., Schulte, G., and Gustafsson, T. (2016). CX3CL1--a macrophage chemoattractant induced by a single bout of exercise in human skeletal muscle. Am. J. Physiol. Regul. Integr. Comp. Physiol. *310*, R297-304.

Strömberg, A., Rullman, E., Jansson, E., and Gustafsson, T. (2017). Exercise-induced upregulation of endothelial adhesion molecules in human skeletal muscle and number of circulating cells with remodeling properties. J. Appl. Physiol. Bethesda Md 1985 *122*, 1145–1154.

Styp-Rekowska, B., Hlushchuk, R., Pries, A.R., and Djonov, V. (2011). Intussusceptive angiogenesis: pillars against the blood flow. Acta Physiol. Oxf. Engl. *202*, 213–223.

Sun, X., Lin, J., Zhang, Y., Kang, S., Belkin, N., Wara, A.K., Icli, B., Hamburg, N.M., Li, D., and Feinberg, M.W. (2016). MicroRNA-181b Improves Glucose Homeostasis and Insulin Sensitivity by Regulating Endothelial Function in White Adipose Tissue. Circ. Res. *118*, 810–821.

Tadokoro, S., Ide, S., Tokuyama, R., Umeki, H., Tatehara, S., Kataoka, S., and Satomura, K. (2015). Leptin promotes wound healing in the skin. PloS One *10*, e0121242.

Takahashi, A., Kureishi, Y., Yang, J., Luo, Z., Guo, K., Mukhopadhyay, D., Ivashchenko, Y., Branellec, D., and Walsh, K. (2002). Myogenic Akt signaling regulates blood vessel recruitment during myofiber growth. Mol. Cell. Biol. *22*, 4803–4814.

Takemoto, M., Asker, N., Gerhardt, H., Lundkvist, A., Johansson, B.R., Saito, Y., and Betsholtz, C. (2002). A new method for large scale isolation of kidney glomeruli from mice. Am. J. Pathol. *161*, 799–805.

Tanaka, J., Qiang, L., Banks, A.S., Welch, C.L., Matsumoto, M., Kitamura, T., Ido-Kitamura, Y., DePinho, R.A., and Accili, D. (2009). Foxo1 links hyperglycemia to LDL oxidation and endothelial nitric oxide synthase dysfunction in vascular endothelial cells. Diabetes *58*, 2344–2354.

Tartaglia, L.A., Dembski, M., Weng, X., Deng, N., Culpepper, J., Devos, R., Richards, G.J., Campfield, L.A., Clark, F.T., Deeds, J., et al. (1995). Identification and expression cloning of a leptin receptor, OB-R. Cell *83*, 1263–1271.

Tedesco, F.S., Dellavalle, A., Diaz-Manera, J., Messina, G., and Cossu, G. (2010). Repairing skeletal muscle: regenerative potential of skeletal muscle stem cells. J. Clin. Invest. *120*, 11–19.

Teichert, M., Milde, L., Holm, A., Stanicek, L., Gengenbacher, N., Savant, S., Ruckdeschel, T., Hasanov, Z., Srivastava, K., Hu, J., et al. (2017). Pericyte-expressed Tie2 controls angiogenesis and vessel maturation. Nat. Commun. *8*, 16106.

Teng, S., and Huang, P. (2019). The effect of type 2 diabetes mellitus and obesity on muscle progenitor cell function. Stem Cell Res. Ther. *10*, 103.

Terman, B.I., Dougher-Vermazen, M., Carrion, M.E., Dimitrov, D., Armellino, D.C., Gospodarowicz, D., and Böhlen, P. (1992). Identification of the KDR tyrosine kinase as a receptor for vascular endothelial cell growth factor. Biochem. Biophys. Res. Commun. *187*, 1579–1586.

Thomas, M.M., Trajcevski, K.E., Coleman, S.K., Jiang, M., Di Michele, J., O'Neill, H.M., Lally, J.S., Steinberg, G.R., and Hawke, T.J. (2014). Early oxidative shifts in mouse skeletal muscle morphology with high-fat diet consumption do not lead to functional improvements. Physiol. Rep. *2*.

Thurston, G., Murphy, T.J., Baluk, P., Lindsey, J.R., and McDonald, D.M. (1998). Angiogenesis in mice with chronic airway inflammation: strain-dependent differences. Am. J. Pathol. *153*, 1099–1112.

Tikhanovich, I., Cox, J., and Weinman, S.A. (2013). Forkhead box class O transcription factors in liver function and disease. J. Gastroenterol. Hepatol. *28 Suppl 1*, 125–131.

Tilton, R.G., Hoffmann, P.L., Kilo, C., and Williamson, J.R. (1981). Pericyte degeneration and basement membrane thickening in skeletal muscle capillaries of human diabetics. Diabetes *30*, 326–334.

Tilton, R.G., Miller, E.J., Kilo, C., and Williamson, J.R. (1985). Pericyte form and distribution in rat retinal and uveal capillaries. Invest. Ophthalmol. Vis. Sci. *26*, 68–73.

Tischer, E., Gospodarowicz, D., Mitchell, R., Silva, M., Schilling, J., Lau, K., Crisp, T., Fiddes, J.C., and Abraham, J.A. (1989). Vascular endothelial growth factor: a new member of the platelet-derived growth factor gene family. Biochem. Biophys. Res. Commun. *165*, 1198–1206.

Toth, M.J., Palmer, B.M., and LeWinter, M.M. (2006). Effect of heart failure on skeletal muscle myofibrillar protein content, isoform expression and calcium sensitivity. Int. J. Cardiol. *107*, 211–219.

Tsuchiya, K., and Accili, D. (2013). Liver sinusoidal endothelial cells link hyperinsulinemia to hepatic insulin resistance. Diabetes *62*, 1478–1489.

Tsuchiya, K., Tanaka, J., Shuiqing, Y., Welch, C.L., DePinho, R.A., Tabas, I., Tall, A.R., Goldberg, I.J., and Accili, D. (2012). FoxOs integrate pleiotropic actions of insulin in vascular endothelium to protect mice from atherosclerosis. Cell Metab. *15*, 372–381.

Turner, N., Bruce, C.R., Beale, S.M., Hoehn, K.L., So, T., Rolph, M.S., and Cooney, G.J. (2007). Excess lipid availability increases mitochondrial fatty acid oxidative capacity in muscle: evidence against a role for reduced fatty acid oxidation in lipid-induced insulin resistance in rodents. Diabetes *56*, 2085–2092.

Uchida, C., Nwadozi, E., Hasanee, A., Olenich, S., Olfert, I.M., and Haas, T.L. (2015). Muscle-derived vascular endothelial growth factor regulates microvascular remodelling in response to increased shear stress in mice. Acta Physiol. Oxf. Engl. *214*, 349–360.

Udan, R.S., Vadakkan, T.J., and Dickinson, M.E. (2013). Dynamic responses of endothelial cells to changes in blood flow during vascular remodeling of the mouse yolk sac. Dev. Camb. Engl. *140*, 4041–4050.

Uezumi, A., Fukada, S., Yamamoto, N., Takeda, S., and Tsuchida, K. (2010). Mesenchymal progenitors distinct from satellite cells contribute to ectopic fat cell formation in skeletal muscle. Nat. Cell Biol. *12*, 143–152.

Uezumi, A., Ito, T., Morikawa, D., Shimizu, N., Yoneda, T., Segawa, M., Yamaguchi, M., Ogawa, R., Matev, M.M., Miyagoe-Suzuki, Y., et al. (2011). Fibrosis and adipogenesis originate from a common mesenchymal progenitor in skeletal muscle. J. Cell Sci. *124*, 3654–3664.

Umek, N., Horvat, S., Cvetko, E., Kreft, M., Janáček, J., Kubínová, L., Stopar Pintarič, T., and Eržen, I. (2019). 3D analysis of capillary network in skeletal muscle of obese insulin-resistant mice. Histochem. Cell Biol. *152*, 323–331.

Vanlandewijck, M., He, L., Mäe, M.A., Andrae, J., Ando, K., Del Gaudio, F., Nahar, K., Lebouvier, T., Laviña, B., Gouveia, L., et al. (2018). A molecular atlas of cell types and zonation in the brain vasculature. Nature *554*, 475–480.

Vempati, P., Popel, A.S., and Mac Gabhann, F. (2014). Extracellular regulation of VEGF: isoforms, proteolysis, and vascular patterning. Cytokine Growth Factor Rev. *25*, 1–19.

Vincent, M.A., Barrett, E.J., Lindner, J.R., Clark, M.G., and Rattigan, S. (2003). Inhibiting NOS blocks microvascular recruitment and blunts muscle glucose uptake in response to insulin. Am. J. Physiol. Endocrinol. Metab. *285*, E123-129.

Vincent, M.A., Clerk, L.H., Lindner, J.R., Klibanov, A.L., Clark, M.G., Rattigan, S., and Barrett, E.J. (2004). Microvascular Recruitment Is an Early Insulin Effect That Regulates Skeletal Muscle Glucose Uptake In Vivo. Diabetes *53*, 1418–1423.

Wang, J., Liu, R., Hawkins, M., Barzilai, N., and Rossetti, L. (1998). A nutrient-sensing pathway regulates leptin gene expression in muscle and fat. Nature *393*, 684–688.

Wang, Y., Nakayama, M., Pitulescu, M.E., Schmidt, T.S., Bochenek, M.L., Sakakibara, A., Adams, S., Davy, A., Deutsch, U., Lüthi, U., et al. (2010). Ephrin-B2 controls VEGF-induced angiogenesis and lymphangiogenesis. Nature *465*, 483–486.

Weber, D.S. (2008). A novel mechanism of vascular smooth muscle cell regulation by Notch: platelet-derived growth factor receptor-beta expression? Circ. Res. *102*, 1448–1450.

Wilhelm, K., Happel, K., Eelen, G., Schoors, S., Oellerich, M.F., Lim, R., Zimmermann, B., Aspalter, I.M., Franco, C.A., Boettger, T., et al. (2016). FOXO1 couples metabolic activity and growth state in the vascular endothelium. Nature *529*, 216–220.

Williams, D.A., and Segal, S.S. (1992). Microvascular architecture in rat soleus and extensor digitorum longus muscles. Microvasc. Res. *43*, 192–204.

Williams, I.M., Valenzuela, F.A., Kahl, S.D., Ramkrishna, D., Mezo, A.R., Young, J.D., Wells, K.S., and Wasserman, D.H. (2018). Insulin exits skeletal muscle capillaries by fluid-phase transport. J. Clin. Invest. *128*, 699–714.

Wong, J., Bennett, W., Ferguson, M.W.J., and McGrouther, D.A. (2006). Microscopic and histological examination of the mouse hindpaw digit and flexor tendon arrangement with 3D reconstruction. J. Anat. *209*, 533–545.

Wörsdörfer, P., and Ergün, S. (2018). Do Vascular Mural Cells Possess Endogenous Plasticity In Vivo? Stem Cell Rev. Rep. *14*, 144–147.

Yamauchi, T., Nio, Y., Maki, T., Kobayashi, M., Takazawa, T., Iwabu, M., Okada-Iwabu, M., Kawamoto, S., Kubota, N., Kubota, T., et al. (2007). Targeted disruption of AdipoR1 and AdipoR2 causes abrogation of adiponectin binding and metabolic actions. Nat. Med. *13*, 332–339.

Yang, G., Ju, Y., Liu, S., and Zhao, S. (2019). Lipopolysaccharide upregulates the proliferation, migration, and odontoblastic differentiation of NG2+ cells from human dental pulp in vitro. Cell Biol. Int. *43*, 1276–1285.

Yang, W.-H., Chen, J.-C., Hsu, K.-H., Lin, C.-Y., Wang, S.-W., Wang, S.-J., Chang, Y.-S., and Tang, C.-H. (2014). Leptin increases VEGF expression and enhances angiogenesis in human chondrosarcoma cells. Biochim. Biophys. Acta *1840*, 3483–3493.

Yang, Y.J., Hope, I.D., Ader, M., and Bergman, R.N. (1989). Insulin transport across capillaries is rate limiting for insulin action in dogs. J. Clin. Invest. *84*, 1620–1628.

Yang, Y.J., Hope, I., Ader, M., Poulin, R.A., and Bergman, R.N. (1992). Dose-response relationship between lymph insulin and glucose uptake reveals enhanced insulin sensitivity of peripheral tissues. Diabetes *41*, 241–253.

Yang, Y.J., Hope, I.D., Ader, M., and Bergman, R.N. (1994). Importance of transcapillary insulin transport to dynamics of insulin action after intravenous glucose. Am. J. Physiol. *266*, E17-25.

Yau, S.W., Henry, B.A., Russo, V.C., McConell, G.K., Clarke, I.J., Werther, G.A., and Sabin, M.A. (2014). Leptin enhances insulin sensitivity by direct and sympathetic nervous system regulation of muscle IGFBP-2 expression: evidence from nonrodent models. Endocrinology *155*, 2133–2143.

Yazdani, S., Jaldin-Fincati, J.R., Pereira, R.V.S., and Klip, A. (2019). Endothelial cell barriers: Transport of molecules between blood and tissues. Traffic Cph. Den. *20*, 390–403.

Yianni, V., and Sharpe, P.T. (2018). Molecular Programming of Perivascular Stem Cell Precursors. Stem Cells Dayt. Ohio *36*, 1890–1904.

Zeng, G., Nystrom, F.H., Ravichandran, L.V., Cong, L.N., Kirby, M., Mostowski, H., and Quon, M.J. (2000). Roles for insulin receptor, PI3-kinase, and Akt in insulin-signaling pathways related to production of nitric oxide in human vascular endothelial cells. Circulation *101*, 1539–1545.

Zhang, Y., and Chua, S. (2017). Leptin Function and Regulation. Compr. Physiol. *8*, 351–369.

Zhang, X., Kazerounian, S., Duquette, M., Perruzzi, C., Nagy, J.A., Dvorak, H.F., Parangi, S., and Lawler, J. (2009). Thrombospondin-1 modulates vascular endothelial growth factor activity at the receptor level. FASEB J. Off. Publ. Fed. Am. Soc. Exp. Biol. *23*, 3368–3376.

Zhao, L., Fu, Z., Wu, J., Aylor, K.W., Barrett, E.J., Cao, W., and Liu, Z. (2015). Inflammation-induced microvascular insulin resistance is an early event in diet-induced obesity. Clin. Sci. Lond. Engl. 1979 *129*, 1025–1036.

Zhou, A., Egginton, S., Hudlická, O., and Brown, M.D. (1998). Internal division of capillaries in rat skeletal muscle in response to chronic vasodilator treatment with alpha1-antagonist prazosin. Cell Tissue Res. *293*, 293–303.

Zhou, J., Li, Y.-S., and Chien, S. (2014). Shear stress-initiated signaling and its regulation of endothelial function. Arterioscler. Thromb. Vasc. Biol. *34*, 2191–2198.

Zhou, Y.T., Shimabukuro, M., Koyama, K., Lee, Y., Wang, M.Y., Trieu, F., Newgard, C.B., and Unger, R.H. (1997). Induction by leptin of uncoupling protein-2 and enzymes of fatty acid oxidation. Proc. Natl. Acad. Sci. U. S. A. *94*, 6386–6390.

Zhu, X., Bergles, D.E., and Nishiyama, A. (2008). NG2 cells generate both oligodendrocytes and gray matter astrocytes. Dev. Camb. Engl. *135*, 145–157.

Ziegler, M.A., Distasi, M.R., Bills, R.G., Miller, S.J., Alloosh, M., Murphy, M.P., Akingba, A.G., Sturek, M., Dalsing, M.C., and Unthank, J.L. (2010). Marvels, mysteries, and misconceptions of vascular compensation to peripheral artery occlusion. Microcirc. N. Y. N 1994 *17*, 3–20.

Zygmunt, M., Herr, F., Münstedt, K., Lang, U., and Liang, O.D. (2003). Angiogenesis and vasculogenesis in pregnancy. Eur. J. Obstet. Gynecol. Reprod. Biol. *110 Suppl 1*, S10-18.